NUREG/CR--5670

TI91 012495

Multiloop Integral System Test (MIST): MIST Facility Functional Specification

Date Published: April 1991

Authors

T. F. Habib, C. G. Koksal, T. E. Moskal, G. C. Rush, J. R. Gloudemans

Major Contributors

ARC		NPD
D. P. Birmingham	A. L. Miller	G. O. Geissler
J. E. Blake	J. R. Oyster	K. W. Turner
H. R. Carter	K. T. Reynolds	R. A. Turner
M. T. Childerson	D. D. Schleappi	
M. I. Manolescu	D. D. Sproul	

Prepared by

Babcock & Wilcox
Nuclear Power Division
3315 Old Forest Road
Lynchburg, VA 24506-0935

Babcock & Wilcox
Research and Development Division
Alliance Research Center
1562 Beeson Street
Alliance, OH 44601

Prepared for

Division of Systems Research
Office of Nuclear Regulatory Research
U.S. Nuclear Regulatory Commission
Washington, DC 20555
NRC FINs B8909, D1734

Electric Power Research Institute
P.O. Box 10412
Palo Alto, CA 94303

Babcock & Wilcox Owners Group
P.O. Box 10935
Lynchburg, VA 24506-0935

DISCLAIMER

ABSTRACT

The Multiloop Integral System Test (MIST) is part of a multiphase program started in 1983 to address small-break loss-of-coolant accidents (SBLOCAs) specific to Babcock and Wilcox designed plants. MIST is sponsored by the U.S. Nuclear Regulatory Commission, the Babcock & Wilcox Owners Group, the Electric Power Research Institute, and Babcock and Wilcox. The unique features of the Babcock and Wilcox design, specifically the hot leg U-bends and steam generators, prevented the use of existing integral system data or existing integral facilities to address the thermal-hydraulic SBLOCA questions. MIST was specifically designed and constructed for this program, and an existing facility--the Once Through Integral System (OTIS)--was also used. Data from MIST and OTIS are used to benchmark the adequacy of system codes, such as RELAP5 and TRAC, for predicting abnormal plant transients.

The MIST Functional Specification documents as-built design features, dimensions, instrumentation, and test approach. It also presents the scaling basis for the facility and serves to define the scope of work for the facility design and construction.

CONTENTS

Section		Page
1	MIST Design Basis	1-1
	1.1 Design Basis Summary	1-2
	1.2 Loop Configuration	1-12
	1.3 Modeling Atypicalities	1-15
	1.4 Test Procedures	1-19
	1.5 Application of Data	1-21
2	Reactor Coolant System	2-1
	2.1 Reactor Coolant System Arrangement	2-1
	2.2 Reactor Vessel Model	2-14
	2.3 Hot Legs	2-56
	2.4 Steam Generators	2-67
	2.5 Cold Legs	2-85
	2.6 Pressurizer	2-109
	2.7 Continuous Vent Line	2-115
3	Boundary Systems	3-1
	3.1 Simulated Leaks	3-1
	3.2 Simulated Vents	3-5
	3.3 Guard Heating System	3-10
	3.4 Emergency Core Cooling System	3-15
	3.5 Steam Generator Secondary System	3-23
	3.6 Non-Condensible Gas Addition System	3-31
	3.7 Water Chemistry Control	3-34
4	Facility Automatic Control Systems	4-1
	4.1 Core Power Control	4-2
	4.2 Reactor Coolant Pump Rampup and Coastdown Control	4-5
	4.3 Reactor Vessel Vent Valves Control	4-7
	4.4 High-Pressure Injection Control	4-9

CONTENTS (Continued)

Section		Page
	4.5 Auxiliary Feedwater Control	4-12
	4.6 Steam Pressure Control	4-19
	4.7 Guard Heater Control	4-24
	4.8 Pressurizer Heater Control	4-26
	4.9 Low-Pressure Injection Control	4-29
5	Data Acquisition System	5-1
	5.1 Data Acquisition and Data Processing Hardware	5-1
	5.2 Software Overview	5-7
6	Characterization Test Results	6-1
	6.1 Primary and Secondary System Volume	6-1
	6.2 Primary Loop Irrecoverable Pressure Losses	6-11
	6.3 Reactor Vessel Vent Valve Performance	6-17
	6.4 Reactor Coolant Pump Performance	6-18
	6.5 Guard Heater Performance	6-22
	6.6 MIST Loop Heat Loss Without Guard Heaters	6-27
	6.7 Leak Quality System Performance	6-37
7	Test Specifications	7-1
	7.1 Mapping Tests -- Group 30	7-4
	7.2 Boundary System Tests -- Group 31	7-6
	7.3 Leak-HPI Configuration Tests -- Group 32	7-9
	7.4 Feed and Bleed Tests -- Group 33	7-10
	7.5 Steam Generator Tube Rupture Tests -- Group 34	7-11
	7.6 Non-Condensible Gas and Venting Tests -- Group 35	7-12
	7.7 Reactor Coolant Pump Operation Tests -- Group 36	7-13
	7.8 Phase 4 Tests	7-15
8	References	8-1

ILLUSTRATIONS

Figure		Page
2.1	Overall Loop Arrangement Showing Major Subsystems	2-3
2.2	Reactor Coolant System Arrangement	2-4
2.3	Reactor Coolant System Layout	2-5
2.4	Support Locations for the Reactor Coolant System	2-9
2.5	Reactor Vessel for a 177 Fuel Assembly Plant	2-15
2.6	Reactor Vessel Model Arrangement	2-17
2.7	Downcomer to Reactor Vessel Crossover Piping	2-19
2.8	Reactor Vessel Ground Plate	2-21
2.9	Core Simulation	2-22
2.10	Fuel Pin Simulator	2-24
2.11	Axial Heat Flux Profile in Model Core	2-26
2.12	Reactor Vessel Top and Upper Plenum	2-28
2.13	Reactor Vessel Hot Leg and Vent Valve Connections	2-29
2.14	Reactor Vessel Instrumentation	2-31
2.15	Reactor Vessel Downcomer	2-35
2.16	Upper Downcomer Detail	2-37
2.17	Upper Downcomer Instrumentation	2-40
2.18	Upper Downcomer Instrumentation Detail	2-41
2.19	Lower Downcomer Instrumentation	2-42
2.20	Reactor Vessel Vent Valve Simulation	2-48
2.21	Effect of RVVV Setpoints on Core Power-to-Flow Characteristic	2-49
2.22	Reactor Vessel Vent Valve Slotted Orifice	2-51

ILLUSTRATIONS (Continued)

Figure		Page
2.23	Internal Geometry of Isolation Valves in RVVV Simulation	2-52
2.24	Reactor Vessel Vent Valve Instrumentation	2-54
2.25	Comparison of Plant and MIST Hot Leg Elevations	2-57
2.26	Hot Leg Instrumentation	2-61
2.27	Hot Leg Fluid Thermocouple Installation	2-62
2.28	Hot Leg Detail at U-Bend	2-64
2.29	MIST Gamma Densitometer Design	2-66
2.30	MIST Once-Through Steam Generator	2-68
2.31	Comparison of MIST and Plant Tube Support Plate Geometry	2-70
2.32	MIST Auxiliary Feedwater Head-Flow Characteristic	2-71
2.33	Auxiliary Feedwater Nozzle Configurations	2-72
2.34	Primary to Secondary Tube Leak Simulation	2-73
2.35	Steam Generator A Instrumentation	2-75
2.36	Cross-Sectional Location of Steam Generator A Instrumentation	2-76
2.37	Steam Generator B Instrumentation	2-79
2.38	Steam Generator B Radial Thermocouple Distribution	2-80
2.39	Steam Generator B Thermocouples to Observe AFW Spreading	2-81
2.40	Steam Generator B Primary Pitot Tubes and Tubesheet Temperature	2-82
2.41	Comparison of Plant and MIST Cold Leg Elevations	2-87
2.42	C2 Cold Leg Discharge Piping Detail	2-89
2.43	Comparison of MIST and Scaled Plant RCP Head-Flow Characteristics	2-90
2.44	Comparison of MIST and Scaled Plant RCP Locked Rotor Resistance	2-91
2.45	MIST Reactor Coolant Pump Design	2-93

ILLUSTRATIONS (Continued)

Figure		Page
2.46	RCP Boost Pump Circuit	2-95
2.47	Rotor Cavity Cooling Circuit for Model Reactor Coolant Pump	2-96
2.48	Plant RCP Startup and Coastdown Characteristics	2-97
2.49	Comparison of MIST and Scaled Plant NPSHR Characteristics	2-98
2.50	Cold Leg Flow and Density Measurements	2-100
2.51	Loop A Cold Leg Differential Pressure Measurements	2-102
2.52	Loop B Cold Leg Differential Pressure Measurements	2-103
2.53	Loop A Cold Leg Fluid Temperature Measurements	2-104
2.54	Loop B Cold Leg Fluid Temperature Measurements	2-105
2.55	Thermocouple Rake in Cold Leg Discharge Piping	2-106
2.56	Cold Leg Guard Heater System Measurements	2-108
2.57	Pressurizer and Pressurizer Surge Line	2-110
2.58	Pressurizer Heater Installation	2-111
2.59	Pressurizer Spray Nozzle Installation	2-112
2.60	Pressurizer Surge Line Diffuser	2-113
2.61	Continuous Vent Line Connection to Steam Generator	2-117
2.62	MIST Continuous Vent Line	2-118
2.63	Continuous Vent Line Instrumentation	2-120
3.1	10 cm^2 Critical Leak Flow Control Orifice	3-2
3.2	Cold Leg Leak System	3-4
3.3	Two-Phase Venting System	3-6
3.4	Reactor Coolant Pump Connections to Two-Phase Venting System	3-8
3.5	Guard Heater Arrangement	3-12
3.6	High-Pressure Injection System	3-16

ILLUSTRATIONS (Continued)

Figure		Page
3.7	High-Pressure Injection Head-Flow Control Functions	3-18
3.8	Core Flood System	3-19
3.9	Core Flood Surge Line Detail	3-21
3.10	Low-Pressure Injection System	3-22
3.11	Low-Pressure Injection System Head-Flow Characteristic	3-24
3.12	Secondary System	3-25
3.13	Feedwater Circuit Instrumentation	3-28
3.14	Steam Generator Steam Line Instrumentation	3-30
3.15	Non-Condensible Gas Addition System	3-32
3.16	Facility Water Supply and Cleanup System	3-37
3.17	Secondary Low-Pressure Cleanup System	3-38
3.18	Primary In-Line Filter System	3-39
4.1	Reactor Vessel Core Power Control	4-2
4.2	Reactor Coolant Pump Control	4-6
4.3	Reactor Vessel Vent Valve Control	4-8
4.4	High-Pressure Injection Control	4-10
4.5	Steam Generator Constant Level Control	4-14
4.6	Auxiliary Feedwater Band Level Control	4-20
4.7	Steam Pressure Control	4-21
4.8	Guard Heater Control	4-25
4.9	Pressurizer Pressure Control	4-27
4.10	Low-Pressure Injection Control	4-29
5.1	Analogic Data Acquisition System Configuration	5-2
5.2	MIST Data Acquisition and Data Processing Program	5-5

ILLUSTRATIONS (Continued)

Figure		Page
5.3	Real-Time Software for Data Acquisition and Test Support	5-8
5.4	MIST Reactor Coolant System On-Line Status Display	5-10
5.5	Post-Test Data Processing Software	5-12
6.1	MIST Primary Loop Configuration	6-3
6.2	Component Identification for Reported Hydraulic Resistances .	6-13
6.3	Reactor Coolant Pump Head-Flow Characteristics	6-20
6.4	Reactor Coolant Pump Head-Flow Characteristics at 18% Speed .	6-20
6.5	Reactor Coolant Pump Spinup Characteristics	6-23
6.6	Reactor Coolant Pump Coastdown Characteristics	6-24
6.7	Facility Overall Heat Loss	6-31
6.8	Reactor Vessel Heat Loss	6-31
6.9	Reactor Vessel Downcomer Heat Loss	6-32
6.10	Steam Generator Heat Loss	6-32
6.11	Hot Leg Heat Loss	6-33
6.12	Cold Leg Suction Heat Loss	6-34
6.13	Reactor Coolant Pump Heat Loss	6-35
6.14	Cold Leg Discharge Heat Loss	6-36
6.15	Leak Enthalpy Uncertainty for 10 cm^2 Leak Phase 4 Tests	6-40
6.16	Leak Enthalpy Uncertainty for 100 cm^2 Leak Phase 4 Test	6-40

TABLES

Table		Page
1.1	TAG Evaluation of Issues	1-4
1.2	SBLOCA Events	1-6
1.3	Loop Compromises and Impacts	1-16
1.4	Potential Use of MIST to Address MIST Atypicalities	1-19
2.1	Plant and MIST Elevations	2-6
2.2	Fluid and Metal Volumes for MIST and the Ideally Scaled Plant	2-10
2.3	Composite Core Heat Flux Profile	2-25
3.1	Facility Water Chemistry Specifications	3-34
4.1	Reactor Vessel Vent Valve Actuation Setpoints	4-9
4.2	Span and Zero Correction Functions for Steam Generator Level	4-16
4.3	Span and Zero Correction Functions for Pressurizer Level	4-29
5.1	Analog Voltage Card Types for the Data Acquisition System	5-3
5.2	Sample Data Tape Header File	5-15
5.3	Engineering Data Reduction Types, Reference VTABs, and Conversion Constants	5-23
5.4	Engineering Data Error Codes	5-34
6.1	Component Volume Versus Level Functions	6-4
6.2	Elliot Tank Volume Versus Differential Pressure Functions	6-9
6.3	Component Level Measurement Uncertainties	6-10
6.4	Summary of Component Hydraulic Resistances	6-12
6.5	Average Reactor Coolant Pump Locked-Rotor Resistance	6-14
6.6	Cold Leg Flow Loop Equivalent Hydraulic Resistance	6-15
6.7	Hot Leg Flow Loop Equivalent Hydraulic Resistance	6-16

TABLES (Continued)

Table		Page
6.8	Reactor Vessel Vent Valve Open Setpoints	6-18
6.9	Reactor Vessel Vent Valve Close Setpoints	6-18
6.10	Reactor Coolant Pump Locked-Rotor Resistance	6-21
6.11	Guard Heater Control Parameters	6-26
6.12	Guard Heater Control Functions	6-28
6.13	Locations of Major Facility Heat Losses	6-38
6.14	Leak Quality System Characterization Data	6-39
7.1	MIST Test Groups	7-1
7.2	Mapping Tests -- Group 30	7-5
7.3	Boundary System Tests -- Group 31	7-6
7.4	Leak-HPI Configuration Tests -- Group 32	7-9
7.5	Feed and Bleed Tests -- Group 33	7-10
7.6	Steam Generator Tube Rupture Tests -- Group 34	7-12
7.7	Non-Condensible Gas and Venting Tests -- Group 35	7-14
7.8	Reactor Coolant Pump Operation Tests -- Group 36	7-14
7.9	Phase 4 Tests	7-16

QUALITY ASSURANCE STATEMENT

To the best of my knowledge and belief, MIST Phase 3 was conducted in accordance with the requirements of Quality Assurance Plan 85004, Revision 2, dated September 12, 1985, and MIST Phase 4 was conducted in accordance with the requirements of Quality Assurance Plan 87004, Revision 0, dated May 13, 1987.

5-8-90

G. W. Roberts
Section Manager, Quality Assurance

Section 1

MIST DESIGN BASIS

The multi-loop integral system test (MIST) was part of a multiphase program to address small-break loss-of-coolant accidents (SBLOCAs) specific to the Babcock & Wilcox-designed nuclear steam system. MIST was sponsored by the U.S. Nuclear Regulatory Commission (NRC), the Electric Power Research Institute (EPRI), the Babcock & Wilcox Owners Group, and Babcock & Wilcox (B&W). Test data from the MIST facility have been used to benchmark the predictive capabilities of several system codes — RELAP5 and TRAC — for predicting abnormal plant transients.

In 1982, a Test Advisory Group (TAG) was formed to identify experimental data needs for the B&W-designed nuclear steam system. The TAG developed a list of 17 issues perceived to lack experimental data and to be of sufficient interest that such data were needed. The issues were categorized into four major topics: natural circulation, small-break loss-of-coolant accidents, feed and bleed, and steam generator tube rupture.

Due to the unique features of the Babcock & Wilcox system design, specifically the hot leg U-bend configuration that results with the once-through steam generator (OTSG), previous large integral system test facilities did not simulate the appropriate natural circulation conditions. There was uncertainty regarding the effects of the non-condensible gases, high point vents, and the reactor vessel vent valves on natural circulation. The validity of the boiler-condenser mode of heat removal was also questioned. Since a major phenomenon in an SBLOCA in a B&W plant is the natural circulation mode of heat removal, the TAG recommended that the natural circulation phenomena be addressed on an integral system basis. Parameters such as break size and location, isolation of the break, sensitivity to emergency core cooling system (ECCS) operation, and the effects of reactor coolant pump operation were to be evaluated. This would also permit evaluation of the reactor vessel vent valves on an integral system basis. The

group recommended that tests be performed to assess the computer code capability of predicting the feed and bleed mode of heat removal. Finally, since the once-through steam generator presents a significantly different configuration from a U-tube steam generator, it was concluded that integral system testing of tube ruptures would be beneficial. Both single- and multiple-tube ruptures were to be considered, along with a steam line break in conjunction with a tube rupture.

Section 1 of this report provides a summary of the design basis, scaling method, and the resulting loop configuration of the MIST facility. Detailed description of the scaling and design selection of each component of the MIST facility is available in Reference 1. Also discussed in Section 1 are the modeling atypicalities and the testing performed to assess the impact of the atypicalities.

1.1 DESIGN BASIS SUMMARY

MIST was developed to provide integral-system data for code benchmarking. The major features of the MIST facility as well as the essential tests were agreed to by the Test Advisory Group.

1.1.1 TAG Issues

The TAG was comprised of representatives of the Nuclear Regulatory Commission, Babcock & Wilcox Owners, Babcock & Wilcox, and the Electric Power Research Institute. The TAG addressed four tasks[2]:

1. Identify experimental needs.
2. Identify operating plant and experimental data available now or in the near future.
3. Evaluate how well these data address the identified data needs.
4. Provide recommendations for future programs.

One result of the first three of these tasks was the development of a list of issues.

The 17 TAG issues are those that the TAG felt should be addressed through an IST (Integral Systems Test) facility. The TAG spent arduous sessions developing and refining this list. The 17 issues are listed in Table 1.1. The priority assignments also shown in Table 1.1 in several instances reflect compromise priorities among the TAG participants. There was a reluctance to prioritize these issues simply because they were each felt to be important — an NRC representative indicated that this list already represented a culling from an extensive list of issues. (The TAG list of issues does not show two issues that the NRC wished to include — "Natural Circulation Cooldown" and "Cyclic Issues"[2].)

The TAG evaluation of the issues involved two considerations: 1) the perceived importance of each issue and 2) the current state of knowledge regarding each issue. An issue deemed to be relatively important and thought to need additional characterization was given a high ranking. The availability of existing test and/or plant data was used to indicate knowledge. Thus by definition the TAG issues for testing address areas in which there is a perceived paucity to relevant data and correlations.

The TAG agreed not only to the testing issues but also to a test matrix and to the essentials of a test facility. The planned tests, of course, related to the TAG issues. The agreed-to test facility was a 2 x 4 model of a 177 (Fuel assembly) lowered-loop (B&W) plant. Major features of the model included:

- Two Hot Legs and four Cold Legs (2 x 4),
- Full elevation,
- Power and volume scaled by 817 (based on the use of two model generators of 19 tubes each),
- Hot Leg diameters of 3 inches (subsequently reduced to 2.5 inches),
- Maximum power of approximately 10% of scaled full power,
- Full-loop guard heating,
- Four model reactor coolant pumps, and
- Full-length model core of prototypical cellular dimensions.

Table 1.1

TAG EVALUATION OF ISSUES
(From Reference 2)

Natural Circulation	**Priority**
Single-phase natural circulation	D
Two-phase natural circulation	C
Boiler condenser natural circulation	A
Steam generator-driven instabilities	B
Cold leg oscillations	B
Interruption/reestablishment	B
High point vents	A/D
Non-condensible gases	B
Reactor vessel vent valves	C
Small Break Loss-of-Coolant Accident	
Break size	C
Emergency core cooling system operation	C
Reactor coolant pump operation	B
Location of break	D
Break isolation	B
Reactor vessel vent valves	B
Feed and Bleed	D
Steam Generator Tube Rupture	B

NOTE: Priority denotes the ranking of issues based on both the importance of the issue, and the degree of current knowledge of the issue. Priorities span "A" through "D", priority A being the highest. Priority "A/D" for High Point Vents (in Natural Circulation) denotes NRC ranking "A" and B&W Owners Group ranking of "D".

The facility and tests were recommended by the TAG to provide a sufficient data base for use in computer code assessment. The assessed computer code is the link between the test data and the operating plant. Test facility results cannot be extrapolated to predict plant performance.

The TAG reached agreement on the testing issues and the MIST tests needed to address these issues. The MIST design has been synthesized from ongoing integral system testing experience, from knowledge and estimates of B&W plant interactions following a SBLOCA, and from the issues identified by the TAG. The TAG issues formed the basis for the design selection. To obtain more readily quantified design selection criteria, the SBLOCA events were identified and related to the TAG issues.

1.1.2 SBLOCA Events

Twenty-five post-SBLOCA events were identified for ranking against the TAG issues. These ranked (and weighted) events then provided the basis for selecting and evaluating the MIST system and component designs. Presumably no single SBLOCA transient would encounter each of the events; the events were defined to include the major interactions likely to be of significance in any post-SBLOCA scenario. For example, each of the three major methods of heat removal (feed and bleed cooling, leak-HPI cooling, and primary-to-secondary heat transfer) were listed, but all three methods may not occur in a single transient. The generation of this events list was subjective. It presumed that current testing experience, observations of plant performance, conceptual estimates, and code predictions were sufficient in the aggregate to identify the key features of post-SBLOCA interactions. The 25 post-SBLOCA events are identified in Table 1.2. They are listed in roughly chronological order; events which may occur repeatedly (e.g., single-phase natural circulation) were listed only once. The events are comparable to these described by Burchill[3] in his general discussion of SBLOCA transients, but reflect greater detail and emphasize only the B&W design.

Table 1.2

SBLOCA EVENTS

Approximately chronological events of a composite post-SBLOCA sequence. Each event listed only once.

Event Chronological Number	Event
	Initiation
1	Leak Flow
2	Pressurizer Draining
3	Primary Depressurization
4	Power and Flow Transient: Reactor and Reactor Coolant Pump Trips, Transfer of Steam Generator Feed
5	Single Phase Natural Circulation
	Intermittent Spillover Circulation
6	Hot Leg U-Bend Saturation and Voiding
7	Reactor Vessel Upper Head Voiding
8	Reactor Vessel Vent Valve Actuation
9	Decoupling of Steam Generator, Steam Generator Depressurization
10	Primary Repressurization
11	Leak-HPI (High Pressure Injection) Cooling
12	Feed and Bleed (Primary) Cooling
13	Downcomer and Cold Leg Voiding and Condensation
14	Asymmetric Conditions Among Cold Legs
	Boiler Condenser Mode
15	Steam Generator Condensation of Primary Steam
16	Primary Depressurization to Core Flood Tank/LPI Pressures
17	Steam Generator Repressurization
	Primary Refill
18	Compression of Primary Steam
19	Venting of Primary Fluid
20	Subcooling of Primary Components
21	Spillover Circulation (Hot Leg U-Bend Refilled)
22	"Pump Bump"
	Cooldown
23	Controlled Steam Generator Depressurization and Primary Cooldown
24	Reinitiation of Natural Circulation
25	Cooling of Idled Loop

The post-SBLOCA events were ranked against the TAG Issues to be able to apply these events in the MIST design selection. The most significant events to address the TAG issues were adjudged to be: Hot Leg U-Bend Saturation and Voiding; Reactor Vessel Vent Valve Actuation; and Leak-HPI (High Pressure Injection) Cooling. Six events were deemed to be of intermediate importance; these included Re-initiation of Natural Circulation, Downcomer and Cold Leg Voiding and Condensation, and Reactor Vessel Upper Head Voiding. Four events were perceived to be least significant: Primary Depressurization to Core Flood Tank/Low Pressure Injection Pressures; Subcooling of Primary Components; Steam Generator Repressurization; and Pressurizer Draining. The event ranking also indicated that all the events are of quite similar significance – the deletion of the least-significant events did not appear to be warranted.

1.1.3 Scaling Technique

The composite list of transient interactions, ranked against the TAG Issues, were used to develop and evaluate MIST scaling. This scaling process was performed for the primary system and for each major component (reactor vessel, hot leg, downcomer). For each scaling application, a six-step procedure was performed:

1) Identify those characteristics (of the system or component) which could significantly affect the integral-system interactions;

2) Evaluate the importance of each characteristic by determining the interactions it would influence, the degree of this influence, and the significance of the affected interactions;

3) Order the characteristics from most to least important;

4) Determine the ideal scaling or design for each characteristic, individually;

5) Synthesize a design which preserves the more important characteristics and, if necessary, compromises the least important characteristics; and

6) Evaluate the typicality of the component or system by verifying its estimated performance against the ranked events.

This procedure is subjective in several respects, particularly in the estimates of the influence of the individual atypicalities. The procedure is

also amenable to iteration or, as was performed, the development of several alternate designs with varying degrees of appropriateness for the multiple characteristics to be preserved. For example, several reactor vessel downcomer and vent valve arrangements were developed and compared during the scaling effort. The following description of the MIST system scaling demonstrates the scaling procedure.

1.1.4 System Scaling

The system characteristics thought to be most relevant to post-SBLOCA interactions included elevation, two-phase behavior, volume, wall effects, and irrecoverable pressure losses. These characteristics were verified against the ranked events. Elevation was considered of major significance in 9 of 25 events, including decoupling of primary-to-secondary heat transfer and events involving fluid buoyant forces. System two-phase behavior (voiding, phase separation, flooding, etc.) was of at least intermediate significance in more than two-thirds of the events. Fluid volume was ranked third of the five system characteristics. It was of particular significance in voiding and vapor compression events. Wall effects, notably steam condensation upon vapor compression, was ranked fourth. Last was irrecoverable pressure drop (fluid momentum loss) which nonetheless received one-third the score of the first-ranked event.

The ordered system characteristics were examined individually to determine the optimum model scaling or design.

Elevation. Elevation was ranked as the most significant model characteristic for the preservation of post-SBLOCA events, and thereby for testing germane to the TAG issues. The ideal model maintains full plant elevations at every flow junction, spillover elevation, and flowpath low point. Full elevation makes use of the existing model steam generator and its extensive testing and benchmarking. Full elevation facilitates the adaptation of model-verified codes to plant predictions. Most importantly, elevation differences govern key post-SBLOCA events, such as heat-transfer decoupling of the primary and secondary systems and natural circulation flow reversals.

Two-Phase Behavior. System two-phase behavior encompasses the following interactions: hot leg U-bend voiding and phase separation; hot leg (horizontal and vertical) flow regimes and lower region (reactor vessel upper head, downcomer, and cold leg discharge piping) voiding and condensation. Considering only the hot legs there are conflicting requirements regarding two-phase behavior because flow regimes and flooding have been correlated both to superficial velocity and to a modified Froude number. Superficial velocity is preserved in the model by scaling the hot leg flow area as power. The modified Froude number is dependent on pipe diameter such that its preservation requires a somewhat larger model pipe. The preservation of hot leg void fraction due to system liquid inventory depletion requires a power-scaled hot leg volume (for a full-elevation model, this again devolves to power-scaling the flow area). The large-system versus small-system criteria based on the existence of bubbly flow obtains a model hot leg diameter larger than using power-scaled area. The diameter beyond which flooding becomes independent of geometry, which is an extreme indication of possible model effects, obtains the largest model hot leg diameter of those discussed (3.4 inches at 200 psia and varying inversely with pressure). Consideration of hot leg U-bend effects introduce additional considerations which are not addressed here.

Volume. System volume scaling governs fluid transport time as well as the rate of change of fluid energy content. The ideal model system scales volume as power and retains the volume-versus-elevation proportions of the plant. Coupled with power-scaled boundary flowrates, the ideal system then loses inventory and level, and changes fluid properties, in entirely prototypical fashion. A hot leg pipe diameter of approximately 1.3 inches preserves power-to-volume scaling for full-length pipes.

Wall Effects. System bounding containment effects include: thermal energy storage, containment conduction across a fluid thermal gradient (and hence interphase energy transfer), and heat losses to ambient through the containment. The ideal model scales containment structural volume as contained fluid volume and avoids atypical metal appendages (massive instrument probes, flanges, conducting supports, and the like). Even with ideal metal scaling, fluid-to-metal coupling is atypically effective in reduced-size pipes, because the convective resistance is reduced as the heat transfer surface area per contained fluid volume is increased. Moreover, the

required pipe wall thickness decreases roughly as the square root of the pipe diameter reduction, thus high pressure models inherently suffer this atypicality. The optimum model simply minimizes pipe wall metal while avoiding the massive appendages previously noted.

Heat losses to ambient are particularly relevant to post-SBLOCA studies. Scaled decay core power levels may be less than the model heat losses if only passive insulation is used; the scaled plant heat losses, on the other hand, are still much smaller than model losses to ambient. The optimum model thus must actively counter ambient losses. Guard heating (automatically controlling on the sign of the temperature gradient in the insulation just beyond the pipe periphery) is well suited for this purpose. Wall effects during vapor compression may be paramount, particularly in light of the excess model metal and increased fluid-to-metal coupling already noted. Because the optimum model still suffers these atypicalities, it is important to identify and quantify the mechanisms of condensation. Instruments may then be selected and located to record the predominant mechanism(s). The likely modes of condensation heat transfer are: heat storage in the walls, direct steam-water interface heat transfer, and indirect interface heat transfer by axial conduction within the walls. Heat storage in the walls is the predominant condensation mode, the other two modes are an order of magnitude smaller. (Fortunately, wall heat storage is readily calculated in either the model or the plant).

Irrecoverable Pressure Drop. The ideal model preserves plant irrecoverable pressure drops (fluid momentum losses) at (power-) scaled flowrates. Furthermore, the ideal model preserves component as well as system losses, and the ratio of losses between form (shock) and friction.

Recognizing the recurring need for scaling compromises, additional guidelines may be discussed: with parallel flow branches, plant-typical hydraulic symmetry must be maintained. With branch points at the hot leg nozzles and at the steam generator outlets, it is desirable that the hydraulic resistances within each branch leg be maintained. Finally, with major inner and outer flow loops (reactor vessel vent valve versus loop, both through the downcomer - reactor vessel), the resistance of each loop should be maintained.

Model piping diameters may be estimated to preserve frictional irrecoverable pressure drop at power-scaled mass flowrates. Because of differences in component geometry between the plant and the model, this model pipe diameter may have to be modified to approximately conserve total (form plus friction) irrecoverable pressure drop. For example, the preservation of only frictional pressure drop indicates larger than area-scaled model pipes, thus the model form losses associated with contractions and expansions are less than those of the plant. This decrease of form loss must be accommodated by a corresponding increase of friction loss (using a diameter slightly smaller than calculated by friction considerations only). The actual model system loss calculations are automated using the flow network code SAVER[4].

Summary. The several model system characteristics have been explored for their scaling implications. Elevation is the most significant characteristic. The model must preserve full plant elevations to even be able to simulate plant post-SBLOCA events. The existence of a full-elevation model steam generator, with a wealth of testing experience and model development has also been noted. The ease of re-application of codes benchmarked using a full-elevation model is another benefit.

The remaining characteristics (two-phase behavior, volume, wall effects, and irrecoverable pressure drop) have been explored largely in the context of a full-elevation model. Because the system configuration is vertically oriented, full elevation requires piping runs that are nearly full (plant) length. The model system characteristics have each yielded an ideal hot leg pipe diameter. A hot leg pipe diameter of 1.3 inches preserves power-to-volume scaling for a full-length pipe; such a diameter also preserves fluid velocities, i.e., equates those in the model to those in the plant, for scaled mass flowrate in the model piping.

A hot leg pipe diameter greater than approximately 2 inches is required to allow bubbly flow, and hence to exhibit phase separation at the hot leg U-Bend. A 2.9-inch hot leg inside diameter is obtained from frictional pressure drop considerations. Calculations of the model system hydraulic losses indicated that a diameter as small as approximately 2-1/4 inches could be used; it is desirable to slightly over-size based on irrecoverable pressure

drop, to admit system orifices for flow metering and to allow some margin for loss calculation inaccuracies.

Consideration of wall effects alone would simply select the largest model pipe and the smallest permissible pipe wall thickness. The larger pipe decreases fluid-to-metal coupling (fluid volume/adjacent metal surface area) toward that of the plant.

The preceding considerations led to a full-elevation model with somewhat oversized hot legs and cold legs. The system and key components and their atypicalities are described below and are addressed in more detail in the Facility Specification[1]. The model reactor vessel vent valves were judged to be the least typical component, primarily because of their inability to simulate the partially-open operation of the plant valves. The most limiting system characteristic was wall effects, specifically the ratio of heat transfer surface area to adjacent fluid volume in the model.

1.2 LOOP CONFIGURATION

MIST is a 2 x 4 loop designed for prototypical fluid conditions, with emphasis on leak tightness and the minimization of heat losses. MIST is full elevation throughout. Only the elevations of the top of the pressurizer, the reactor vessel top plenum, the steam generator inlet and inlet plenum extremes, and of several incidental stagnant fluid zones are compromised.

System two-phase behavior during hot leg U-bend voiding and flow interruption is sufficiently prototypical, i.e., both the plant and the model will experience phase separation early in the post-SBLOCA transient (after the reactor coolant pumps are tripped). The model hot leg pipes are sufficiently large to admit bubbly flow. The model reactor vessel upper internals are designed to obtain prototypical phase separation.

The model fluid volume is 30% larger than power-to-volume scaled; the hot legs, cold legs, and upper downcomer are oversized. This undesirable typicality is imposed by the previously mentioned model system characteristics, and by the consideration of model regional fluid irrecoverable

pressure drops. The hot leg excess volume slows the rate of hot leg level decrease for a power-scaled draining rate, and similarly retards the rate of level increase for a power-scaled injection rate. Although the excess loop fluid volume delays system heatup and cooldown, this effect is minor compared to the long-term impact on system energy of leak versus HPI (High Pressure Injection) cooling. The concentration of model excess volume in the piping runs decreases fluid velocities in the hot legs and cold legs, and hence lengthens the loop fluid transit time.

Model wall effects are amplified by the atypically large ratio of wall heat transfer surface area to contained fluid volume. Therefore, model heat losses and metal mass are closely controlled. Heat losses are minimized by using full-system active guard heating.

Metal mass is minimized by avoiding flanges and conducting supports, and by using minimum pipe wall thickness consistent with code requirements. The resulting ratio of metal volume to fluid volume in the model is roughly 35% greater than that in the plant. This excess model metal dampens system pressure changes, but these metal effects can be modeled and predicted.

System irrecoverable pressure drops are well preserved. The designed system allows for the introduction of extra grids at the inlet to the core, and for the insertion of flow-metering devices in the cold leg suction piping.

1.2.1 Components

The model core and steam generator use cellular modeling. The core consists of a 7 x 7 array of rods (45 heated; 4 unheated simulating guide tubes), of prototypical length and unit-cell geometry and dimensions; likewise the model steam generators contain 19 full-length tubes each, in prototypical arrays. The hot legs use 2.32-inch ID pipe (2-1/2 inch Schedule 80); this diameter admits to bubbly flow and approximates the irrecoverable pressure drop, the Schedule 80 pipe obtains a metal-to-fluid ratio only 20% greater than that of the plant. The HL horizontal runs are approximately 1 foot to accommodate the gamma densitometers. The surgeline connection to the ("A") hot leg is at the plant elevation. The hot leg U-bend maintains the hot leg pipe diameter, a

1.61-foot bend radius is used to conform to the model system layout; phase separation at the U-bend is predicted to occur at approximately 18% of full power versus 8% in the plant. Beyond the hot leg U-bend, the model hot leg piping extends 12 feet (versus 1-1/2 feet in the plant) to span the height of the plant steam generator inlet plenum. The model steam generator contains an orifice plate (for flow redistribution) between the steam generator inlet and the upper tube sheet.

The four model cold legs preserve elevation throughout. Two-inch Schedule 80 piping is used, primarily on the basis of irrecoverable pressure drop. This piping also preserves cold leg Froude number, which governs HPI-RVVV (Reactor Vessel Vent Valve) fluid mixing. The cold leg horizontal piping runs are shortened, but the plant declination of the cold leg discharge sloping run is approximately maintained. HPI is injected into this sloping piping at the appropriate elevation. The diameter of the model HPI nozzle is selected to preserve the ratio of fluid momentum between the cold leg and HPI. A model reactor coolant pump is mounted in each cold leg. Suction and discharge orientations are prototypical. The model pumps are virtually leak tight and do not distort the system energy balance. The pumps deliver full power-scaled flow at (plant) rated head. The coastdown of the plant pumps can be simulated. The model pumps preserve neither specific speed nor the two-phase degradation characteristics of the plant pumps, however.

MIST employs an external annular downcomer. Inter-cold leg decoupling is obtained by using fins in the downcomer annulus to form quadrants. The annular gap is 1.4 inches; the gap at each fin is 0.4 inch. Each downcomer quadrant is connected to a separate RVVV simulation and cold leg nozzle. The two core flood tank nozzles are each led to (the interface between) two downcomer quadrants. The model downcomer geometry is annular down to the elevation of the top of the core. Just above the top of the core, the downcomer is gradually reconfigured to form a single pipe for the remaining elevation; this lower downcomer region obtains roughly power-scaled fluid volume over the elevation of the core. The downcomer irrecoverable losses are mis-scaled using the model hardware just described, but the flow loop and branch losses are preserved (other than the inter-cold leg flow which encounters decreased circumferential resistance in the downcomer).

The four model RVVVs may be controlled individually or in unison. Individual controllers provide automatic actuation on the upper plenum to downcomer-quadrant pressure differences. These RVVVs thus provide the gross head-flow response of the plant valves; partially-open operation is not possible in the model, and the detailed valve dynamics of the plant flapper valves are absent.

The MIST pressurizer is power-to-volume scaled and contains heaters and spray. The lower pressurizer elevations are prototypical, as are those of the surge line. The model pressurizer height is reduced from that of the plant to increase the model pressurizer diameter. This facilitates guard heating, lessens atypical fluid stratification and the likelihood of spray impingement on the walls; the larger diameter also admits to the introduction of excess model heater capacity without amplifying fluid velocities within the pressurizer (toward entrainment velocities) upon relief actuation.

Boundary systems are sized to power-scale the plant boundary conditions. HPI and auxiliary feedwater head-flow characteristics are obtained from the composite plant characteristics. The core flood tank volume is power-to-volume scaled. Vent, relief, and controlled-leak sizes are similarly obtained by power scaling the nominal plant values. Boundary system simulations thus emphasize the impact of boundary flows on system energy, as opposed to their effects on system fluid inventory.

1.3 MODELING ATYPICALITIES

An extensive list of MIST atypicalities and scaling compromises was presented to the MIST Design Review Board and is reproduced in Table 1.3. The list is ordered by component, each compromise is listed with its estimated impact and the reason for the compromise. The compromise regarding cold leg slope has since been determined to be less severe than as listed. The cold leg slope (maximum declination of the piping centerline) is 45° in the plants and 59° in MIST. Also, under the steam generator entry regarding auxiliary feedwater multi-dimensional effects, it is indicated that bracketing auxiliary feedwater wetting effects will be obtained by using minimum and maximum wetting nozzles.

This list of MIST scaling atypicalities and compromises provided the basis for the deliberations regarding inter-facility coordination. The number of atypicalities was reduced by considering only those perceived to have a major impact on the application of a code, benchmarked using MIST data, to a plant. The atypicalities which can be addressed by MIST are summarized in Table 1.4. MIST was assigned to address three of its 12 atypicalities. Of these three: MIST can well address auxiliary feedwater multi-dimensional effects in MIST; MIST is of limited usefulness regarding the steam generator metal mass atypicality (precluding substantial facility modifications); and a secondary system modification is required to address its Secondary Side atypicality.

Table 1.3

LOOP COMPROMISES AND IMPACTS

Component	Compromise	Impact	Reason for Compromise
Reactor Vessel	Simplified upper internals, modeled only for flow-path elevation, pressure losses, and de-entrainment; other hardware eliminated	Small: The major impact of RV upper internals on SBLOCA are due to flow and phase branching among the several flowpaths. These are preserved in the model.	Geometry: The hardware not simulated is not significant to preserve SBLOCA phenomena and cannot be geometrically scaled.
	Elevations of the upper plenum (the region above the RVVV's).	None: Phenomena in this region are controlled by voiding rather than elevation head.	Scaling: Elevations in the upper nonflow regions are modified to obtain plenum power-to-volume scaling.
	Core Heater Power Leads	Unknown: Thought to be minor, atypical core inlet flow geometry, atypical pressure drop.	Contract: Ability to upgrade to 100% core power capability required.
	Heater Time Constant and Stored Energy	None: Transferred and generated power are approximately equal throughout SBLOCA starting from 10% of full power.	Heater design limitations.
Hot Leg and Hot Leg U-Bend	Two-Phase Flow Regime and Void Fraction	(1) Separation, none: HLUB phase separation is expected to occur early in the SBLOCA transient, in both the plant and the model.	Avoid small-pipe flow behavior in which bubbly flow is precluded and preserve irrecoverable pressure drop.

Table 1.3 (Continued)

LOOP COMPROMISES AND IMPACTS

Component	Compromise	Impact	Reason for Compromise
Hot Leg and Hot Leg U-Bend (Continued)	Two-Phase Flow Regime and Void Fraction	(2) Inventory and timing of circulation interruption, in consequential: Although timing is affected, the predicted post-SBLOCA events (circulation interruption, re-pressurization, etc.) are expected to occur in the model.	
	Volume (excess volume 3 times scaled value)	Same as Two-Phase Flow Regime and Void Fraction	Same as Two-Phase Flow Regime and Void Fraction
Steam Generator	Bounding Elevations of Inlet and Outlet Plenums	Minor: Elevation retained by extending hot leg and cold leg suction.	Geometry: Model SG plenum-to-pipe transitions are of reduced length using conventional reducers.
	Metal Mass	Intermediate: Dampens fluid thermal transients, especially primary re-pressurization.	ASME/ANSI Design Codes
	AFW Multi-Dimensional Effects	Unknown: The anticipated influence of AFW bracketed by use of minimum/maximum wetting.	Geometry: The small scale of the 19-tube steam generator precludes prototypical AFW wetting effects.
Cold Leg	Volume	Same as for hot leg volume.	Same as for hot leg volume.
	Slope of Cold Leg Discharge Line (~2 times plant angle)	Minor: Since the hydraulic jump, which impacts mixing and condensation, is expected to occur in the plant and model.	Geometry: Physical constraints.
Pumps	(1) Net Positive Suction Head Requirements (2) Two-Phase Degraded Performance	Intermediate: The extremes of develop head (i.e., single-phase water and steam) are prototypical; however, degraded two-phase performance will be atypical. Also, the plant pump is expected to cavitate whereas the model pump will not under certain conditions.	(1) Geometry: The small scale precludes simulation of NPSH in conjunction with head-flow. (2) Geometry: Specific speed sacrificed to maintain leak and energy requirements.

Table 1.3 (Continued)

LOOP COMPROMISES AND IMPACTS

Component	Compromise	Impact	Reason for Compromise
Downcomer	(1) Volume above top of core (2) Local flow and density variations (stemming from cold leg to downcomer mixing, RVVV effluent - downcomer interactions, etc.) (3) Tangential pressure difference. (4) External downcomer.	Unknown: Separate effects test to be performed to obtain some measure of impact.	The several downcomer compromises are selected to obtain a measure of downcomer fluid conditions and hydraulics segregation and thus to challenge system codes.
RVVV	(1) Partial opening (at intermediate differential pressures) (2) Slow response (3) Four RVVV design	Probably Minor: In single-phase circulation, 1 valve may actuate causing model valve driven asymmetric performance. The on/off operation of the model valves may accentuate this tendency.	Partial opening characteristics were sacrificed for leak tightness (stem and seat), known control characteristics and known position for flow determination.
	Valve Simulation Piping Volume and Transient Time	Minor: Model valve located next to downcomer, piping guard-heated.	Scaling: External annular downcomer requires cross-connect piping.
Pressurizer	Length reduced from full elevation to preserve volume.	Small: Elevations are large enough to allow equilibrium between spray and steam.	Diameter was increased to allow internal circulation, prevent spray from hitting walls, reduce surface area to volume misscaling, etc. Had to decrease length to preserve volume scaling.
System	Volume	Event timing impacted, decreased hot leg void fraction. Impact inconsequential to code verification because key events are expected to occur.	Piping: Large pipe/small pipe two-phase flow criteria, irrecoverable pressure drop. Upper Downcomer: Annulus required to segregate quadrant fluid, gap required to preclude atypical wall effects.
	Wall Effects	Increases fluid-to-wall heat transfer.	Small-scale full-pressure model.

Table 1.4

POTENTIAL USE OF MIST TO ADDRESS THE MIST ATYPICALITIES

MIST ATYPICALITIES	Was MIST assigned to address this atypicality?		Can MIST address this atypicality?				Can the MIST information be applied directly to the plant modeling effort?		
	Yes	No	Yes	Limited	Mod'n Req'd	No	Yes	Limited	Limited & Mod'n Req'd
1. Hot Leg Separation		X	X					X	
2. S.G. Metal Mass	X			X				X	
3. AFW Multi-Dimensional	X		X					X	
4. RCP Two Phase Characteristics		X		X				X	
5. Downcomer Flow & Density Field	X			X				X	
6. Downcomer Tangential Resistance		X			X				X
7. RVVV Simulation		X		X				X	
8. Piping Metal Mass		X		X				X	
9. Low Pressure Injection	X		X					X	
10. Secondary Side	X				X				X
11. One Phase, Two Temperature Stratified Flow		X			X				X
12. Hot Leg Flow Regime		X	X					X	

MIST can also be used to address two other of its atypicalities without modification – Hot Leg Separation and Hot Leg Flow Regime. MIST testing to address MIST atypicalities is generally of limited use regarding the direct application of this information to the code modeling effort. MIST testing is of similar benefit and applicability for all of the issues affected by each atypicality.

1.4 TEST PROCEDURES

1.4.1 General Approach and Techniques

MIST test procedures were keyed to test types, which include: Debug, Characterization, Mapping, and Transient. "Debug" tests were used to verify system and component operability.

MIST Characterization tests were performed to determine the behavior and impact of key subsystems. For example, RVVV/Downcomer interactions were tested, as were the steam generator secondary control functions. Test conditions were selected to highlight the interaction or subsystem being examined, rather than for plant-transient typicality. Loop conditions thus range widely, from subcooled at atmospheric pressure to saturated at 2350 psia (the MIST PORV setpoint). Formal test specifications and procedures were developed for each of the Characterization tests. Data taking employs the full set of instruments and both the high-speed and low-speed data acquisition systems, as well as supplementary data recording techniques (strip charts and video tapes). The data scan frequency was keyed to the rapidity and duration of the interactions being characterized.

MIST Mapping Tests (Test Group 30) examined the events which occur early in the post-SBLOCA sequence, namely saturation, two-phase circulation, intermittent circulation, flow interruption, and the boiler-condenser mode (BCM). Rather than being transient tests, pseudo-steady states were obtained by holding the system boundary conditions constant throughout each test; system total liquid inventory is alternately decreased gradually and held constant. The full set of instruments and recording techniques were used.

The MIST Transient Tests are integral system transients, from 1-1/2 minutes beyond reactor trip through post-refill cooldown.

Tests were conducted both parametrically (with limited simulation of operator actions, to enhance the understanding, comparison, and prediction of these tests) and with the more significant operator actions simulated. The loop was generally to be initialized in subcooled natural circulation at 3.5% of scaled full power plus 0.4% losses to ambient. The initial steam generator secondary control pressure was held constant at 1010 psia — this sets the secondary saturation temperature (and reactor coolant temperature at the steam generator outlet, T_{cold}) at 545°F, and thus determines reactor outlet temperature, T_{hot} (at approximately 590° to 600°F depending on the SG thermal center elevation). A test was initiated by opening the specified leak and then actuating the appropriate boundary systems (power decay ramp, HPI, and increased auxiliary feedwater) as the pressurizer drains. This sequence obtains plant-similar conditions as the upper-elevation hot leg fluid saturates. System

thermodynamic conditions thus range from multiphase (subcooled, saturated, and superheated) fluid at high pressures to predominantly subcooled at ~200 psia. The full set of instruments were utilized. Recording methods included the low-speed and high-speed data acquisition systems, strip charts recordings of selected signals, and video tapes of the viewport displays.

1.5 APPLICATION OF DATA (to Resolve the Issues or to Address the Atypicalities)

The application of MIST to the MIST atypicalities (and effected issues) is summarized in Table 1.4. Atypicalities are taken up individually in the following subsections. The description of each atypicality is generally excerpted from Part I of the MIST Facility Specification[1].

1.5.1 MIST Atypicality 1: Hot Leg Separation

Background. Separation will occur when the hot leg liquid inventory is insufficient to support the co-current flow of two phase, i.e., when a liquid-vapor interface develops in the hot leg.

The leak fluid inventory loss rate was used to estimate the rate of change of hot leg void fraction with fluid inventory. These were combined with an assumed draining time, to provide an estimate of hot leg void fraction due to imposed liquid deficiency. The intersections of the drift-flux model void fractions with those imposed by draining indicated a time at which hot leg phase separation occurs. Also, the time (after trip and the start of draining) at which the drift-flux based void fraction decreases below 25% signals the transition from slug to bubbly flow. These transition times (for the various assumed conditions, including maximum vapor superficial velocity) ranged from 3 minutes to almost 9 minutes after trip.

Reactor vessel vent valve (RVVV) operation impacts these estimates. With increasing RVVV vapor flowrate, the drift-flux model void fractions versus time decrease more rapidly. Bend-induced separation also has an impact. The hot leg U-bend volume above the spillover elevation is a small portion of the total hot leg volume, e.g., ~8% in the plant and ~5% in the model (using a 1.6-foot bend radius).

Phase separation at the U-bend occurs at roughly 10% power, or less than one minute after reactor trip. Based on the relatively small volume of the upper U-bend, and the propensity of the bend to cause phase separation, it is expected that the draining of a relatively small amount of primary fluid will lead to the interruption of circulation of the plant and model hot leg U-bend.

Testing. MIST Test Group 30, Mapping Tests, examined the interactions which occur early in the SBLOCA transient, including phase separation. Conditions were selected to highlight these interactions and to investigate their response to the major boundary conditions, e.g., core power level, magnitude of HPI-leak cooling, RVVV performance, etc. These conditions were held constant throughout a mapping test, only primary system total liquid inventory was varied during testing. Inventory was reduced in steps by imbalancing the leak and HPI flow rates; it was then held constant at inventory plateaus to observe system interactions at pseudo-steady state. This testing approach facilitated the code benchmarking of these results. The inter-test conditions variations identifies those conditions having the greatest impact, and the range of conditions over which the system performance changes were most pronounced. Code predictions at conditions of most interest are thereby facilitated.

Application. The Mapping Tests were directed to the generation of pseudo-steady state data during events which occurred early in the post-SBLOCA sequence. Conditions were varied among the tests to obtain the sensitivity of events to major variations of boundary conditions. These results can be used to compare observations to the code predictions of the early events (including hot leg separation). These comparisons, combined with the information from the separate-effects facilities, will enhance the ability of the codes to predict these early events in the plant.

1.5.2 MIST Atypicality #2: SG Metal Mass

Atypicality. Steam generator wall effects include heat losses to ambient (primary to secondary to ambient) and energy storage in the steam generator metal. Losses to ambient are countered by active guard heating of the entire steam generator; these guard heaters act to maintain adiabaticity at the steam generator outer metal surface.

The model steam generator used prototypical tubes, tube support plates, and tube sheet material and geometry, thus eliminating internal metal-effects atypicalities. The steam generator shell is overly thick in the scaled model; similarly the ratio of peripheral cells to unit (internal) cells is too large, this increased coupling of steam generator fluid to the shell through heat transfer exacerbates the impact of excess shell metal in the model. The excess MIST steam generator metal mass increases the ratio of stored energy to fluid energy, tending to dampen oscillatory events and increase the amount of energy removal required for cooldown.

Testing. Supplementary MIST tests addressed the impact of steam generator metal on system interactions or cooldown. The steam generator guard heater controls could be adjusted to vary the amount of energy stored in the metal. MIST testing did include a guard-heaters-off test (310302). Assuming that the energy stored in the larger steam generator metal mass is more responsive to metal conduction than to surface convection, variations of the metal stored energy may largely be constrained to increases from nominal. The transient events perceived to be most affected by metal stored energy effects would then be repeated with the altered metal energy content. The single metal thermocouple per steam generator tubesheet could be augmented to better-indicate the metal stored energy.

Application. The sensitivity of system response to metal stored energy could readily be compared to the code-predicted response. The required modeling detail would be determined. This code modeling information would be directly applicable to the plant modeling effort.

1.5.3 MIST Atypicality #3: AFW Multi-Dimensionality

Atypicality. Auxiliary feedwater (AFW) effects refer primarily to the localized peripheral feed introduction and the resulting pronounced radial and circumferential heat transfer differences. Because three-dimensional effects do not admit to geometric scaling, atypical AFW effects are likely in any scaled model. With full elevation in the steam generator, the tube bundle dimensions and hence the impedance to horizontal (steam) flow between heat transfer regions on the secondary side of the steam generator are reduced.

(Bracketing methods of feed introduction – maximum wetting and minimum wetting – were provided in MIST.)

The relatively few tubes in the model steam generator bring into close proximity the tube regions wetted upon AFW introduction and those which are unwetted. The impact of this dimensional atypicality can be addressed by using extremes of AFW wetting; the introduction of AFW through one relatively large nozzle wets only one or a few SG tubes; at the other extreme, AFW injection using three dispersion nozzles wets virtually all the tubes (at the same AFW flowrate at which only a few tubes are wetted using the minimum-wetting configuration). Tests using the extremes of tube wetting provided insight into tube wetting effects. They do not achieve plant similarity in this regard, at either extreme of tube wetting.

Testing. Selected transients or portions of transients were repeated using the maximum AFW wetting configuration rather than minimum wetting (Test 3111AA). Interactions due to variation of AFW wetting configuration include: natural circulation with a relatively low secondary level, boiler-condenser mode heat transfer, and the steam generator tube leak transient.

Applications. Selected events observed with minimum AFW wetting would be contrasted to the behavior with maximum wetting. The code models of AFW effects could then be revised to reflect the wetting change, and exercised through the events of interest. The code sensitivity to AFW wetting would thus be established, and may suggest model improvements. Neither (minimum nor maximum) wetting model replicates the plant AFW effects, however. The suggested code comparison at wetting extremes simply highlights the code adequacy in this area, because of the atypically shortened horizontal dimensions of the model tube bundle. Additional code work would be required to apply this AFW wetting information to plant predictions.

1.5.4 MIST Atypicality #4: Reactor Coolant Pump Two-Phase Characteristics

The MIST model pump design sacrifices two-phase performance for mass and energy closure, single-phase performance, and mechanical reliability. Model pump two-phase degradation will be prototypical only by coincidence. But

model pump degradation could be characterized by testing. This degradation data may then be used in conjunction with a systems code to predict system behavior through a degrading-pumps event. A code so benchmarked, with a plant pump degradation model substituted for that of the model pump, can then be applied to the plant with increased confidence. This utility of the model data notwithstanding, it should be reiterated that model degraded-pump behavior is unlikely to shed any light on plant pump behavior.

1.5.5 MIST Atypicality #5: Downcomer Flow and Density Fields

Atypicality. The MIST baffled quadrant downcomer preserves the plant elevations of each zone of flow-stream interaction. The model downcomer voiding and condensation typicality is hindered by excess fluid volume over the upper downcomer elevation and by excess metal associated with the RVVV piping. Both influences should be amenable to prediction, but the interactions of the four RVVVs with the voiding and condensation events may cause difficulty. The model downcomer volume is excessive above the top of the core (to obtain the annular configuration without excessive downcomer wall retardation of flow). The model downcomer volume below the top of the core is approximately power-to-volume scaled.

Local downcomer hydraulics are only coarsely modeled in the MIST baffled quadrant downcomer arrangement (although it is the best of the candidate arrangements in this regard). Axial and tangential irrecoverable pressure drops are mis-scaled, their ratio is approximated. Axial pressure drop in the inner flow loop containing the downcomer was compensated for by adding a venturi flow meter to the lower downcomer. Wall effects are atypically operative, but they can be modeled.

Testing. The MIST downcomer and RVVV performance were examined during Characterization testing. Test conditions were selected to highlight the RVVV and downcomer performance, rather than to obtain transient typicality. These Characterization tests examined vapor flow through the vent valves and also single-phase liquid circulation. Test conditions included both symmetric and asymmetric loop conditions. The RVVVs were controlled to actuate independently, ganged, and manually; tests were performed both with and without HPI and leak flow.

Downcomer (and/or RVVV) modifications could be made to accentuate a characteristic of particular interest. For example, the existing downcomer baffles could be modified to perturb the tangential hydraulic resistance. Such modifications would be relatively costly, however.

Application. The MIST RVVV/downcomer Characterization Tests provide detailed model component (steady-state) performance over a range of imposed boundary conditions. This information will facilitate the detailed code benchmarking of model RVVV/downcomer interactions. Although these MIST interactions are not transferable to the plants, the code modeling information and the prediction techniques required to adequately represent MIST will apply to the plant modeling effort.

1.5.6 MIST Atypicality #6: Downcomer Tangential Resistance

This atypicality has been included in the preceding discussion of downcomer flow and density fields (Atypicality #5).

1.5.7 MIST Atypicality #7: Reactor Vessel Vent Valve Simulation

Atypicality. The resistance of the model reactor vessel vent valve (RVVV) arrangement is composed of frictional and form losses, versus form losses in the plant. The model RVVV imposes most of the plant RVVV resistance at the slit-orifice located adjacent to the discharge into the downcomer. To accomplish this, the RVVV piping is oversized and the valve resistance is minimized. The orifice was sized to obtain the remaining resistance. The model RVVV resistance has been increased to enhance its stability with vapor flow.

The model RVVV opens at a differential pressure of 0.125 psi. The simulated valve obtains full open head-flow response between 0.125 and 0.26 psi, but the plant RVVV head-flow response varies over this range. For differential pressures greater than 0.26 psi, the model obtains power-scaled flow rates for plant-similar fluid conditions, except for its increased hydraulic resistance.

The two-phase behavior differs between the MIST RVVV and that of the prototype. The RVVV should experience two-phase conditions only when the reactor vessel liquid level approaches the elevation of the RVVV. The plant valve inlet height is roughly five times that of the model. Also, the plant RVVV velocities are greater than those in MIST, tending to increase the effective vertical dimension of the plant RVVV via vapor pull-through and liquid entrainment; the model RVVV is thus less likely to entrain than that of the plant.

The four-RVVV design chosen for MIST obtains the quickest response for the valve stroke time of the various design options. There is a time delay associated with the flow of the fluid through the piping, however. For continuous RVVV flow, the transit time should not have any effect. Fluid transit delay time does impact RVVV effects at valve actuation. In order to minimize this impact, the guard heaters surrounding the model RVVV piping lengths are controlled to approximately maintain the RVVV fluid at the reactor vessel upper head conditions.

Testing and Application. Two MIST tests vary RVVV control. The valves were maintained closed in one test and (manually) open in the second test (Tests 310101 and 310201, respectively). Both tests otherwise correspond to the boundary conditions of the Nominal MIST transient. RVVV Characterization tests were also performed. These tests and their application have been discussed in Atypicality #5 (Downcomer Flow and Density Fields).

1.5.8 MIST Atypicality #8: Piping Metal Mass

Atypicality. Model wall effects are amplified by the atypically large ratio of wall heat transfer surface area to contained fluid volume. Therefore, model heat losses and metal mass are closely controlled. Heat losses are minimized by using full-system active guard heating. Metal mass is minimized by avoiding flanges and conducting supports, and by using minimum pipe wall thickness consistent with code requirements. The resulting ratio of metal volume to fluid volume in the model is roughly 35% greater than that in the plant. This excess model metal dampens system pressure changes, but these metals effects can be modeled and predicted.

OTIS results[6] have indicated that piping metal has little impact during the depressurization and draining phases of the post-SBLOCA transient. But the (upper-elevation) metal stored heat (and the superheating of the adjacent vapor) govern the repressurization upon refill and thus become significant relatively late in the transient. The wall conditions at this time depend on the detailed fluid-wall-ambient energy balance over the several hours preceding refill.

Testing and Application. A MIST test (310302) with the guard heaters off was performed. Additional tests could be conducted with altered guard heating. Such tests would serve to better-quantify the role of piping metal stored energy in the refill and post-refill events. This test information would indicate the necessity for the code modeling of detailed system piping heat transfer, and would thus be directly applicable to the plant modeling and prediction effort.

1.5.9 MIST Atypicality #9: Low Pressure Injection

MIST Phase 3 tests were performed without a low pressure injection (LPI) system simulation. LPI system actuation is most prevalent at the low pressures achieved with larger (small) breaks. LPI system operation also affects operator actions during cooldown. A low pressure injection system was added for Phase 4 testing, and tests were performed to evaluate the system's influence on SBLOCA events. These tests are described in Section 7.

1.5.10 MIST Atypicality #10: Secondary Side

The MIST secondary side characteristics limit the rate of secondary side depressurization and thus the ability of MIST to simulate a steam-line-break transient. The MIST secondary system could be modified to increase its maximum depressurization rate; for example, a large feed reservoir could be added such that the model secondary system could be depressurized by discharging to atmosphere. However, MIST is currently limited to 10% of scaled full power; the earlier portion of the steam line break transient cannot be simulated. A combined tube rupture and (limited) steam line break transient was performed.

1.5.11 MIST Atypicality #11: Stratified Single-Phase Flow

Atypicality. The MIST pipe diameters are reduced from those of the plant in order to maintain approximate power-to-volume scaling while preserving the plant elevations. In vertical piping runs, the reduced MIST pipe diameters suppress liquid-liquid counterflow; the degree and duration of fluid stratification is thus atypically increased.

The shortened MIST horizontal piping runs combined with the reduced pipe diameters tend to suppress horizontal liquid-liquid counterflow as well. This phenomenon is perceived to be most significant in the cold leg discharge piping. The OTIS results[6] indicate that such counterflow (or an equally-effective mixing process) did commonly occur in the single, small-diameter cold leg piping of OTIS.

Testing and Application. MIST cannot be used to study counterflow variations without piping modifications between tests. MIST does have an alternate leak site at the top of the (B1) cold leg discharge pipe. (This alternate leak site would have to be equipped with the requisite leak flow control and metering systems.) Tests using this pipe-top leak could be compared to tests with the customary pipe- bottom leak site. Stratification, counterflow, and mixing will alter the leak fluid conditions, and system mass balance, between these tests. Such information could be used to exercise the relevant code models (or to indicate the need for code capabilities in single-phase counterflow). This information could be applied to plant modeling via suitable separate-effects test having large pipe diameters.

1.5.12 MIST Atypicality #12: Hot Leg Flow Regime

The discussion of Hot Leg Separation (Atypicality #1) also pertains to this Hot Leg Flow Regime atypicality.

Section 2

REACTOR COOLANT SYSTEM

The multi-loop integral system test (MIST) facility is an integral 2 x 4 (two hot legs and steam generators; four cold legs and reactor coolant pumps) test loop consisting of several independent subsystems as illustrated in Figure 2.1. The major facility subsystems are the reactor coolant system, the emergency core coolant system, the secondary (feedwater and steam) system, single-phase leak system, two-phase vent/leak system, the gas addition system, and the water supply and cleanup system. The reactor coolant system is discussed in this section. The remainder of the facility subsystems are described in Section 3.

In the description of each component or subsystem, a brief summary of the instrumentation in the component is provided. For a detailed description of the instrumentation, instrument designations, precise locations, and explanation of the instrument placement, the reader is directed to Reference 5.

2.1 REACTOR COOLANT SYSTEM ARRANGEMENT

The MIST facility reactor coolant system consists of a reactor vessel, downcomer, four reactor vessel vent valves (RVVV), two hot legs, two 19-tube once-through steam generators, four cold legs, and four reactor coolant pumps. The overall arrangement of the reactor coolant system and a comparison of the MIST elevations, volumes, and metal mass to the corresponding ideally scaled loop parameters is presented here.

Figure 2.2 illustrates the overall arrangement of the MIST reactor coolant system and identifies the diameters and schedules of the pipe sections and components. The reactor coolant system is approximately 75 feet tall and 11 feet across (including the pressurizer). As indicated in Figure 2.3, the

downcomer is external to the reactor vessel and centrally located in the MIST configuration. The four cold legs, two from each loop, enter the downcomer around its circumference at 90° spacings. One reactor coolant pump is located in each cold leg at the highest cold leg elevation, thus defining the spillover point in the cold leg. The two 19-tube once-through steam generators are full-length sub-sections of their plant counterparts and are located to preserve similarity in flow path and length for each loop. The two hot leg takeoffs from the reactor vessel are positioned circumferentially to maintain equal flow lengths. The horizontal length of the hot leg takeoffs is as short as possible to minimize the volume atypicality. The pipe length from the reactor vessel nozzle to the hot leg U-bend is approximately 45 feet. A pipe section extends from the downstream side of the hot leg U-bend to the upper tubesheet of each steam generator to maintain the prototypical elevation of the steam generator primary inlet.

2.1.1 Elevations

A comparison of plant and loop elevations is provided in Table 2.1. The plant and MIST elevations are referenced to the secondary face of the steam generator lower tubesheets. The MIST steam generators are full length from tubesheet to tubesheet (secondary faces); therefore, the plant elevations over the secondary heat transfer surface are preserved. The MIST core is also full-length thus preserving the plant elevations over the primary heat transfer surface.

The MIST piping generally matches the plant spillover and spillunder elevations. The MIST hot leg U-bend and the plant hot leg U-bend elevations are the same at the bottom inside surface of the pipe. The elevation of the bottom of the MIST reactor vessel vent valve matches the bottom elevation of the plant vent valve. The plant and model reactor coolant pump spillover elevations agree as do the cold leg spillovers and the suction pipe horizontal run at the outlet of the steam generator. The MIST surge line low elevation matches the top inside of the plant surge line at its low point. In addition, the elevations of the MIST cold leg nozzle, hot leg nozzle and surge line to hot leg connection correspond to the centerline elevations of their plant counterparts.

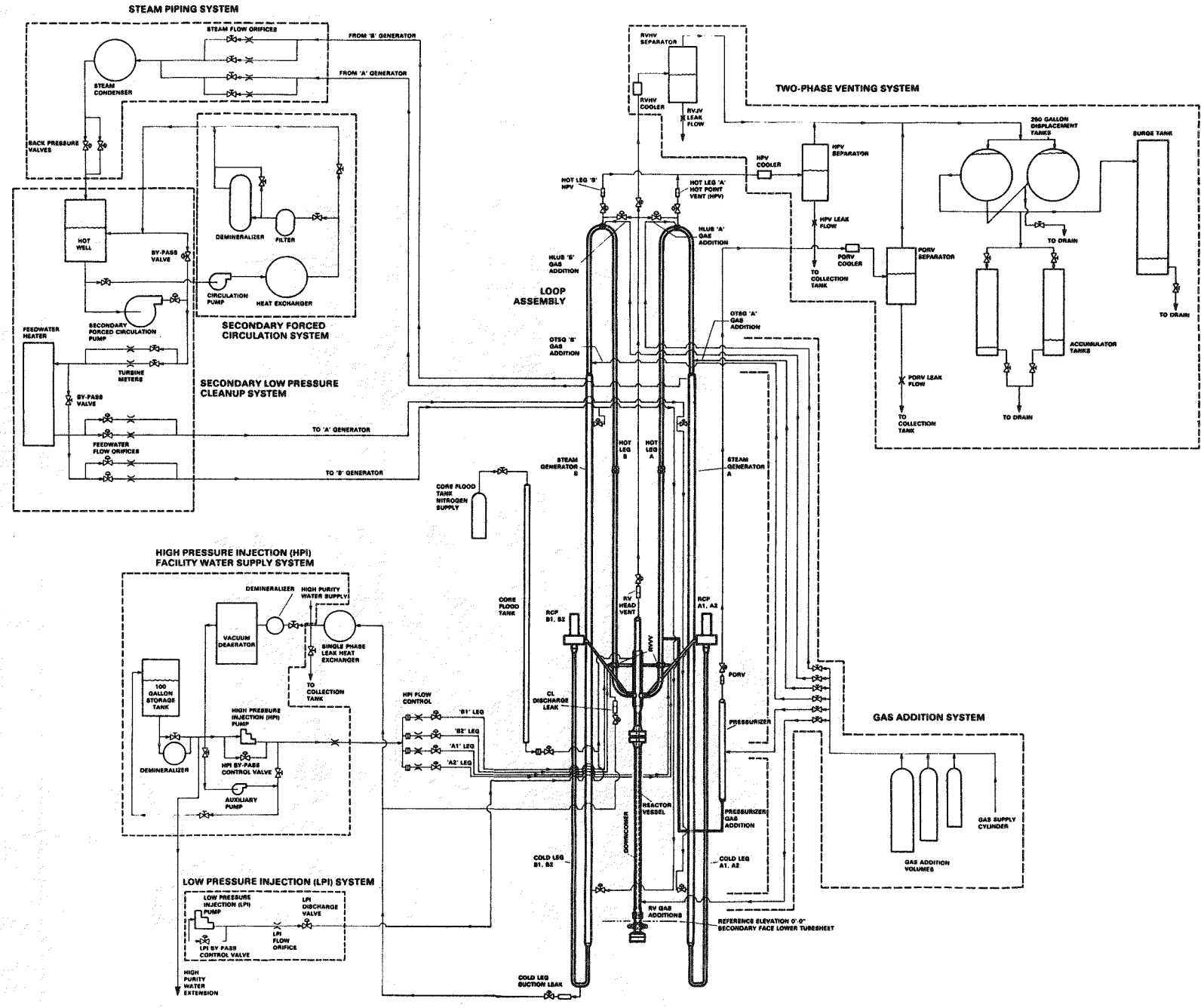

Figure 2.1 Overall Loop Arrangement Showing Major Subsystems

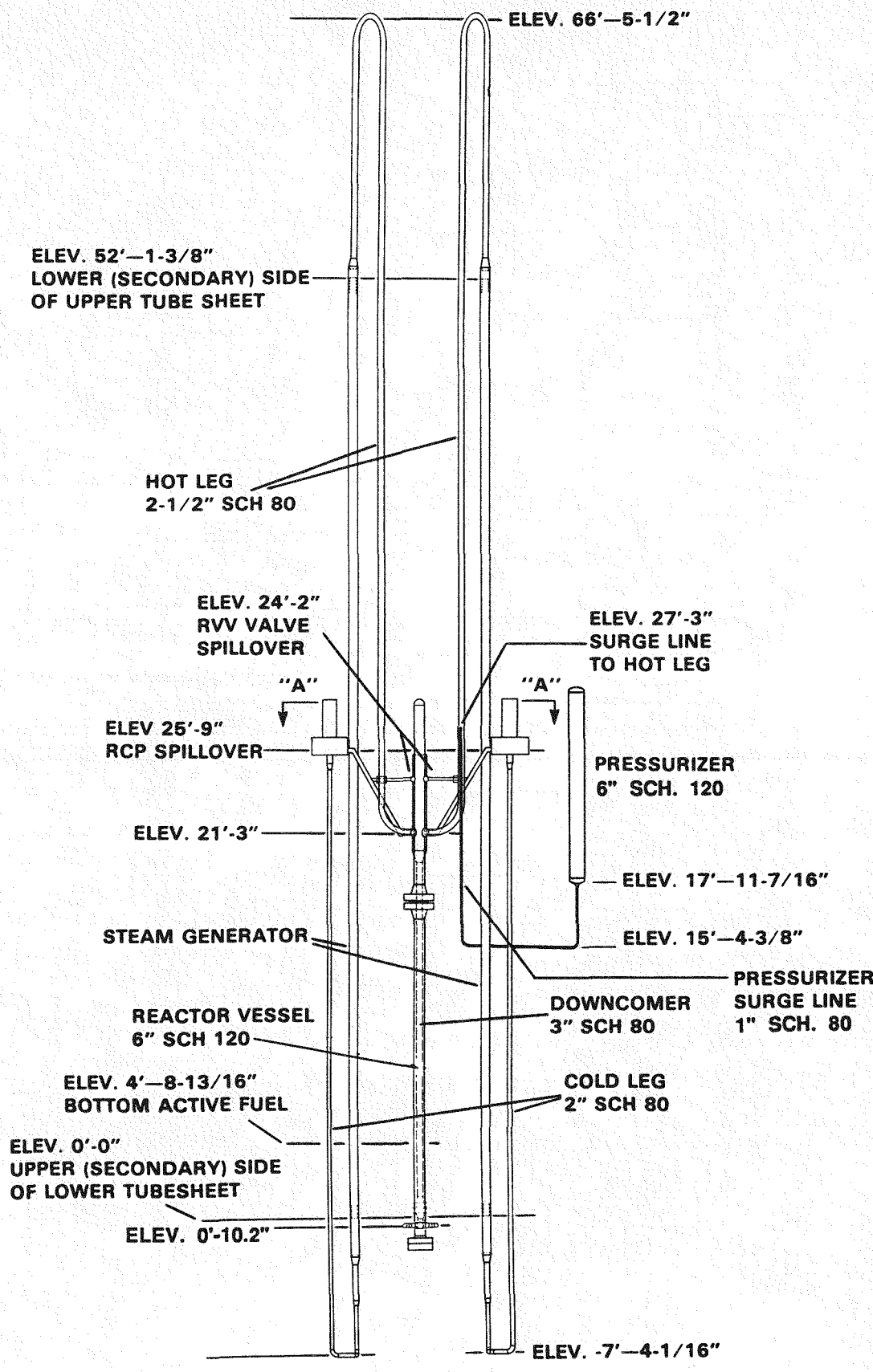

Figure 2.2 Reactor Coolant System Arrangement

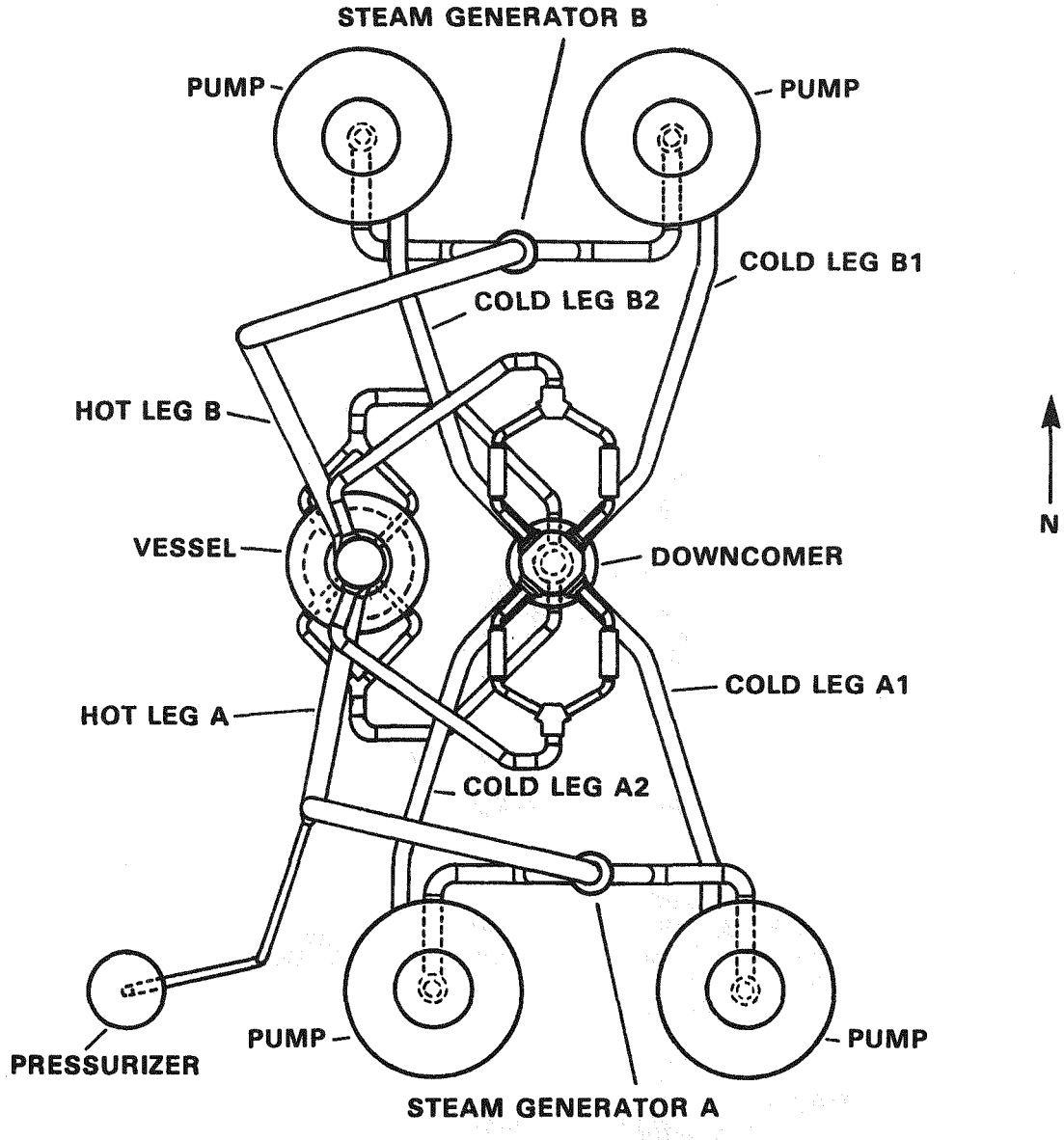

Figure 2.3 Reactor Coolant System Layout

Table 2.1

PLANT AND MIST ELEVATIONS

Component	Item	Plant Ft (Relative to Datum)*	MIST** Ft (Relative to Datum)
Steam Generator	Inlet Nozzle-Upper Plenum Interface	61.46	52.91
	Upper Tube Sheet		
	-Upper face	54.11	53.38
	-Lower face	52.11	52.12
	Auxiliary Feedwater Nozzle	49.20	50.87
	Lower Tubesheet		
	-Upper face	0.00	0.00
	-Lower face	-2.00	-2.00
	Outlet		
	-Outlet Nozzle-Lower Plenum Interface	---	2.54
	-Lower Plenum-Cold Leg Interface	-6.77	-6.35
	- Outlet Plenum Bottom	-6.94	---
Cold Leg	Horizontal Run Steam Generator to Reactor Coolant Pump Top of Pipe	-7.34	-7.34
	Cold Leg to Reactor Coolant Pump Interface	22.08	25.56
	Reactor Coolant Pump Spillover	25.75	25.75
	Discharge		
	-Bottom of Discharge Pipe	23.58	25.75
	-HPI Injection Nozzle, Centerline	23.02	23.58
	-Cold Leg to Reactor Vessel Nozzle, Centerline	21.25	21.25
	-Pressurizer Spray Nozzle, Centerline	24.75	25.83
Pressurizer	Surge Line		
	-Hot Leg to Surge Line Connection	27.25	27.25
	-Low Point, Top of Pipe	15.36	15.36
	Surge Line-Pressurizer Nozzle Interface	16.25	---
	Bottom	17.95	17.91
	Top	59.85	29.30
	Spray	58.76	28.98

* The reference datum used for all elevations was the steam generator secondary face of the lower tubesheet.
** MIST elevations are from as-built measurements.

Table 2.1 (Continued)

PLANT AND MIST ELEVATIONS

Component	Item	Plant Ft (Relative to Datum)*	MIST** Ft (Relative to Datum)
Pressurizer (continued)	PORV and Safety		
	-Valves (inside shell)	59.57	29.30
	-Bottom Heater Centerline	23.06	18.61
	-Top Heater Centerline	26.56	19.78
Reactor Vessel (RV)	Downcomer		
	-Top	27.08	24.37
	-Vent Valve Spillover	24.17	24.17
	-Vent Valve Centerline	24.75	24.21
	-Core Flood Nozzle, Centerline	23.25	23.25
	-Elevation of Lowest Flow Hole	0.85	0.85
	Core		
	-Lower Grid, Top	4.19	---
	-Lower Grid, Bottom	1.52	---
	-Bottom of Active Fuel	4.74	4.73
	-Fuel, Midplane	10.74	10.73
	-Top of Active Fuel	16.74	16.73
	-Upper Grid, Top	18.62	---
	-Upper Grid, Bottom	17.58	---
	Outlet		
	-Upper Plenum, Top Bottom Face of Plenum Cover	28.19	25.27
	-Outlet Nozzle Centerline	21.25	21.25
	-Plenum Cylinder Large Hole, (R = 16-3/4"), Centerline	25.35	24.30
	-Plenum Cylinder Large Hole, (R = 11-3/4"), Centerline	25.85	24.99
	-Plenum Cylinder Small Hole, (R = 3"), Middle Hole Centerline	21.25	21.25
	-Plenum Cylinder Small-Hole, (R = 3"), Top Hole Centerline	22.58	21.25
	-Top Inside of Reactor Vessel	33.98	29.39
Hot Leg (HL)	Upturn to Vertical	26.25	22.86
	Hot Leg U-Bend		
	-Start and End	62.96	64.95
	-Spillover	66.46	66.46
	Hot Leg to Steam Generator Nozzle Interface	61.46	52.91
	Hot Leg to Reactor Vessel Nozzle Centerline	21.25	21.25

* The reference datum used for all elevations was the steam generator secondary face of the lower tubesheet.

** MIST elevations are from as-built measurements.

Several MIST elevations are atypical. The model steam generators are full-length between the tubesheets, but the upper tubesheet thickness and the inlet and outlet plenums are much shorter than the corresponding plant components. Therefore, the hot leg-to-steam generator inlet and steam generator outlet-to-cold leg elevations are not plant typical. Additional piping in these locations is required to maintain key plant elevations; in particular, the hot leg U-bend spillover and cold leg spillunder points.

Thermal expansion at operating conditions can increase the overall height by several inches. Support locations for the loop were chosen to minimize thermal expansion induced piping stresses. The location of the loop's rigid supports are shown in Figure 2.4. The steam generator and reactor vessel are rigidly mounted on thermally insulated supports to minimize heat loss to ambient. The hot legs are supported by the connections to the reactor vessel and steam generator, and are laterally supported with guide supports at the elevation shown in the figure. The pumps are supported by mountings that fix the vertical position of the pumps, but permit lateral movement to accomodate thermal expansion. The cold legs are welded to the pump inlet and outlet connections, which provide vertical support for the cold leg suction and discharge piping. Additional lateral support for the cold leg piping is provided by guide supports located at the points indicated in Figure 2.4.

2.1.2 Volumes

Primary component fluid volumes are given in Table 2.2 for both the ideally scaled 177-FA plant and MIST. The ideally scaled plant component volumes are scaled by 1/817.42 from the 177-FA plant values, as fixed by the number of tubes in the MIST steam generators and the power scale of the MIST core simulation. These volumes are computed for the loop (plant and MIST) at ambient temperature. The volumes are presented for each primary component of the reactor coolant system.

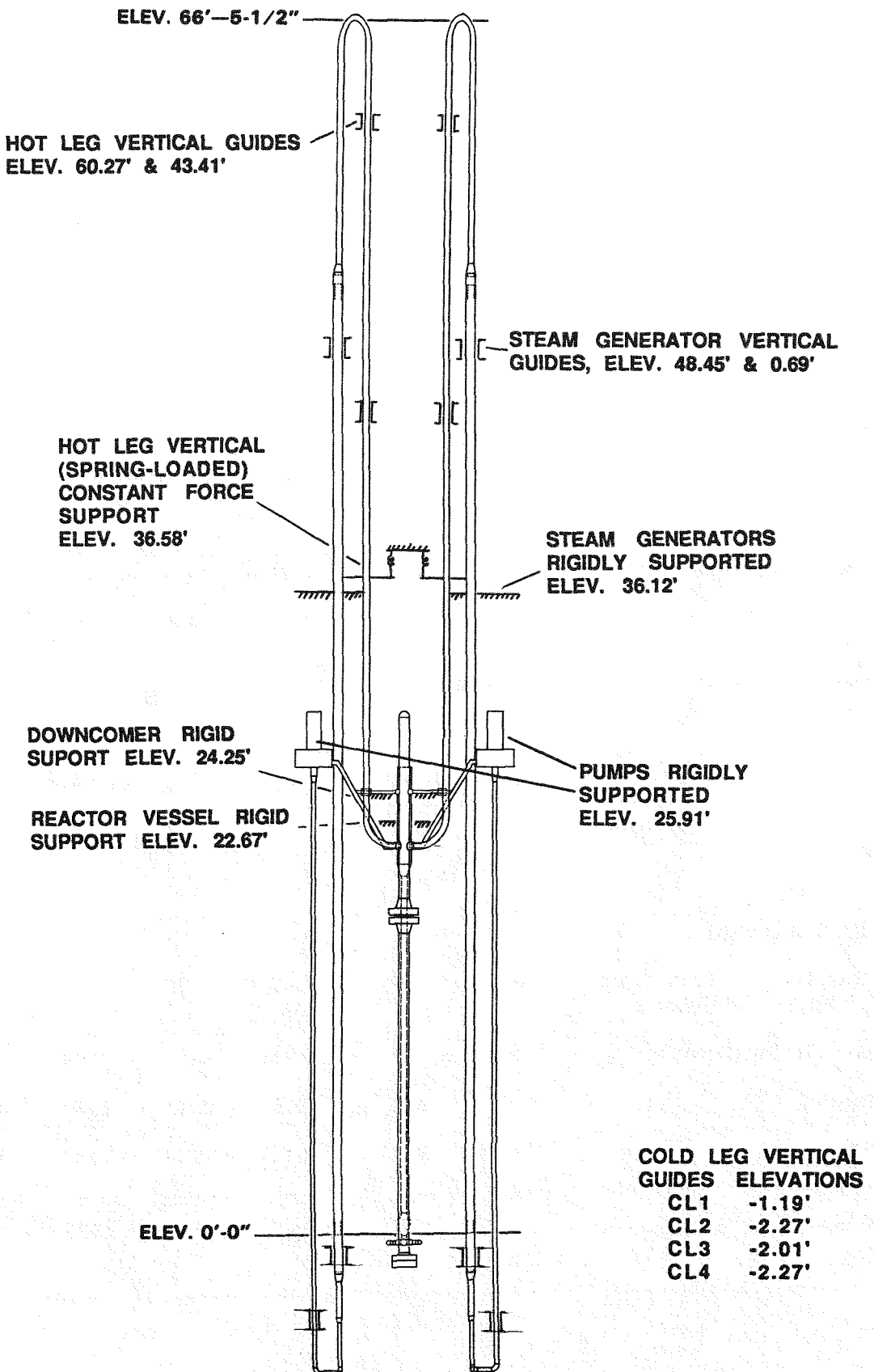

Figure 2.4 Support Locations for the Reactor Coolant System

Table 2.2

FLUID AND METAL VOLUMES FOR MIST AND THE IDEALLY SCALED PLANT[1]

Component	Ideally Scaled Plant			MIST		
Reactor Vessel	Fluid (in^3)	Metal (in^3)	Metal Fluid (-)	Fluid (in^3)	Metal (in^3)	Metal Fluid (-)
1. Upper Downcomer - Above the centerline of the cold leg nozzle.	541	652	1.21	859[2]	1629[2]	2.00
2. Lower Downcomer - From center of cold leg nozzle to lowest hole of flow distributor[3]	1580	1907	1.21	2776	2145	0.77
3. Lower Plenum - From bottom of Reactor Vessel to bottom of active fuel	1316	587	0.45	655	3220[4]	4.92
4. Core - Active fuel region	1640	461	0.28	1298	2181	1.68
5. Upper Plenum - From top of active fuel to the plenum cover[5]	2313	862	0.37	2385	1931	0.81
6. Top Plenum - From plenum cover to top of Reactor Vessel	1171	695	0.59	1143	664	0.58
Totals	8561	5164	0.60	9116	11,770	1.29
Hot Leg (1 only)						
1. Horizontal Section - From Reactor Vessel Nozzle to 90° Upbend	83	37	0.45	20	11	0.55
2. Upbend - The 90° Elbow	117	53	0.45	129	69	0.53
3. Vertical Pipe[6]	526	238	0.45	2141	1149	0.68
4. U-Bend[7]	280	126	0.45	257	137	0.53
Totals	1006	455	0.45	2547	1366	0.54

Table 2.2 (Continued)

FLUID AND METAL VOLUMES FOR MIST AND THE IDEALLY SCALED PLANT[1]

Component	Ideally Scaled Plant			MIST		
	Fluid (in^3)	Metal (in^3)	Metal/Fluid (-)	Fluid (in^3)	Metal (in^3)	Metal/Fluid (-)
Pressurizer						
1. Surge Line - From surge line nozzle at Hot Leg to pressurizer nozzle interface	84	43	0.51	59	122	2.07
2. Pressurizer Vessel - Total volume of pressurizer	3213	906	0.28	3201	1579	0.49
3. Spray Line - From spray line nozzle to cold leg nozzle	3.1	2.6	0.84	5.0	7.0	1.4
Totals	3300	951	0.29	3265	1708	0.52
Steam Generator (1 only)						
1. Upper Plenum - Includes inlet nozzle and upper tubesheet	583	575	0.99	612[8]	424	0.69
2. Tubes	3104	367	0.12	2959	857	0.29
3. Lower Plenum - Includes lower tubesheet and plenum half sphere	535	415	0.78	31[9]	456[10]	14.7
Totals	4223	1357	0.32	3602	1737	0.48
Cold Leg (1 only)						
1. Suction Piping - Includes Steam Generator nozzle and piping to Reactor Coolant Pump interface	362	155	0.43	1488[11]	707	0.48
2. Reactor Coolant Pump	207[12]	49,800lbs[12]	-	207	3054[13]	14.7
3. Discharge Piping - Includes piping from Reactor Coolant Pump to Reactor Vessel downcomer	197	41	0.21	259	129	0.50
Totals	559	196	0.35	1954	836	0.43

Table 2.2 (Continued)

FLUID AND METAL VOLUMES FOR MIST AND THE IDEALLY SCALED PLANT[1]

Totals	Ideally Scaled Plant		MIST	
	Fluid (in^3)	Metal (in^3)	Fluid (in^3)	Metal (in^3)
1. Reactor Vessel	8561	5164	9116	11553
2. Hot Legs (2)	2012	910	5094	2732
3. Pressurizer	3300	951	3265	1708
4. Steam Generators (2)	8446	2715	7204	3474
5. Cold Legs (4)	2235	784	7318	3344
Grand Totals	24554	10524	31997	22811

[1] Ideally scaled plant refers to power or volume scaled (1:817.4) B&W 177-FA Lowered Loop plant.

[2] Includes external reactor vessel vent valve circuit.

[3] MIST preserves the spillunder elevation or the highest hole of flow distributor.

[4] Includes large mass of Reactor Vessel heater rod seal flange.

[5] For the plant, the outlet annulus is included.

[6] For the plant, this includes section from 90° elbow to 18" below the U-bend (U-bend - SG interface elevation). For MIST, this includes vertical pipe from 90° elbow to start of U-bend.

[7] For the plant, this includes 18" of straight pipe on both ends of the U-bend.

[8] For MIST, includes vertical pipe from end of U-bend to upper tubesheet.

[9] Does not include fluid in tubes.

[10] Includes 24" thick tubesheet.

[11] Fluid volume with cold leg venturis installed. Add 45 in^3 for tests without venturis installed.

[12] Information supplied by pump manufacturer (Byron-Jackson).

[13] Includes mass of lower portion (volute casing) of pump.

The hot leg volume includes the piping from the hot leg nozzle at the reactor vessel to the inlet nozzle on the steam generator. The steam generator volume includes the inlet nozzle, the upper plenum, the tubes, and the lower plenum. In MIST, the additional piping required between the hot leg U-bend and steam generator inlet is included as part of the upper plenum. The generator outlet nozzle is included with the cold leg suction piping. In addition to the suction piping, the cold leg includes the reactor coolant pump fluid volume and the discharge piping to the downcomer. The reactor vessel volume includes the downcomer (RVVV circuit included for MIST), the lower plenum, core, and the upper and top plena. The surge line is included with the pressurizer as is the spray line.

Total loop fluid volumes are 31,997 in^3 for MIST and 24,554 in^3 for the ideally scaled 177-FA plant. Thus the total volume of the MIST reactor coolant system exceeds the ideally scaled plant value by 30%.

2.1.3 Metal Mass

Table 2.2 also provides the metal volumes for both the ideally scaled 177-FA plant and MIST at ambient temperature. The metal volumes are associated with the same components as the fluid volumes. Metal mass can be calculated from the metal volumes using the metal density. For the plant, the metal can be assumed to be carbon steel while for MIST the metal is stainless steel.

The total loop metal volumes are 22,811 in^3 for MIST and 10,524 in^3 for the ideally scaled 177-FA plant. The resulting ratio of MIST-to-plant metal volume is 2.17.

The ratio of metal volume to fluid volume is given in Table 2.2 for the primary-side components. The MIST ratios (0.68 overall) are higher than the plant ratios (0.43 overall) as would be expected for a scaled high pressure and temperature model. Metal mass in MIST was minimized where possible, while meeting the requirements of the applicable ANSI and ASME Pressure Parts Codes.

2.2 REACTOR VESSEL MODEL

The plant reactor vessel modeled by the MIST facility is shown schematically in Figure 2.5. As shown in this figure, the core is contained in a cylindrical core barrel located inside the reactor (pressure) vessel. Reactor coolant flow enters the reactor vessel from the cold legs, flows downward in the annulus between the core barrel and reactor vessel shell, turns upward to enter the core barrel through core barrel flow holes, and continues into the core. From the core, flow enters the reactor vessel's upper and top plenums, and leaves the reactor vessel to enter the RCS hot legs. The hot legs are connected to the vessel's upper plenum. The vessel's top plenum is a low flow region where the control rod drive units penetrate the reactor vessel. During abnormal operating conditions, an additional significant flow path is available to flow within the reactor vessel through flapper-type vent valves. The vent valves are located in the side wall of the core barrel and connect the vessel's upper plenum to the annular downcomer region. The valves are located a short distance above the hot leg and cold leg connections to the reactor vessel, and open when the pressure in the upper plenum exceeds the downcomer pressure enough to overcome the weight of the hinged flapper valve assembly.

The MIST facility reactor vessel models the plant reactor vessel from the spillunder point at the uppermost flow hole of the core barrel, the core region, the top and upper plenums, and connections to the hot legs and the prototype's reactor vessel internal flapper-type vent valves. A downcomer simulation is provided by a separate vessel. The separate downcomer vessel models the annular region between the prototype's core barrel and cylindrical pressure boundary, and connections to the cold legs. The model downcomer vessel is connected to the model reactor vessel at the bottom (core barrel spillunder point) and at the reactor vessel vent valve simulation. The MIST facility downcomer vessel models the prototype's annular downcomer from the cold leg connections to the reactor vessel to the spillunder point at the uppermost flow hole in the core barrel. The simulation of the annular downcomer also extends above the cold leg connections to slightly above the reactor vessel internal vent valve connection point to provide a prototypic flow path for steam flow from the upper plenum to the downcomer during periods of vent valve operation.

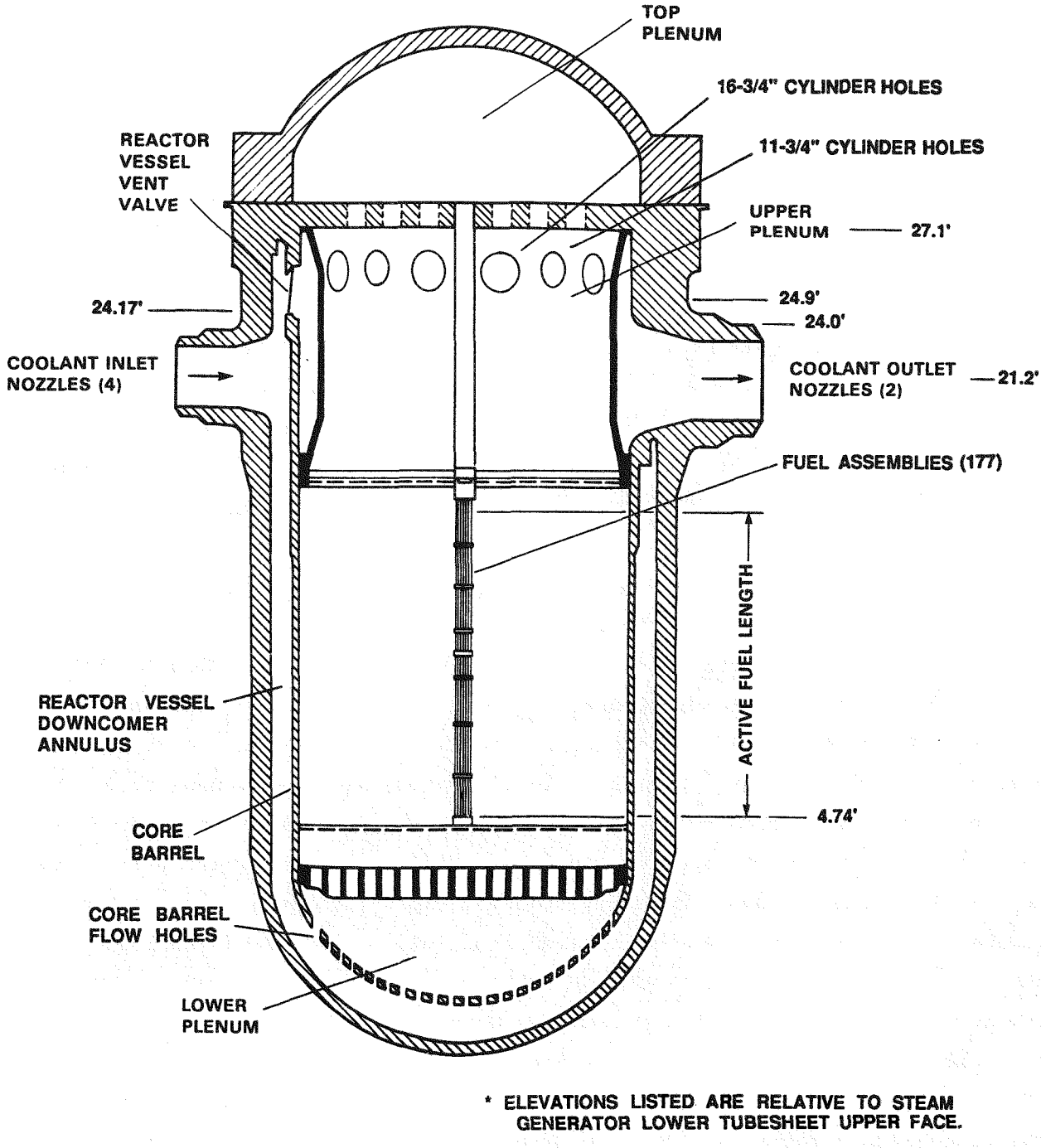

Figure 2.5 Reactor Vessel for a 177 Fuel Assembly Plant

The model's reactor vessel and downcomer vessel are connected at elevations corresponding to the prototype's spillunder point at the uppermost flow hole in the core barrel and at the elevation corresponding to the spillover point in the prototype's internal vent valves. Connections of the MIST cold leg piping to the downcomer vessel preserve the elevation corresponding to the plant's cold leg to reactor vessel nozzle centerline. Similarly, connections of the MIST hot leg piping to the reactor vessel preserve the plant's hot leg to reactor vessel nozzle centerline elevation.

2.2.1 Reactor Vessel

The MIST reactor vessel, shown in Figure 2.6, is divided into two sections by a pair of weld neck flanges which provide access to the top of the fuel pin simulators during assembly. The flanges are located at an elevation just slightly above the top of the core simulation. Therefore, the lower section of the reactor vessel contains the core simulation, and the upper section contains the upper plenum internals.

2.2.1.1 Lower Reactor Vessel Section. The lower reactor vessel section contains the core simulation and provides the volume corresponding to the plant reactor vessel's lower plenum. The core simulation consists of 45 electrically heated fuel pin simulators, and four guide tubes prototypically spaced in a square array. The fuel pin simulators and guide tubes enter the reactor vessel through a flanged head at the bottom of the reactor vessel. The sealing technique at the lower head was designed to provide a leak-tight seal while accomodating differential thermal expansion between the fuel pin simulators and the reactor vessel, and to minimize heat loss to ambient.

The lower head of the reactor vessel was constructed of a lap joint flange. The lower head seal arrangement consisted of extension tubes installed in each of the 49 holes drilled through the stub of the lap joint flange assembly. The tubes were attached to the upper face of the lower head by expansion rolling and welding, and protrude from the lower face of the lower head. The fuel pin simulators and guide tubes exit the reactor vessel through the extension tubes and are sealed by a braze joint in the annulus between the fuel pin simulator and extension tube.

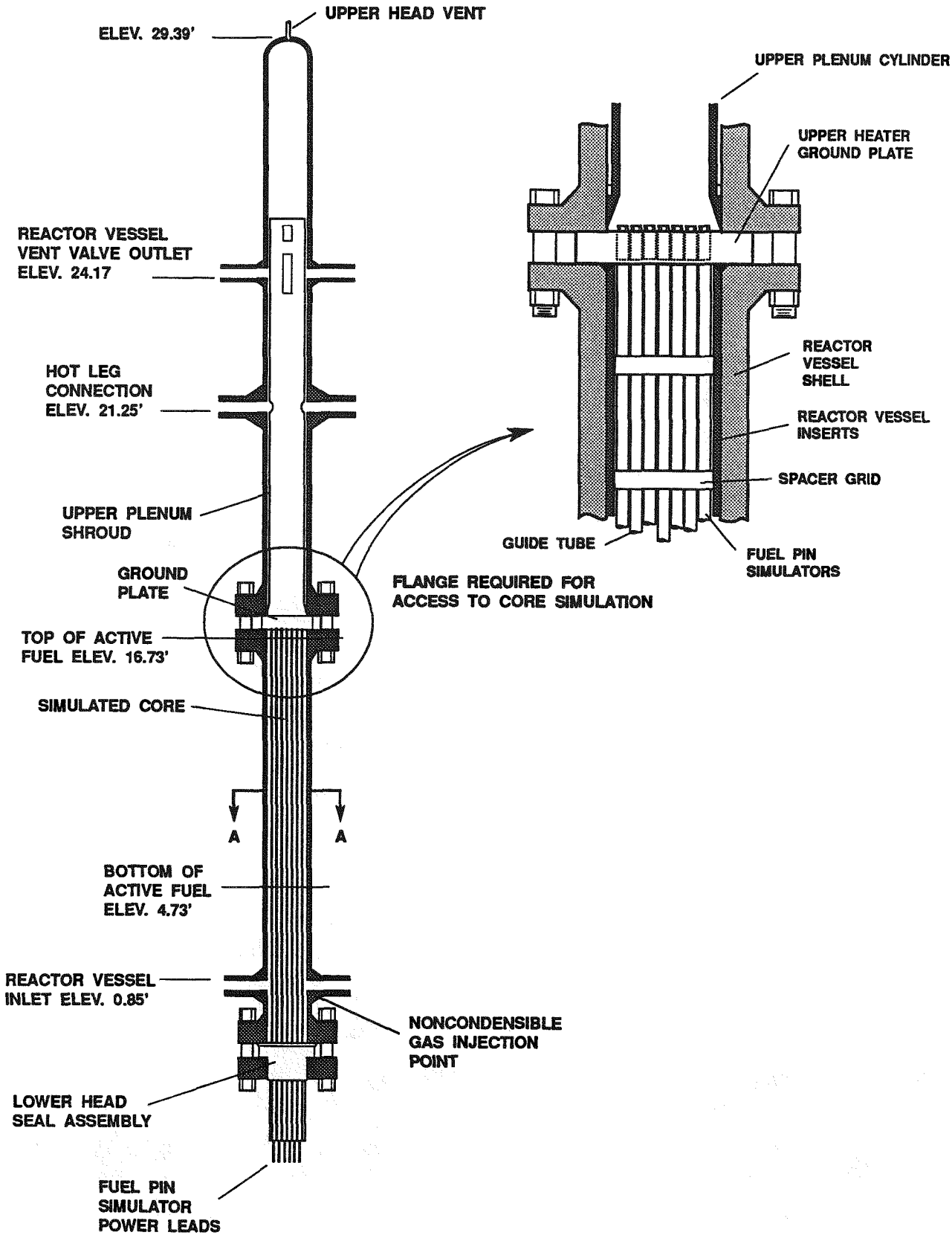

Figure 2.6 Reactor Vessel Model Arrangement

The upper ends of the fuel pin simulators are attached to a ground plate installed between the opposing faces of the weld neck flanges that separate the reactor vessel into an upper and lower section. The ground plate is used both to anchor the fuel pin simulators at their upper end, and to conduct current between the fuel pin simulators and the negative connection of the power supply. The flange joint is bolted and seal welded closed using Omega seals to seal weld the ground plate to both the upper and lower reactor vessel sections.

The braze joint at the lower head firmly attaches the lower end of the fuel pin simulators to the lower head of the reactor vessel shell. The top ends of the fuel pin simulators are bolted to the ground plate attached to the reactor vessel shell. Differential thermal expansion between the fuel pin simulators and the reactor vessel shell is accomodated by pretensioning the fuel pin simulators during installation. This pretensioning leads to facility operation limitations in order to avoid overstressing or buckling the fuel pin simulators. The limitations were determined by benchscale pull tests, and calculations to translate the strength limits into differential temperature limitations. These operational limitations imposed by the sealing arrangement did not limit the testing performed in the facility.

The fuel pin simulators extend fully from the lower head assembly to the ground plate. From the lower end of the fuel pin simulator to the elevation corresponding to the bottom of the plant fuel pins, the fuel pin simulators are essentially unheated. The heated length of the fuel pin simulators was equal in length to the plant MK-B fuel pins, thus preserving the heated length of the reactor core.

Flow enters the lower reactor vessel shell section through four 2-inch schedule 80 pipes. Four crossover pipes connecting the downcomer to the reactor vessel were used to lower the inlet velocity of incoming flow to avoid flow induced vibration. The inlet pipes connect to the reactor vessel on each side of the square array of fuel pin simulators, as shown in Figure 2.7. A gas addition site for noncondensible gas testing was installed in the lower reactor vessel below the downcomer-to-reactor vessel crossover piping.

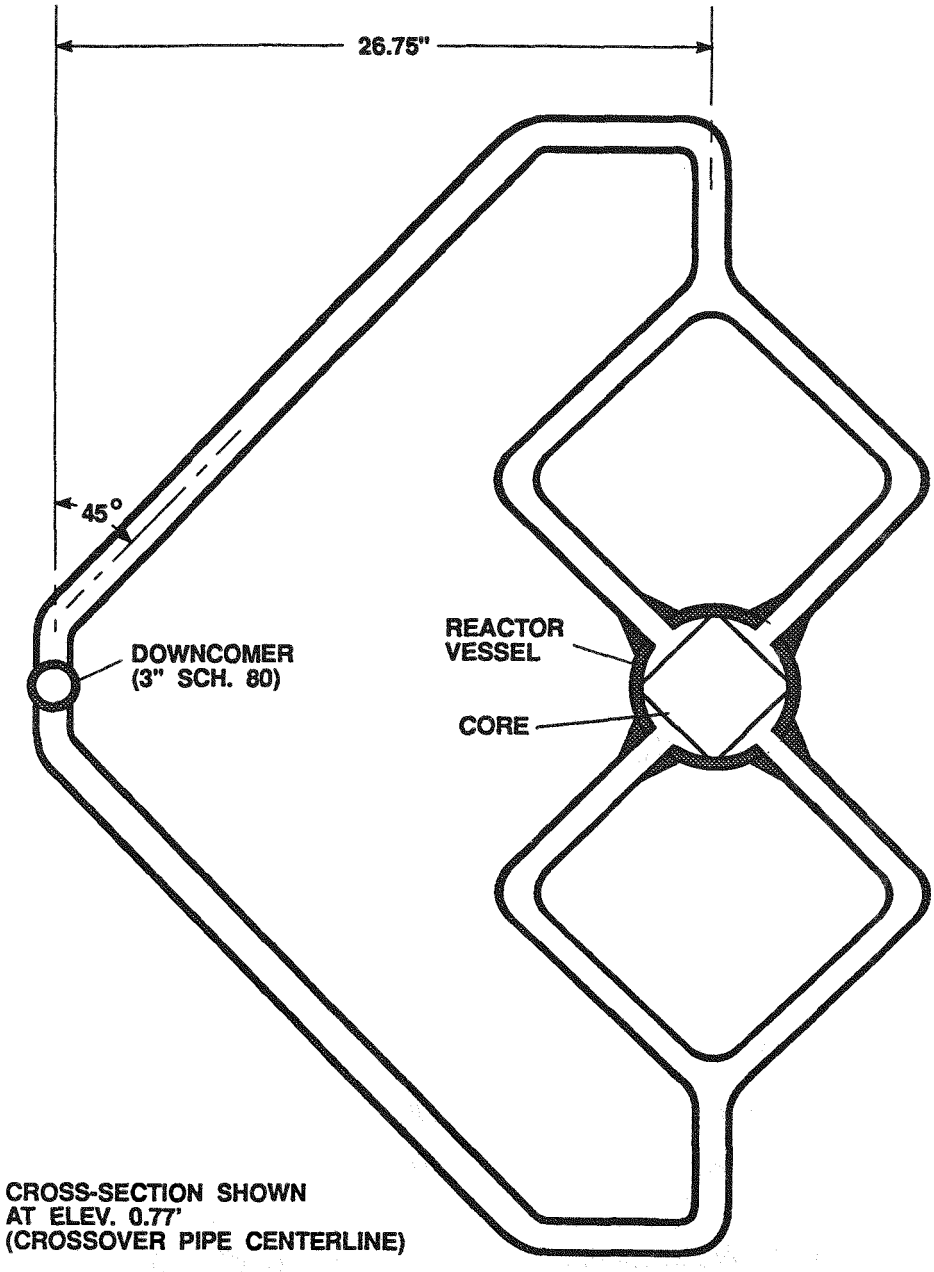

Figure 2.7 Downcomer to Reactor Vessel Crossover Piping

Above the inlet piping, inserts were used to occupy the open area between the outside of the square array of fuel pin simulators and the inside of the round reactor vessel shell. The inserts were gun drilled along their length to minimize the metal mass added to the reactor vessel. The gun drilled design resulted in a 57% reduction in metal mass, compared to solid metal inserts. The drilled holes in the inserts were capped on each end to keep them air filled throughout operation. Upon installation, the reactor vessel inserts

provided a square flow channel having a flat to flat dimension of 4.118 inches. The fuel pin simulators were 0.430-inch diameter, installed in a 7 x 7 square pitch of 0.568 inch. Therefore, the peripheral gap between the inside surface of the reactor vessel inserts and the outermost point of the fuel pin simulators was 0.140 inch. This gap sizing was selected to preserve the enthalpy rise of the fluid passing up the peripheral gap, relative to fluid within the array of fuel pin simulators. The reactor vessel inserts are supported axially from the top end, where they are bolted to the underside of the ground plate. Lateral support is provided at several places along the insert's length by a sliding pin arrangement. The sliding pin accommodates axial thermal expansion of the inserts relative to the reactor vessel shell, while retaining the insert against the surface of the shell to maintain the desired peripheral gap for the core simulation.

At the top of the core, the heating element in each fuel pin simulator is grounded to an end plug. The end plugs were drilled and tapped in order to bolt to the reactor vessel ground plate. The ground plate conducts the 2500 amps of direct current (at scaled 10% of full power) between the 45 fuel pin simulators and the power supply negative terminal. The ground plate was fabricated of Inconel in order to conduct the current without becoming a significant heat source itself. The plate was machined to provide a flow path between the core simulation and the upper plenum. The flow area in the plate was maximized by the pattern shown in Figure 2.8 in order to minimize pressure loss through the plate, while maintaining the required strength to anchor the fuel pin simulators.

The upper reactor vessel shell section provides the top and upper plenum simulation. Connections to the hot legs and reactor vessel vent valves are provided in the upper vessel section. Further details of the upper reactor vessel section are provided in Section 2.2.1.3.

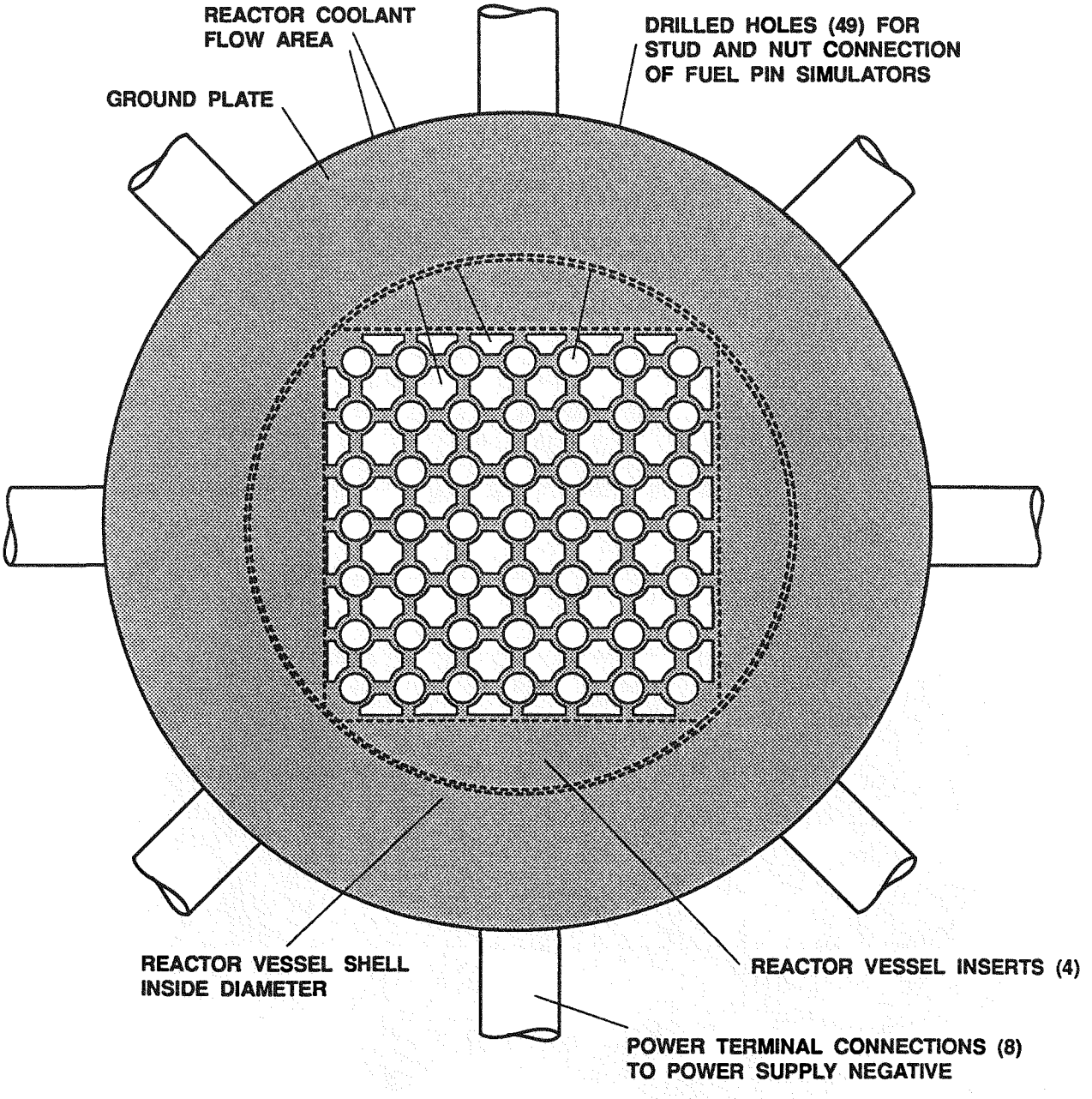

Figure 2.8 Reactor Vessel Ground Plate

2.2.1.2 Core. The core simulation in the reactor vessel lower section consists of 45 electrically heated filament-type heater rods. Each electrically heated rod is geometrically similar to a B&W Mark B fuel pin, and is powered to simulate the fuel rod surface heat flux and cladding outer surface temperature during transient testing. The fuel pin simulators are placed in a 7 x 7 array, with four unheated guide tubes as shown in Figure 2.9. Four guide tubes in the MIST core simulation approximately preserve the area occupied by unheated tubes in a typical Mark B fuel assembly.

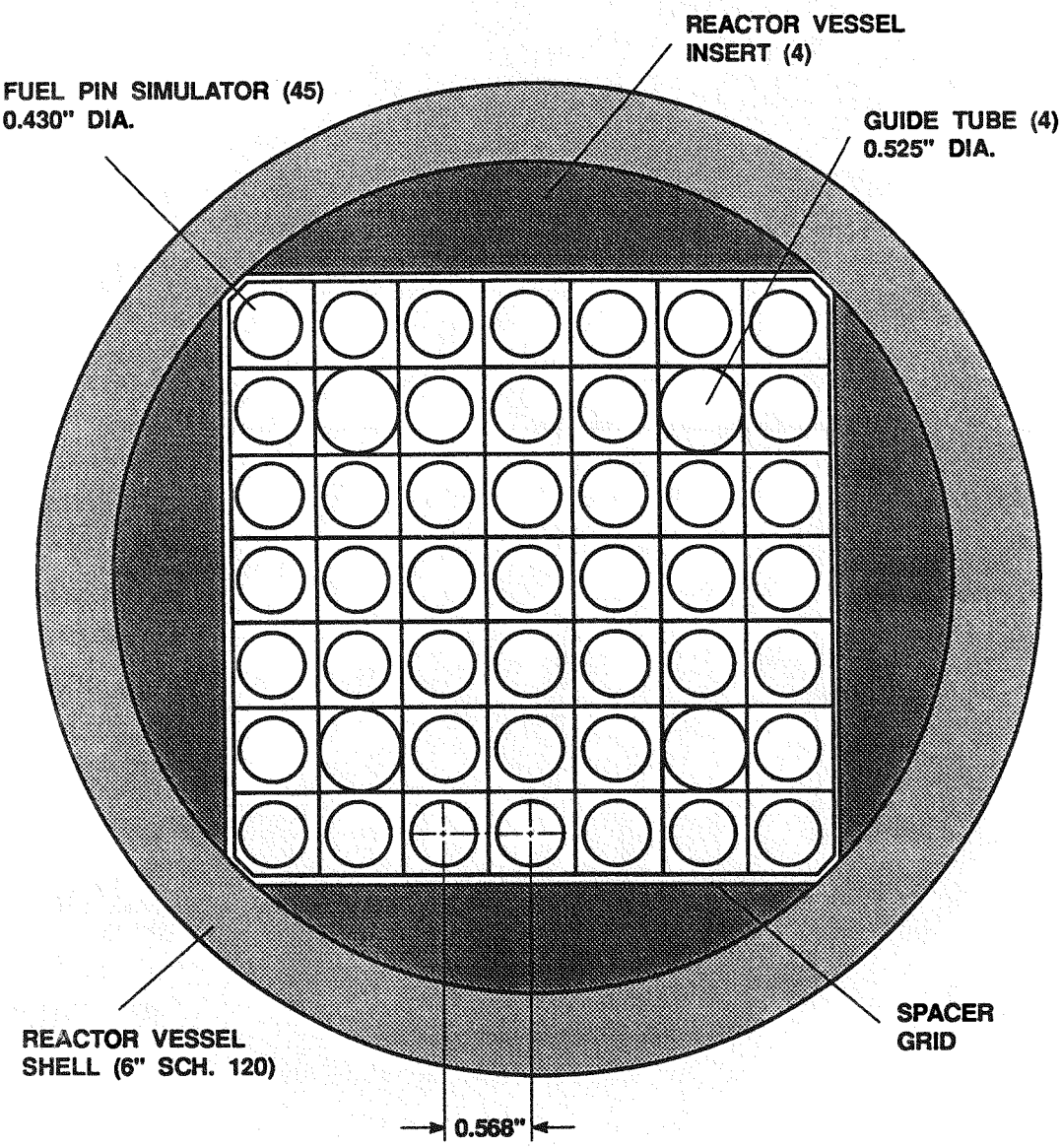

Figure 2.9 Core Simulation

Spacing between fuel pin simulators was maintained with prototypic B&W Mark B spacer grids. The production spacer grids were modified to reduce its peripheral dimensions to fit the 7 x 7 array. Fourteen spacer grid assemblies were installed along the length of the MIST core. The upper eight are located along the heated length of the core to preserve the placement typical of a Mark B fuel rod assembly. The remaining six spacer grids (lower six) were installed to minimize flow induced vibration at the reactor vessel entrance where flow enters crosswise relative to the fuel pin simulators.

Each fuel pin simulator has an outside diameter of 0.430 inch and is approximately 20.5 feet long. As shown in Figure 2.10, this length consists of 144 inches of heated length beginning approximately 2 inches from one end, and 100.5 inches of unheated length at the opposite end. Over the lowermost 33 inches of the unheated length, the outside diameter of the heater rod was reduced to 0.360 inch to accommodate the lower head seal arrangement.

Each fuel pin simulator is capable of operating at 70 kW, which corresponds to 100% power simulation. However, for the MIST program, each heater rod was operated up to a maximum of 7 kW, which corresponds to 0 to 10% power simulation. Over the 144-inch heated length, the axial power profile approximated a 1.25 peak-to-average sinusoidal profile. This was accomplished by a stepwise approximation consisting of 11 discrete plateaus. The heating element was a coiled Cupron wire approximately 0.081 inch in diameter. The axial power shaping was obtained by varying the pitch of the coil (that is, the number of turns of the coil per unit length down the heater rod). The as-built axial power profiles were calculated for each fuel pin simulator and for the core as a whole using heating element zonal resistance measurements taken during the heaters fabrication procedure and radiograph inspection of the zonal lengths of the completed core heater rods. Resistance changes that occur in each zone upon completion of final swaging and heat treatment were accounted for.

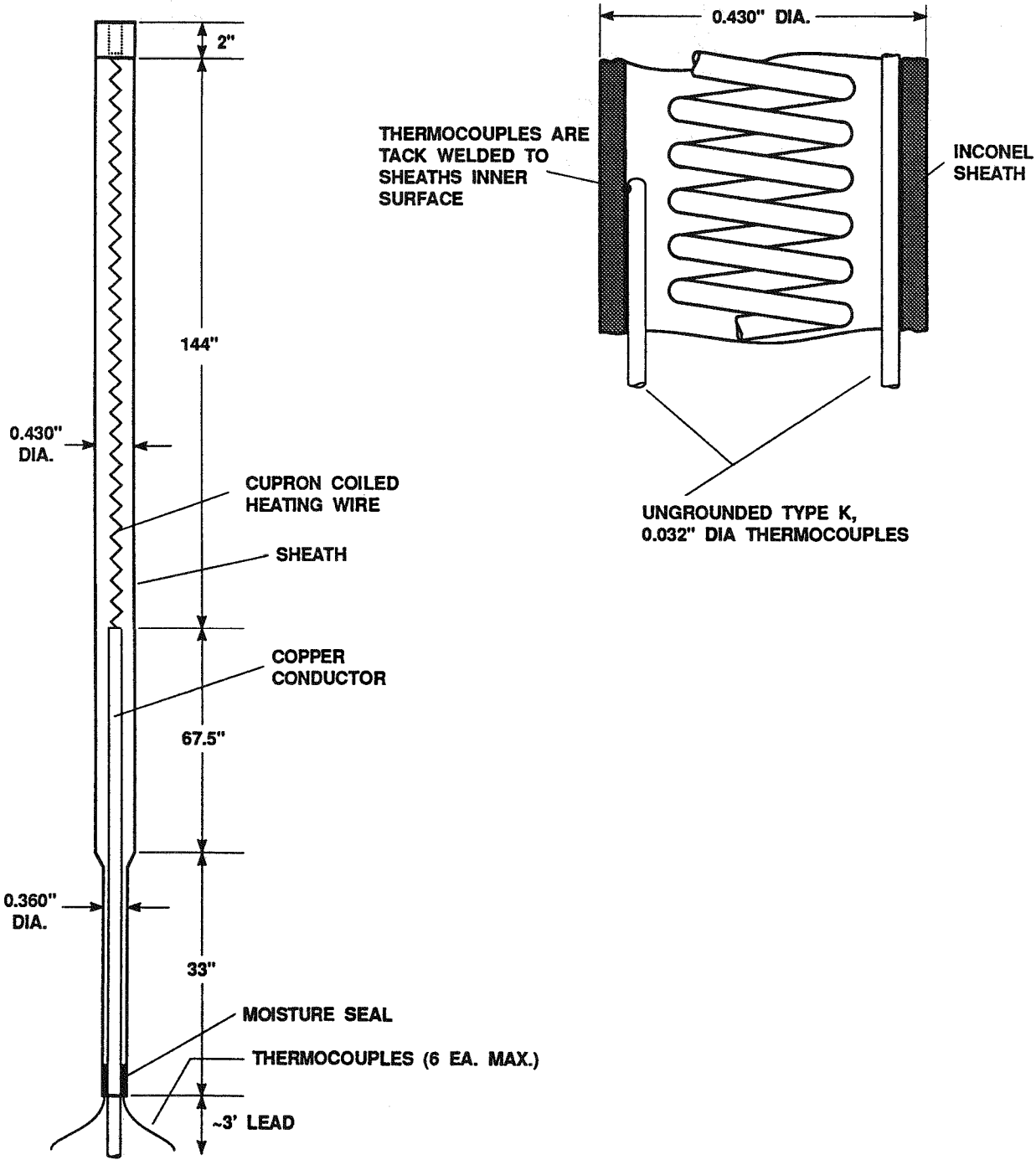

Figure 2.10 Fuel Pin Simulator

Summing the resistance of the series of power zones in each fuel pin simulator, the total core resistance of the 45 heat rods installed in parallel in the MIST core simulation was 0.0536 ohm. The distance from the top of the fuel pin simulator (which fit up to the underside of the reactor vessel ground plate) to the top of the composite core's heated length is 1.963 inches. The top of the heated length of individual heater rods vary from this average by no more than $\pm$0.2 inch. The composite core develops the surface heat flux profile along the heated length of the core given in Table 2.3. In this tabulation, Zone 1 is at the top of the core's heated length, and heat flux values for each zone are normalized on the average heat flux of the composite core. The heat flux profile, or equivalently the power profile along the length of the core, is shown plotted in Figure 2.11. Also shown in this figure is the 1.25 peak-to-average, chopped sinusoidal axial power profile approximated by the MIST core simulation.

Table 2.3

COMPOSITE CORE HEAT FLUX PROFILE

Zone No.	Zone Length (inches)	Heat Flux (normalized)*
1	6.04	0.548
2	11.92	0.703
3	12.08	0.860
4	11.91	1.050
5	12.06	1.180
6	36.24	1.295
7	12.11	1.178
8	12.11	1.029
9	12.06	0.862
10	12.00	0.698
11	6.01	0.546

* Zone heat flux values normalized on core average heat flux.

Average Heat Flux = 375.63 W per square inch at scaled 100% power level.

Total Heated Length = 144.54 inches; Zone 1 begins at the top of the core.

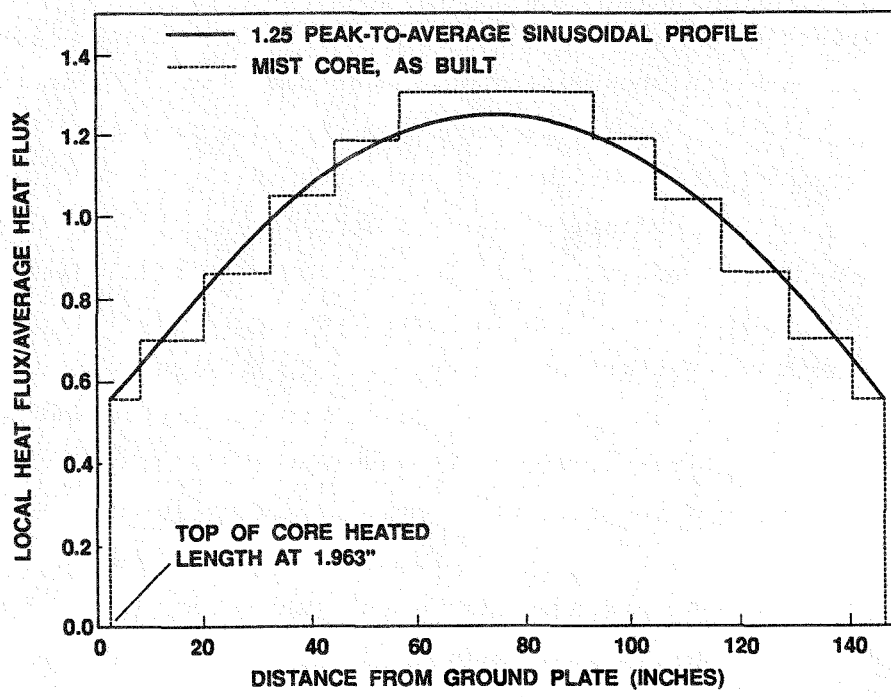

Figure 2.11 Axial Heat Flux Profile in Model Core

The time constant of the coiled wire design core heater rod was estimated to be 0.2 second by a lumped parameter analysis. Previous B&W analyses have indicated a time constant of 5.5 seconds for a nuclear fuel rod. In Loss of Coolant Accident (LOCA) test facilities, such a large disparity between model and prototype would indicate the need for a core power control system incorporating feedback of heater rod surface temperature in order to compensate for the difference in stored energy between the electrical heater rod and the nuclear fuel rod. However, MIST facility testing was initiated at power levels on the decay heat curve at less than 10% full power. At power levels less than 10%, the rate of change of fuel rod surface heat flux is slow enough to preclude the necessity of compensating core power to account for stored energy differences, and a preprogrammed power transient was considered adequate for Small Break Loss of Coolant Accident (SBLOCA) testing.

The core simulation is powered by a direct current power supply. A voltage of 420.6 volts would operate the core at 3.3 MW (100% power) and obtain an average heat flux of 375.6 watts per square inch. During MIST testing, the total power output was limited to 330 kW by the capacity of power supply purchased.

2.2.1.3 **Upper and Top Plenums**. The upper reactor vessel shell section forms the top and upper plenums of the MIST reactor vessel. An upper plenum cylinder is located inside the upper shell section as shown in Figure 2.12. A top cover plate on the cylinder divides the upper reactor vessel into an upper plenum (inside the cylinder), and a top plenum (above the cover plate). The upper plenum cylinder is bolted to the reactor vessel shell at the cylinder's lower end. The connection is sealed sufficiently that essentially all reactor vessel flow is directed into the upper plenum cylinder. The upper end of the cylinder is laterally supported in the reactor vessel by centering pins.

Hot leg connections to the reactor vessel are located to preserve the centerline elevation of the plant reactor vessel nozzle. Reactor vessel vent valve connections are located to preserve the spillover elevation of the plant flapper-type vent valves. That is, the bottom elevation of the MIST RVVV connection matches the bottom elevation of the plant RVVVs.

Figure 2.13 shows the cross section of the upper reactor vessel at the hot leg and reactor vessel vent valve connections. The downcomer vessel was located at the center of the reactor coolant system; the two steam generators were equidistant from the downcomer, one directly to the North, and the other directly to the South. The circumferential positions of the two hot legs were selected to mimimize the hot leg horizontal length, obtain equal and prescribed hot leg U-bend radii, and to permit symmetric cold leg connections to the downcomer. Thus, the hot leg connections were oriented as shown in Figure 2.13, and were 142.5° from one another. The reactor vessel vent valve locations were located to obtain symmetric flow paths between the reactor vessel and the downcomer.

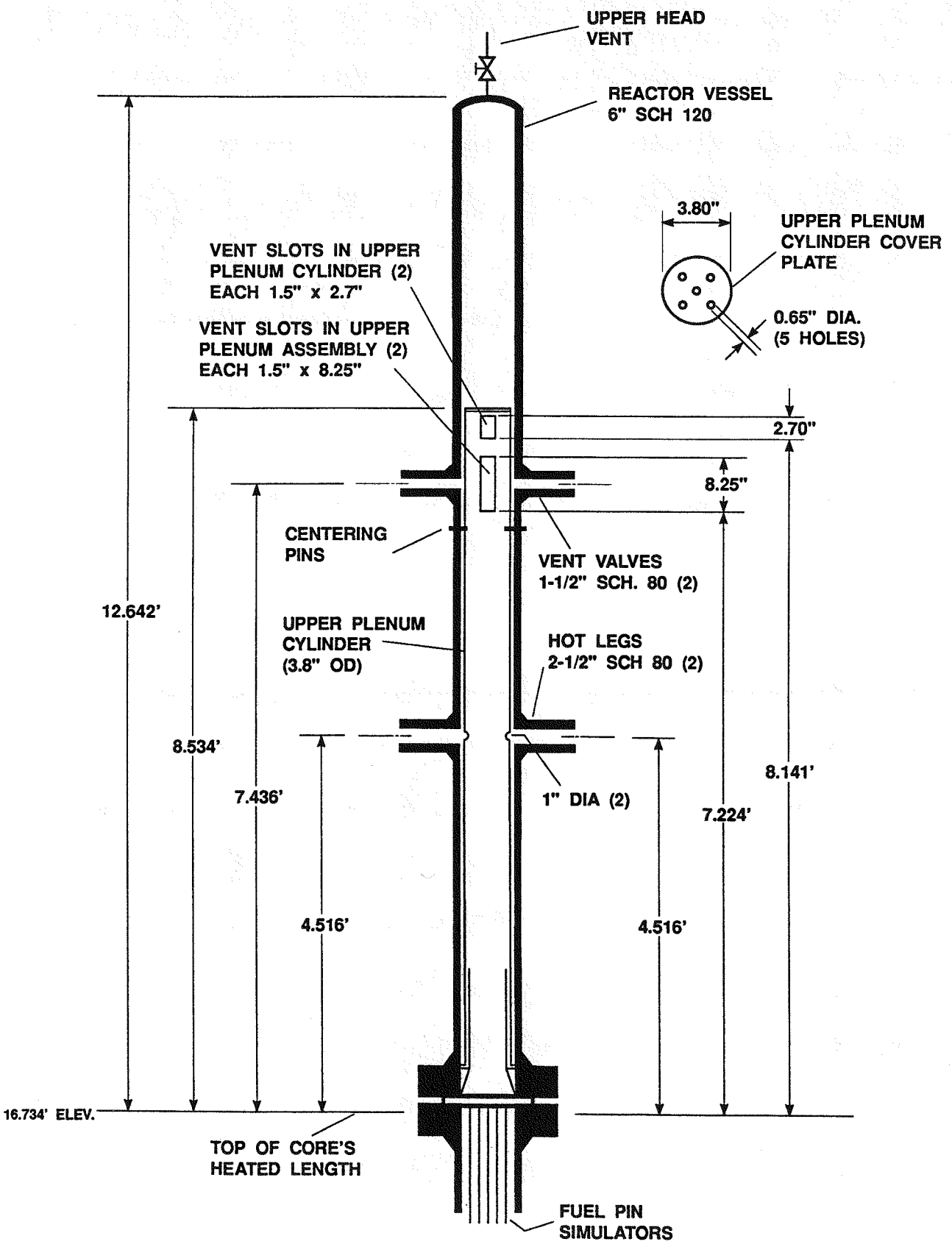

Figure 2.12 Reactor Vessel Top and Upper Plenum

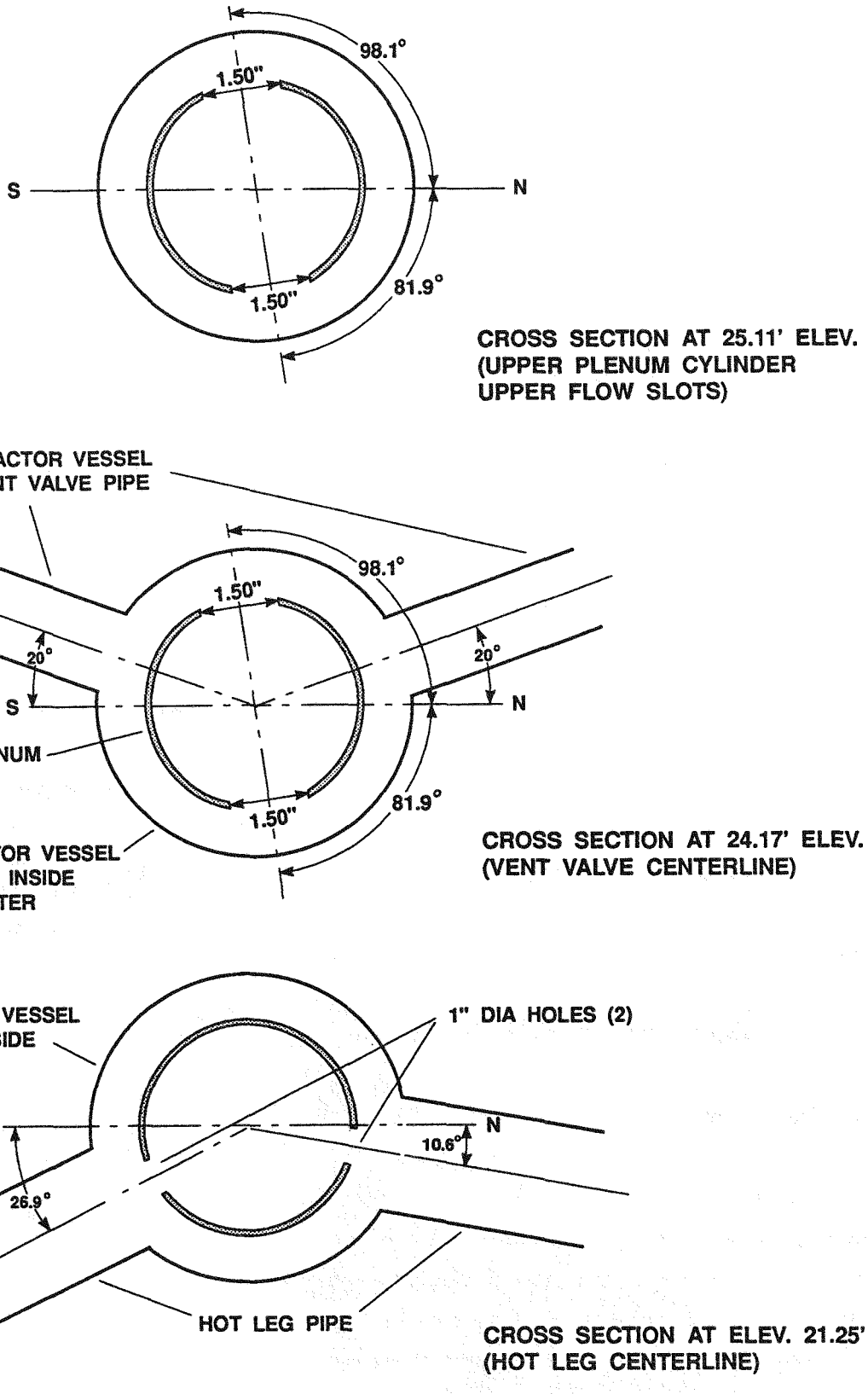

Figure 2.13 Reactor Vessel Hot Leg and Vent Valve Connections

Also shown in Figure 2.13 are the locations of the flow holes in the upper plenum cylinder. The hot leg pipe terminates at the outer vessel. Directly in line with each hot leg connection is a 1-inch diameter flow hole in the upper plenum cylinder. Flow can also enter each hot leg by flowing down the annulus formed between the reactor vessel shell and the upper plenum cylinder. Similarly, the vent valve connections terminate at the outer vessel. The flow holes near the vent valve connections are vertical slots in the upper plenum cylinder. Two sets of vertical slots (each set consisting of two flow holes) are provided in the upper plenum cylinder. The lower slots are 1.5 inches wide by 8.5 inches tall to provide the flow area of the plant's 16-3/4-inch diameter plenum cylinder holes. The upper slots are 1.5 inches wide by 2.7 inches tall to provide the flow area of the plant's 11-3/4-inch diameter plenum cylinder holes. The vertical placement of each set of slots in MIST preserves the spillover elevation of the plant's plenum cylinder holes. The vertical slots are not located directly in line with the vent valve connections. Rather, they are located to bisect the vent valve piping connections.

The top cover plate of the upper plenum cylinder is 1/4-inch thick, having the same diameter as the plenum cylinder. The cover plate has five 21/32-inch diameter holes to provide the desired flow resistance between the upper and top plenums. The flow area of the various openings in the upper plenum cylinder (hot leg openings, vertical slots, top cover plate) were sized to preserve the plant's flow resistance between the top and upper plenum, and to preserve the flow split among these various flow paths between the plena.

2.2.1.4 Reactor Vessel Instrumentation

Fluid Temperatures. Twenty-three fluid thermocouples installed in the reactor vessel were connected to the data acquisition system. Ten of these thermocouples were located in a central flow channel within the heater rod bundle and two were located in a flow channel adjacent to a guide tube. A total of five thermocouples, including one in each of the two flow channels just discussed, were located at the core exit. Four more thermocouples were located in the upper regions of the reactor vessel, as shown in Figure 2.14.

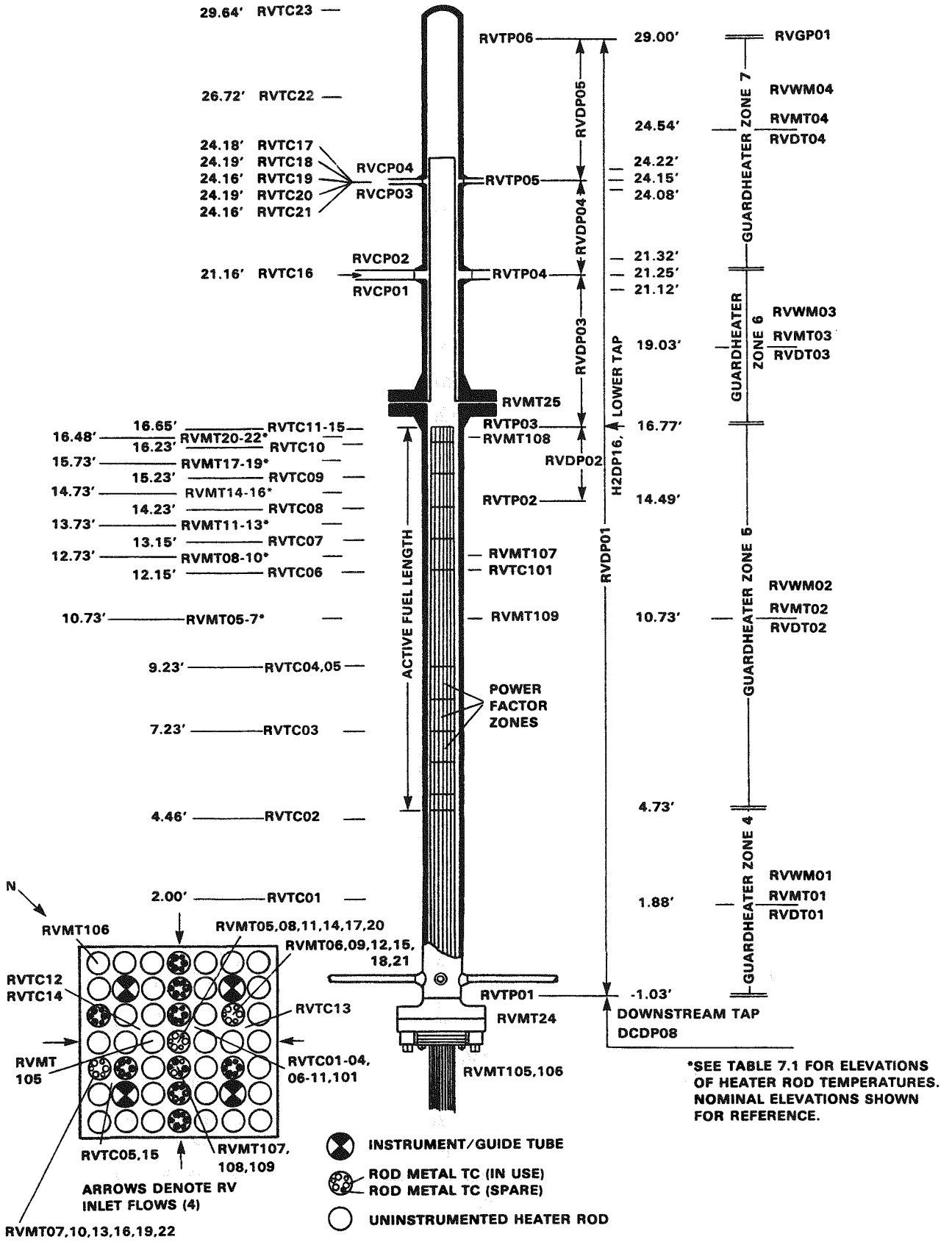

Figure 2.14 Reactor Vessel Instrumentation

Two of the central bundle thermocouples were placed in the lower plenum, one just below the beginning of the heated core region and one mid-way through the lower plenum from the downcomer/reactor vessel crossover elevation. A resistance temperature detector was installed in the reactor vessel to downcomer piping. Together these instruments indicated the core inlet temperature. The remaining eight central bundle thermocouples were located in the heated region of the rod bundle, concentrated in the upper half of the heated length.

Pressure and Differential Pressure. The reactor vessel was instrumented with one pressure and five differential pressure transmitters. The tap locations are shown in Figure 2.14. The differential pressure transmitters were used for collapsed liquid level and void fraction calculations in the reactor vessel. Differential pressure transmitters used for measurements across each of the four vent valve lines and are discussed in Section 2.2.3.

Guard Heater Measurements. Active and passive insulation techniques are employed to minimize heat loss from each component of the MIST reactor coolant system. To minimize heat loss, heat input to the trace heating system installed outside the pipe wall is adjusted to maintain an approximately adiabatic boundary condition at the pipe wall. Pipe wall metal and insulation temperature measurements are required for controlling heat input. Guard heating concepts and characterization are discussed more completely in Section 6.

Four guard heater zones were used on the reactor vessel itself. Guard heater total power for the four zones was obtained from the controller output signal.

Limit Switch. A limit switch installed on the remotely actuated isolation valve for the reactor vessel upper head vent was used to provide a positive indication of an open upper head vent.

Core Instrumentation. Twelve of the 45 fuel pin simulators were instrumented with six internal thermocouples each to measure the heater rod's sheath temperature along the heated portion of the rod. The thermocouples were installed during fabrication in the dielectric insulation between the coiled wire heating element and the outer sheath, and welded to the sheath at the sensing tip to ensure thermal contact. The six elevations at which thermo-

couples were installed correspond to the mid-point of each of the six upper power level plateaus. This relatively close spacing of the thermocouples near the top of the active core length allowed the detection and measurement of core uncovery. The location of the instrumented fuel pin simulators is shown in Figure 2.14 (inset).

Eighteen fuel pin simulator sheath temperatures were recorded by the data acquisition system; six in each of the three fuel pin simulators shown in Figure 2.14. In addition to the three heater rods connected to the data acquisition system, three supplied temperature measurements for core power trip based on high heater rod temperature. The remaining instrumented fuel pin simulators served as spares in case of thermocouple failures. None of these were utilized over the course of the MIST test program.

Energy input to the reactor coolant by the core heaters was calculated from core voltage and amperage measurements. Current was measured by the voltage drop across a 16 micro-ohm shunt.

2.2.2 Reactor Vessel Downcomer

The reactor vessel downcomer is the zone of recombination for several fluid streams returning to the reactor vessel and is the site of fluid and thermal phenomena which are likely to be multidimensional. The downcomer is the juncture between the outer reactor coolant flow path (through the cold legs) and the inner flow path (through the reactor vessel vent valves). Emergency core cooling system fluid from the core flood tank enters the downcomer near the vent valves. And, the downcomer and the cold leg discharge piping define the region of interaction between liquid high pressure injection or return loop flow and reactor vessel vent valve stream.

2.2.2.1 Reactor Vessel Downcomer Design. Scaling requirements to preserve the diverse and multidimensional downcomer phenomena which occur during different plant transients result in conflicting design characteristics. The MIST reactor vessel downcomer design represents a compromise which preserves the most significant post-SBLOCA plant phenomena.

Design characteristics for the MIST downcomer were ranked in order of importance based on available data, correlations, and technical analyses. The most important design characteristic is elevation. Next most important are volume and geometric effects on transient timing, condensation, and voiding characteristics. Geometric details which preserve local flow and fluid density differences, axial and tangential irrecoverable pressure drop, and wall (stored energy) effects are of lesser, but not insignificant, importance to the downcomer design.

Power-scaled volume for a plant-typical reactor vessel and downcomer arrangement requires an extremely narrow annular gap. This results in atypical wall effects on fluid flow and surface to fluid energy transfer. Scaling to avoid wall effect atypicalities, while maintaining a plant-typical arrangement, results in grossly excessive downcomer fluid volume and atypical core cooling characteristics. As a result, an external downcomer (separate from the reactor vessel) was specified for MIST.

Practical considerations factored into the downcomer design included leak tightness and the ability to make relevant measurements. The downcomer design also must promote segregation for entering fluid streams to preserve loop to loop pressure and temperature variations. For MIST, power-scaled leaks are very small so the avoidance of unplanned leaks is extremely important. Applied to the downcomer simulation, the avoidance of unplanned leaks requires positive closure for the reactor vessel vent valves in addition to leak tightness across pipe boundaries. These factors contributed to the specification of an external downcomer for MIST.

The MIST downcomer vessel has two distinct regions (Figure 2.15), with different scaling emphasis, to best preserve important transient phenomena. The scaling emphasis for the upper downcomer is on elevation, geometric details which preserve typical fluid stream segregation and allow asymmetric behavior, and volume to a lesser extent. The scaling emphasis for the lower downcomer is on elevation and power scaled fluid volume.

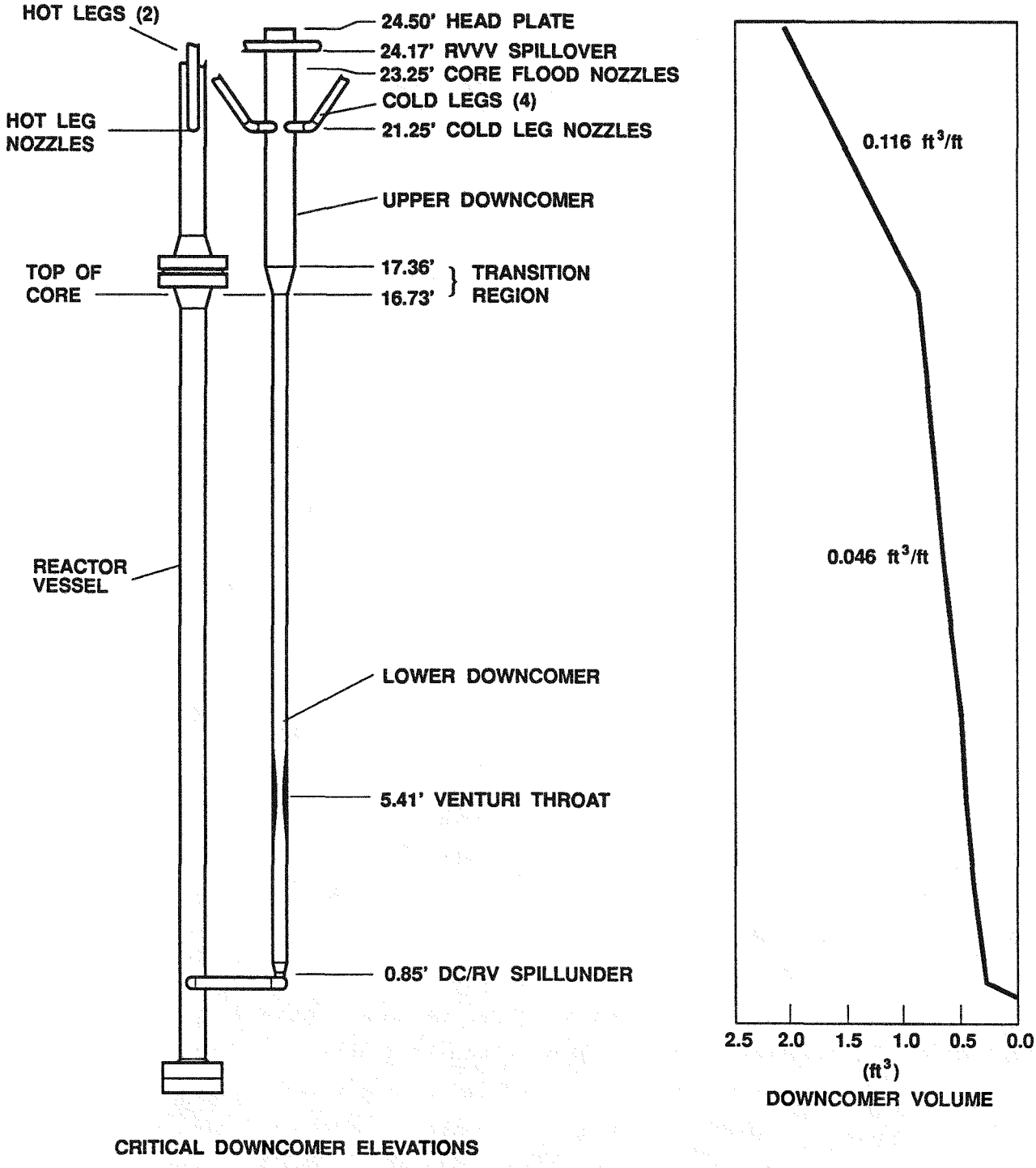

Figure 2.15 Reactor Vessel Downcomer

The upper downcomer design (Figure 2.16) supports limited multidimensional loop-to-loop coupling with an annular, partially segregated mixing zone for loop, reactor vessel vent valve, cold leg, high pressure injection, and core flood fluids. Baffle plates extend part of the distance across the annular gap for the full length of the upper downcomer, separating it into four quadrants. These baffles restrict tangential flow around the annulus preventing atypical interactions between adjacent cold leg flows and allowing limited loop-to-loop coupling to preserve resulting asymmetries.

Nozzles for fluid streams entering the upper downcomer from the reactor vessel vent valves, core flood tank, and cold legs are designed to preserve plant-typical flow momentum and avoid atypical stored energy transfer by wetting of the inner pipe and baffles.

The upper downcomer outer annular boundary is provided by an 8-inch, schedule 160 pipe with an inside diameter of 6.813 inches. The inner annular boundary is formed by a 3-1/2-inch, schedule 160 pipe with an outside diameter of 4.000 inches. The resulting annular gap is 1.407 inches. The inside pipe is welded to the top downcomer plate and sealed at the bottom to maintain a voided condition and reduce thermal storage.

The baffles, which separate the upper downcomer into quadrants, extend to within 0.25 inch of the outer annular boundary. Vertically, the baffles extend the entire length of the upper downcomer, from the top at 24.50 feet to the point in the downcomer having the same elevation as the top of the active core at 16.73 feet (elevations relative to the steam generator lower tubesheet, secondary face).

As shown in Figure 2.16, the upper downcomer region includes a transition section to the lower downcomer 3-inch, schedule 80 pipe. The transition from 8-inch, schedule 160 pipe to 3-inch schedule 80 pipe is accomplished in 7-1/2 inches. To provide for fluid plume segregation as far as possible into the downcomer, the annular geometry is maintained through the transition section using a machined conical section and tapered baffle plates. Gaps between the inner and outer annular boundaries and between the baffles and the outer annular boundary are maintained to the bottom of the transition.

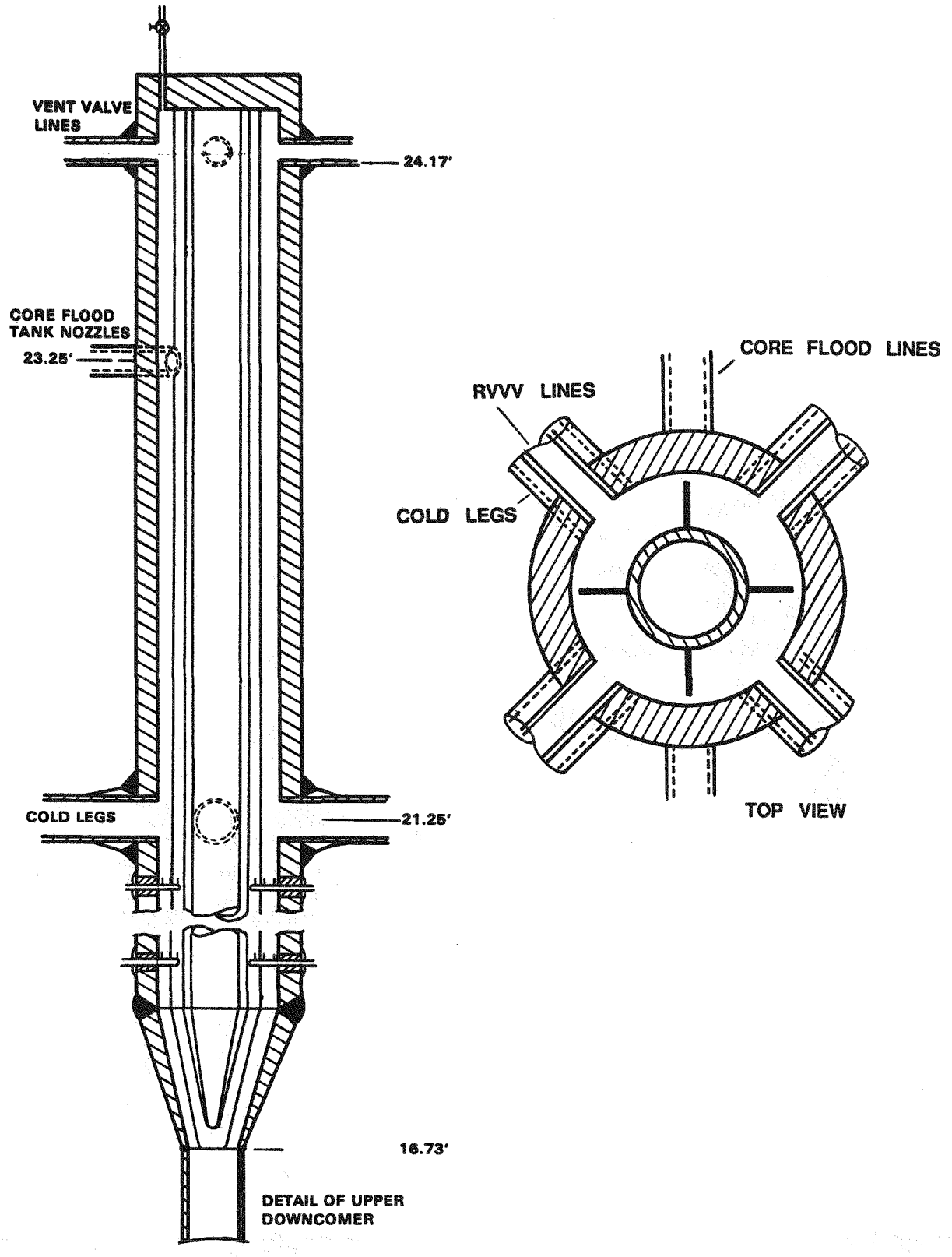

Figure 2.16 Upper Downcomer Detail

Plant typical natural circulation driving forces for the upper and lower downcomer are obtained by preserving the elevations of the reactor vessel vent valve nozzles, the cold leg discharge nozzles, the core flood tank nozzles, and the downcomer to lower reactor vessel plenum flow path. The uppermost plant downcomer elevation of 26.44 feet is not maintained for the MIST downcomer design. Fluid above the vent valve elevation is less important to the natural circulation driving force since it is out of the normal flow path, so the uppermost MIST downcomer elevation is lowered to provide more typical power scaled fluid volume in the upper downcomer. Key downcomer elevations are provided in Figure 2.15. Downcomer fluid volume as a function of elevation is also noted.

Upper downcomer fluid volume exceeds the ideal power-scaled volume despite the external downcomer configuration and the reduced uppermost elevation. This results from maintaining the required annular configuration while minimizing atypical wall effects on fluid friction and surface to fluid energy transfer. Both atypical wall effects and excessive fluid volume in the upper downcomer adversely influence condensation and voiding typicality. The specified design represents the best achievable compromise between excessive fluid volume and atypical wall effects, best preserving plant-typical phenomena.

The ratio of axial to tangential flow resistance for the upper downcomer is similar to the plant, however both resistances are somewhat lower than typical. Axial pressure drop for the reactor coolant path through the vent valves is preserved by the added resistance of a venturi in the lower downcomer.

Lower downcomer design supports plant typical manometric and core cooling characteristics. To this end, plant typical elevations and power-scaled volumes are preserved. The lower downcomer extends from 16.73 feet to 0.69 foot and includes the downcomer to lower reactor vessel plenum connective piping. The lower downcomer is fabricated from 3-inch, schedule 80 pipe with an inside diameter of 2.900 inches. The spillunder for the downcomer to lower plenum connective piping matches the top of the uppermost flow hole in the lower plenum cylinder.

Flow exits the lower downcomer vertical piping through two 180° opposed pipes. The flow is further split and returns to the reactor vessel through four equally spaced nozzles. This design for the connective piping reduces flow velocity entering the core, reducing the potential impact of flow induced vibrations on the core heater rods. The four nozzles also promote a more uniform axial flow profile through the core. Downcomer to lower plenum connective piping is fabricated from 2-inch, schedule 80 piping with an inside diameter of 1.939 inches.

2.2.2.2 Reactor Vessel Downcomer Characterization. Reactor vessel vent valve operation and downcomer performance are closely linked. For MIST, downcomer response to various modes of vent valve actuation and control was characterized for both liquid and vapor phases. The results of these characterization tests are noted briefly in the following paragraph and expanded upon in Section 6.

The MIST reactor vessel vent valve and downcomer configuration is necessarily atypical of the plant in several notable aspects. These include valve layout, and actuation characteristics, fluid flow patterns, and flow path lengths. Noting these atypicalities, the MIST downcomer is a satisfactory simulation of the plant in that it supports both primary loop and downcomer transverse asymmetries in fluid conditions without creating additional asymmetries due to the simulation itself. These findings apply for both liquid and vapor conditions in the downcomer.

2.2.2.3 Reactor Vessel Downcomer Instrumentation. The reactor vessel downcomer is extensively instrumented to provide detailed, multidimensional thermal hydraulic data. Instrument locations and installation details are defined in Figures 2.17, 2.18, and 2.19. Seventy-two instruments are recorded by the MIST data acquisition system, including: 46 fluid thermocouples, eight differential pressure transmitters, four metal thermocouples, four thermocouples associated with a cooled thermocouple probe, three differential temperature pairs, three wattmeters, three limit switches, and one resistance temperature detector. The majority of these instruments are concentrated in the upper downcomer.

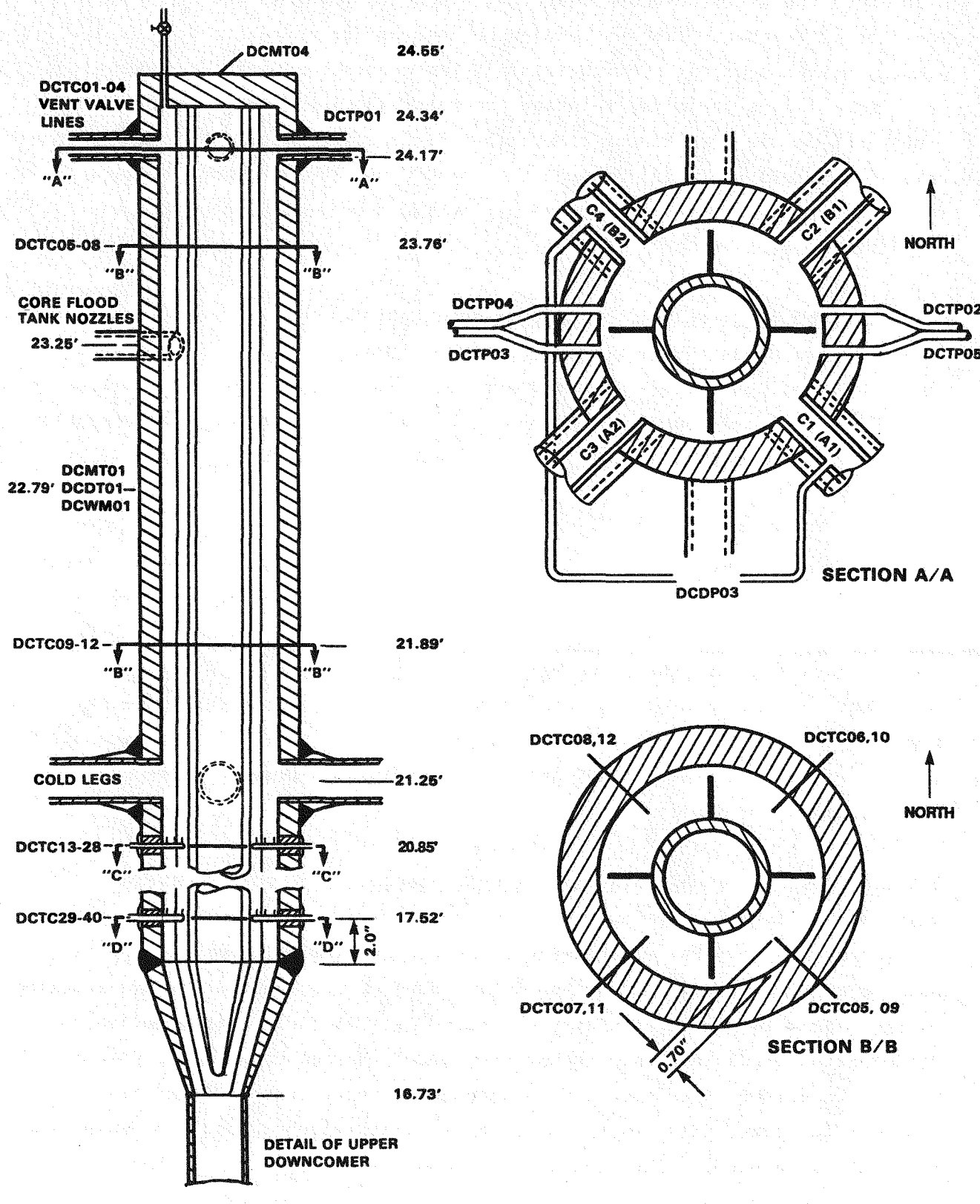

Figure 2.17 Upper Downcomer Instrumentation

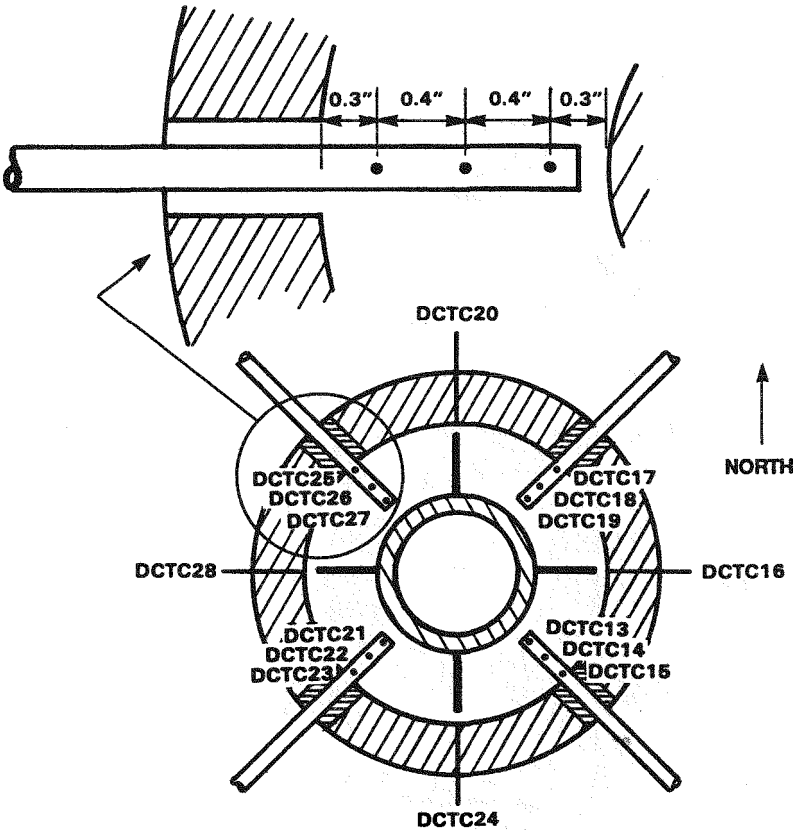

SECTION C/C

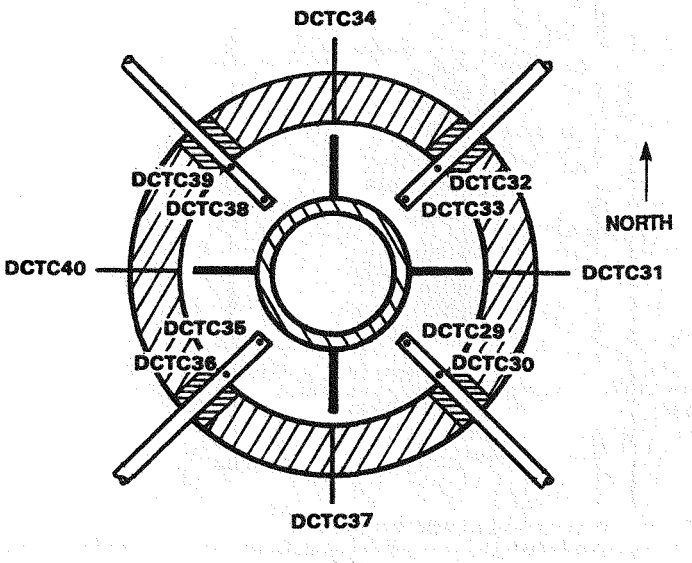

SECTION D/D

Figure 2.18 Upper Downcomer Instrumentation Detail

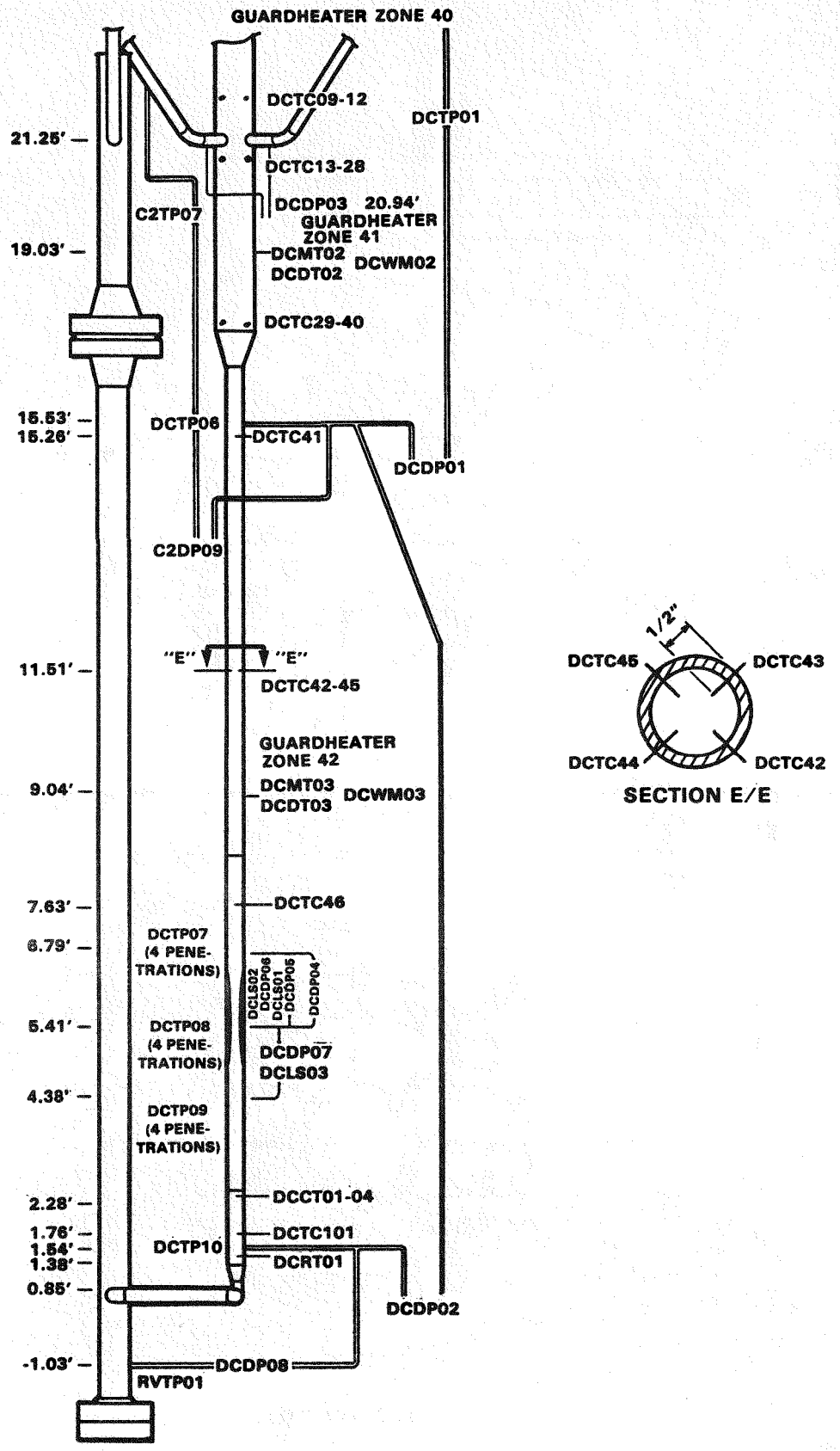

Figure 2.19 Lower Downcomer Instrumentation

Fluid Temperature Measurements. The upper reactor vessel downcomer is instrumented to record loop-to-loop asymmetries and multidimensional effects. Forty fluid thermocouples are concentrated in the upper downcomer to detail mixing information for reactor vessel vent valve, core flood, and cold leg fluid streams. These thermocouples are grouped at four planes bracketing each entering fluid stream as shown in Figure 2.17, and are arranged radially and tangentially as shown in Figures 2.17 and 2.18. In addition, four thermocouples are located, one each, in the four vent valve lines, downstream of the valves. These thermocouples are used to indicate a positive seal when the vent valves are closed and to record fluid temperature.

The geometry of Section B/B, Figure 2.17, is typical of the two planes of four thermocouples which bracket the core flood tank nozzles. The upper plane is located approximately midway between the vent valve and core flood nozzles, at 23.76 feet. The lower plane is located 8 inches above the cold leg discharge nozzles, at 21.89 feet. Each thermocouple is inserted to a depth of 0.7 inch (half the annulus) and aligned with the cold leg discharge nozzles. These thermocouples record potential thermal asymmetries due to vent valve activity and indicate the mixing of core flood tank fluid.

The two planes of thermocouples at 20.89 feet and 17.52 feet are used to define mixing patterns for cold leg discharge effluent and the heterogeneous fluid already in the upper downcomer. At each plane, thermocouples are radially spaced in each quadrant and located in the gaps between the baffle plates and the outer annular boundary. The 40-inch axial separation between the two instrument planes makes an indication of fluid stream segregation supported by the baffle plates possible.

Section C/C, Figure 2.18, illustrates the geometry for the thermocouple plane at 20.89 feet, 4 inches below the cold leg discharge nozzles. Rakes of three thermocouples each are installed in each upper downcomer quadrant, aligned with the cold leg discharge nozzles. The outermost thermocouple of each rake is 0.3 inch from the outer annular boundary; the center thermocouple is aligned with the Section B/B thermocouples at the annulus midline, and the innermost thermocouple is 0.3 inch from the inner annular boundary. Individual rake thermocouples are oriented vertically and extend five thermocouple

diameters out of the rake assembly to avoid conduction effects on measured temperature. The four gap thermocouples at 20.89 feet, are inserted 0.094 inch to the midpoint between the baffle plate and the outer annular boundary.

The thermocouple plane at 17.52 feet is arranged like the plane at 20.89 feet except that the center thermocouple for each rake is omitted. The remaining thermocouples are aligned under their counterparts at 20.89 feet, as shown by Section D/D of Figure 2.18.

Lower downcomer temperature instrumentation shown in Figure 2.19 is installed to record axial variations and to indicate the completeness of mixing for fluid streams exiting the upper downcomer region. At 11.51 feet, four thermocouples are inserted to a depth of 0.5 inch and aligned with the cold leg discharge piping and the rake thermocouples in the upper region. These thermocouples are intended to provide additional mixing information. The two remaining fluid thermocouples and the RTD in the lower region are spaced evenly and inserted to the pipe centerline.

Upper downcomer fluid thermocouples are 0.063 inch, ungrounded, Type J with an approximate time constant of 5 seconds. Lower downcomer thermocouples are 0.125 inch, ungrounded, Type J with an approximate time constant of 15 seconds. The resistance temperature detector is 1/4 inch in diameter with an approximate time constant of 5.5 seconds.

The time constant is defined as the time required to reach 63.2% of an instantaneous temperature change. The time constant values given throughout this report for the various thermocouples and resistance temperature detectors were provided by the sensor manufacturer. The reported values are quite conservative. The reported values were calculated for air at room temperature and atmospheric pressure moving with velocity of 65 ft/sec. The response time for these sensors is improved (reduced) substantially when immersed in steam or water.

Differential Pressure Measurements. Differential pressure measurements in the MIST downcomer are used to calculate collapsed liquid levels, fluid mass flow rates, irrecoverable pressure drop, and to measure loop-to-loop pressure

asymmetries. Pressure tap locations and spans for for these instruments are noted on Figure 2.19.

Two differential pressure transmitters are used for the downcomer collapsed liquid level calculation. The upper measurement extends from the top of the upper downcomer to 15.26 feet, just below the transition section. The lower measurement extends from 15.26 feet to 1.54 feet, just above the downcomer-to-lower reactor vessel plenum crossunder.

The downcomer venturi is designed with identical inlet and outlet cones, allowing forward and reverse flow measurements. Four differential pressure transmitters are used for the flow rate measurement. The transmitters are spanned to cover overlapping forward flow rate ranges up to 100 percent scaled primary flow and low reverse flow rates. Limit switch indications on the low and mid range forward flow transmitters and on the reverse flow transmitter confirm when each is within its calibrated differential pressure range.

Tap-to-tap differential pressure measurement continuity for the primary loop is preserved through the downcomer using transmitters which connect to pressure taps outside the downcomer. These transmitters allow measurement of irrecoverable pressure drop around the primary loop.

A final differential pressure transmitter spans the upper downcomer at the cold leg discharge nozzle elevation. This transmitter measures loop-to-loop pressure asymmetries. Pressure taps for this measurement are located in the Loop A1 and B2 cold leg nozzles as shown by Section A/A of Figure 2.17.

Guard Heater Measurements. Heat input to the downcomer pipeguard heaters is adjusted to maintain an approximately adiabatic boundary condition at the pipe wall. Three guard heater control zones are used in the MIST downcomer. The zone boundaries are chosen to enclose areas of similar heat transfer characteristics. The uppermost zone extends from the top of the downcomer to the cold leg discharge nozzles and includes the vent valve piping downstream of the valves themselves. The middle zone extends from the cold leg discharge nozzles to the top of the lower downcomer, including the transition. The lowest zone covers the entire lower downcomer region, including the downcomer-to-lower plenum crossunder piping.

Pipe wall metal and insulation temperatures are recorded at the midline of each zone. Required power input is also recorded. Redundant wall metal and insulation temperatures are used for guard heater power control. A metal temperature measurement on the upper downcomer head plate provides an indication of thermal storage and release for this metal mass.

Cooled Thermocouple Measurement. A cooled thermocouple probe was installed in the lower MIST reactor vessel downcomer at an elevation of 2.28 feet. The probe was intended to measure low flow rates near stalled conditions. The probe is also theoretically able to distinguish flow direction when both upstream and downstream thermocouples are in service.

2.2.3 Reactor Vessel Vent Valves

Reactor vessel vent valves in Babcock & Wilcox plants are intended to vent core-generated steam to the reactor vessel downcomer under abnormal operating conditions. Eight valves are typically located in the core barrel wall, separating the reactor vessel upper plenum and the downcomer. Weighted, hinged disks close during normal plant operating conditions and open during abnormal transients.

The vent valves play a significant role in abnormal transients without forced circulation. Under these conditions, pressure differentials sufficient to open the vent valves develop between the reactor vessel upper head and the downcomer, providing a direct flow path into the upper downcomer. The resulting interaction between vented upper head fluids and colder emergency core cooling fluids provides an effective mode of core heat removal, sufficient to offset primary loop repressurization during certain transients.

Plant vent valves begin to open with a differential pressure of approximately 0.125 psid across the valve and achieve their full open position at approximately 0.26 psid. Once open, the valves reseat at approximately 0.04 psid. Between 0.04 psid and 0.26 psid, valve open angle and hydraulic resistance vary as a function of differential pressure.

2.2.3.1 Reactor Vessel Vent Valve Design. The external MIST reactor vessel downcomer configuration supports the use of four reactor vessel vent valves. Each vent valve admits fluid to an upper downcomer quadrant and simulates two plant vent valves. Relevant vent valve operational characteristics are opening differential pressure, flow rate versus differential pressure, convective energy transport, and time response. Positive vent valve closure and the ability to make relevant measurements are required. A symmetric valve arrangement is also required to preclude design-imposed fluid condition asymmetries.

The MIST reactor vessel vent valve circuit is symmetrically arranged as illustrated in Figure 2.20. The common lines between the reactor vessel and the individual vent valve lines are fabricated from 1-1/2-inch, schedule 80 pipe with an inside diameter of 1.500 inches. Each individual vent valve line empties into an associated downcomer quadrant and is fabricated from 1-inch, schedule 80 pipe with an inside diameter of 0.957 inch. Remotely actuated, 1-inch Edwards sealed-stem valves, in the individual vent valve lines, ensure positive closure and maintain primary loop leak tightness.

The MIST reactor vessel vent valves are atypically limited to open or closed operation by the requirement for positive closure. A plant-typical hinged disk valve arrangement, scaled for MIST, could simulate variable flow resistance, but would be prone to erratic operation. Leakage across these valves would be likely and difficult to quantify. Edwards sealed-stem valves are expected to open and close reliably for several thousand cycles.

Valve actuation is based on the measured differential pressure between the reactor vessel upper plenum and the downcomer quadrant associated with each vent valve. The valves open at a nominal difference of 0.125 psid (reactor vessel minus downcomer quadrant) and close at 0.040 psid. The valves can be actuated independently or in unison based on a single differential pressure signal.

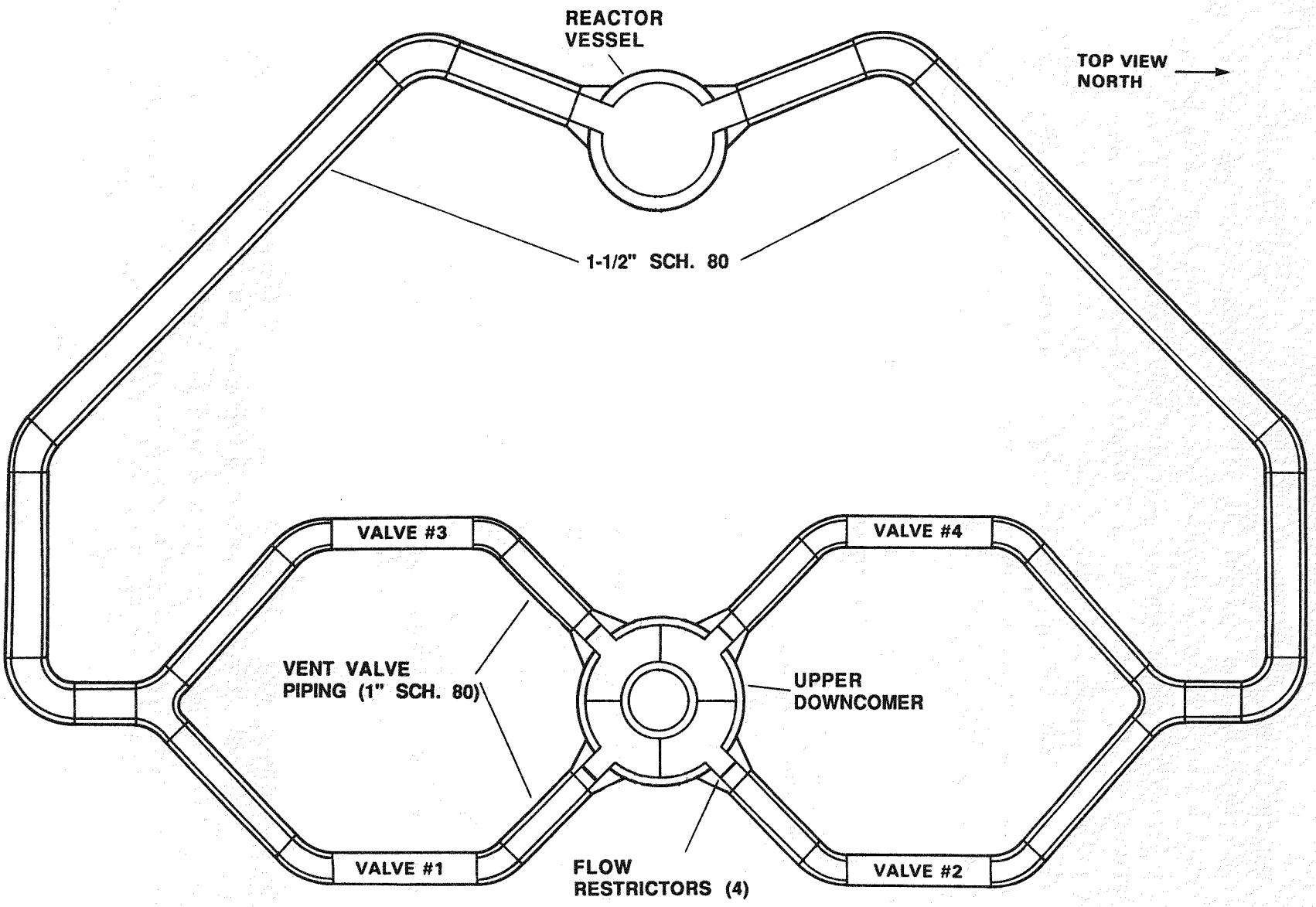

Figure 2.20 Reactor Vessel Vent Valve Simulation

The MIST vent valve simulation provides limited head-flow typicality. Plant vent valves open at 0.125 psid and exhibits a continuously varying resistance to flow up to 0.26 psid, at which point the vent valve is fully opened and a fixed pressure loss coefficient is achieved. MIST vent valves achieve a full open, fixed loss coefficient immediately upon opening at 0.125 psid. Compared to partially opened plant vent valves, the fully opened MIST valves may relieve the developed pressure difference more quickly, increasing the potential for atypical cycling. To reduce this potential, a slotted orifice located at the discharge of each vent valve line into the downcomer increases MIST hydraulic resistance to approximately ten times greater than the plant. For this resistance, valve actuation setpoints of 0.125 psid and 0.040 psid produce valve operating characteristics similar to the plant in single-phase natural circulation. The influence of the MIST vent valve simulation on primary flow is compared to the corresponding plant vent valve influence in Figure 2.21.

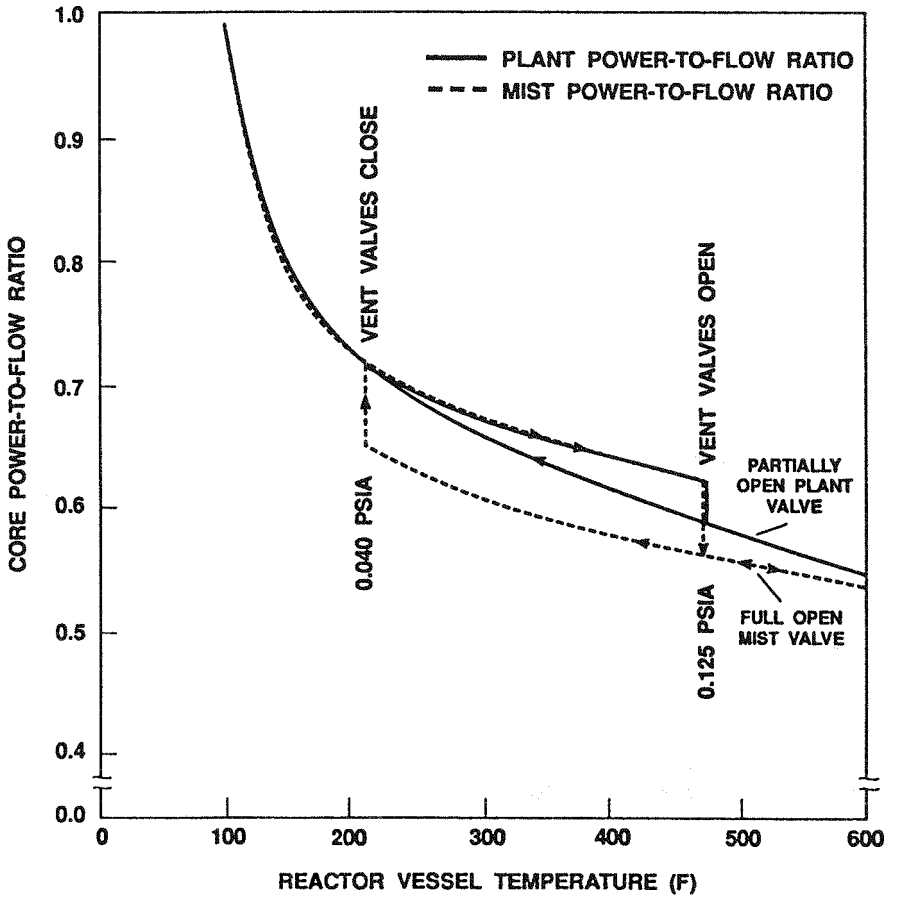

Figure 2.21 Effect of RVVV Setpoints on Core Power-to-Flow Characteristic

Figure 2.21 shows the results of an evaluation of vent valve characteristics during single-phase natural circulation. With the vent valves closed, the natural circulation flow rate (through the core) and the core power are related by a simple ratio which varies with fluid temperature. The relationship is shown in Figure 2.21 as the core power-to-flow ratio. As the fluid temperature increases, so does the differential pressure across the vent valves. At 0.125 psid, the plant vent valves open partially. The open vent valves increase the natural circulation flow rate in the core, and the core power-to-flow ratio abruptly decreases at 0.125 psid. During a cooldown from an open vent condition, the plant core power-to-flow ratio varies continuously since the valve position decreases with pressure difference and reaches full closed at 0.04 psid. On the heatup cycle, the MIST vent valves achieve the plant-typical core power-to-flow ratio characteristic until the vent valves open at 0.125 psid. Because the MIST vent valves open fully, the core power-to-flow ratio drops to a characteristic lower than plant-typical. On the cooldown cycle, the MIST vent valves remain on the full open characteristic until the vent valve differential pressure reaches 0.04 psid. Upon closing, the MIST circuit regains the plant-typical core power-to-flow ratio characteristic.

The vent valve discharge orifice design is illustrated in Figure 2.22. Although liquid-vapor separation in the reactor vessel upper plenum is expected to be highly efficient, two-phase conditions are expected in the lines when the liquid level in the reactor vessel approaches the vent valve elevation. A vertical slot orifice is used in the vent valve lines to minimize impact on stratified liquid and vapor phases. Slot dimensions are 0.095 inch in width by 0.957 inch in height. Total hydraulic resistance for the vent valve simulation is dominated by the resistance of these orifices.

The energy content of fluid convected through the plant vent valves is a function of elevation, the de-entrainment characteristics for the reactor vessel internals, and the vertical dimension of the valves. For MIST, the vent valve connections to the reactor vessel and downcomer are located so that the plant typical spillover elevation of 24.17 feet, which occurs at the valve seats, is preserved. Also, the design of the MIST reactor vessel internals preserves plant de-entrainment characteristics. However, the MIST vent valve

simulation is less likely than the plant to entrain liquid in predominantly vapor flow due to reduced entering flow velocity and vent valve height for MIST. Therefore, plant typical vent valve fluid energy content is preserved for single-phase liquid and vapor conditions, but may not be preserved for two-phase conditions.

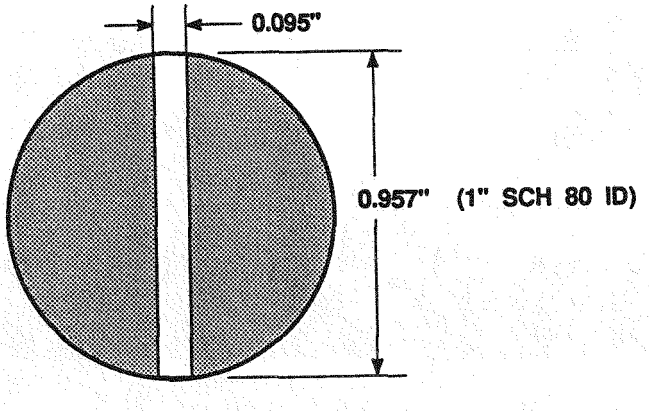

Figure 2.22 Reactor Vessel Vent Valve Slotted Orifice

In addition to supporting plant typical fluid energy transport, preserving the reactor vessel vent valve spillover elevation and other critical reactor vessel and downcomer elevations results in plant typical natural circulation driving forces for the inner reactor coolant flow loop. Figure 2.23 details the internal geometry of the 1-inch Edwards valves.

Fluid transit time for reactor vessel fluid through the vent valves to the MIST external downcomer is atypical of the plant. The MIST reactor vessel vent valve circuit is designed to minimize this atypicality. First, the piping upstream of the vent valves is guard heated to approximate reactor vessel upper head temperature. This effectively extends the reactor vessel boundary to the inlet of the four valves. In addition, the valves are positioned as close to the downcomer as physically possible. This minimizes the delay after opening the vent valves, before fluid at reactor vessel conditions reaches the downcomer.

The reactor vessel vent valve actuators are equipped with high-capacity solenoids which allow the valves to open or close in less than 1 second. This further reduces fluid transit time as well as reducing atypical valve cycling.

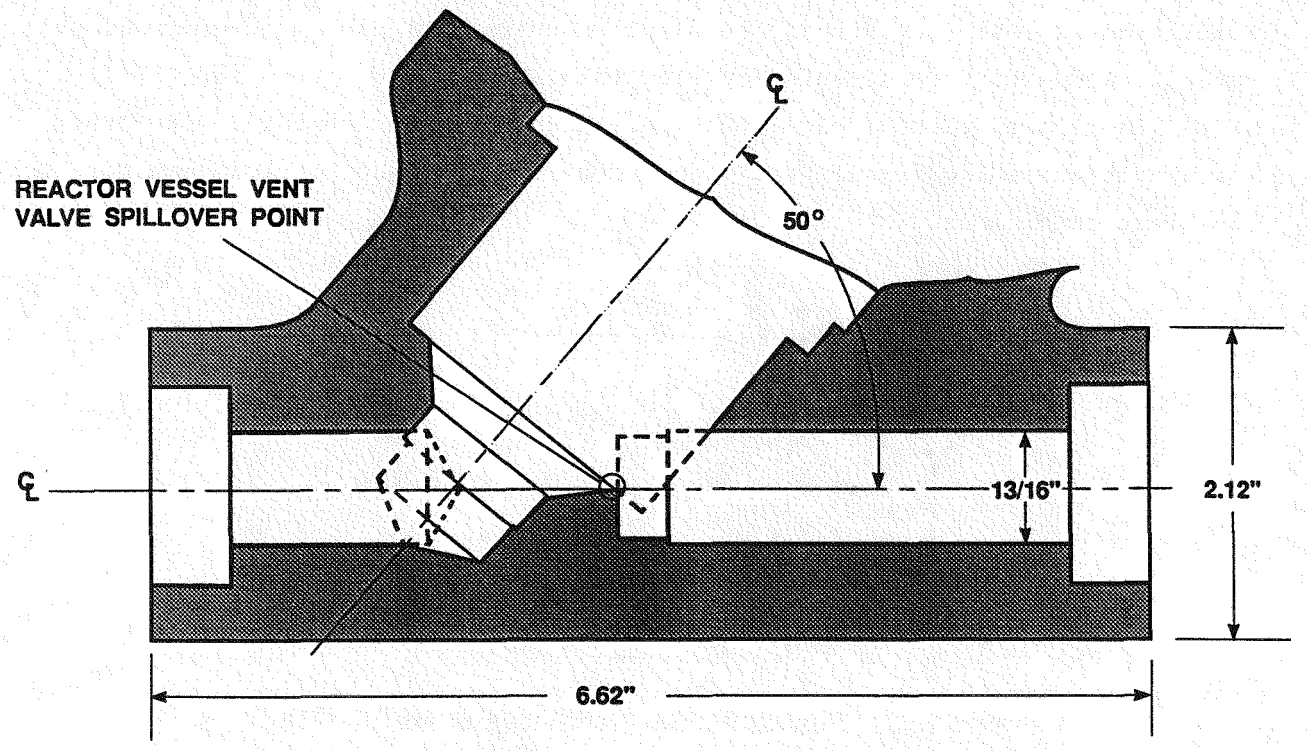

Figure 2.23 Internal Geometry of Isolation Valves in RVVV Simulation

2.2.3.2 Reactor Vessel Vent Valve Characterization. Reactor vessel vent valve actuation and control were characterized in liquid and vapor conditions. Results of the characterization are noted briefly in this section and expanded upon in Section 6. Automatic, independent control of the vent valves was determined to be the desired mode of vent valve operation in preference to automatic, ganged control, manual control, or a combination of control modes.

Individual valve open and close setpoints were adjusted to within 0.006 psi of the required setpoints (0.125 and 0.040 psid). The repeatability of the setpoints was demonstrated as was the adequacy of the associated control system. The actual differential pressure at valve actuation varied slightly depending on whether liquid or vapor conditions prevailed at the vent valves. This effect resulted due to a slight difference in pressure tap elevations between the reactor vessel upper plenum and the downcomer.

The vent valves were shown generally to actuate in order of their individual setpoints rather than in response to imposed loop asymmetries. This indicated that the pressure difference supported between downcomer quadrants was small compared to the tolerance on the vent valve actuation setpoints.

The vent valves were shown to operate in a stable manner and not prone to cyclical behavior. The reduction in differential pressure due to valve opening was generally insufficient to result in rapid reclosing of the valve, or valves for ganged control.

2.2.3.3 Reactor Vessel Vent Valve Instrumentation. The reactor vessel vent valve simulation is instrumented to record fluid temperatures, differential pressures, flow rates, and guard heater data. Instruments associated with the vent valve simulation are classified as reactor vessel or downcomer instrumentation depending on location relative to the valves. Locations for vent valve instruments are defined in Figure 2.24.

Fluid Temperature Measurements. Fluid thermocouples are positioned immediately upstream and downstream of the vent valves, inserted to the centerline of the individual flow paths. These thermocouples confirm positive valve closure in addition to recording individual vent valve line fluid temperatures. Reactor vessel vent valve thermocouples are 0.063 inch, ungrounded, Type J with an approximate time constant of 5 seconds.

Differential Pressure Measurements. Four transmitters record the differential pressure between the reactor vessel upper plenum and each individual downcomer quadrant. A common tap at the reactor vessel wall supplies the high pressure signal to all four transmitters. Individual taps, in the downcomer quadrant associated with each vent valve line, supply low side pressure signals. All pressure taps are positioned at the same nominal elevation of 24.21 feet, although very small differences in the final installed elevations do exist. Each transmitter is spanned from -4 to 26 inches of cold water (-0.144 to 0.939 psid).

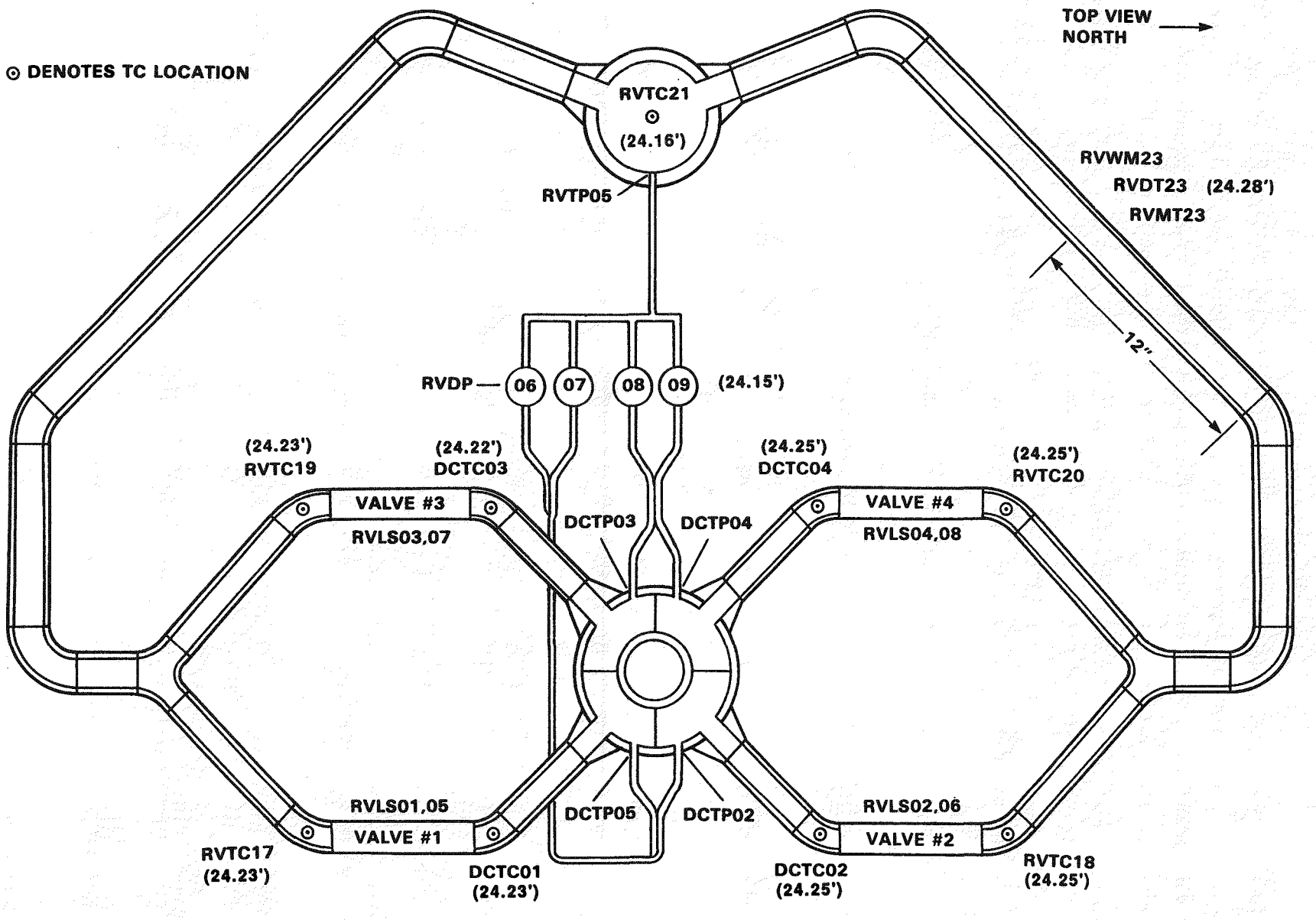

Figure 2.24 Reactor Vessel Vent Valve Instrumentation

Differential pressures measured by the four transmitters signal actuation for the four reactor vessel vent valves. At measured differential pressures of 0.125 psid, plant air is supplied to the "normally closed" vent valve actuators, opening the valves. At 0.040 psid, oversized solenoid valves quickly exhaust the actuator air, allowing the vent valves to close. Open and close times are less than 1 second for the vent valves.

Measured differential pressure between the reactor vessel upper plenum and each downcomer quadrant is also used to compute vent valve flow rates. Loss coefficients for flow paths through each valve in the fabricated vent valve assembly were determined as a function of Reynolds number prior to final installation in the MIST Facility. Pipe sections, typical of reactor vessel and downcomer geometry were used to maintain entrance and exit loss similarity for the vent valve calibration.

Limit Switch Indications. Eight limit switches are used to define the state of the MIST reactor vessel vent valves. Two limit switches are associated with each valve; one to indicate a fully opened condition and one to indicate a fully closed condition. A negative indication from both limit switches indicates a partially opened, or transient condition.

Guard Heater Measurements. The reactor vessel vent valve simulation is guard heated using one control zone and part of another. The portion of the vent valve assembly upstream of the valves to the reactor vessel wall makes up one full control zone. Control metal and differential temperature measurements are located as shown in Figure 2.24, in one of the two common vent valve lines. A control differential temperature of 0.0°F is used to maintain fluid in this piping at reactor vessel upper plenum conditions.

Reactor vessel vent valve piping downstream of the valves is guard heated as a part of the uppermost downcomer control zone. Control instrumentation for this zone is located in the upper downcomer and was discussed previously.

2.3 HOT LEGS

The hot legs carry effluent from the reactor vessel nozzles to the inlet of each steam generator. The two hot legs are identical except for the pressurizer surge line connection on the A loop hot leg and instrument placement. Primary coolant flow exits the reactor vessel at the hot leg nozzles and flows horizontally for a short distance before turning upward. At an elevation above the steam generator inlets, the hot legs bend 180 degrees and carry flow downward to the steam generators.

Several hot leg characteristics are significant to small break loss of coolant transients. Two-phase behavior, critical elevations, wall effects, and fluid volume in the hot legs are significant to hot leg U-bend voiding, interruption of steam generator heat transfer, and subsequent primary loop repressurization. Critical elevations and wall effects are important to primary refill, spillover at the U-bends, and re-establishment of natural circulation. Critical elevations and hot leg irrecoverable pressure drop are important to primary loop natural circulation.

2.3.1 Hot Leg Design

The MIST hot legs are illustrated in Figure 2.25 and compared to the plant hot legs. Each MIST hot leg is fabricated from 2-1/2-inch, schedule 80 pipe with an inside diameter of 2.323 inches. The hot leg nozzles are centered at a nominal elevation of 21.25 feet and extend horizontally 0.40 foot before turning upward. The radius of curvature for the upward bends is 1.61 feet. Vertical risers extend to 64.95 feet; the beginning of the hot leg U-bends.

Each U-bend has a 1.61-foot radius of curvature and a spillover elevation of 66.46 feet. Vertical sections, downstream of each U-bend, extend downward to 53.00 feet to meet the transition to the steam generator upper plenums. Plant-typical natural circulation driving forces for the primary flow loop are maintained by preserving elevations for the hot leg nozzles and the hot leg U-bend spillovers.

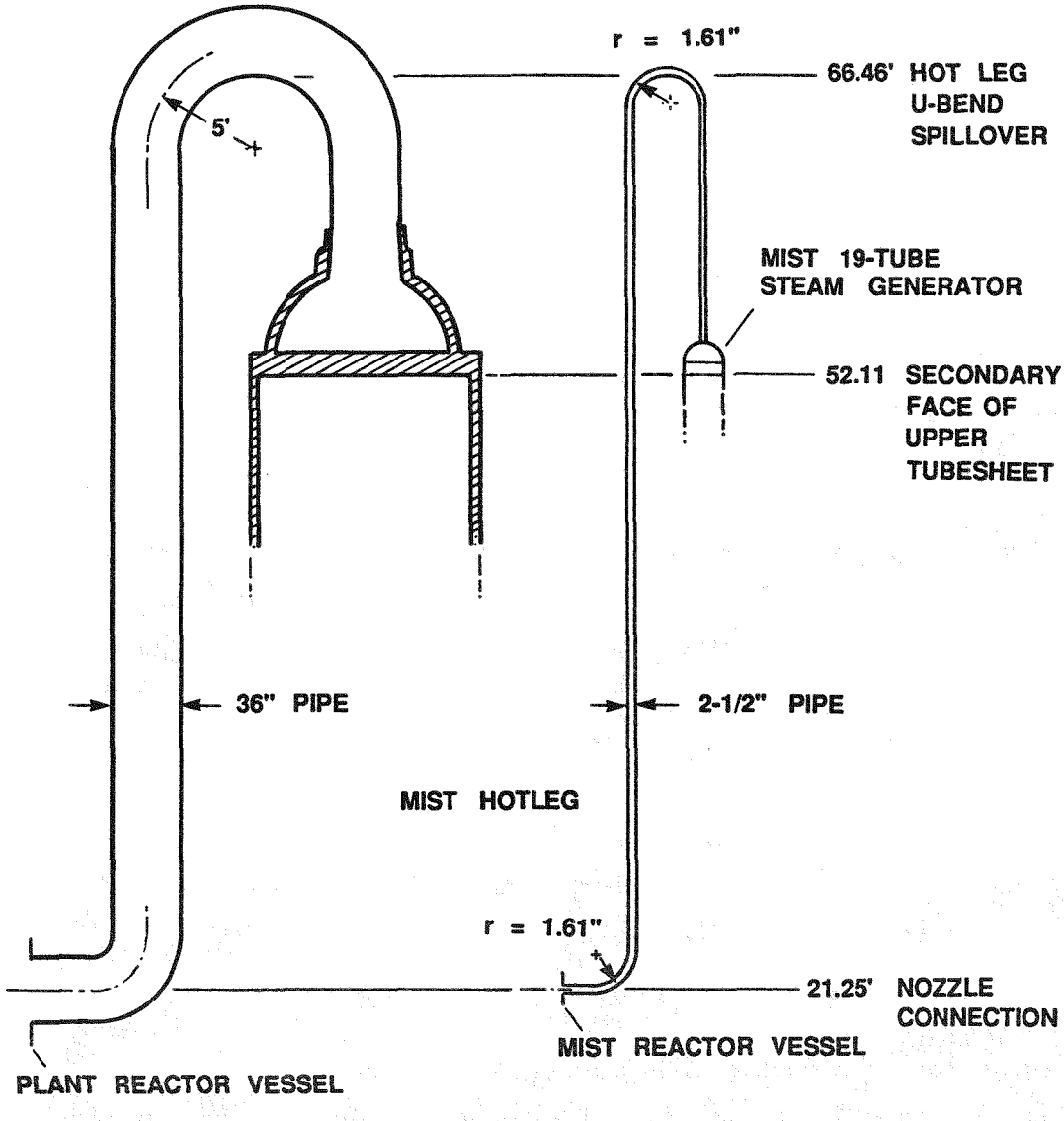

Figure 2.25 Comparison of Plant and MIST Hot Leg Elevations

Different materials are used for the portions of the hot legs upstream and downstream of the U-bends. Inconel 600 is used for the riser portion of each hot leg; 304 stainless steel is used for the U-bend section and the for the straight run downstream of the U-bend. The resulting hot leg differential thermal expansion offsets differential thermal expansion resulting from the use of carbon steel for the steam generator shells and stainless steel for the remainder of the primary loop.

High point vent simulations are installed at the apex of each hot leg U-bend. Critical orifice assemblies control vent flow; typically 1 cm^2, scaled. Detailed MIST boundary system descriptions are provided in Section 3 of this document.

The MIST hot leg design represents a compromise which preserves most significant post-SBLOCA phenomena. In general, scaling to preserve plant two-phase flow regime and irrecoverable pressure drop opposes scaling to preserve plant flow velocities and power-to-volume ratio. Also, wall metal effects on contained fluid volume are increasingly atypical as pipe diameter decreases.

Two-Phase Flow Characteristics. Scaling to preserve the two-phase flow regimes expected for various plant transient scenarios was the most important MIST hot leg design consideration. As discussed below, vertical sections of the MIST hot legs support all expected plant two-phase flow regimes, although transitions between flow regimes may be somewhat delayed.

The MIST hot leg pipe diameter of 2.323 inches is sufficiently large to permit plant-typical bubbly two-phase flow. Vertical pipe diameters of at least 2 inches are required to support "large system", bubbly two-phase flow behavior.

The transition from bubbly to slug flow occurs as core vapor production and hot leg void fraction increase, allowing smaller bubbles to coalesce into larger bubbles. The ratio of core power to hot leg fluid volume is critical to preserving this phenomena. The ratio for MIST is approximately 30 percent of the plant ratio, delaying the transition to slug flow relative to the plant.

The transition to churn two-phase flow results from the interaction between rising vapor slugs and a falling liquid film, causing the slugs to break apart. For MIST-typical hot leg pipe diameters and operating pressures, the interaction is generally responsive to vapor Froude number. Plant-typical vapor Froude number is preserved for a MIST hot leg diameter of 2.46 inches, approximately the diameter of 2-1/2-inch, schedule 80 pipe.

The transition from churn to annular two-phase flow occurs as vapor flow rates increase sufficiently to reverse the direction of the previously downward flowing liquid film. Core vapor production and hot leg void fraction determine vapor flow rates in the hot legs. Therefore, the transition to annular flow occurs at greater core powers for MIST than for the plant due to the relatively lower MIST core power to hot leg fluid volume ratio.

Under the influence of gravitational and centrifugal forces, the MIST hot leg U-bends and upturns act as phase separators. Phase separation by void migration and accumulation at the U-bends is expected to occur more readily in the MIST hot legs than in the plant, based on a comparison of plant and MIST bubble rise times and U-bend transit times. U-bend transit times are similar for the plant and MIST, but rise times are considerably shorter for MIST due to reduced pipe diameter. Void accumulation sufficient to interrupt natural circulation is expected to occur earlier for MIST due to greatly reduced volume above the hot leg spillover elevation.

Two-phase flow regime is expected to develop rapidly in the plant and MIST horizontal hot leg nozzles, permitting fully stratified flow in both. MIST hot leg horizontals and upturns are capable of supporting all expected plant two-phase flow regimes, with atypicalities limited to transitions between flow regimes.

Irrecoverable Pressure Loss. Fluid density gradients and component irrecoverable pressure losses determine primary loop branch flow rates. Plant-typical hot leg irrecoverable pressure loss is preserved for hot leg diameters of about 2.9 inches. The MIST hot leg diameter of 2.323 inches results in irrecoverable pressure losses which are approximately three times greater than plant-typical. Since flow resistance in the hot legs is a relatively small portion of overall primary loop flow resistance, the excess hot leg resistance has a minor effect on primary flow rates and the flow split between the inner flow loop and the outer flow loop.

Wall Effects. Energy storage in pipe wall metal is critical to hot leg voiding and the interruption of natural circulation. Ratios of fluid volume

to metal volume for the plant and MIST hot legs are roughly the same: 2.2 for the plant and 1.9 for MIST. Therefore, the influence of stored energy in pipe wall metal on hot leg fluid is approximately plant-typical.

Fluid Volume. MIST hot leg fluid volume, using 2.323-inch diameter pipe, is 3.4 times greater than power-scaled. As noted above, this delays the transition between certain two-phase flow regimes and also impacts the timing of transient initiation and hot leg U-bend voiding events. However, the increased hot leg diameter permits all expected plant two-phase flow regimes and minimizes atypicalities in irrecoverable pressure drop and wall energy storage.

2.3.2 Hot Leg Instrumentation

Hot leg instrumentation includes fluid temperature measurements, metal and differential temperature measurements, measurements of total guard heater power, differential pressure measurements, gamma densitometers and conductivity probes. Viewport cameras record video data at critical locations in each hot leg.

Instrument locations and installation details are defined in Figure 2.26. Instrumentation installed in the hot leg with the pressurizer surge line connection (A loop) is designated as "H1"; instrumentation in the opposite hot leg (B loop) is designated as "H2". The hot legs are essentially symmetric in instrument layout with one additional differential pressure transmitter installed in hot leg 2.

A total of 121 instruments were recorded by the MIST data acquisition system, including: 38 fluid thermocouples, 31 differential pressure transmitters, 20 conductivity probes, eight wattmeters, eight metal thermocouples and differential temperature pairs, four gamma densitometer signals, two resistance temperature detectors, and two limit switches.

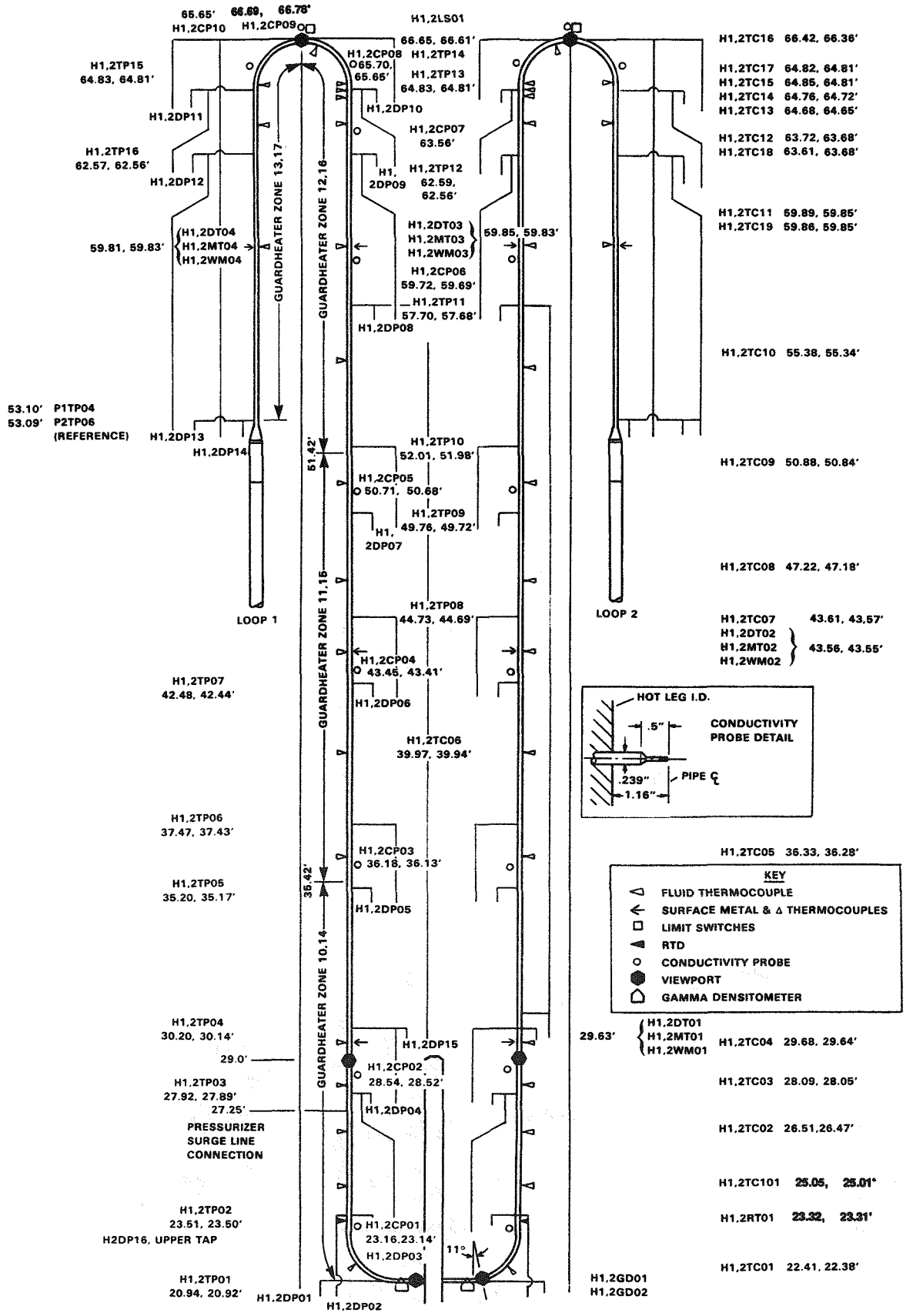

Figure 2.26 Hot Leg Instrumentation

Fluid Temperature Measurements. Nineteen fluid thermocouples and one resistance temperature detector are installed in each hot leg to record local fluid temperatures and indicate thermal and density gradients. As shown in Figure 2.26, at least one fluid temperature measurement is associated with each narrow range differential pressure transmitter. Measurements are grouped more densely in areas of developing or changing temperature profiles, especially in the region of the pressurizer surge line connection. In addition, three closely spaced thermocouples at the beginning of each U-bend provide thermal gradient information, near the fluid interface, as the hot leg level approaches spillover.

One resistance temperature detector is located in each hot leg riser, immediately downstream of the upturn. Along with steam generator inlet resistance temperature detectors, these are used as reference measurements for in-place hot leg thermocouple calibrations.

Hot leg thermocouples are 0.063-inch, ungrounded, Type J with a time constant of approximately 5 seconds. Each thermocouple is formed, as shown in Figure 2.27, prior to installation and inserted to a depth of 0.612 inch. This installation procedure avoids thermocouple damage due to flow induced vibrations in forced flow. Resistance temperature detectors are 1/4 inch in diameter with an approximate time constant of 5.5 seconds. Each is inserted to the pipe centerline.

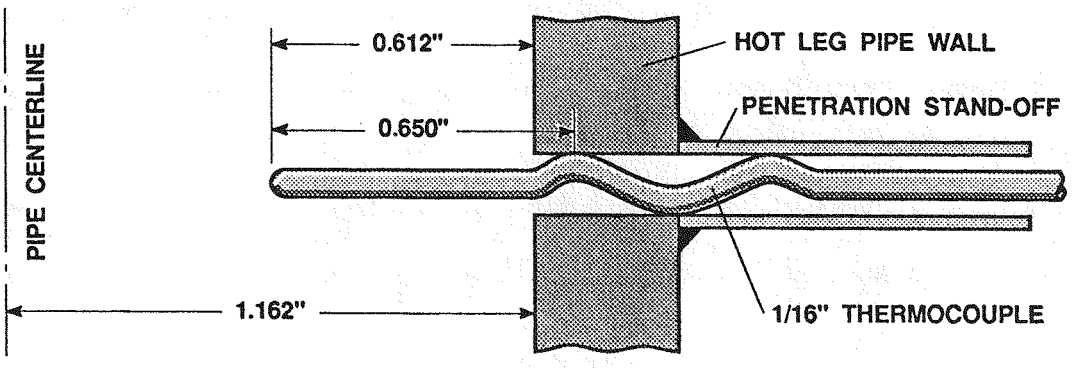

Figure 2.27 Hot Leg Fluid Thermocouple Installation

Differential Pressure Transmitters. Fifteen differential pressure transmitters are installed in the A loop hot leg (H1) and 16 are installed in the B loop hot leg (H2). With the exception of a transmitter spanning the reactor vessel to B loop hot leg nozzle, these transmitters are distributed symmetrically between the two hot legs.

Overall differential pressure transmitters, upstream and downstream of each hot leg U-bend provide input to collapsed fluid level calculations. Additional narrow range transmitters provide input to void fraction calculations at several locations. These transmitters are concentrated around the hot leg upturns and U-bends and are otherwise evenly spaced in the hot leg risers. Void fraction measurements using these transmitters represent an average between pressure taps. Narrow and intermediate range transmitters in both hot legs are summed to provide a check on overall differential pressure measurements.

The differential pressure transmitter spanning the reactor vessel to B loop hot leg nozzle allows characterization of overall primary loop irrecoverable pressure drop. Nozzle symmetry is assumed and no corresponding A loop transmitter is installed. Characterization of primary loop irrecoverable pressure drop is discussed in Section 6.

Conductivity Probes. Ten conductivity probes are installed in each hot leg; most located at midspan for a narrow range differential pressure transmitter. This geometry allows a direct comparison between point void fraction estimates using the conductivity probes and average void fractions using differential pressures. However, the primary function of the conductivity probes is to provide wet or dry indications.

Conductivity probe sensing tip geometry is illustrated by the inset for Figure 2.26. All probes, except at the hot leg high point, are inserted to the pipe centerline. The probes located at each hot leg high point define phase for high point vent effluent and are positioned as shown in Figure 2.28. The probes is designed to minimize metal mass.

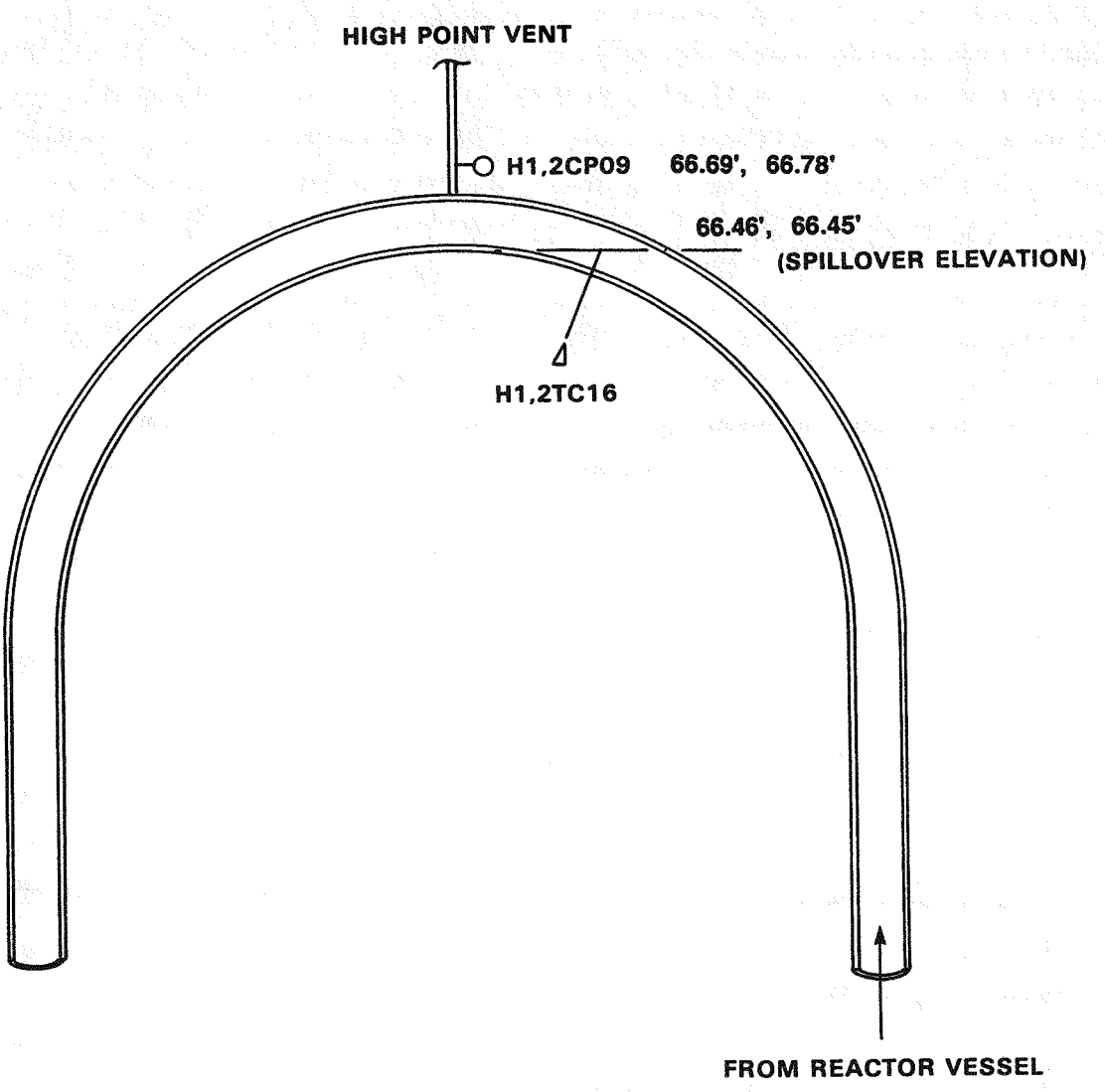

Figure 2.28 Hot Leg Detail at U-Bend

Guard Heater Measurements. Four guard heater control zones are used for each MIST hot leg. Three zones of approximately equal length are used upstream of each U-bend high point. The lowest zones extend from the hot leg nozzles to 35.42 feet (relative to the secondary face of the lower tubesheet). The middle zones extend from 35.42 to 51.42 feet. The top zones extend from 51.42 feet to the top of the U-bends.

One zone is used for each hot leg stub, extending from the top of the U-bends to the steam generator inlets. Pipe wall metal and insulation temperatures are recorded near the the midline of each zone. Required power input is also recorded.

Gamma Densitometers. Dual-beam gamma densitometers are installed in each horizontal hot leg nozzle, as shown in Figure 2.26. The MIST densitometer design is presented in Figure 2.29. A gamma photon source, embedded in each densitometer spool piece, emits in all directions and a statistically known fraction is counted by each of two associated detectors for an empty pipe. The presence of fluid between the source and the two detectors reduces the fractions of gamma photons counted. This reduction is directly proportional to the density of the fluid in the photon path. The use of two beams and the choice of beam orientation optimizes the accuracy of the cross sectional average density calculation.

Viewports. Three viewports are positioned in each of the two hot legs; one at each U-bend, one in each hot leg riser at approximately 29 feet, one in the hot leg A horizontal, and one 11 degrees into the hot leg B upturn. Viewports at the hot leg U-bends are oriented so that the lower pipe surface at the spillover is in view. The field of view for the riser viewports includes the hot leg pipe centerline. Viewports in the horizontals allow definition of flow regime in the vicinity of the gamma densitometers.

Video cameras allow monitoring of hot leg activity including the presence or absence of circulation and flow regime. Video recorders preserve image data at each viewport for post-test review.

Limit Switches. Limit switches are used to define the state of the simulated hot leg high point vents. One limit switch is associated with each high point vent to indicate an open or closed condition.

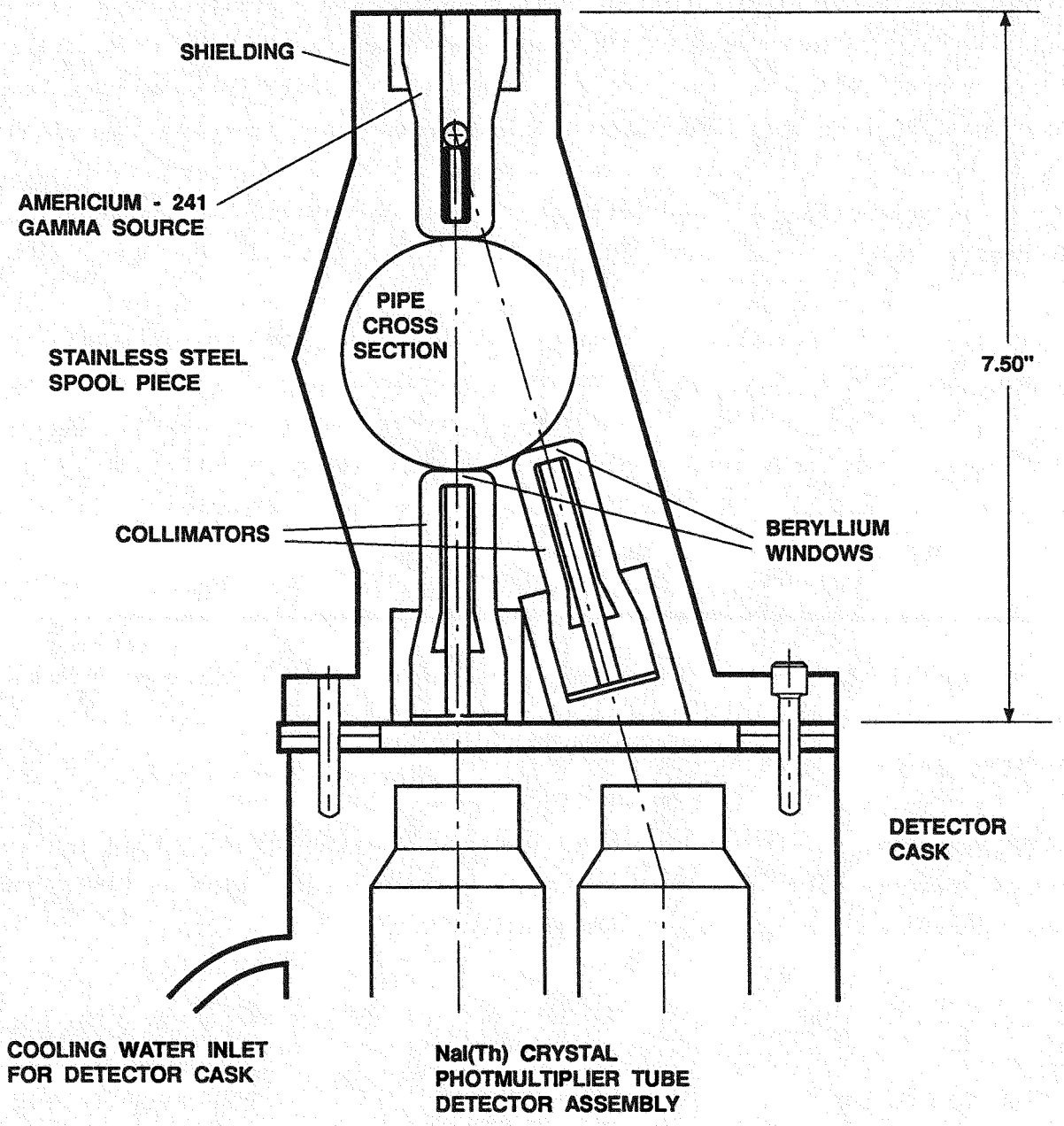

Figure 2.29 MIST Gamma Densitometer Design

2.4 STEAM GENERATORS

Plant Once-Through Steam Generators contain 15,531 straight tubes which carry primary reactor coolant flow. Heat transfer across the primary tubes heats secondary inventory flowing around the tubes. During normal operation, secondary feedwater is injected into a downcomer where it is preheated to saturation by aspiration of secondary steam. The preheated feedwater then flows into the generator, just above the lower tubesheet. During auxiliary feedwater operation, unheated feedwater is injected directly into the tube bundle near the top of the steam generator through a feed ring.

Several scaling characteristics are relevant to the MIST steam generator design for post-SBLOCA events. Critical steam generator elevations and heat flux distribution impact natural circulation driving forces and steam generator heat removal. Multi-dimensional auxiliary feedwater wetting effects and wall effects, including ambient heat losses, fluid-to-metal coupling, metal energy storage, and conduction, also impact steam generator heat removal. Fluid volume impacts the ratio of power to volume and transient timing.

2.4.1 Steam Generator Design

The MIST Facility includes two 19-tube steam generators, identical to one another in all respects except instrumentation. Each steam generator is a full-length subsection of the plant counterpart. For each, primary flow enters at the top, flows downward through 19 plant-typical Inconel 600 tubes, and exits at the bottom. Flow distributor plates in each inlet plenum promote uniform flow distribution to the 19 tubes. The ratio of the number of plant to MIST steam generator tubes defines the MIST scaling factor of 817. Key connections and elevations are illustrated in Figure 2.30. As indicated, elevations are referenced to the secondary (upper) face of the lower tubesheet.

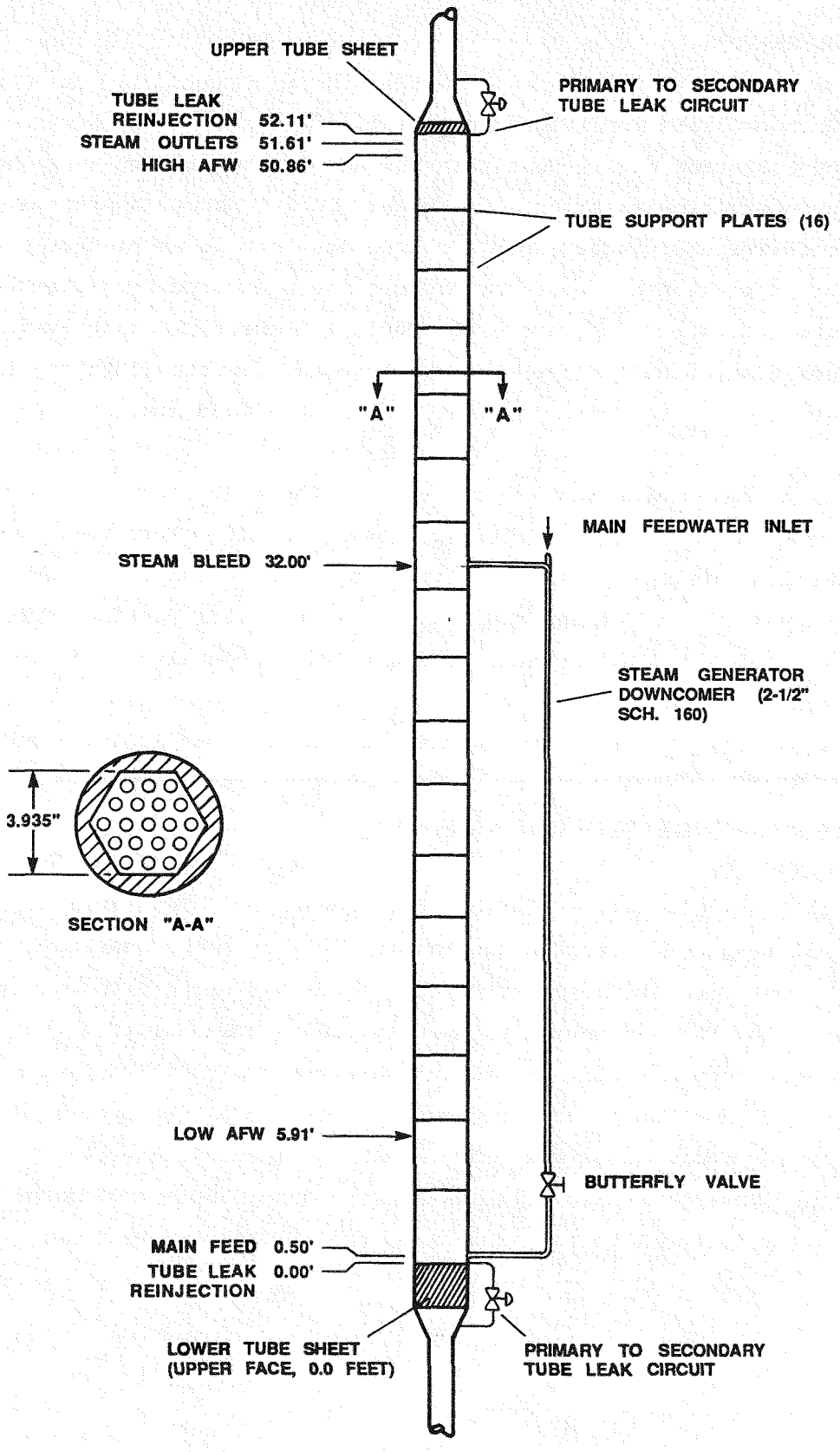

Figure 2.30 MIST Once-Through Steam Generator

The steam generator tubes have an outside diameter of 5/8 inch and are arranged on a triangular pitch of 7/8 inch, as shown in Section A-A of Figure 2.30. Inside tube diameter is 0.577 inch. Sixteen 1-1/2-inch carbon steel support plates, spaced approximately 3 feet apart, hold the tube bundle in place. Each tube support plate is drilled to approximate the broached plant hole pattern and area (see Figure 2.31).

Carbon steel tubesheets, 52.11 feet between secondary faces, complete the primary to secondary pressure boundary. Upper and lower tubesheets are 3 and 24 inches thick, respectively, and clad with Inconel 600 on the primary face.

Primary tubes pass through each tubesheet and are seal-welded to the primary faces. The tube bundle, support plates, and tubesheets are enclosed in a hexagonal carbon steel shell, 3.935 inches between flat faces, to maintain plant-typical secondary flow cell geometry.

Full-length scaling for the MIST steam generators supports plant-typical natural circulation driving forces for both primary and secondary systems. Also preserved are sensible and boiling heat transfer regions, heat transfer to secondary steam, and the saturated pool and enhanced heat transfer to entering auxiliary feedwater.

Plant-typical steam generator elevations and internal flow cell geometry result in plant-typical heat flux distributions. Primary and secondary power-scaled fluid volume are also preserved as are internal steam generator wall effects and primary-to-secondary coupling. Active guard heating maintains a nearly adiabatic secondary boundary.

As for other reduced scale MIST components, steam generator shell metal mass is atypically large, possibly delaying some post-SBLOCA transient events. The ratio of fluid to shell metal volume is approximately four times greater than for the plant. In addition, secondary fluid-to-shell coupling is atypical, with the ratio of peripheral to internal flow cells greater than the plant.

19-TUBE OTSG TUBE SUPPORT PLATE (DRILLED)

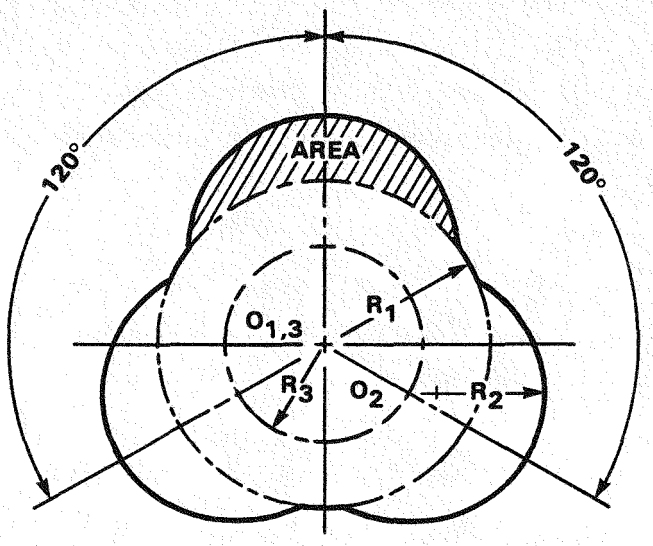

R_1 (IN.)	R_2 (IN.)	R_3 (IN.)	AREA (IN.)
0.32031	0.250	0.1907	0.051518

FULL SIZE OTSG TUBE SUPPORT PLATE (BROACHED)

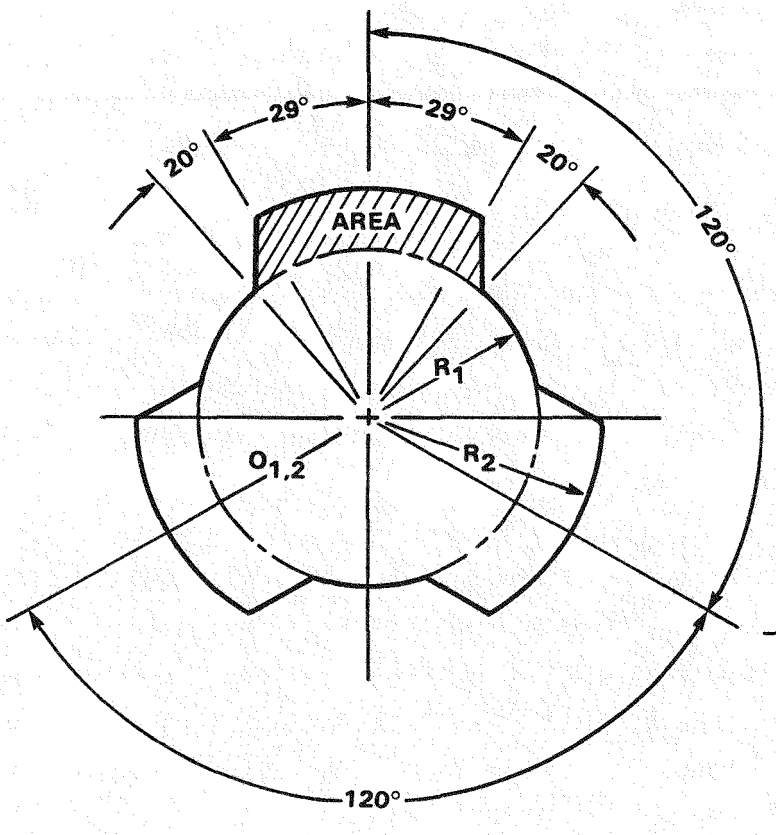

R_1 (IN.)	R_2 (IN.)	AREA $(IN.)^2$
0.323	0.430	0.051866
0.320	0.430	0.053075
0.320	0.427	0.051445
0.323	0.427	0.050233

Figure 2.31 Comparison of MIST and Plant Tube Support Plate Geometry

Each steam generator is equipped with an aspirating downcomer, fabricated from 2-1/2-inch, schedule 160 pipe with an inside diameter of 2.125 inches to preserve power-scaled fluid volume. A butterfly valve in the vertical portion of each downcomer allows variable resistance to fluid flow. Steam bleed and main feed connections to the generator shell are at plant-typical elevations of 32.00 feet and 0.50 foot, respectively.

Plant-scaled, auxiliary feedwater injection is available according to the head-flow characteristic of Figure 2.32. Manual and constant automatic flow control modes are also available for auxiliary feedwater. Injection sites are installed at 5.91 feet and 50.86 feet, with the high elevation injection nozzles plant-typically located relative to the highest tube support plate. The low elevation injection site is typical of a 205-FA plant, and was not used in the MIST test program. As in the plant, auxiliary feedwater is injected cold into the steam generator.

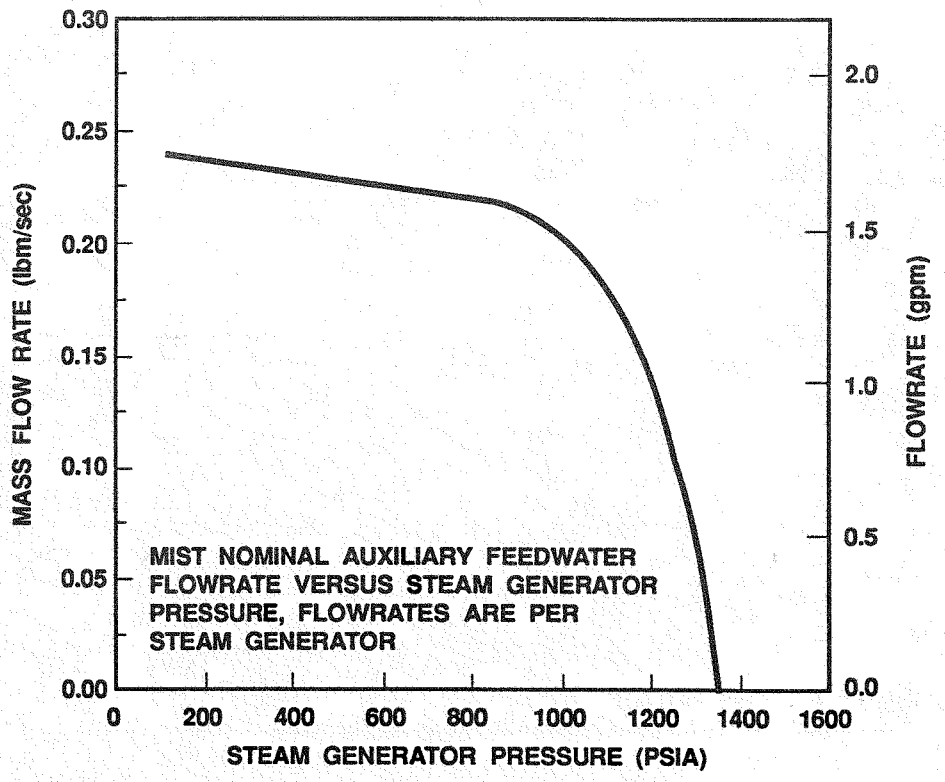

Figure 2.32 MIST Auxiliary Feedwater Head-Flow Characteristic

Different auxiliary feedwater dispersion nozzles can be used to bracket feed-induced multi-dimensional heat transfer characteristics. Minimum tube wetting is accomplished using a single 0.430-inch injection nozzle, adjacent to primary tube J in Figure 2.33. MIST test results indicate that tube J is fully wetted and tubes A,B,C,H, and K are partially wetted using the minimum wetting configuration. This is a higher degree of wetting than expected; earlier benchscale tests at atmospheric pressure had indicated that only one tube (J) would be wetted by the minimum wetting nozzle[13].

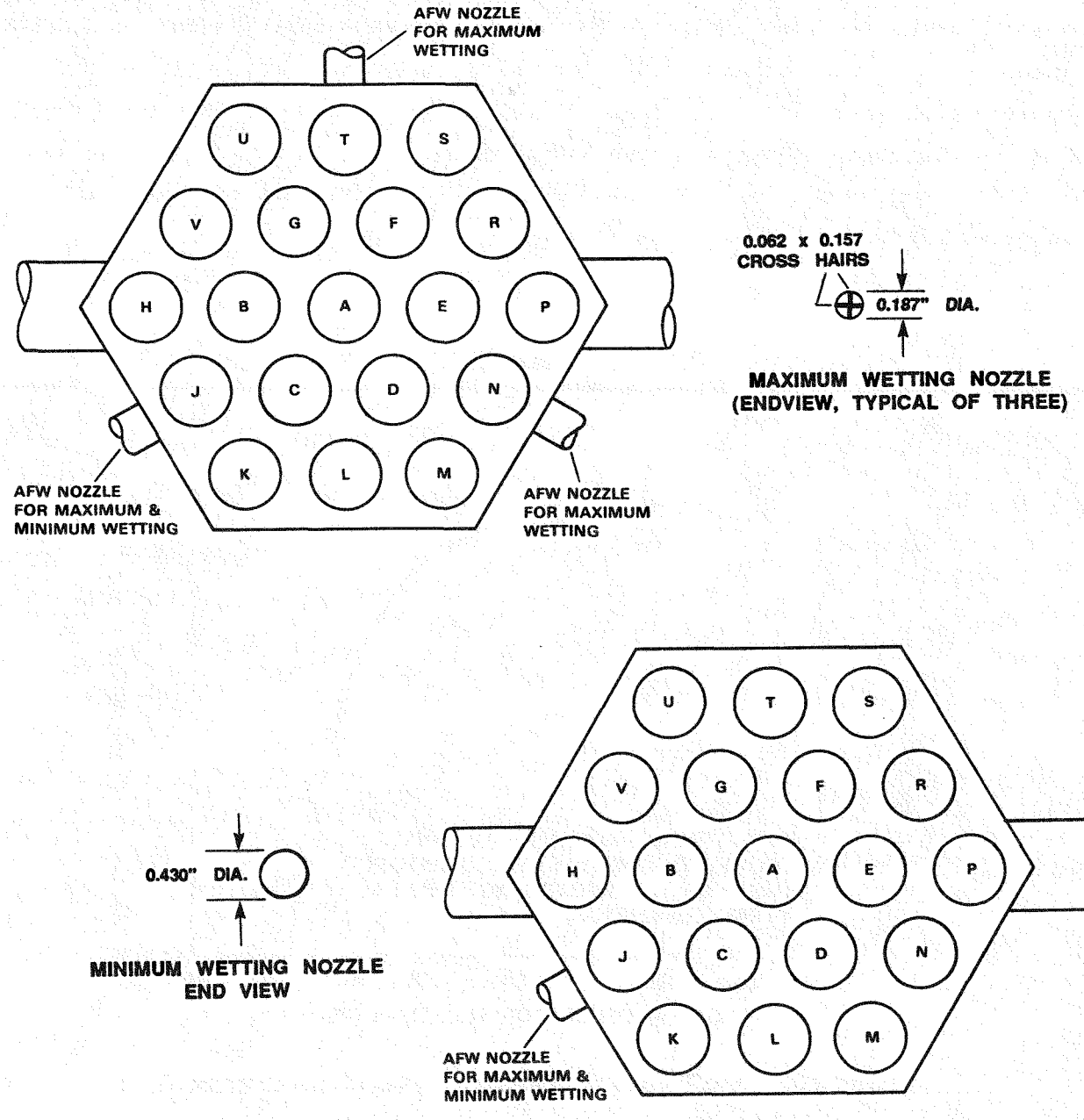

Figure 2.33 Auxiliary Feedwater Nozzle Configurations

Maximum tube wetting is accomplished using injection nozzles adjacent to tubes N and T in addition to the J nozzle. As shown in Figure 2.33, maximum wetting nozzles are 0.187 inch in diameter with 0.062-inch cross hairs. All primary tubes are substantially wetted using the maximum wetting configuration.

The B steam generator includes two simulated primary-to-secondary tube ruptures — one upper elevation and one lower elevation. For the upper tube rupture, primary fluid is taken from the upper plenum and reinjected into the secondary immediately below the upper tubesheet, as shown in Figure 2.34. An analogous arrangement is used for the simulated low elevation tube rupture. Tube rupture flow is controlled by critical flow orifices which are installed to simulate single-tube, single ended breaks or a ten-tube, double ended breaks.

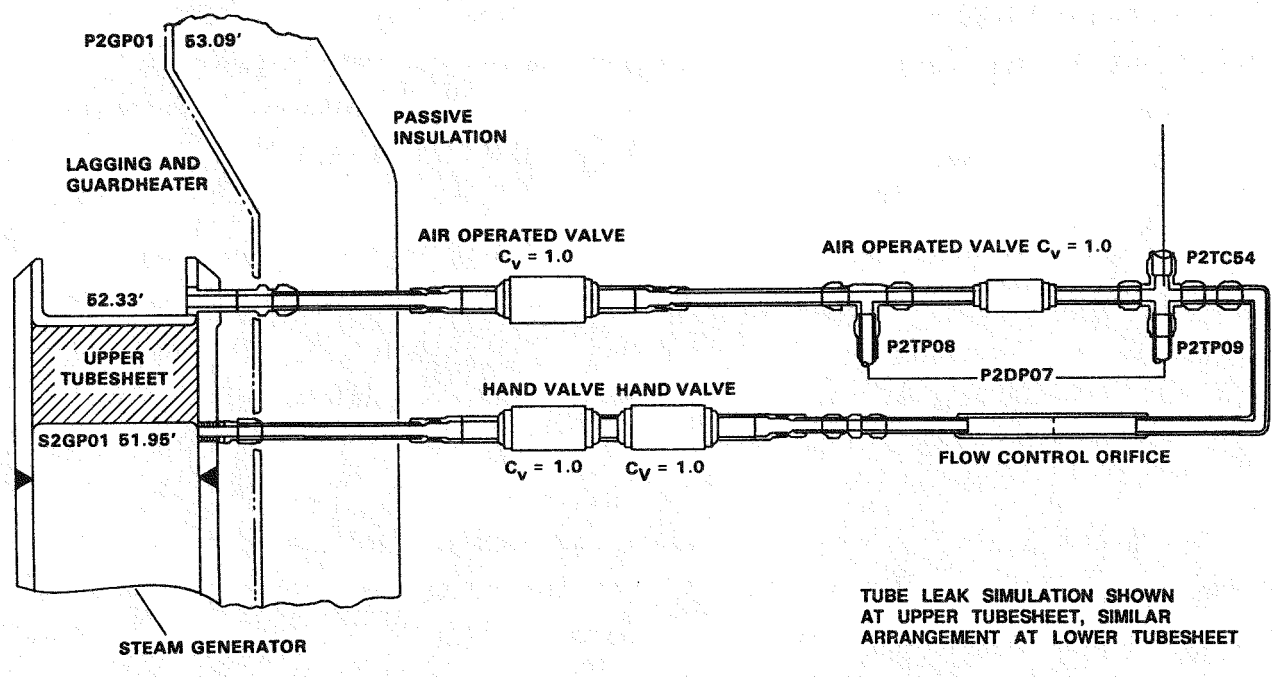

Figure 2.34 Primary to Secondary Tube Leak Simulation

2.4.2 Steam Generator Instrumentation

MIST steam generator instrumentation provided fluid temperatures, metal and differential temperatures, total guard heater powers, differential and gauge pressures, and fluid conductivities. The A steam generator was constructed prior to the MIST program and was instrumented at that time, while the B steam generator was constructed and instrumented specifically for MIST.

2.4.2.1 A-Loop Steam Generator Instrumentation

Ninety-three instruments are recorded by the MIST data acquisition system for the A loop steam generator: 64 fluid thermocouples, seven differential pressure transmitters, six metal thermocouples, five differential temperature thermocouple pairs, five wattmeters, two limit switches, two gauge pressures, and two resistance temperature detectors. Locations and installation details for these instruments are defined in Figures 2.35 and 2.36.

Forty fluid temperature measurements were recorded for the A steam generator. Resistance temperature detectors measure fluid temperatures in the inlet and outlet steam generator plenums. Thirty-eight fluid thermocouples are installed in the primary tubes. String thermocouples, each with 10 axially spaced measurement junctions, are located in tubes J, R, and N, Figure 2.35. Each assembly is inserted through the upper steam generator plenum so that measurement junctions are located between 23.06 and 51.06 feet, more densely spaced near the high elevation auxiliary feedwater injection site. Each measurement point is maintained on tube centerline by a centering spring-wire arrangement. Other primary thermocouples are available at limited locations in the A generator, as shown in Figure 2.36. Fluid thermocouples are also installed in pitot tubes, which are installed in tubes J, R, and N near the lower face of the lower tubesheet, at -2.00 feet (elevation, relative to the upper face of the lower tubesheet).

Tube J and R string thermocouple assemblies contain 0.020-inch individual thermocouples inside a 0.144-inch O.D. sheath. The tube N assembly contains 0.020-inch individual thermocouples inside a 0.125-inch sheath. Pitot tube thermocouples are 0.020 inch in diameter and remaining primary thermocouples are 0.063 inch in diameter. All A steam generator primary thermocouples are Type J and ungrounded.

Twenty-six fluid thermocouples are installed in the A generator secondary at the locations noted in Figures 2.35 and 2.36. Twenty-four of these thermocouples record fluid temperature in secondary flow channels, over the full length of the generator. The two remaining thermocouples record fluid temperature in the steam generator downcomer; at the steam bleed and main feedwater nozzle elevations.

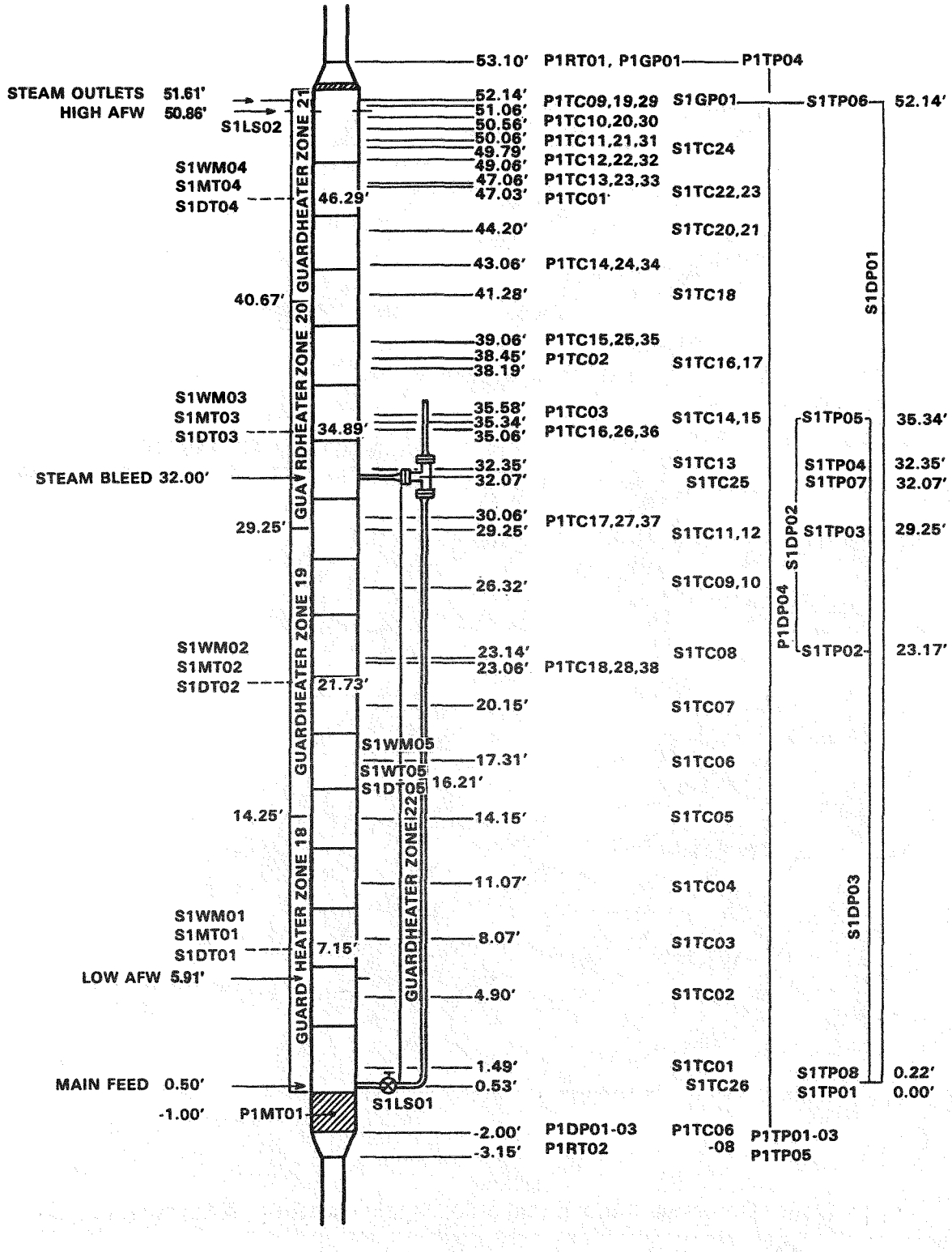

Figure 2.35 Steam Generator A Instrumentation

INSTRUMENT TYPE	TUBE IDENTIFICATION	VTAB
STRING TC	J	P1TC09-18
	R	P1TC19-28
	N	P1TC29-38
PITOT TUBE (AND FLUID TC)	J	P1DP01, P1TC06
	R	P1DP02, P1TC07
	N	P1DP03, P1TC08

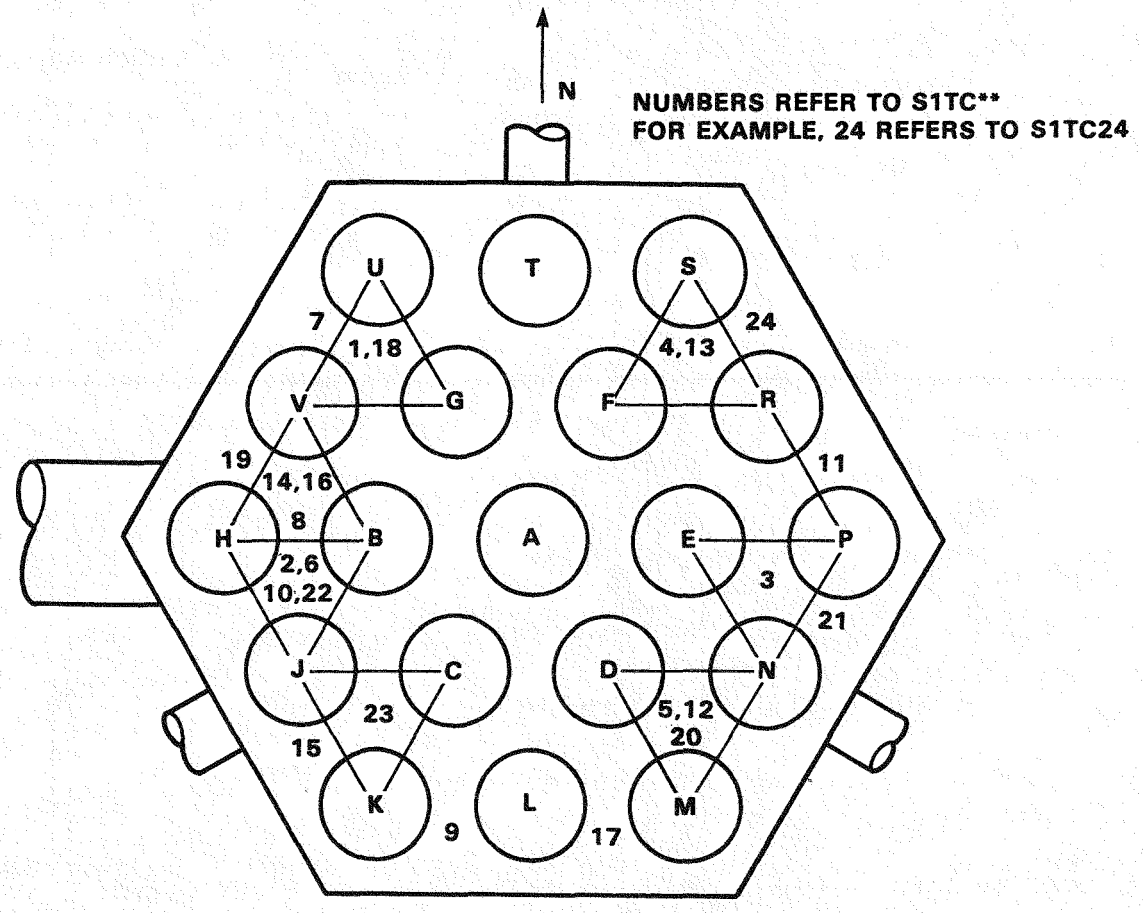

Figure 2.36 Cross-Sectional Location of Steam Generator A Instrumentation

Secondary thermocouples in the A steam generator are 0.063-inch diameter, ungrounded Type J, sheathed with 0.125-inch O.D. tube for mechanical strength. The outside sheath extends no closer than 0.313 inch (5 diameters) from the thermocouple junction to avoid impact on measured temperature.

Seven differential pressure transmitters are installed in the A steam generator — four in the primary and three in the secondary. In the primary, an overall transmitter, spanned from -3.15 to 53.10 feet, provides input to the collapsed fluid level calculation and three transmitters measure the differential pressure developed at pitot tubes in primary tubes J, R, and N. Pitot tube transmitters are spanned 0 to 5 inches of cold water (0.000 to 0.181 psid). Secondary transmitters measure differential pressure from 0.00 to 52.14 feet for collapsed fluid level calculations and level control, from 0.00 to 35.34 feet, and from 23.17 to 35.35 feet.

Pipe wall metal and insulation temperature measurements are required for five guard heater zones in the A steam generator. Four approximately equal length control zones are used for the steam generator shell and a fifth is used for the steam generator downcomer. Shell control zones extend from 0.00 to 14.25 feet, from 14.25 to 29.25 feet, from 29.25 to 40.67 feet, and from 40.67 to 52.14 feet. Pipe wall metal and the difference between wall and insulation temperatures are recorded near the midline of each zone, as is required guard heater power input. An additional metal thermocouple is installed in lower tubesheet metal to provide an indication of thermal storage and release for this metal mass.

Steam generator A pressure is recorded at the uppermost primary pressure tap at 53.10 feet and at the uppermost secondary tap at 52.14 feet. These transmitters are spanned to the system design limits of 2500 psia for the primary and 1500 psia for the secondary. The secondary pressure transmitter also supplies the signal for secondary steam pressure control, including simulated ATOG depressurization.

Limit switches indicate the use of auxiliary or main feedwater for the A-loop steam generator.

2.4.2.2 B-Loop Steam Generator Instrumentation

One hundred sixty-six instruments are recorded by the MIST data acquisition system for the B loop steam generator — 110 fluid thermocouples, 20 differential pressure transmitters, 12 conductivity probes, six metal thermocouples, five differential temperature pairs, five wattmeters, four limit switches, two gauge pressures, and two resistance temperature detectors. Locations and installation details for these instruments are defined in Figures 2.37, 2.38, and 2.39.

Fifty-seven fluid temperature measurements are recorded for the B steam generator. Resistance temperature detectors measure average fluid temperatures in the inlet and outlet steam generator plenums. Fifty-three fluid thermocouples are installed in primary tubes, at 14 separate planes over the full length of the generator. These thermocouples are positioned to record axial and radial temperature gradients resulting from several steam generator heat transfer modes. Axial measurement density is greatest in areas of highest heat transfer; near the high auxiliary feedwater addition elevation and the nominal post-trip secondary operating level. Additional primary thermocouples define fluid temperature at upper and lower primary-to-secondary tube leak sites. Axial and radial positions of primary (and secondary) temperature measurements are defined in Figures 2.37 through 2.40.

Auxiliary feedwater wetting results in fluid temperature differences between primary tubes. These differences persist for the entire length of the primary tubes, diminishing in magnitude toward lower elevations. A minimum of three tubes are instrumented at each primary thermocouple plane, with two additional instrumented tubes at planes where radial temperature gradients are most pronounced. Tubes J, A, and R are instrumented at every primary thermocouple plane, with tubes C and F additionally instrumented at three planes and at the pitot tubes. A final plane of six primary thermocouples, arranged as shown in Figure 2.39, is installed between the 14th and 15th tube support plates to define the extent of auxiliary feedwater spreading.

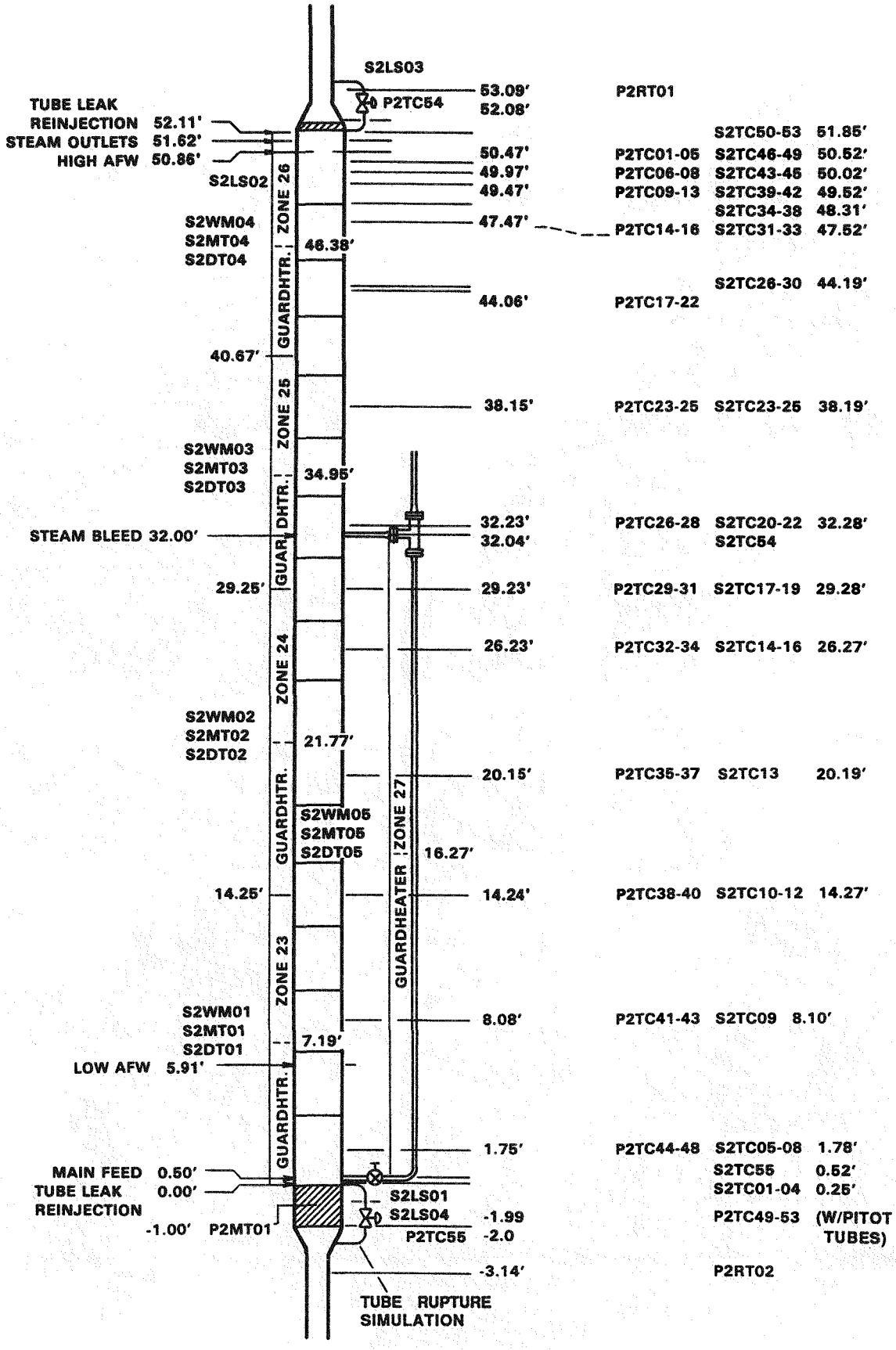

Figure 2.37 Steam Generator B Instrumentation

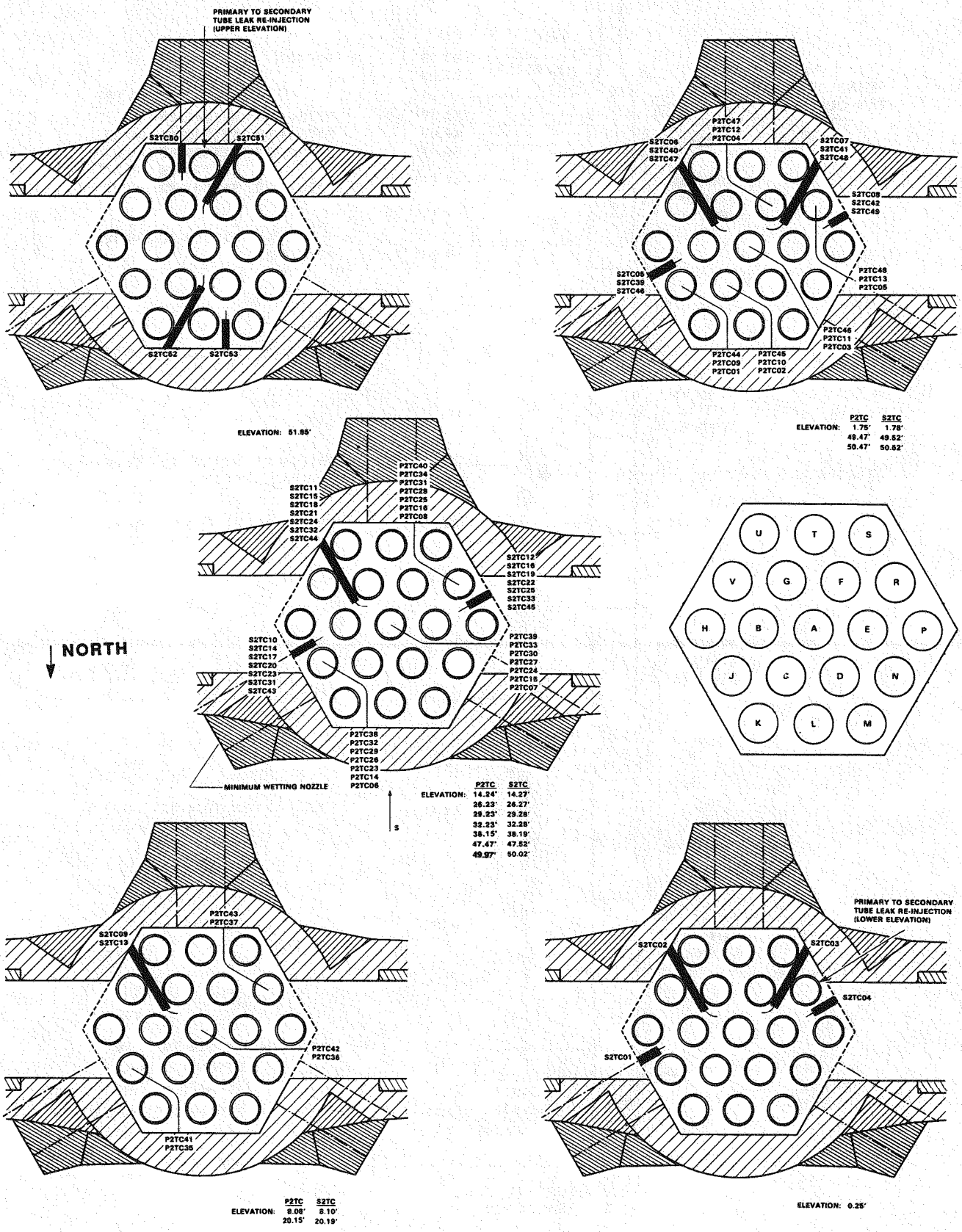

Figure 2.38 Steam Generator B Radial Thermocouple Distribution

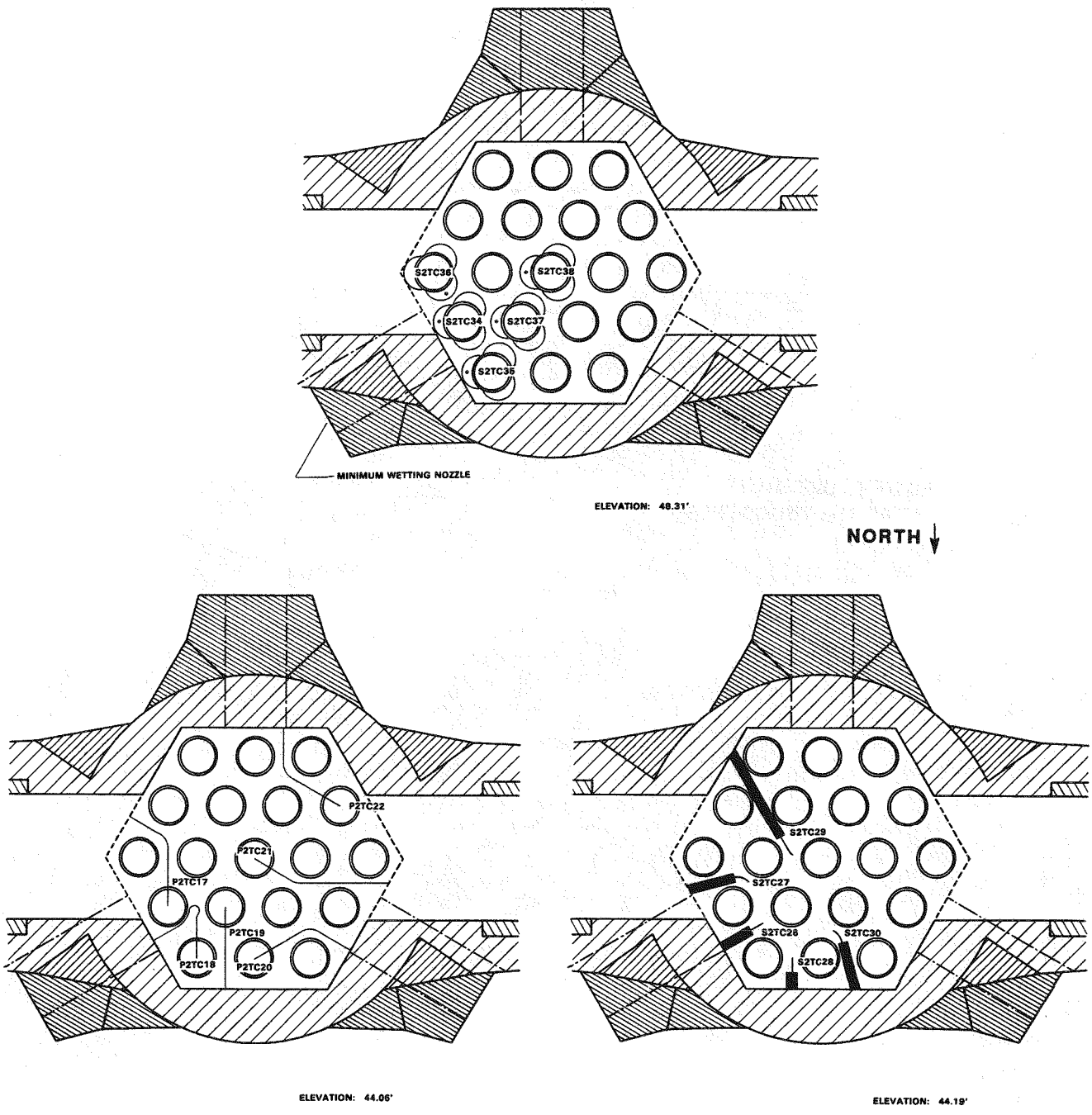

Figure 2.39 Steam Generator B Thermocouples to Observe AFW Spreading

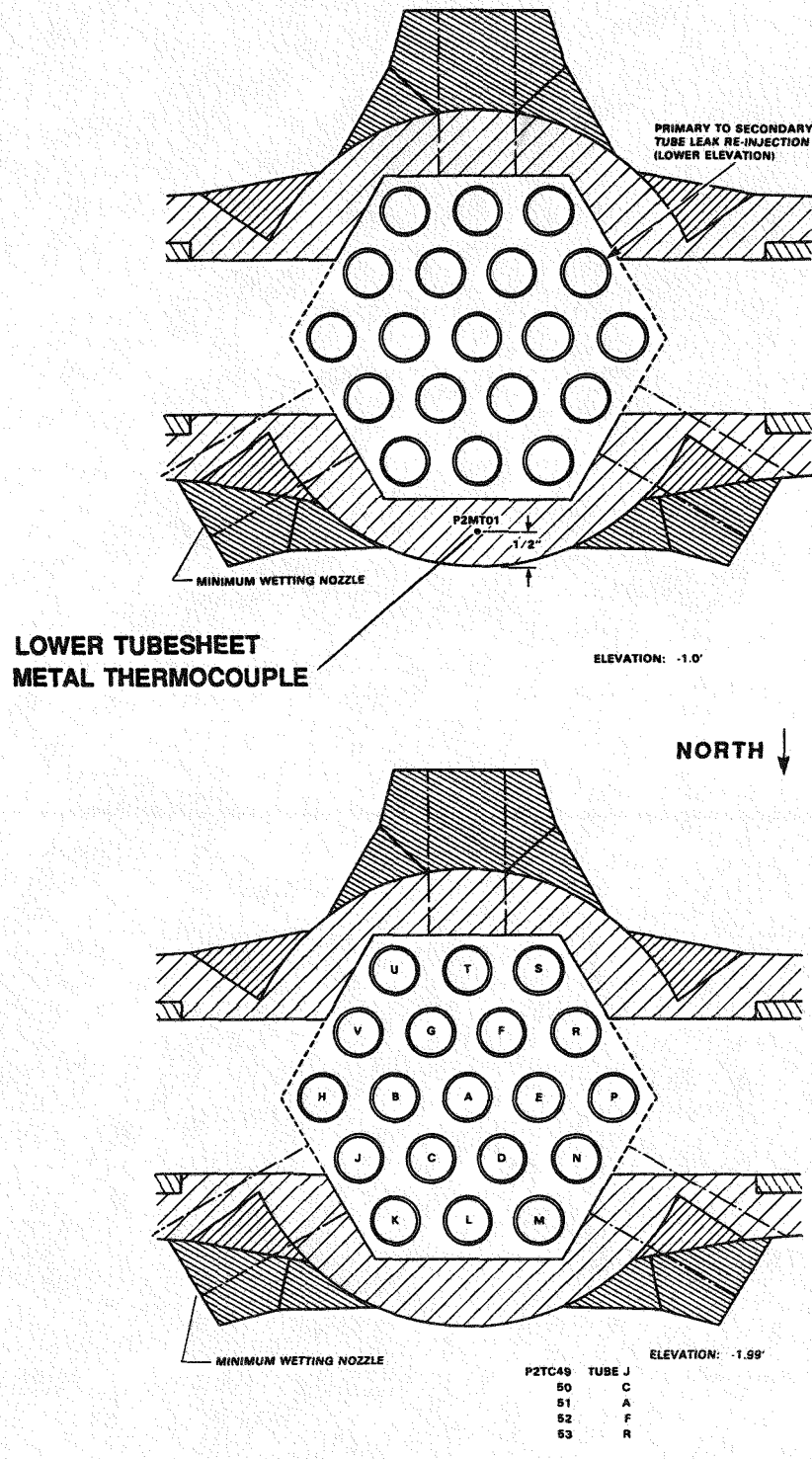

Figure 2.40 Steam Generator B Primary Pitot Tubes and Tubesheet Temperature

As indicated in the figures, steam generator B primary thermocouples are installed through penetrations in the secondary shell and the primary tubes. The thermocouples extend through the secondary flow stream to the centerline of a primary tube. Seal welds maintain pressure boundaries at tube and shell walls. Each thermocouple is installed to minimize stress due to differential thermal expansion. All primary thermocouples are 0.063-inch, ungrounded Type J, with a time constant of approximately 5 seconds. Resistance temperature detectors are 1/4 inch in diameter with a time constant of approximately 5.5 seconds.

Fifty-five fluid thermocouples are installed in the B generator secondary at the locations noted in Figures 2.37, 2.38, and 2.39. Fifty-three of these thermocouples record fluid temperature in secondary flow channels, at 16 distinct planes throughout the generator. The two remaining thermocouples record fluid temperature in the steam generator downcomer — at the steam bleed and main feedwater nozzle elevations.

Secondary thermocouples are positioned following the same rationale used for the primary thermocouples, with 14 of 16 secondary planes coincident with primary planes. As shown in the figures, one to four thermocouples are installed at 13 planes depending on expected radial temperature gradients. The 14th plane contains five thermocouples, installed in broach holes in the highest tube support plate, as shown in Figure 2.39. These thermocouples monitor the presence of a subcooled pool of auxiliary feedwater on the top tube support plate.

The two remaining secondary thermocouple planes are located immediately below the upper tubesheet and immediately above the lower tube sheet and monitor the influence of primary-to-secondary tube leak effluent on secondary fluid temperatures.

Twenty differential pressure transmitters are installed in the B steam generator — eight in the primary and 12 in the secondary. On the primary side, an overall transmitter is spanned from -3.11 to 53.09 feet and provides input to a collapsed fluid level calculation. Additional primary transmitters record the differential pressure across valves in the upper and lower

primary-to-secondary tube rupture circuits for flow measurement calculations. The five remaining primary transmitters record the differential pressure developed at pitot tubes in primary tubes J, C, A, F, and R. Primary-to-secondary tube leak transmitters are spanned 0 to 750 inches of cold water (0.00 to 27.09 psid). Pitot tube transmitters are spanned 0 to 5 inches of cold water (0.000 to 0.181 psid).

Secondary transmitters measure overall, intermediate, and local pressure differences. The overall transmitter is spanned from 0.00 to 51.95 feet and provides input to the secondary collapsed level calculation and fluid level control. The intermediate transmitter is spanned from 0.00 to 33.61 feet. Local secondary transmitters are spanned for 10 narrow range estimates of void fraction between 0.00 and 33.61 feet. Twelve conductivity probes evaluate the highest elevation wet by secondary fluid or froth and provide confirming void fraction data. Differential pressure transmitter and conductivity probe locations for the B steam generator are shown in Figure 2.37.

Pipe wall metal and differential temperature measurements installed for B steam generator guard heater control parallel those installed for the A steam generator. Four approximately equal length shell control zones extend from 0.00 to 14.25 feet, from 14.25 to 29.25 feet, from 29.25 to 40.67 feet, and from 40.67 to 52.14 feet. A fifth control zone is allocated to the B steam generator downcomer. Pipe wall metal and differential temperatures are recorded near the midline of each zone, as is the required guard heater power input. As for the A steam generator, a thermocouple is installed in the lower tubesheet metal of the B generator to provide an indication of thermal storage and release for this metal mass.

B steam generator pressure is recorded at the uppermost primary pressure tap at 53.09 feet and at the uppermost secondary tap at 51.95 feet. As for the A steam generator, these transmitters are spanned to system design limits of 2500 psia for the primary and 1500 psia for the secondary. The secondary transmitter supplies the signal for secondary steam pressure control, including simulated ATOG depressurization.

Four limit switches are recorded for the B steam generator — one each to indicate the use of auxiliary or main feedwater and one each to indicate the use of the upper or lower simulated primary-to-secondary tube rupture.

2.5 COLD LEGS

Four identical cold legs are provided in the reactor coolant system of the MIST facility. Two cold legs originate at the outlet of each steam generator, and drop vertically to the preserve the plant cold legs' spillunder elevation at an elevation of -6.375 feet (relative to the steam generator's lower tubesheet secondary face). The cold legs run horizontally a short distance then turn upward. The cold legs extend vertically upward to the reactor coolant pump such that the spillover elevation in the model pump's volute cavity preserves the plant-typical spillover elevation at 25.83 feet. Downstream of the coolant pumps, the cold legs are sloped (58.9°) downward to the downcomer intersection. Each cold leg connects to a quadrant of the baffled upper downcomer. The cold legs are guard heated to minimize heat loss.

An injection nozzle for high pressure injection (HPI) flow is installed in each cold leg downstream of the reactor coolant pump at an elevation of 23.58 feet. In one cold leg, a connection is provided at the reactor coolant pump discharge for the pressurizer spray line. The cold legs were the principal locations for controlled leak simulations in the MIST reactor coolant system. Leak sites were provided in the sloping cold leg (pump) discharge piping of two cold legs, and in the vertical pipe length on the pump suction side of one cold leg.

2.5.1 Cold Leg Design

Characteristics of the cold legs evaluated to be significant to the MIST simulation of post-trip natural circulation and small-break loss-of-coolant events include heat loss, energy storage and transfer to and from the piping metal mass, fluid mixing, elevations traversed by flow from the steam generator to the reactor vessel downcomer, volume, and irrecoverable pressure losses. Heat losses to ambient are addressed by the guard heating system provided on all components of the reactor coolant system, as discussed in

Section 3.3. Pipe wall stored energy and fluid-to-metal coupling impact the vapor generation and compression events, and are particularly significant during an asymmetric or interrupted circulation condition. Fluid mixing primarily refers to phenomena in the cold leg discharge piping where the high pressure injection and reactor vessel vent valve discharge mix with cold leg flow. Critical elevations include the spillunder and spillover points of the plant cold leg piping. And, as with all components of the reactor coolant system, volume and irrecoverable pressure losses are important to preserve power-to-volume scaling and natural circulation, respectively.

Fluid mixing and pipe metal stored energy are well addressed by the MIST cold leg design. Fluid-to-fluid mixing in the cold leg discharge piping were previously studied in experiments and numerical modeling studies (Appendix H of Reference 1), and was found to be approximately preserved by scaling the model pipe diameter by a modified Froude number. The Froude number scaling dictates a cold leg diameter of 1.9 inches. Stored energy along the length of the cold leg piping is approximately preserved by matching the ratio of fluid to metal volume per unit length. The MIST cold leg piping selected was 2-inch schedule 80 pipe, which obtains a fluid-to-metal volume ratio of approximately 2. The plant cold legs (28-inch piping) have a fluid-to-metal volume ratio of 2.3. The selection of 2-inch pipe for the MIST cold legs also approximately preserves the cold leg irrecoverable pressure loss characteristic.

Cold leg piping elevations are central to natural circulation flow behavior, particularly inter-cold leg flow. The MIST cold legs are illustrated in Figure 2.41 and compared to the plant cold leg critical elevations. Full elevations of the spillunder and spillover points in the cold legs are maintained. As noted in the figure, two cold legs connect to the lower plenum of each steam generator. In MIST, the flow from a steam generator is maintained in a single pipe, until the elevation corresponding to the bottom of the cold leg pipe connection to the plant lower plenum. At this elevation, a Y-connection divides the steam generator effluent between the two cold legs. Separately, the two cold legs from each steam generator then maintain the spillunder point of the plant cold legs, and the long vertical run to the reactor coolant pump suction.

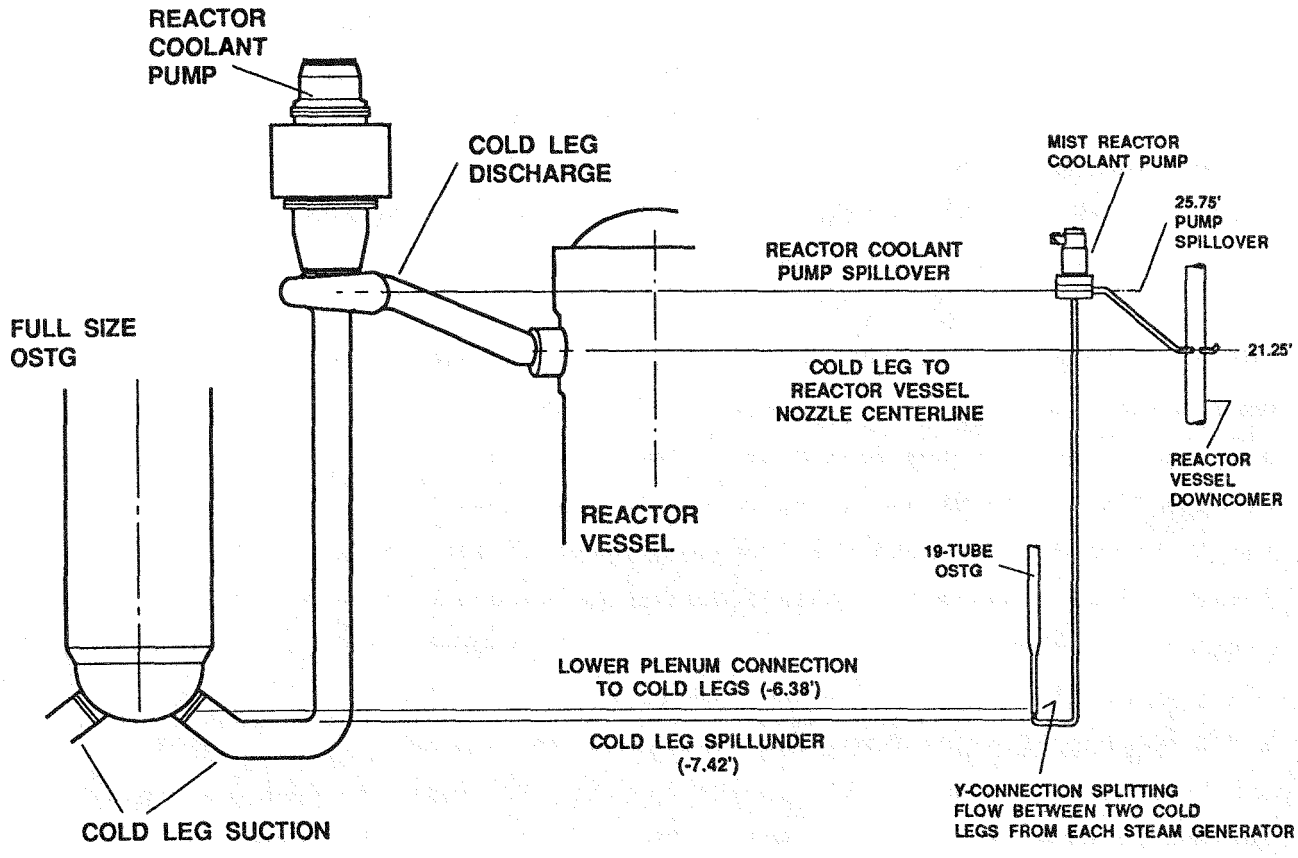

Figure 2.41 Comparison of Plant and MIST Cold Leg Elevations

By maintaining the full elevation of the plant cold legs with individual cold legs from the steam generator lower plenum to the reactor vessel downcomer, the model piping would have to be 1 inch in diameter to preserve power-to-volume scaling. Priority was given to metal mass energy storage and fluid mixing, resulting in atypical volume in the MIST cold legs. The atypicality was minimized by shortening the horizontal lengths of the cold leg piping by approximately 30%.

Reducing the horizontal lengths obtains a slope of 58.9° in the cold leg discharge piping, whereas the plant cold legs have a maximum slope along the pipe centerline of approximately 45° in this region. The cold leg discharge piping contains the high pressure injection nozzles (one in each cold leg),

and leak sites. Cold leg C2 (connected to the B steam generator) contains two leak sites in the discharge piping, and one in the suction piping, as illustrated in Figure 2.42. This figure also provides a detail view of the HPI and leak site connections. As indicated, HPI flow enters the side of each cold leg discharge pipe horizontally. In the C2 cold leg, leak sites are provided just upstream and downstream of the HPI connection; the upstream leak site is connected to the top side of the pipe, and the downstream leak site is connected to the bottom side of the pipe. The bottom of pipe leak site is the nominal cold leg discharge leak site. Cold leg C1 (connected to the A steam generator) contains one leak site in the discharge piping, which is a bottom of pipe leak connection similar to the one illustrated in Figure 2.42. Cold leg C3 (also connected to the A steam generator) contains a connection immediately at the pump discharge that supplies the pressurizer spray line discussed in Section 2.6.

2.5.2 Reactor Coolant Pumps

The MIST facility reactor coolant system contains four identical reactor coolant pumps. One is located in each cold leg at an elevation which preserves the plant reactor coolant pump spillover elevation at 25.83 feet. The pumps are specially designed Chempump canned rotor centrifugal pumps. The pumps design allows them to be installed vertically, such that the pump suction is on the underside of the volute, and the pump discharge is horizontally oriented as shown in Figure 2.42. This preserves the general flow path through the plant's pump internals, and sets the spillover elevation in the cold leg at the bottom of pipe elevation of the model reactor coolant pump discharge piping.

The pump was designed to obtain scaled single-phase performance characteristics. When operated in subcooled water operation, the MIST reactor coolant pump obtains full plant-typical head rise at scaled flow rates. The nominal head-flow curve of the as-built pumps is shown in Figure 2.43. Flow rates are scaled from the plant pump values by 1/817. The pump performance upon installation in the MIST loop is discussed further in Section 6. To obtain this head-flow characteristic, the pump discharge is fitted with a slotted orifice, and the pump's impeller diameter was machined for final adjustment.

The discharge orifice is an integral part of the pump, and was never removed for any portions of MIST testing. The orifice was slotted and installed with the slot oriented vertically in order that the spillover elevation of the pump was minimally affected.

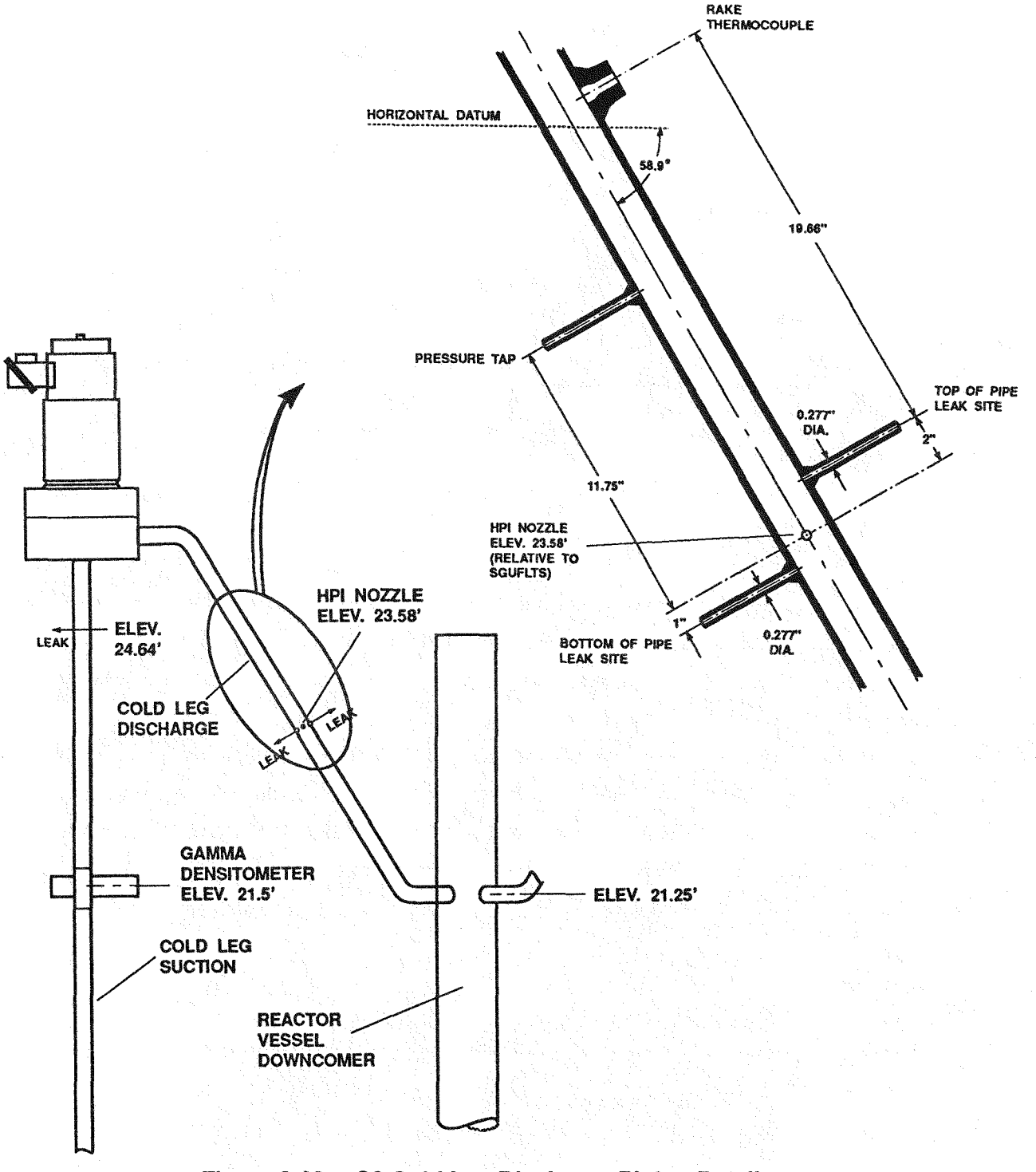

Figure 2.42 C2 Cold Leg Discharge Piping Detail

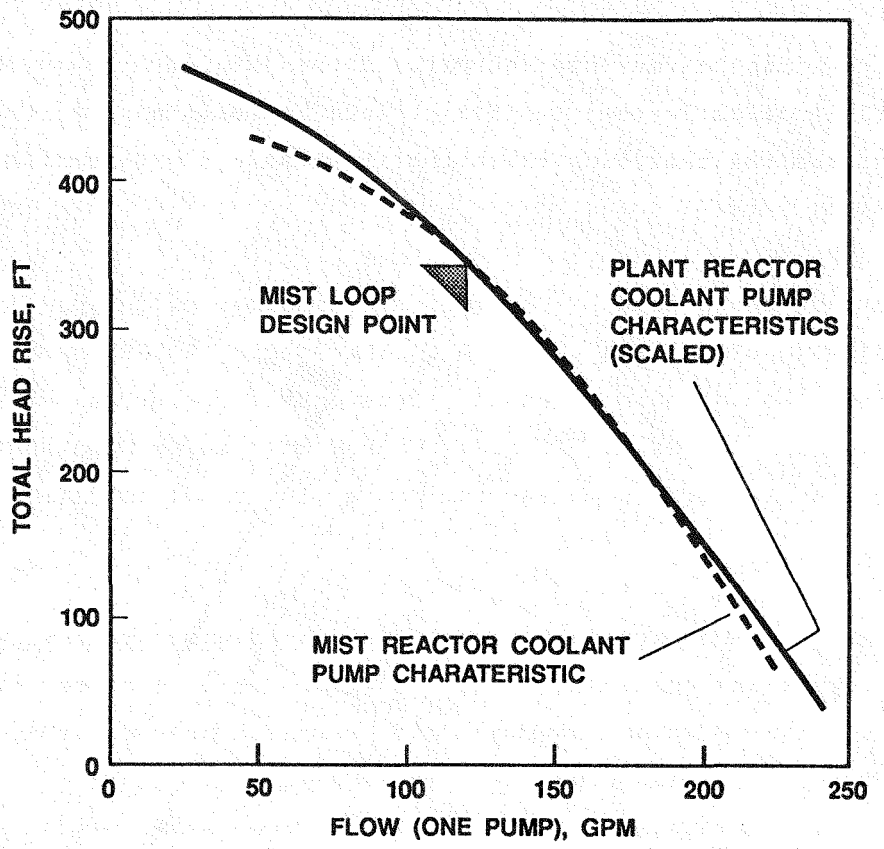

Figure 2.43 Comparison of MIST and Scaled Plant RCP Head-Flow Characteristics

When the pump is not running, the pump impeller can be locked to prevent rotation (windmilling) in either the forward or reverse direction. This aids in the preservation of two plant pump characteristics. First, the full-size reactor coolant pumps are equipped with an anti-reverse rotation mechanism to prevent windmilling in the reverse direction. Second, the MIST cold legs must have prototypical head loss characteristic when the pumps are unpowered. The reactor coolant pumps are part of the cold leg resistance, and the locked rotor in the model pump provides a fixed pump resistance if the rotor is not windmilling. The model pump's rotor is locked by an air-actuated brake assembly.

The locked rotor resistance (differential pressure across the pump with the rotor locked) of the model reactor coolant pumps was less that plant typical, even with the slotted discharge orifice installed. This required that additional cold leg resistance be added to preserve total loop resistance during natural circulation. The resistance was added in the form of cold leg

venturi flowmeters discussed in Section 2.5.3. Figure 2.44 indicates the scaled plant typical locked rotor resistance of the reactor coolant pumps. Similar to the pump operating characteristic, the (scaled) plant typical irrecoverable loss characteristic preserves the full plant typical head loss at scaled (1/817) flow rates. The locked rotor resistance of the as-built MIST reactor coolant pumps (with the discharge orifice considered as an integral part of the pump) is shown in Figure 2.44.

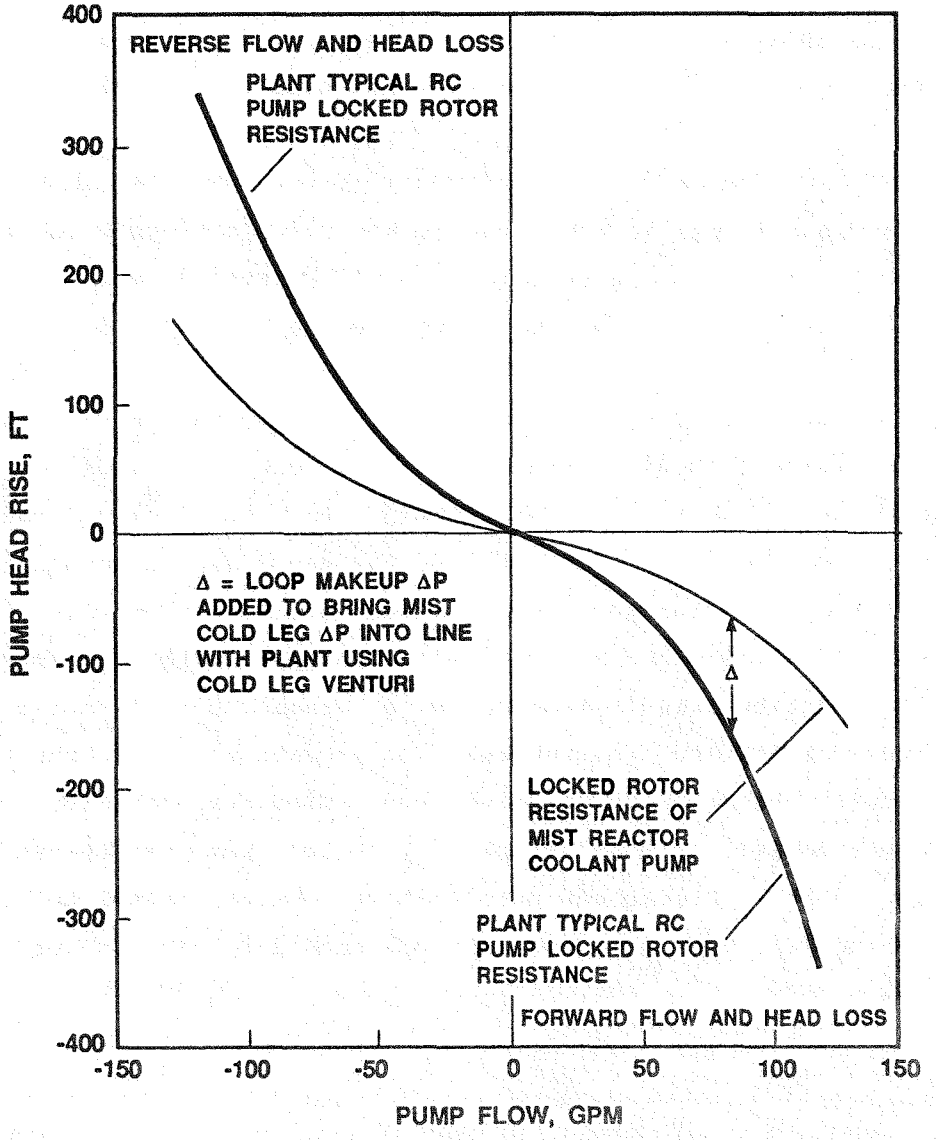

Figure 2.44 Comparison of MIST and Scaled Plant RCP Locked Rotor Resistance

Due to the scale factor used in the MIST facility design, scaled leak rates for small-break loss-of-coolant accidents in MIST are very low in magnitude. Controlled leak discharge rates are as small as 0.005 lbm/sec (scaled 2 cm^2 break, critical flow of saturated liquid at 2000 psia). The design criteria for the MIST reactor coolant pumps was to ensure that system leakage from the pumps was at least an order of magnitude below this (for the four pumps, total). The model reactor coolant pumps are a canned-rotor pump, and thus is a seal-less centrifugal pump design. With this design, the pump impeller/ rotor assembly is totally enclosed by a hermetically sealed pressure boundary. It is thus suited to meet the leakage requirement because the shaft between the rotor and impeller does not penetrate the pressure boundary. A sketch of the MIST reactor coolant pump is shown in Figure 2.45.

The vertical orientation and canned-rotor design make the MIST pumps susceptible to vapor or gas accumulation in the rotor cavity, which would lead to rotor damage if operated with a voided rotor cavity. To minimize this, a spring-loaded mechanical face seal was installed to separate the volute and rotor cavities. During all tests in which the pumps were to be operated, the rotor cavity was maintained full of water by injecting reactor coolant fluid into the rotor cavity with a metering pump. Each pump was serviced by one metering pump. The metering pump was installed to withdraw fluid from the cold leg suction piping, and inject it into the model reactor coolant pump's rotor cavity. Keeping the rotor cavity filled, the injection flow would pass into the pump volute chamber, and thus back into the reactor coolant system. Therefore the injection circuit represents no net mass loss from the system, only a displacement of flow from the cold leg suction piping to the high point in each cold leg. The metering pumps were set to maintain the rotor cavity water filled during periods when the reactor coolant pump was operating in a steam filled cold leg. During characterization testing, it was determined that the metering pump setting provided a maximum of 0.5 lbm/hr (per pump) of injection flow.

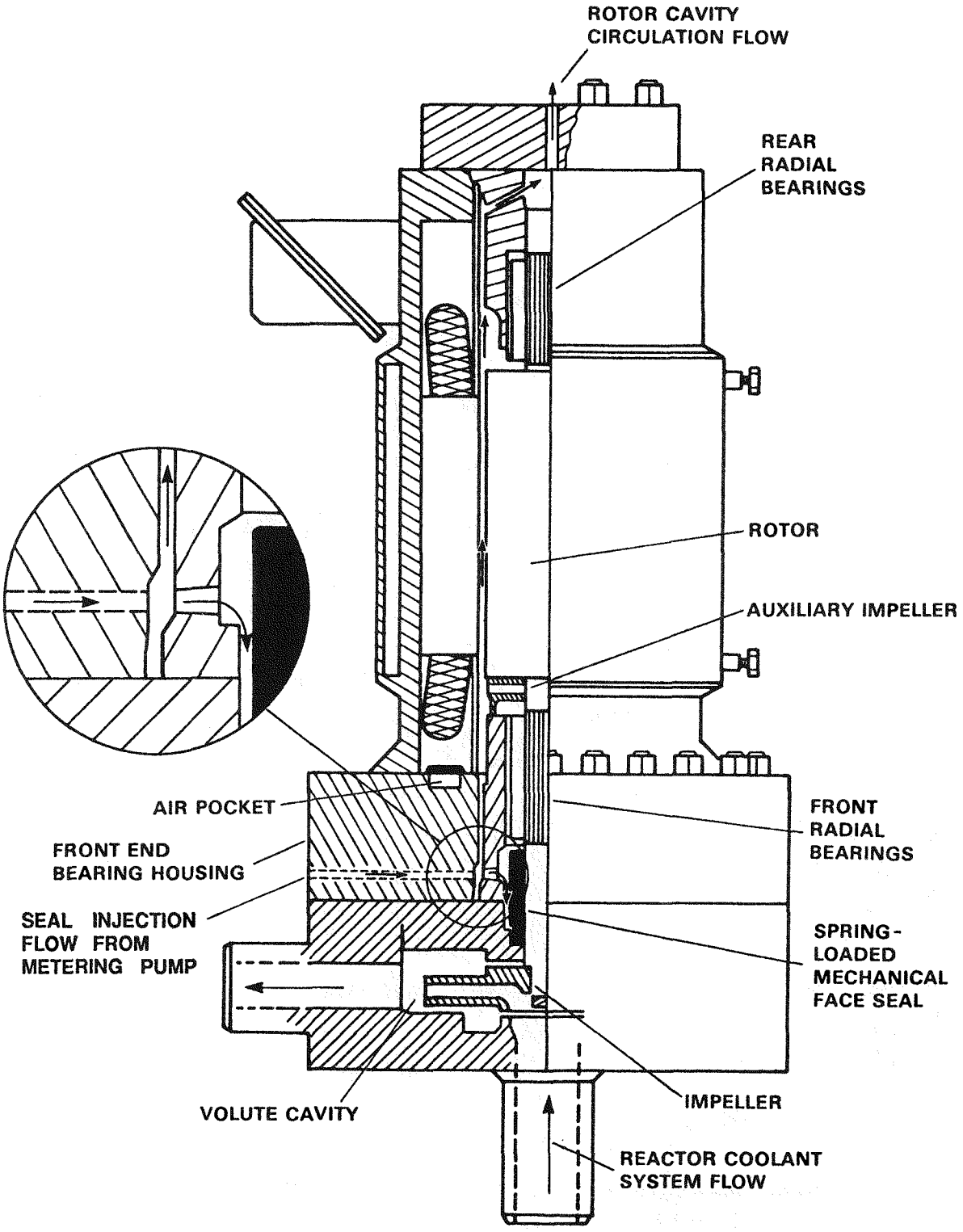

Figure 2.45 MIST Reactor Coolant Pump Design

The circuit containing the metering pumps was referred to as the RCP boost pump circuit, shown schematically in Figure 2.46. As indicated in the figure, the total boost pump circuit flow was drawn from the C2 cold leg suction piping. This flow was divided to supply the four metering pumps. Each metering (boost) pump discharged approximately 0.5 lbm/hr fluid into the vent reservoir of a model reactor coolant pump. The vent reservoir was a component of each reactor coolant pumps rotor cavity cooling circuit.

The fluid in the rotor cavity of the pump is kept cool by circulating it through an external heat exchanger as illustrated in Figure 2.47. The rotor cavity fluid keeps the radial bearings on the impeller/rotor shaft lubricated and removes heat from the motor windings in the stator. The insulation on the pump motor windings must be maintained below 425°F. To minimize heat transfer between the rotor and impeller cavities (which represents a heat loss from the reactor coolant system), air pockets are designed into the front bearing housing (shown in Figure 2.45). Fluid exchange between the cavities was minimized by the spring-loaded face seal in the front bearing housing.

Due to the inefficiency of the model pump impeller and conduction heat transfer from the motor windings, heat energy is added to the reactor coolant system fluid during pump operation. The heat energy input of the MIST pumps was estimated to be 1.3% of full scaled core power (1.3% of 3.3 MW, where 3.3 MW corresponds to 100% scaled full power in the MIST facility core). The full-size reactor coolant pumps at Oconee III have a heat energy input equal to approximately 1.0% of full core power (1.0% of 2568 MW, where 2568 MW corresponds to 100% power at Oconee III).

The pumps were powered by variable speed drives in order to provide controlled startups and coastdowns to simulate conditions during pump bump operation. The full-size reactor coolant pumps are equipped with large flywheels which lead to long startup and coastdown periods. Operator action during a SBLOCA transient may include periodic "pump bumping" in which a pump is started, briefly operated, then shut off and allowed to coastdown. To simulate the effect of these pump bumps, the startup and coastdown scaled flow versus time and suction lift versus scaled flow characteristics are needed. The plant typical startup and coastdown characteristics are shown in Figure 2.48. The

degree to which the MIST pumps were able to simulate these characteristic are discussed in Section 6.

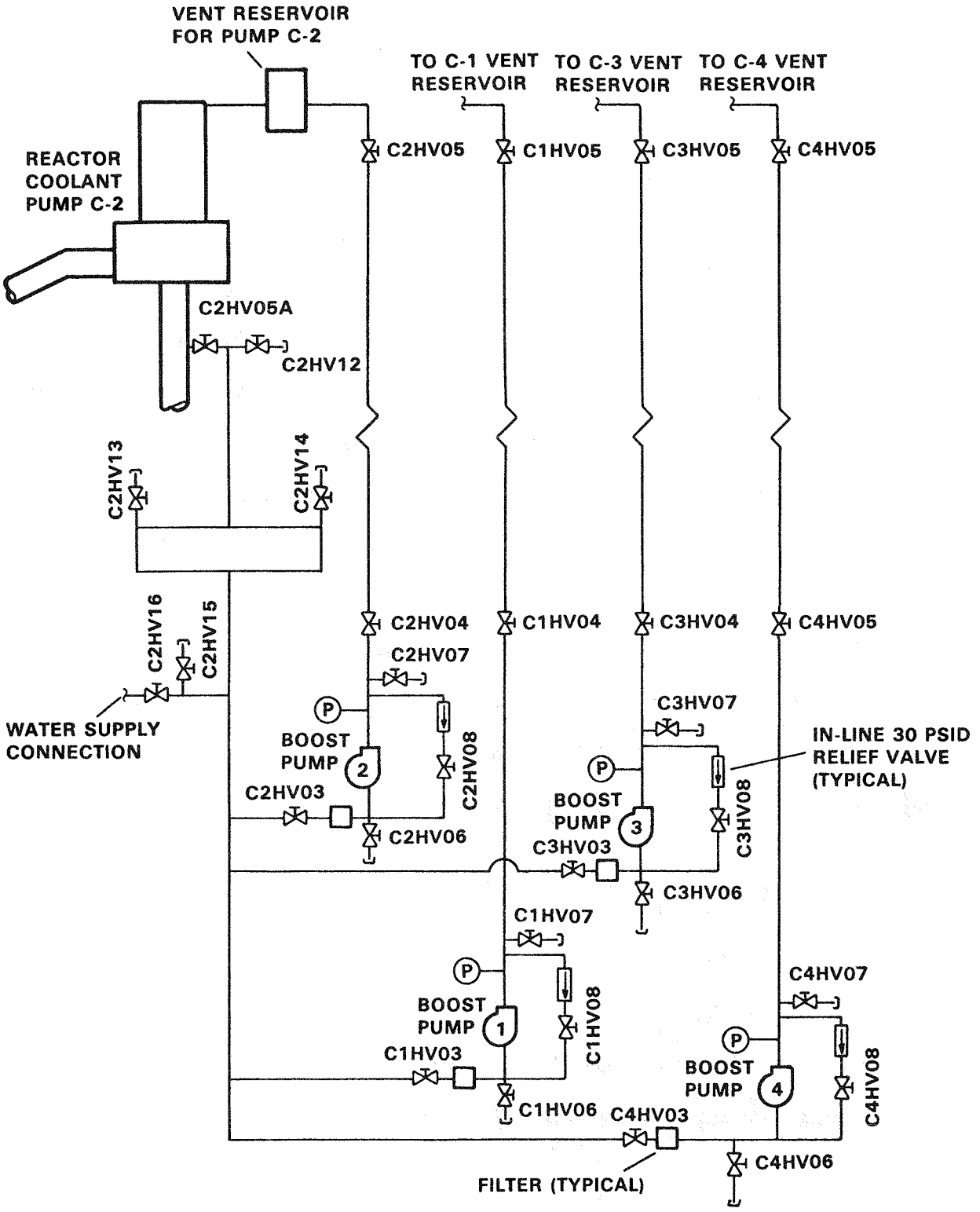

Figure 2.46 RCP Boost Pump Circuit

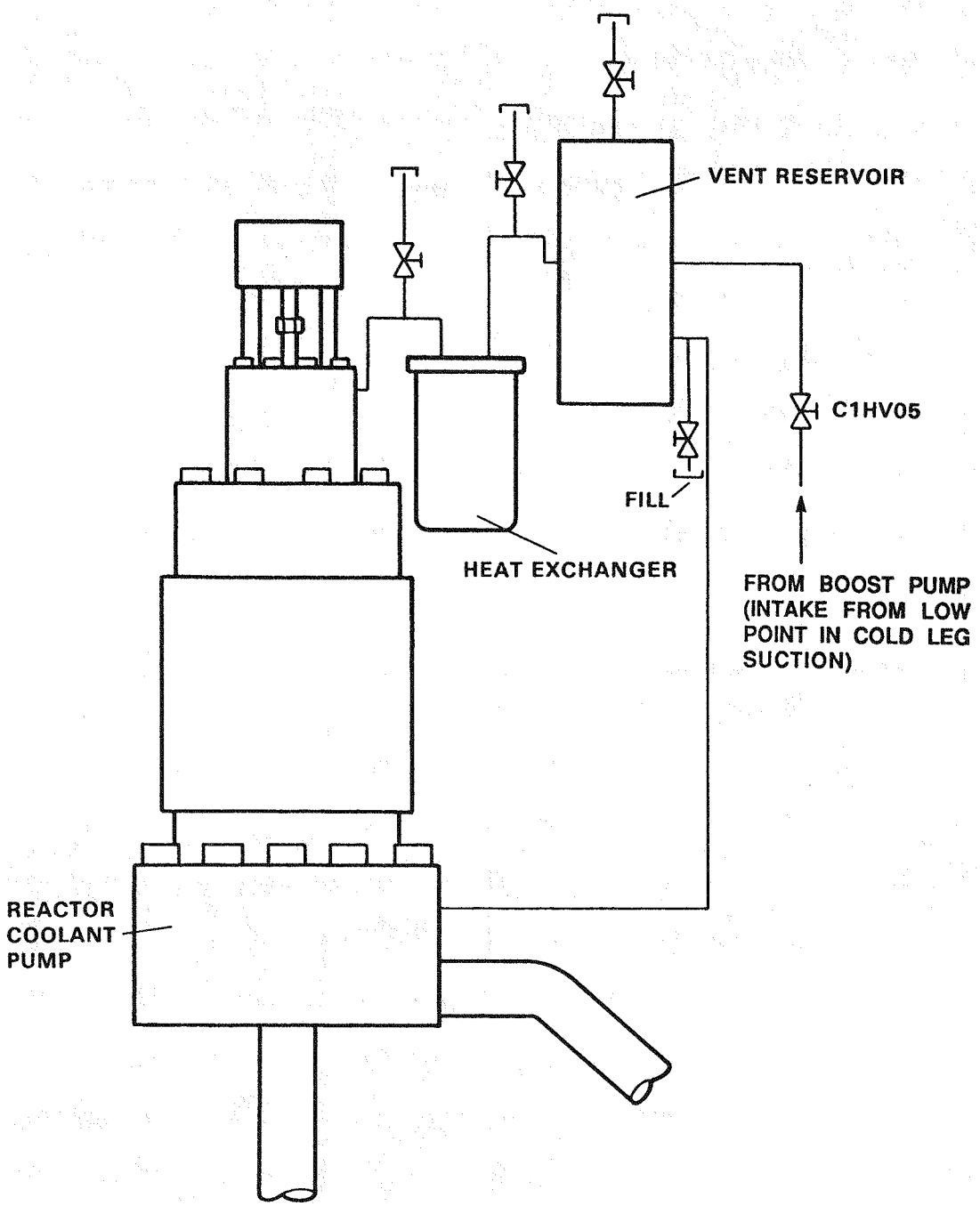

Figure 2.47 Rotor Cavity Cooling Circuit for Model Reactor Coolant Pump

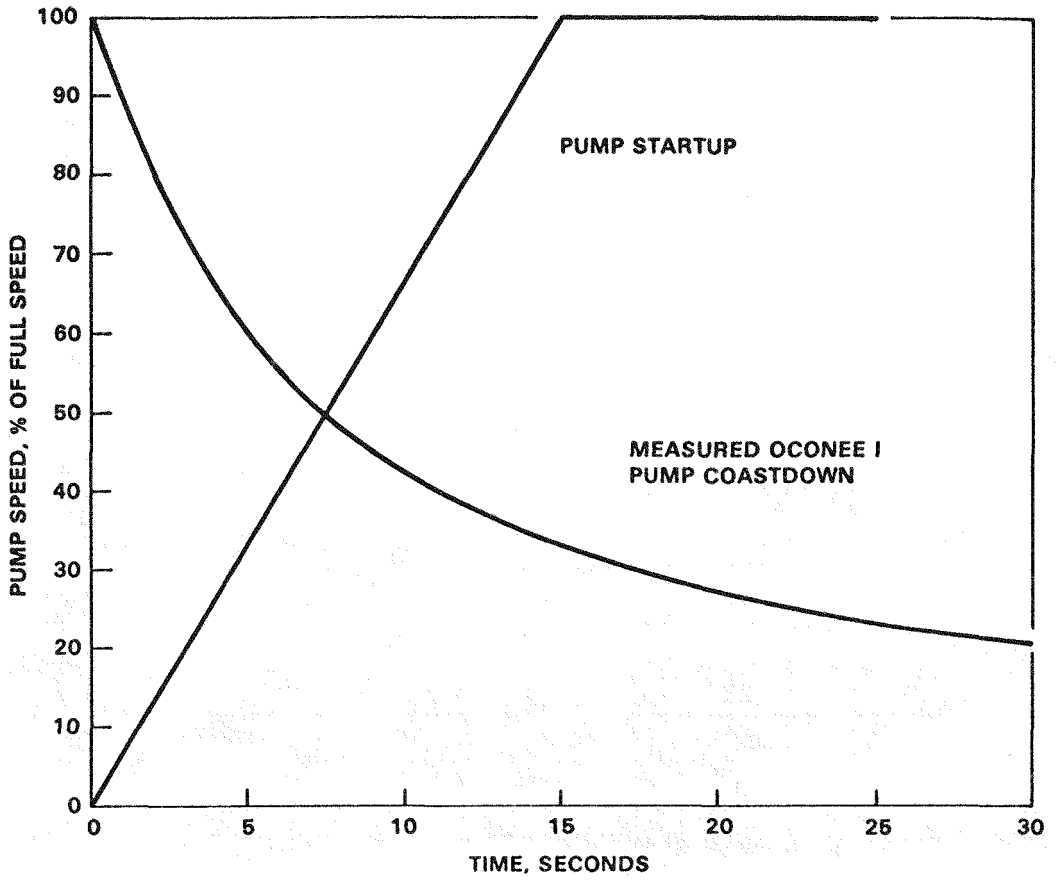

Figure 2.48 Plant RCP Startup and Coastdown Characteristics

In order to simulate the effect of pump bumps or prolonged pump operation during SBLOCAs, the model pumps would need to have prototypical net positive suction lift, and should have the same threshold point for cavitation initiation. The degree to which these characteristics are preserved are examined by comparing plant and model net positive suction head requirement (NPSHR) characteristics. NPSHR is the minimum suction head which must be available at the pump inlet to prevent cavitation in the pumps impeller. Plant and model as-built NPSHR characteristics are compared in Figure 2.49. As indicated, the MIST reactor coolant pumps have a lower NPSHR than the plant pumps. The result of this is that there are a range of reactor coolant system pressures at which the plant reactor coolant pumps would be cavitating because of insufficient net positive suction available and therefore exhibiting two-phase degraded performance, while the MIST pumps would be capable of pumping at the same conditions without signs of cavitation or degraded performance.

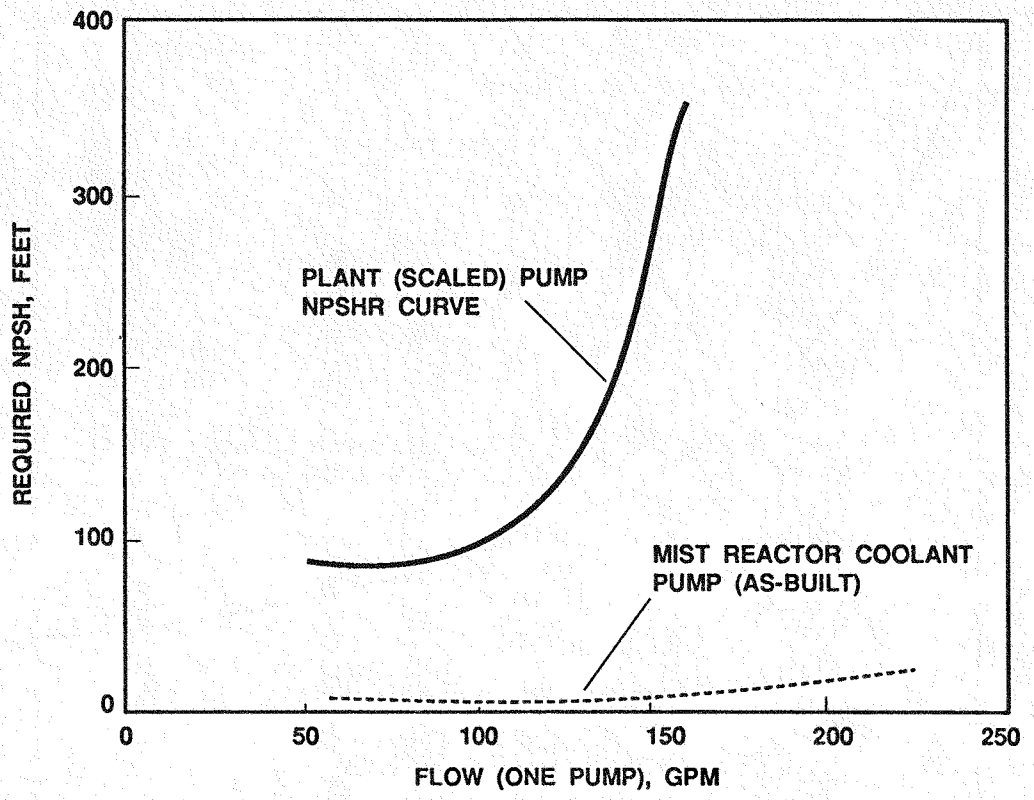

Figure 2.49 Comparison of MIST and Scaled Plant NPSHR Characteristics

Prototypical two-phase pump performance was not obtained by the MIST model reactor coolant pumps. It is believed that in order to obtain prototypical two-phase pump performance (degraded head rise), the specific speed of the plant pump must be preserved. Specific speed (N_S) is defined as:

$$N_S = \frac{N\ Q^{1/2}}{H^{3/4}}$$

where N is shaft speed in rpm, Q is flow rate in gpm, and H is the head rise in feet. This pump characteristic number, calculated at the design point of the head-flow curve, is typically used an an index for identifying pump types. Similar pump types are presumed to have similar two-phase characteristics.

The full-size reactor coolant pumps have an N_S of approximately 4200. The MIST model reactor coolant pumps have an N_S of approximately 489. With the lower specific speed, it is expected that the MIST pumps head rise will degrade more than the plant pumps during two-phase operating conditions.

2.5.3 Cold Leg and RCP Instrumentation

Flow. Venturi flowmeters were used for measurement of natural circulation flow rates prior to the pump tests. The venturis were sized with a nominal throat-to-upstream diameter ratio (β) of 0.203 to provide a high resistance for two reasons: 1) to provide a pressure drop that is readily measured even for low flows and 2) to make up for locked rotor resistance deficiencies in the coolant pumps. The venturis were bidirectional (inlet and exit cones with a total angle of 7°) and have three pressure taps – inlet, throat, and outlet. Multiple ranges of differential pressure transmitters were connected to these taps to provide three ranges of forward flow and one range of reverse flow. As shown in Figure 2.50, the venturi throat was located nominally at elevation +0.59 foot, approximately 50 diameters from the bottom of the pump suction. This location was sufficiently far from the bottom of the pump suction to avoid flow development length problems yet was reasonably low in the loop so as to minimize occurrence of two-phase flow exposure.

For experiments involving pump bumps or extended pump operation, the venturi described above was too restrictive and would cause flashing of the cold leg fluid because of the large pressure drop. For example, the calculated inlet-to-throat and irrecoverable pressure drops through the venturi for 100% flow were about 457 and 65 psi, respectively. Furthermore, two-phase flow would exist in the pump suction and the venturi would not provide a measurement under such conditions. For these experiments, the venturis were removed and full-flow turbine meters used to provide flow measurements. Since pump performance was of interest, the turbine was located as near to the pump suction as possible (approximately 22.50 feet elevation) so that the pump suction density measurement could be used in combination with the turbine output to provide mass flow rate. At this location, the turbines were between the pump and the density measurement (to be discussed later) yet were far enough from the pump to avoid potential problems associated with pump electrical interference on the turbine pickup coils.

Density/Void Fraction. Fluid density/void fraction measurement spools were located at the pump suction vertical run near the pump inlets (approximate elevation of 21.4 feet) and in the cold leg horizontal runs near the downcomer

nozzles as shown in Figure 2.50. Each measurement spool was dual beam, thus, each spool required two complete sets of electronics. Figure 2.50 (inset) shows the beam orientation for the densitometer spools located in horizontal runs.

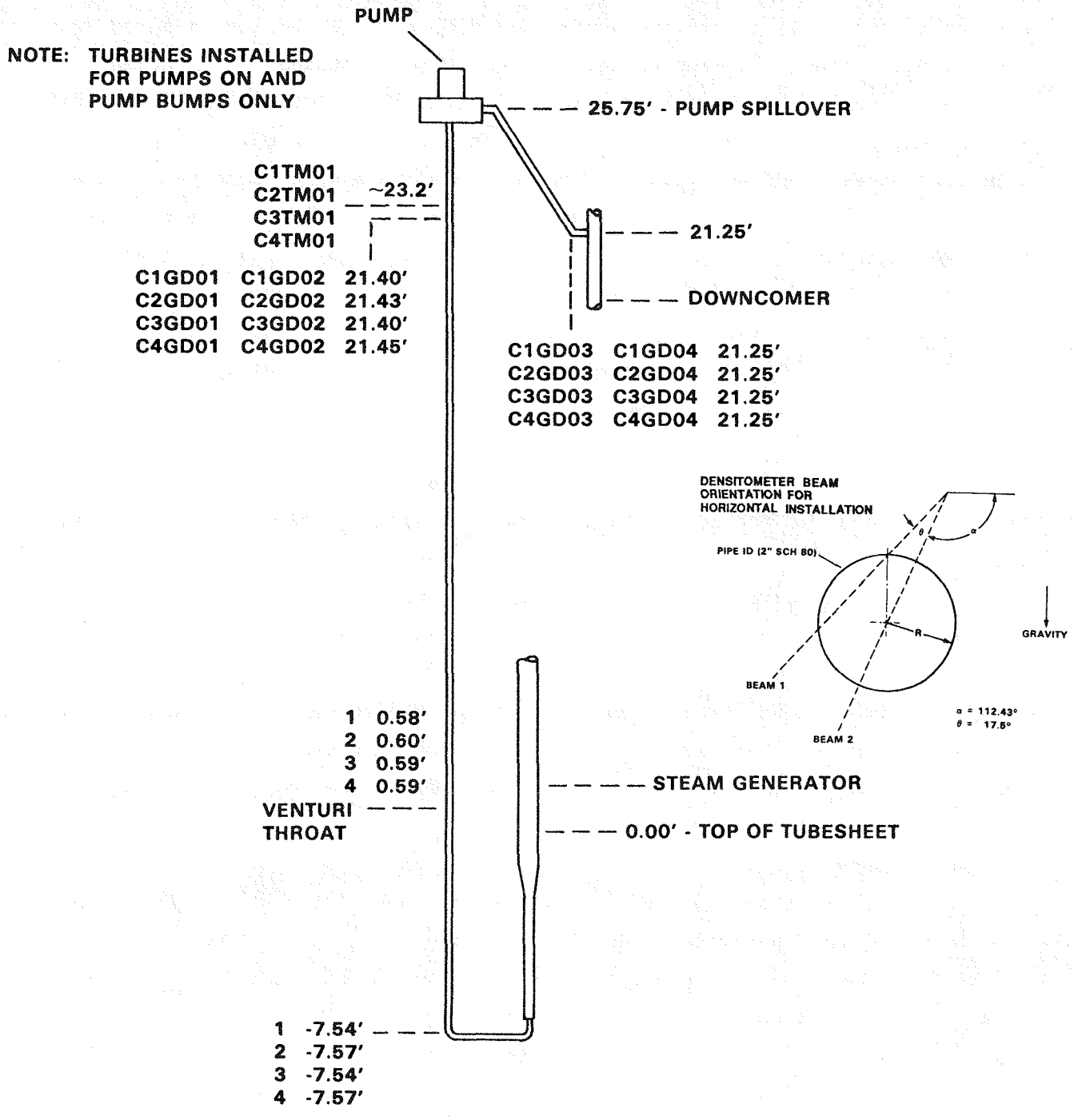

Figure 2.50 Cold Leg Flow and Density Measurements

Differential Pressure. The differential pressure tap location and transmitter hookups are shown in Figures 2.51 and 2.52. Four measurements in each cold leg were allocated to flow measurement for use on the venturis to provide low, medium, and high forward flow ranges and low range reverse flow. The remaining measurements were used to provide pressure drop and/or water level from the steam generator outlet plenum to the bottom of the pump suction, pump suction to pump inlet, and pump outlet to downcomer nozzle. One differential pressure in each loop was used to indicate pump head (differential pressure across the pump). Note that two taps were located in the cold leg near the pump discharge. Tap 06, located close to the pump discharge, was used when liquid level measurements were of most interest (as in natural circulation experiments). Tap 07, located 10 diameters downstream of the pump discharge where the flow should be more thoroughly developed was used when the pumps were operating and a good measurement of pump head rise was desired. C2DP09 provides differential pressure closure between the cold leg and downcomer for overall loop pressure drop characterization.

Fluid Thermocouples. Fluid thermocouple locations for the cold legs are shown in Figures 2.53 and 2.54 for the loops connected to the A and B steam generators, respectively. Measurements included resistance temperature devices, individual fluid thermocouples, and fluid thermocouples mounted on rakes.

Fluid thermocouples were placed mainly to provide an indication of loop temperature distribution. Thermocouples at locations C1-4TC02, C1-4TC03, and C1-4TC04 were used to supply freestream temperatures for the venturis. These temperatures in conjunction with system pressure were used (for an assumed single-phase state) to provide density for computation of mass flows. Pump inlet and outlet fluid temperatures were provided by resistance temperature detectors (RTDs) RT01 and RT02. RTDs were used since the pumps represented a significant heat loss or heat addition to the fluid depending on whether the pumps were operating or shut down. Because the pumps were a heat sink/source, RTDs located on each side of the pump in this manner allowed better and easier calibration of the rest of the cold leg thermocouples.

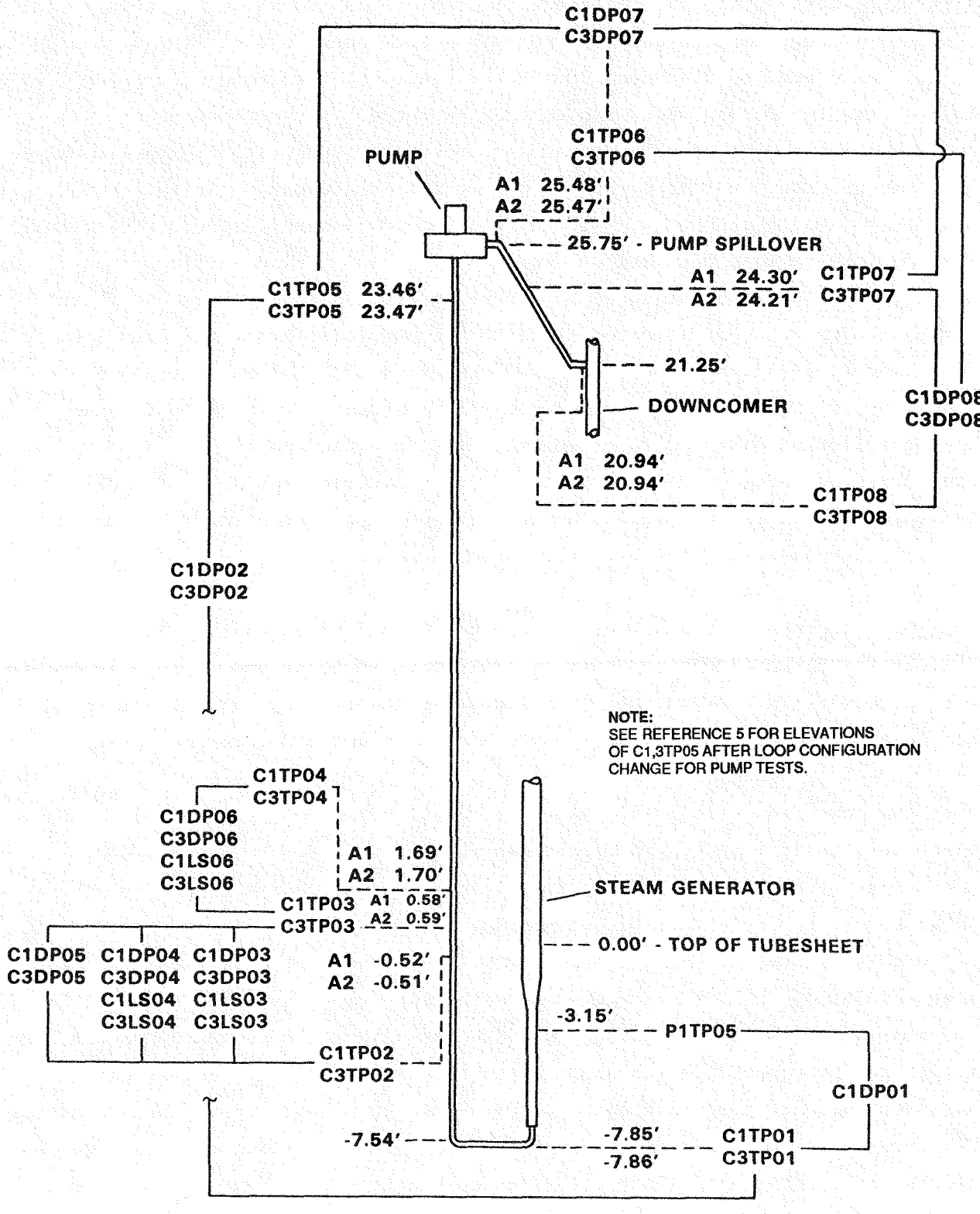

Figure 2.51 Loop A Cold Leg Differential Pressure Measurements

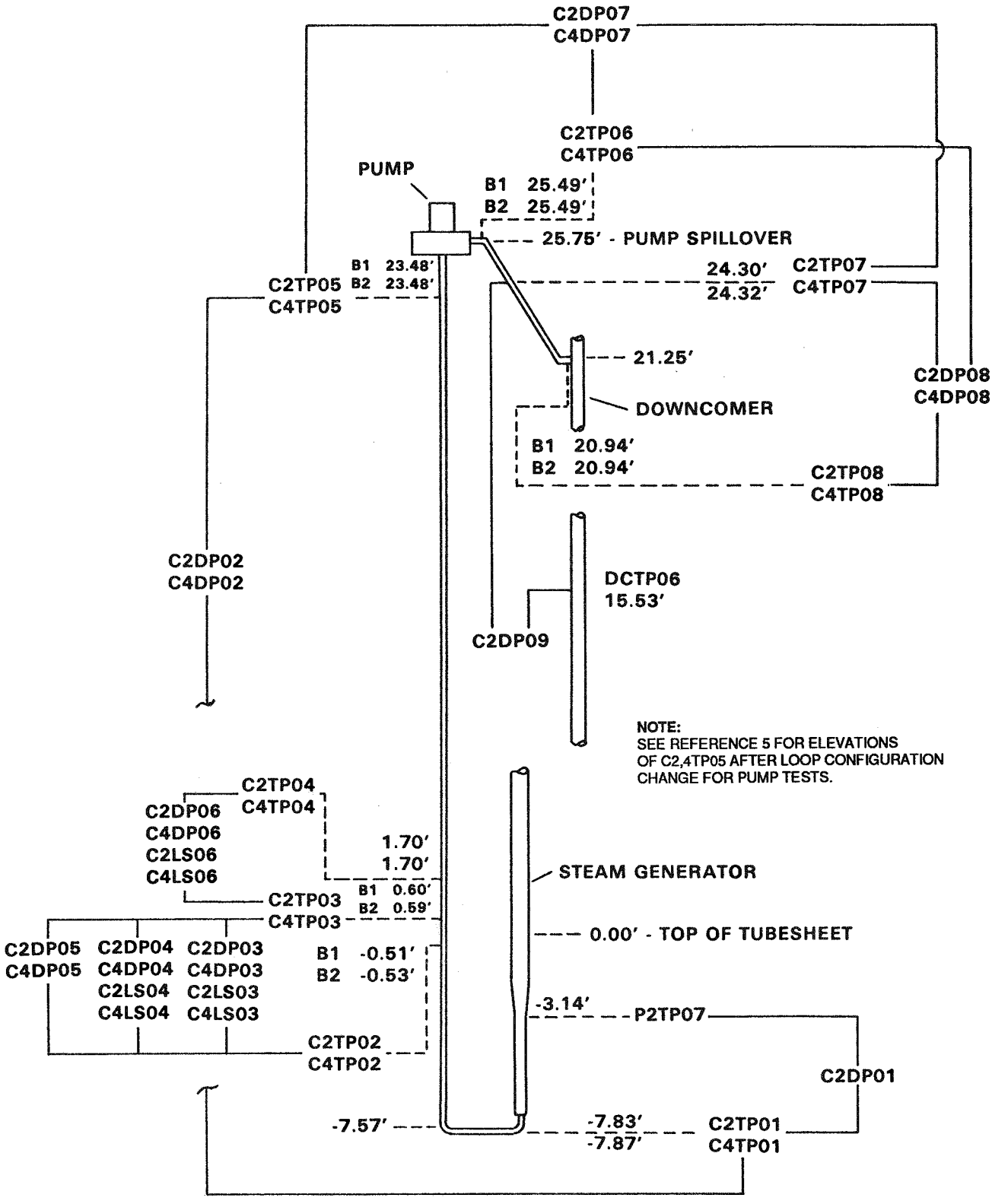

Figure 2.52 Loop B Cold Leg Differential Pressure Measurements

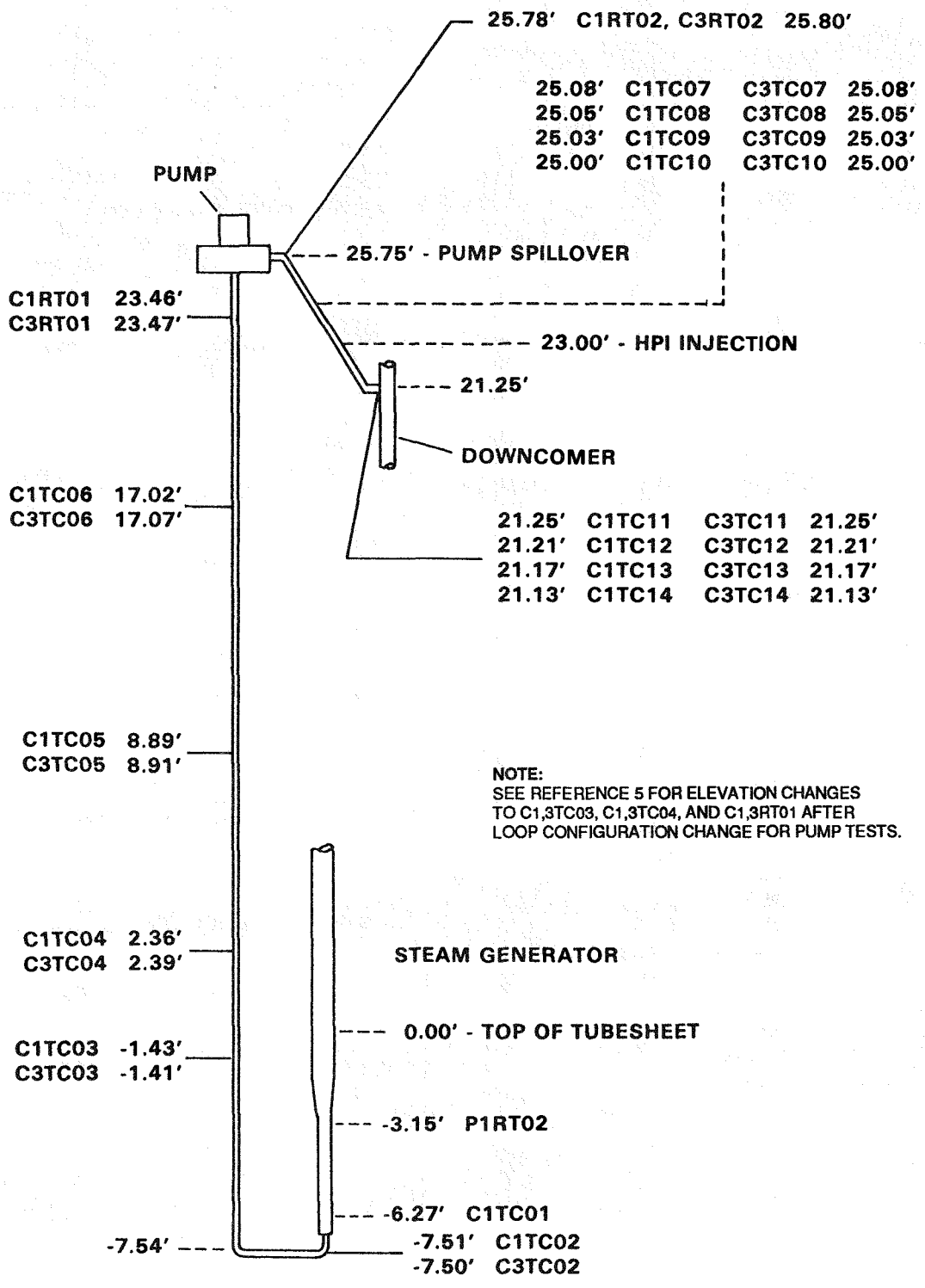

Figure 2.53 Loop A Cold Leg Fluid Temperature Measurements

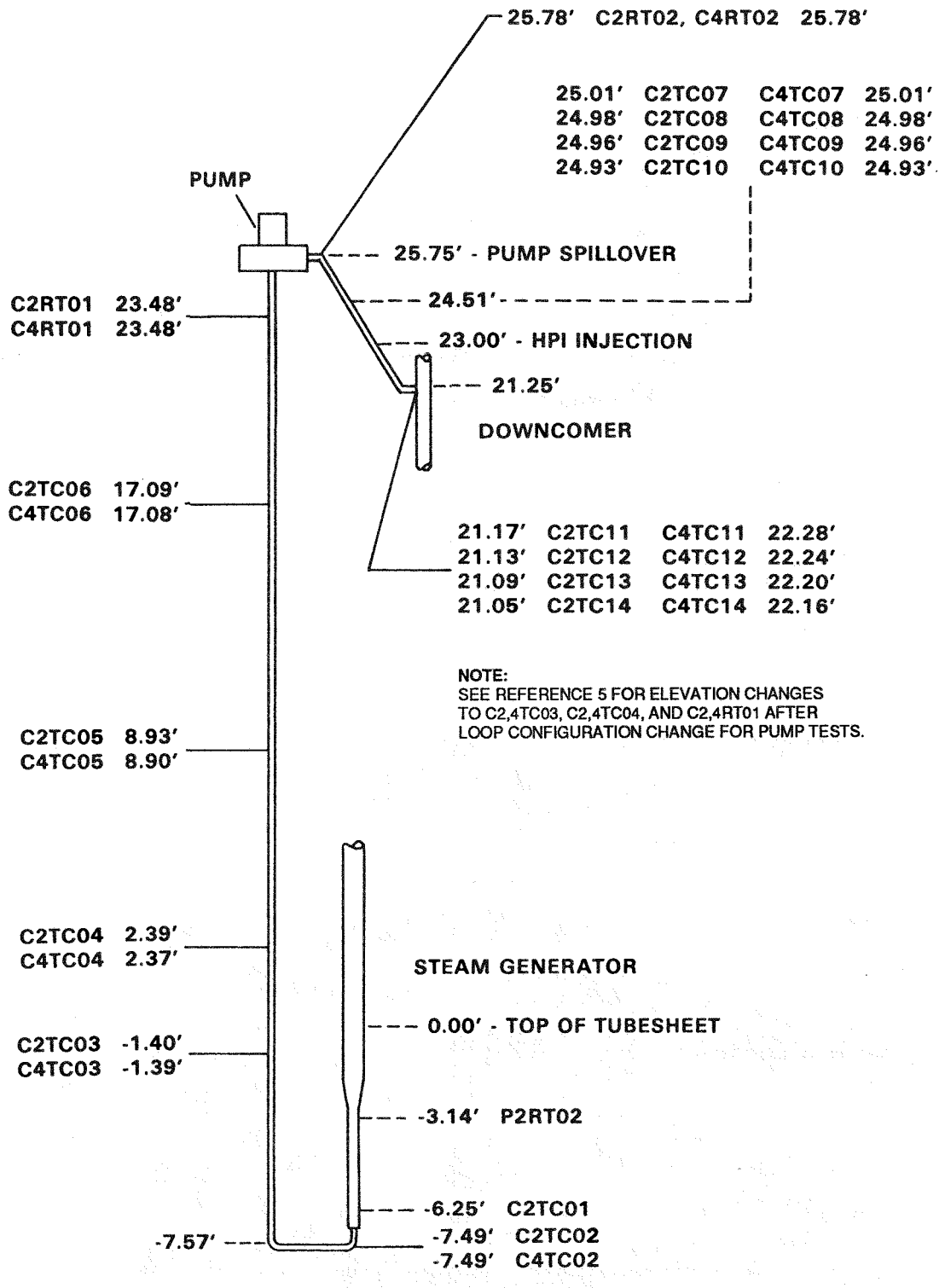

Figure 2.54 Loop B Cold Leg Fluid Temperature Measurements

Thermocouple rakes were located both upstream and downstream of the HPI nozzle in all four cold legs. These rakes were used to help detect liquid-liquid stratification and HPI heatup due to mixing and condensation and to detect the approach to saturation conditions in the cold leg discharge piping. The rake located upstream of the HPI injection point was positioned approximately 10 diameters from the injection location. The rakes thus provided a good indication of thermal stratification effects upstream of the HPI point. The downstream rake was located in the horizontal piping near the flare on the downcomer nozzle. These rakes indicated the temperature profile of the fluid entering/leaving the downcomer. Each rake was composed of four thermocouples mounted on a stalk that radially spanned the flow cross section as illustrated in Figure 2.55. On each rake, the thermocouples were numbered from the top of the stalk in ascending order to the bottom of the stalk.

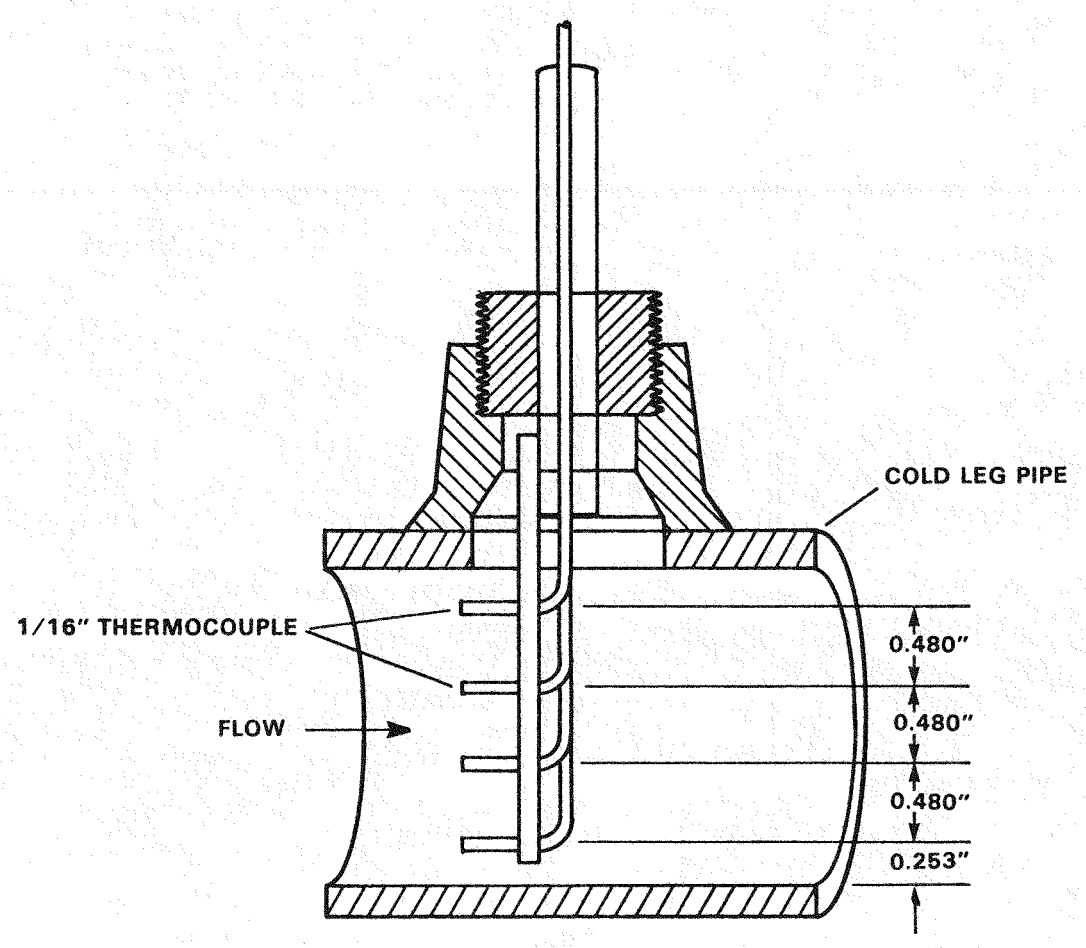

Figure 2.55 Thermocouple Rake in Cold Leg Discharge Piping

Guard Heater Zones, Metal Temperatures, and Insulation Temperatures. Figure 2.56 depicts guard heater zones, piping metal temperatures, and insulation differential temperatures for each cold leg. Three guard heater zones are shown. Two, each approximately 15 feet in length, were located in the pump suction leg and one zone approximately 5 feet in length was located in the pump discharge leg. With the exception of C1-4DT01 and C1-4MT01, the metal and insulation thermocouples were located approximately in the center of the guard heater zones. C1-4DT01 and C1-4MT01 were located 1.6 feet above the center of the zone to avoid interference with the venturi and to be consistent with the fluid temperature at that same elevation.

The thermocouple pairs imbedded in the insulation for guard heater control were located at approximately the same elevation as the pipe metal temperatures. The control thermocouples were axially spaced about 2 inches from the fluid thermocouples to avoid interference.

Power to each guard heater zone was inferred via measurement of the voltage across a precision resistor located upstream of the firing circuit for each heater zone. This power measurement included power components transferred to the pipe and fluid as well as heat loss to the ambient.

Pump Measurements. Pump measurements are also shown on Figure 2.56. In addition to the heat measurement already discussed, pump power, motor current, and rotational speed were recorded.

Each of the loop pumps also had three thermocouples for monitoring motor winding temperature and one thermocouple for monitoring rotor cavity bearing temperature. Also, each pump had provision for installation of an accelerometer (for monitoring vibration and/or cavitation) on the outer surface of the volute housing. These measurements were for process control and safety, and were not recorded on the data acquisition system.

Limit Switches. Limit switches were installed on the low, mid range, and reverse flow range of each of the cold leg venturi DP measurements. These switches facilitated startup procedures and aided operationally to indicate when the measurements are put in service. Limit switches in the turbine meter signal processing electronics provided a flow direction indication.

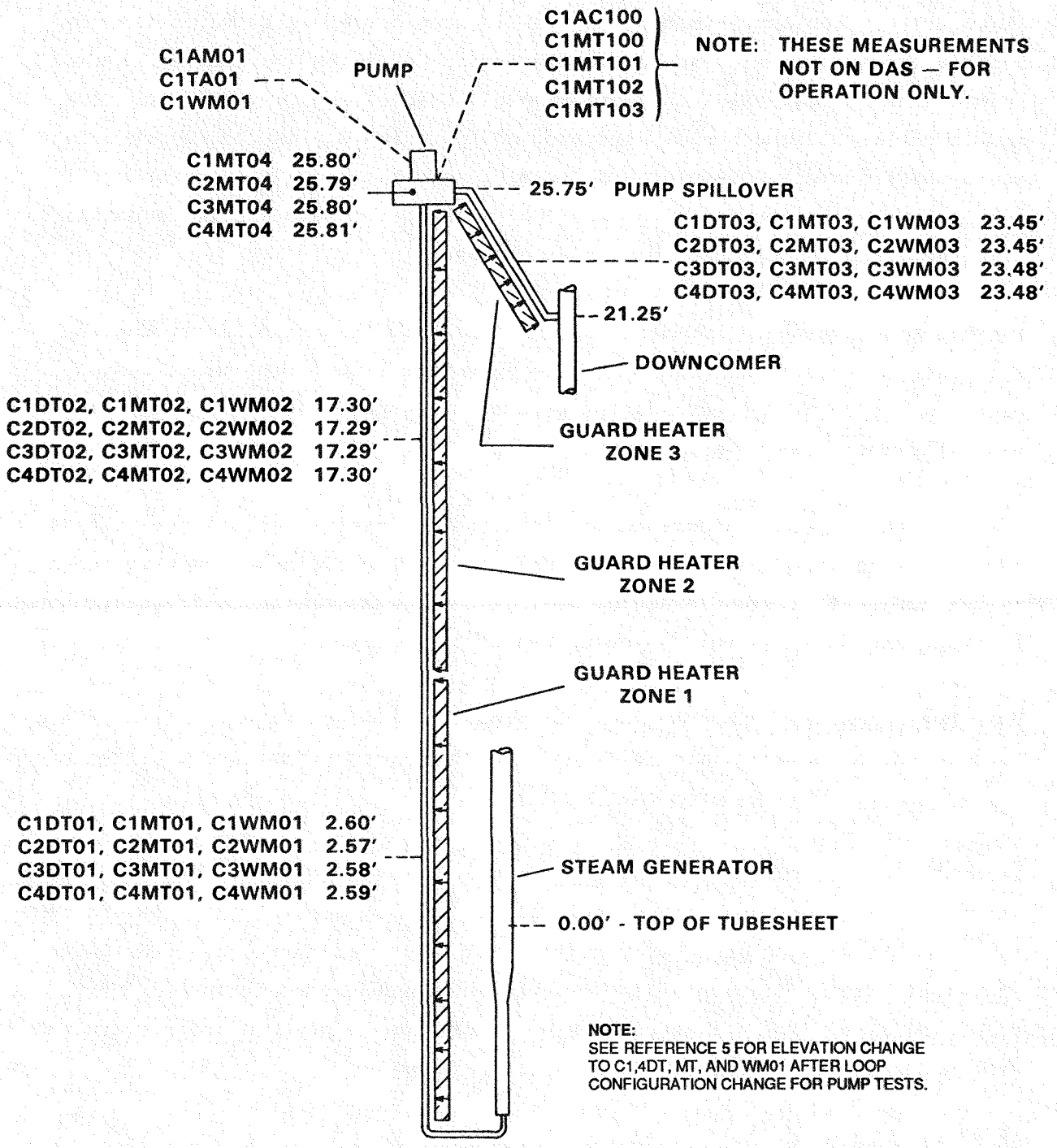

Figure 2.56 Cold Leg Guard Heater System Measurements

2.6 PRESSURIZER

The plant pressurizer provides an additional primary loop volume, equipped with heaters, vents, and spray, which serves to dampen reactor coolant system pressure transients. The pressurizer vessel is outside of the normal reactor coolant flow path, connected by the surge line to the A-loop hot leg. The configuration of the surge line piping provides a loop seal which impacts the flow of primary inventory toward or away from the pressurizer vessel.

Pressurizer scaling and design considerations include volume, the impact of heaters, sprays, and vessel walls on boiling and condensation, and elevation for the surge line loop seal. Pressurizer vessel volume impacts the inventory of available primary coolant and the rate of primary system pressurization or depressurization. Condensation is the primary mechanism for energy removal from pressurizer inventory, in the absence of vent operation. Surge line elevations impact pressurizer drain rates and the venting of primary fluid through the pilot-operated relief valve (PORV).

2.6.1 Pressurizer Design

The pressurizer and surge line configuration is illustrated in Figure 2.57. The pressurizer vessel is fabricated from 6-inch, schedule 120 pipe and is 11.28 feet tall. The resulting contained volume of 3215 cubic inches preserves power-scaled plant pressurizer volume; however, the overall vessel height is reduced in order to increase vessel cross-sectional area. The larger cross section promotes plant-typical internal circulation patterns and fluid stratification and reduces the atypically high ratio of surface area to vapor volume for the MIST pressurizer.

Heat transfer mechanisms for the MIST pressurizer are similar to the plant. For both, heat transfer by condensation of vapor on the vessel wall dominates heat transfer by condensation at the liquid-vapor interface and axial conduction. Heat transfer coefficients for the vertical pressurizer wall are a function of fluid properties and height. Coefficients for MIST are plant-typical since thermodynamic conditions for MIST and the plant are equivalent and since the dependence on height is weak.

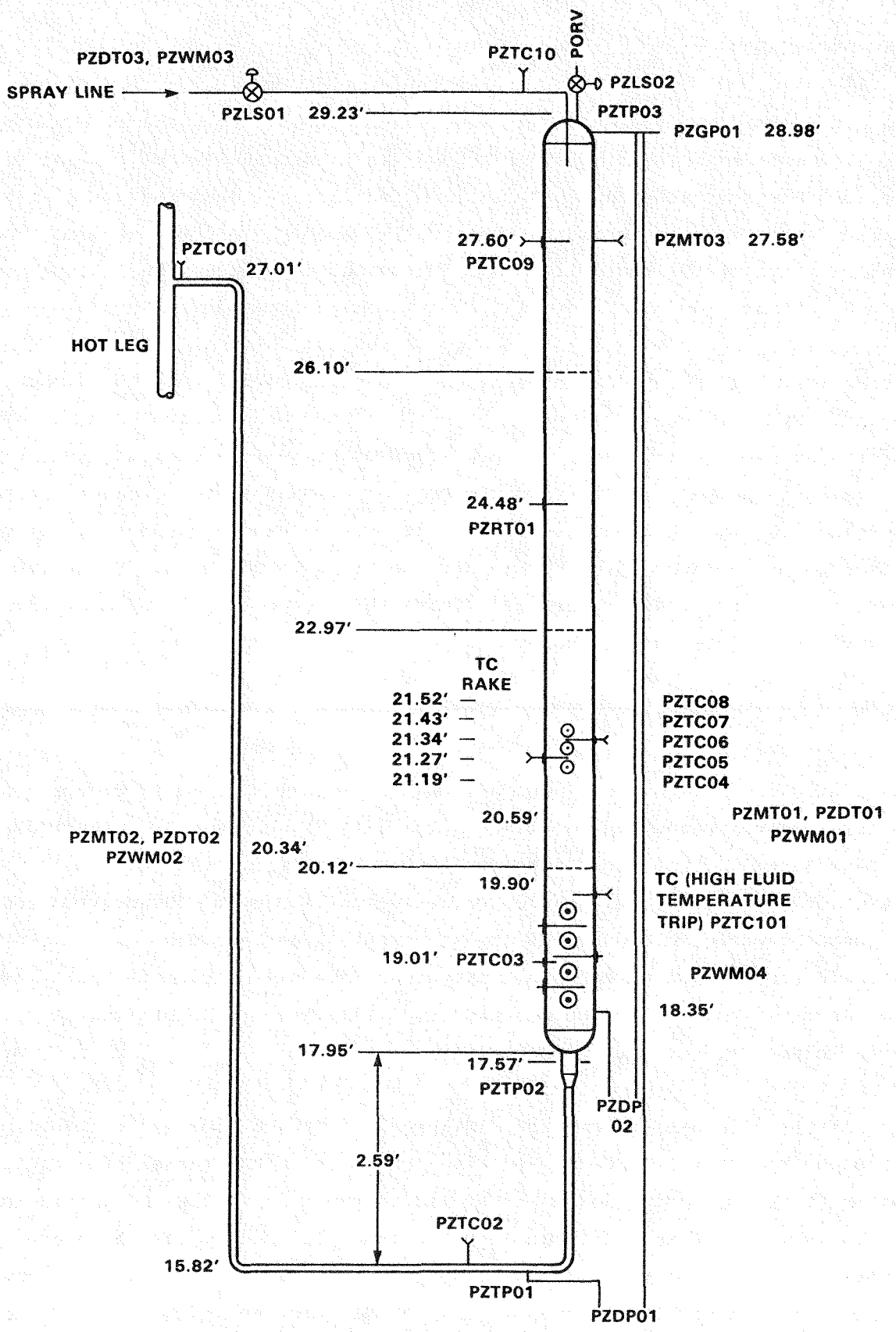

Figure 2.57 Pressurizer and Pressurizer Surge Line

The MIST pressurizer vessel is guard heated to provide an approximately adiabatic condition at the vessel outer surface. One control zone is used since the vessel geometry is simple and compact. The presence of a fluid interface within this is expected to have minimal impact on guard heater performance.

Seven electrical heater rods are installed in the MIST pressurizer for reactor coolant system pressure control. Scaled heater power is 2.0 kW and is provided by three of the seven heater rods. A maximum of 4.7 kW is available for facility control during test setup by using all seven heaters. The heater rods are installed as shown in Figure 2.58, in the lower 1.5 feet of the pressurizer vessel. The heater rods reduce the unrestricted fluid flow area by 17% in this region.

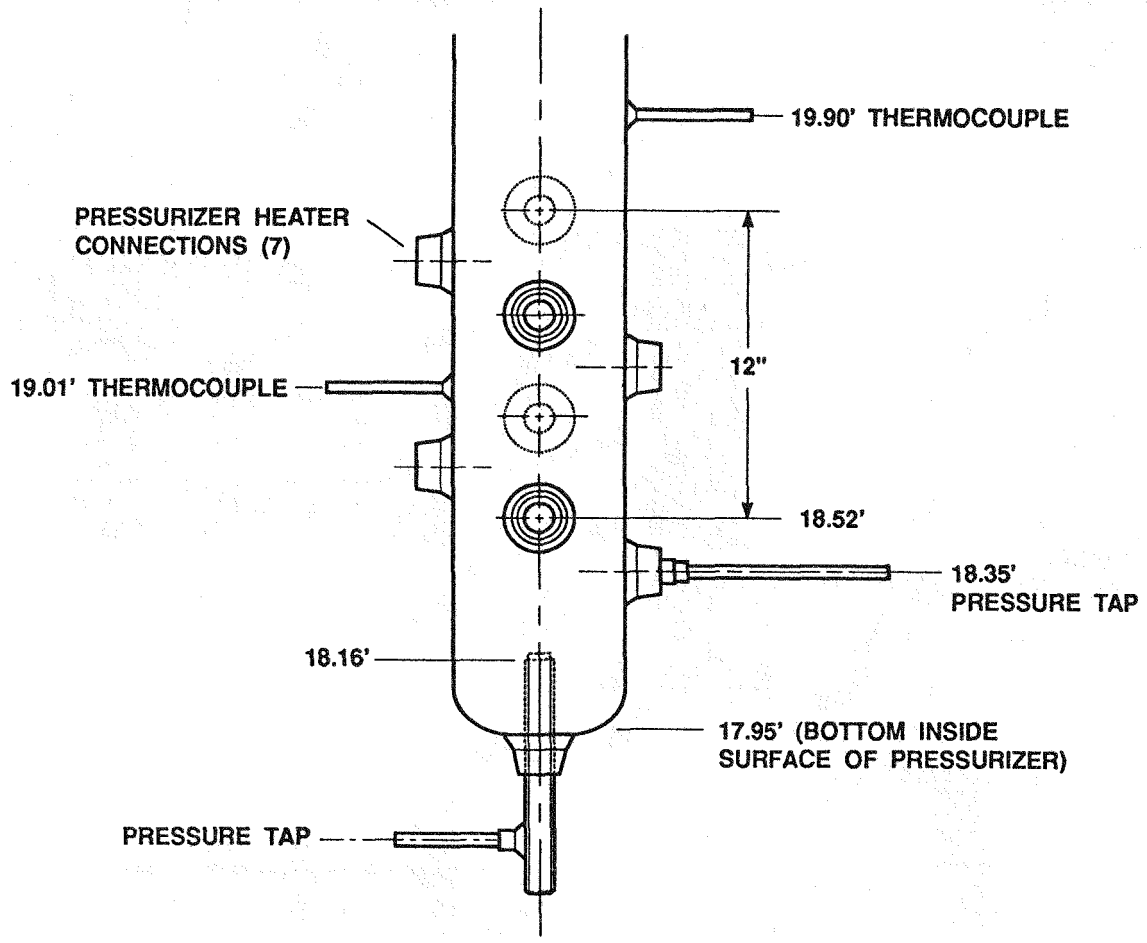

Figure 2.58 Pressurizer Heater Installation

The MIST pressurizer spray line provides additional reactor coolant system pressure control by injecting relatively cool liquid into the pressurizer vapor space. Spray is initiated by opening remotely actuated valves in a line connecting the A2 cold leg discharge piping to the top of the pressurizer. The pressure gradient developed by the operating reactor coolant pumps drives the scaled flow rate of 0.26 gpm into the pressurizer vessel (based on pump discharge to pressurizer pressure difference of 80 psi).

The spray nozzle is designed and installed to minimize the contact of spray droplets with vessel walls. Contact with hot wall metal would result in vapor generation, offsetting the intended effect of the pressurizer spray. The spray nozzle and installation at the top of the MIST pressurizer vessel is shown in Figure 2.59. The nozzle was designed to obtain a spray pattern having less than 4° included angle over 71 inches. The MIST spray line is guard heated to maintain cold leg discharge temperature at the pressurizer spray inlet nozzle.

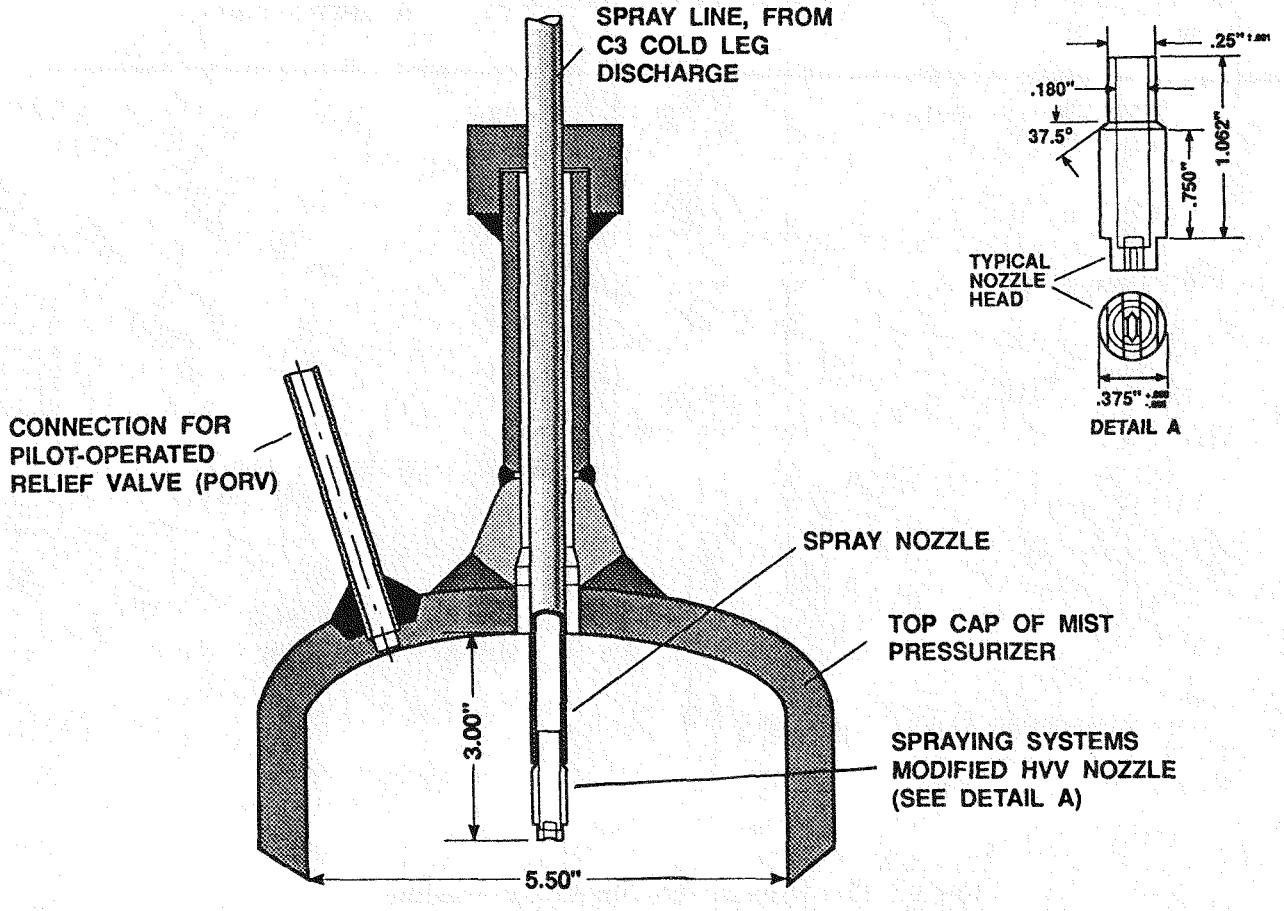

Figure 2.59 Pressurizer Spray Nozzle Installation

The MIST pressurizer includes a vent in the vessel head which is most often used to simulate the plant pilot-operated relief valve (PORV). A scaled 10 cm^2 critical orifice provides modeled flow when the PORV isolation valves are remotely actuated.

The MIST surge line is the communication path between the pressurizer and the A hot leg. The line is fabricated from 3/4-inch, schedule 160 pipe to approximate plant-typical irrecoverable pressure loss and to prevent atypical flooding phenomena. Plant-typical elevations, as noted in Figure 2.57, are preserved for the surge line connections to the pressurizer vessel and the hot leg and for the surge line low point to model the influence of the surge line loop seal on transient response.

The surge line termination in the MIST pressurizer vessel is detailed in Figure 2.60. The MIST surge diffuser preserves the power-scaled flow area of the surge diffuser.

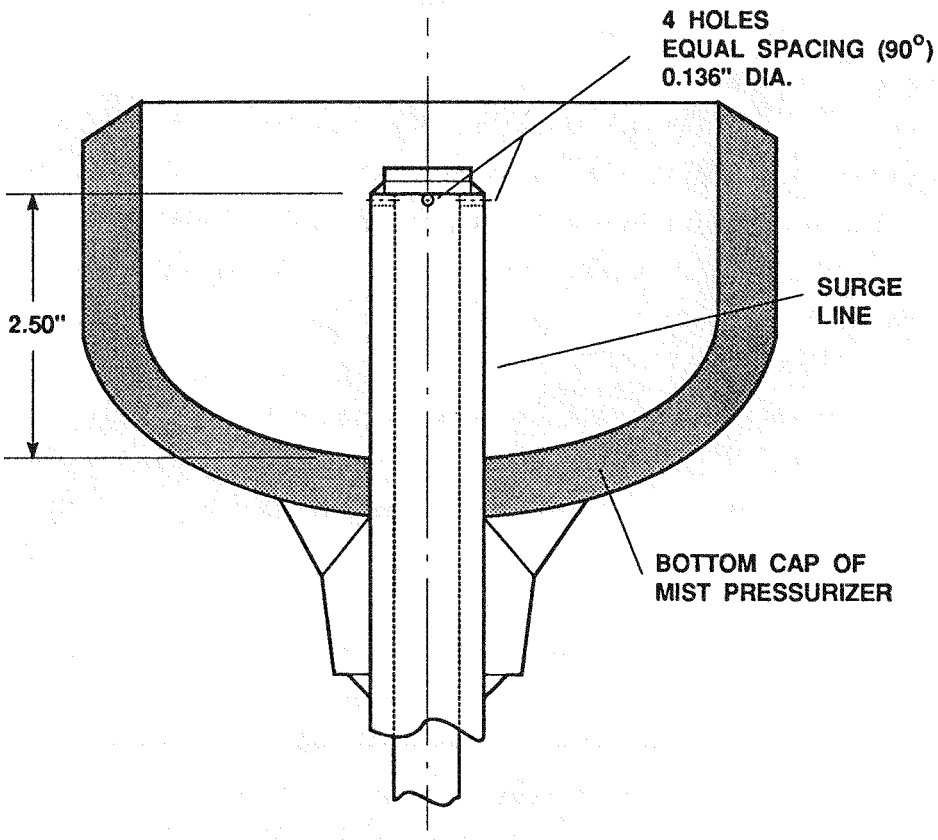

Figure 2.60 Pressurizer Surge Line Diffuser

The surge line is guard heated using one control zone. Power to this zone is manually controlled during establishment of test initial conditions to achieve equivalent surge line outlet and hot leg fluid temperatures. Control is switched to CASCADE (refer to Section 3.3) just prior to transient initiation.

Operation of the pressurizer heaters is limited by several automatic trips. The heaters trip on low liquid level to prevent heater damage. The heaters also trip on high liquid level, high pressure, and high fluid temperature to protect the reactor coolant system from overpressure conditions.

Also for facility protection, power to all guard heaters may be interrupted if abnormal conditions occur in the pressurizer. These conditions are high pressure in the pressurizer vessel or the spray line, high fluid temperature in the vessel, and high wall metal temperature.

2.6.2 Pressurizer Instrumentation

Pressurizer instrumentation recorded by the data acquisition system includes fluid thermocouples, pressurizer (fluid) heaters and guard heater power measurements, differential and metal temperature measurements, gauge and differential pressure measurements, and an RTD. Limit switches are installed on the PORV and spray line isolation valves to indicate when these simulations are active. A total of 26 measurements are recorded in the pressurizer vessel, surge line, and spray line as defined in Figure 2.57.

Fluid thermocouples are installed in the surge line near the connection to the hot leg and at the low point. These thermocouples, along with another installed near the bottom of the pressurizer vessel, define the average fluid temperature for the surge line.

All fluid temperature measurements in the pressurizer are located along the vessel centerline. The lowest elevation thermocouple is installed in the region of the pressurizer heaters. Five more thermocouples are grouped within 4 inches to provide detailed information regarding the liquid-vapor interface. These thermocouples are located near, but below, the established collapsed water level at transient test initial conditions. An RTD is installed near

the vessel mid-elevation and may be used as a standard for thermocouple calibrations. The highest elevation fluid thermocouple may be compared to a wall metal temperature measurement at the same elevation to confirm appropriate guard heater operation.

One fluid thermocouple is installed in the spray line, near the inlet nozzle, to define the entering fluid temperature. This thermocouple also forms one half of the control pair (with C3TC07) for the spray line guard heater.

Two differential pressure measurements are used to compute pressurizer collapsed levels. These measurements, along with the pressurizer gauge pressure measurement, share a common tap in the top vessel head. The lower tap for PZDP02 is located in the vessel, above the surge line diffuser nozzle. This measurement is used for the pressurizer level computation during the rapid drain following transient test initiation to avoid errors resulting from irrecoverable losses at the diffuser nozzle. The lower tap for PZDP01 is located at the surge line low point. This measurement extends the collapsed level computation into the surge line after the vessel empties.

Guard heater power and control temperature measurements are recorded for each of the three control zones associated with the pressurizer. Insulation differential temperatures, metal temperatures, and guard heater power are recorded for surge line and pressurizer vessel guard heater zones. Fluid differential temperature and guard heater power are recorded for the spray line guard heater zone.

2.7 CONTINUOUS VENT LINE

Toledo Edison has installed a continuous vent line in the reactor coolant system of their Davis-Besse plant in lieu of a reactor vessel head-to-containment vent. The vent line extends from the top plenum of the reactor vessel to the upper (inlet) plenum of the A loop steam generator. The vent line has no valves, and therefore is in continuous operation. This would provide a path for steam or noncondensible gases to flow from the reactor vessel head to the hot leg where any possible accumulation could be released through the hot leg high point vents. The vent line also results in a more

rapid cooldown of the fluid in the reactor vessel upper and top plenums since the vent line facilitates greater flow through the reactor vessel head region.

Toledo Edison sponsored the installation of a continuous vent line in the MIST facility, and a series of tests to examine the effect of the vent line on natural circulation cooldown and SBLOCA transients with noncondensible gases. The vent line was only installed for these specific tests, designated the Group 37 test series.

2.7.1 Vent Line Design

The MIST continuous vent line consists of 1/2-inch, schedule 160 pipe extending from the top of the reactor vessel upper head to the upper plenum of the B-loop steam generator. Similar to the plant vent line, it contains no valves and therefore is in continuous operation. Unlike the plant, the vent line in MIST was connected to the upper plenum of steam generator B (i.e., the loop without pressurizer surge connection). The Davis-Besse vent line is connected to the upper plenum of steam generator A. Steam generator B was chosen in MIST because of the generator's extensive instrumentation compared to steam generator A.

An inside diameter of 0.466 inch was chosen for the MIST vent line as a compromise between larger line sizes which would preserve plant-similar two-phase flow regimes and smaller line sizes which would preserve irrecoverable loss characteristics, volume scale (hence elapsed time for flow to traverse the line), and vertical pipe flooding similarity. With this choice, it is necessary to add an orifice in the line to obtain scaled plant-typical resistance; that is, to preserve hydraulic loss characteristics when passing scaled single-phase flows.

Davis-Besse is a raised loop plant (referring to the elevation of the steam generators relative to the reactor vessel), whereas the steam generator placement in MIST replicates B&W's lowered loop plant design. Therefore, the MIST vent line installation cannot preserve Davis-Besse plant vent line elevations. However, as indicated in Figure 2.61, the model vent line does preserve spillunder and spillover elevations of the steam generator upper plenum connection piping.

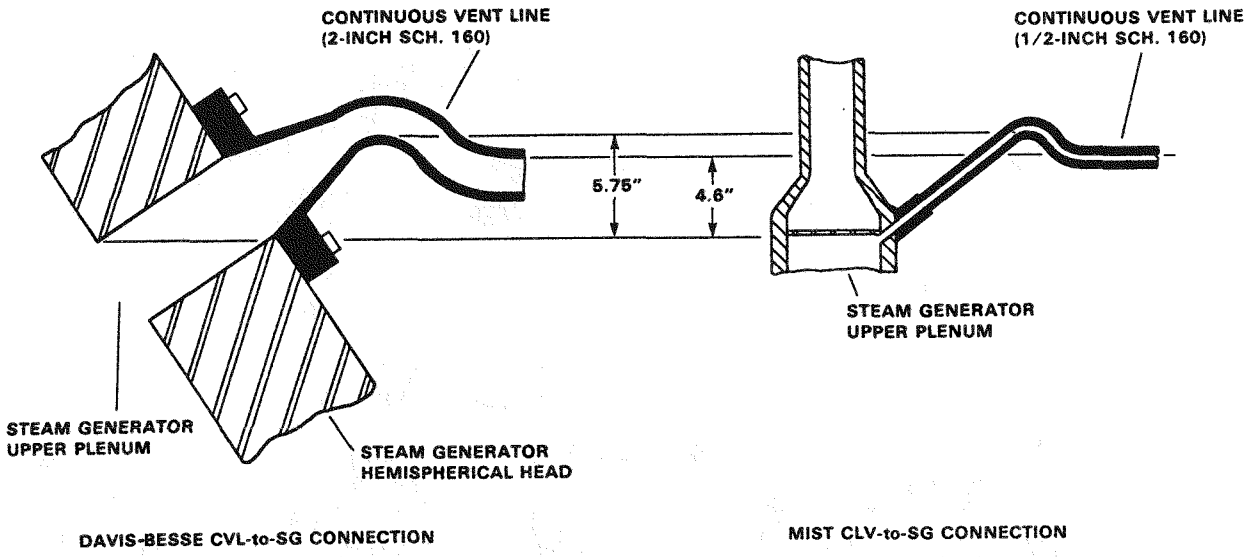

Figure 2.61 Continuous Vent Line Connection to Steam Generator

The steam generators in MIST each have a 50% perforated plate located 2 inches above the primary face of the upper tubesheet. The plates are used to distribute primary flow among the steam generator tubes. As indicated in Figure 2.61, the MIST vent line is connected to steam generator B such that the spillunder point for vent line flow precisely aligns with the underside of the distribution plate.

Figure 2.62 shows the overall geometry of the MIST continuous vent line. As seen in this figure, the orifice in the line is installed in the horizontal run from reactor vessel to steam generator. Since the orifice will also be used to measure vent line flow rates, it is installed approximately mid-length along the straight horizontal pipe section to provide flow development length for flow in either direction.

The orifice is welded into the vent line in the straight horizontal pipe section. With this installation, the model vent line is a completely welded system. The continuous vent line in MIST was also guard heated to prevent atypically high heat losses to ambient.

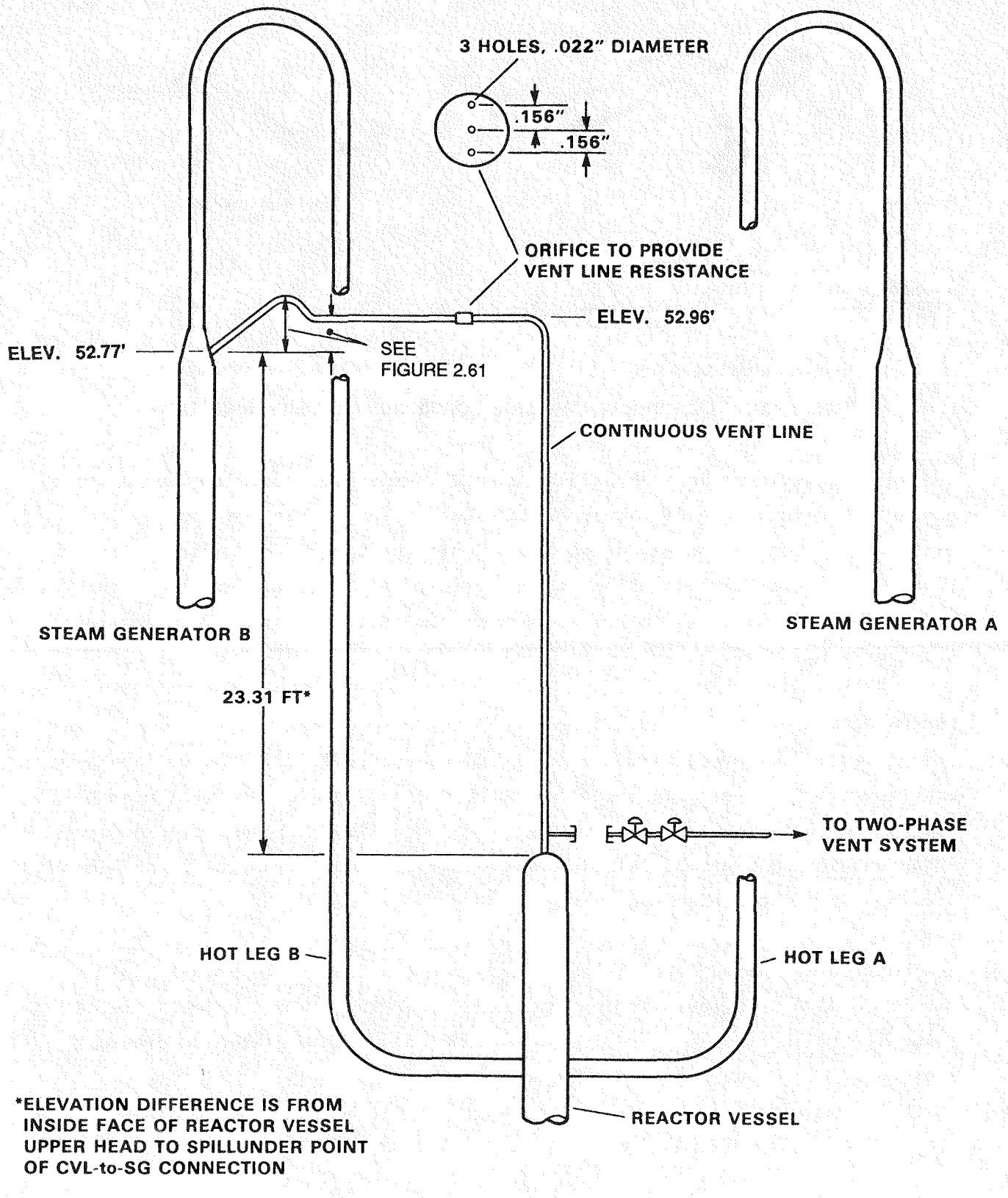

Figure 2.62 MIST Continuous Vent Line

2.7.2 Vent Line Instrumentation

The continuous vent line is schematically shown in Figure 2.63 to indicate instrumentation placement. Three differential pressure measurements were associated with the vent line. HVDP02 spanned the vertical length of the head vent line to provide an overall collapsed liquid level or average void fraction. HVDP01 and HVDP03 are differential pressure measurements across the vent line orifice used for mass flow measurement during single-phase venting conditions. HVDP01 is a low range transmitter for periods of liquid flow through the vent line. HVDP03 is a higher range transmitter ranged to measure vapor flow and higher liquid flow rates through the line. In addition, two pressure taps were installed 27 inches apart along the vertical length of the vent line. A differential pressure measurement between these taps was used to obtain an average local void fraction in the vent line at this approximate mid-point along the vent line's vertical run.

HVTC01 in the vent line measured vent line fluid temperature as it entered the steam generator upper plenum. V2TC02 was installed as part of the two-phase vent system to measure vent line fluid temperature as it entered the vent line from the reactor vessel top plenum. HVMT01 and HVDT01 were used to control power to the vent line's guard heating system.

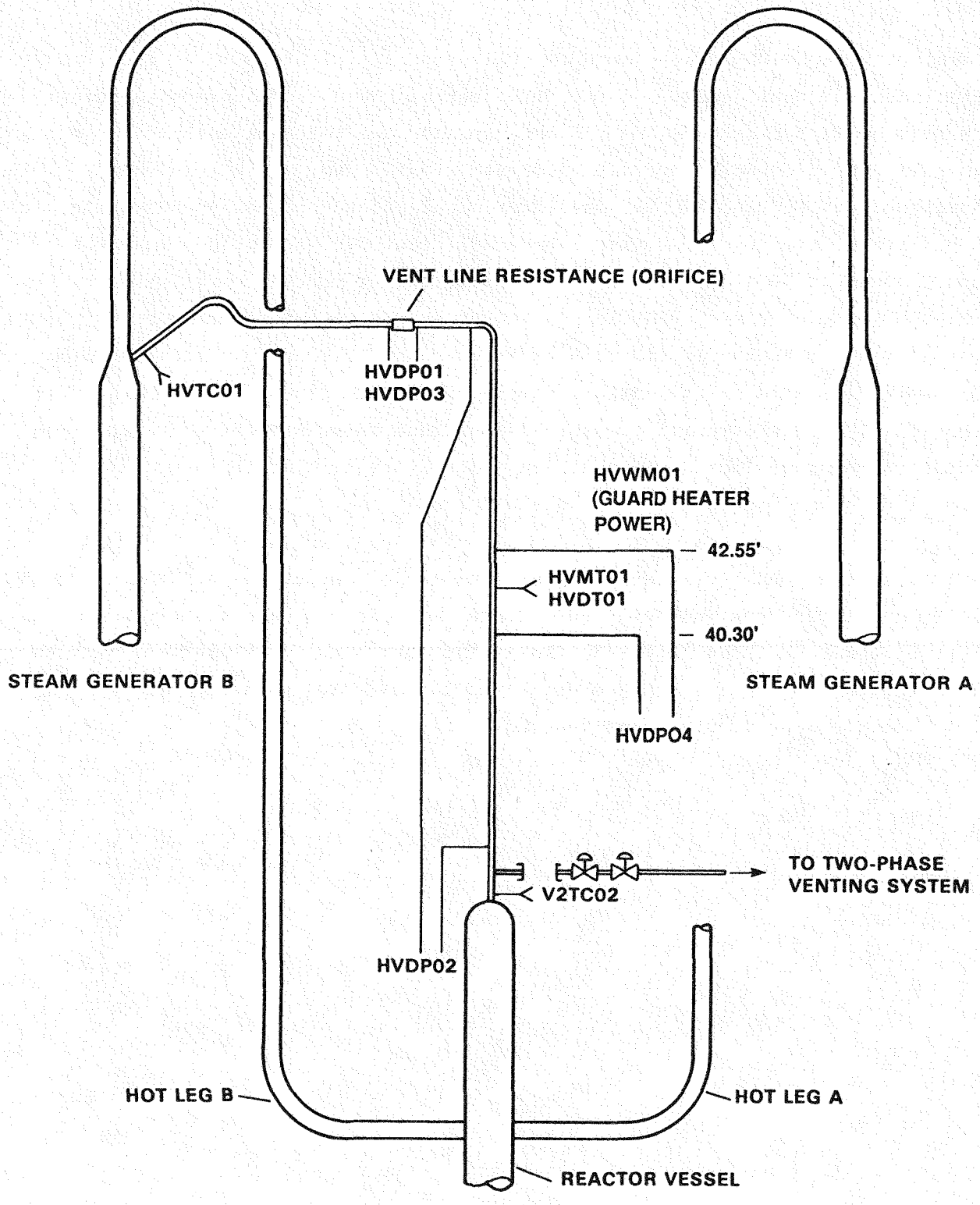

Figure 2.63 Continuous Vent Line Instrumentation

Section 3

BOUNDARY SYSTEMS

The facility boundary systems discussed in this section are the independent subsystems that collect effluent from, add fluid to, minimize heat loss from, and clean up the fluid inventory of the reactor coolant system. The secondary system supporting the steam generators is also discussed as one of the boundary systems, in that the secondary loop provided in MIST only simulates the plant conditions at the immediate entrance and exit of the steam generator's secondary side. The major facility boundary systems consist of the single-phase leak system, two-phase leak/vent system, the guard heating system, the emergency core cooling system, the secondary system, the gas addition system, and the water supply and cleanup system. There are also several minor independent subsystems, such as the reactor coolant boost pump circuit that are discussed throughout the remainder of this report in the sections providing a description of the specific facility component supported by the system.

3.1 SIMULATED LEAKS

Reactor coolant system leaks are simulated at several locations in the MIST facility, corresponding to likely plant leak sites. Scaled leak flows are obtained using critical flow orifices installed just downstream of each leak site. A typical scaled 10 cm^2 leak orifice assembly is shown in Figure 3.1; various scaled orifice sizes are available. As indicated, scaled orifice dimensions and therefore, flow rates are small so avoidance of unplanned leakage from the model reactor coolant systems is very important.

The leak orifice is scaled by multiplying the area of the break by 1/817, consistent with the facility's power scale factor. The leak collection system is designed to minimize back pressure on the leak orifice assembly, in order to ensure a choked flow condition at the orifice. Because the test facility operates at full plant pressures, the critical mass flux is assumed to be

preserved. Therefore, scaling the break area results in a leak mass flow rate that is consistent with the core power scaling.

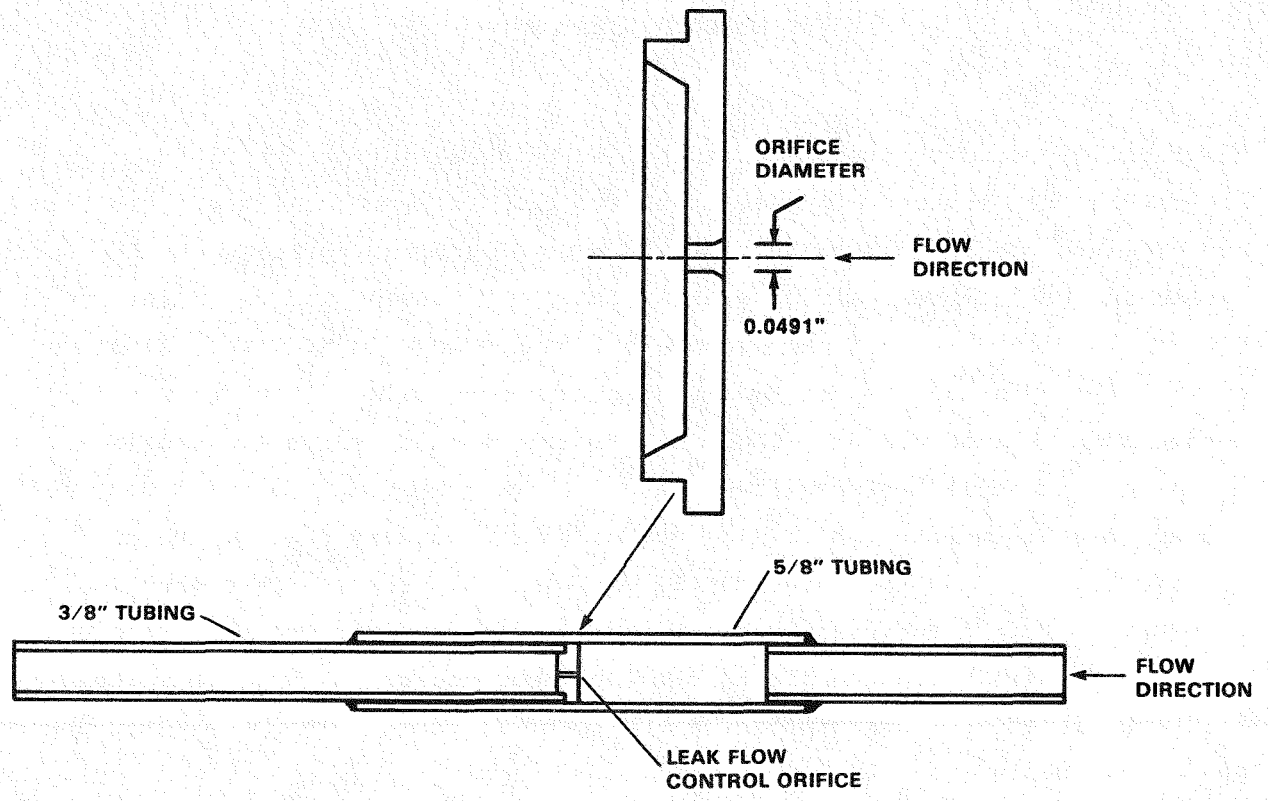

Figure 3.1 10 cm^2 Critical Leak Flow Control Orifice

Remotely actuated, sealed stem valve pairs provide leak tightness and allow selective leak actuation from the MIST control room. Each valve pair isolates an orifice assembly from reactor coolant system pressure, allowing replacement of the orifice assembly without loop shutdown. Depending on the type of leak being simulated, leak effluent is either cooled to ambient conditions before final collection or immediately reinjected into the steam generator secondary. Primary to ambient leak size is limited to 100 cm^2 (scaled) by cooling capacity of the leak collection system.

3.1.1 Leak Sites

Four instrumented leak locations are simulated in the MIST reactor coolant system. The nominal leak site is in the C2 cold leg (i.e., B1 cold leg) discharge piping, below the HPI injection point, on the pipe underside. This site is equipped with a four-branch control orifice assembly (see Figure 3.2) and is connected to a leak quality measurement system. The second leak site in the figure is at the C2 cold leg suction piping low point, on the underside of the pipe. The two remaining instrumented leak sites simulate upper and lower elevation steam generator tube ruptures. These leaks and their associated instrumentation are discussed in Section 2.4 for the B steam generator.

A leak site in the reactor vessel downcomer drain line is available when a symmetric primary loop drain down is required. This leak site is normally not instrumented but effluent from the site can be routed to the cold leg leak flow measurement instrumentation.

3.1.2 Leak Flow Measurements

Cold leg leak flow measurements, required for reactor coolant system mass and energy closure, include leak flow rate, accumulated flow, temperature, and energy. The following instruments are required for these measurements: 12 thermocouples, two mass flow rate meters, two load cells, two pressure transmitters, and 11 limit switches. Another load cell and mass flow meter were added to the cold leg leak system toward the end of the Phase IV test program to measure flow from the letdown system simulation shown in Figure 3.2. Instruments associated with the simulated steam generator tube ruptures are discussed in Section 2.4.2.

Thermocouples define effluent temperature at each cold leg leak site, as shown in Figure 3.2, prior to an isenthalpic expansion across a critical leak flow control orifice. Pressure at each leak site is evaluated using reactor coolant system pressure and differential pressure transmitters.

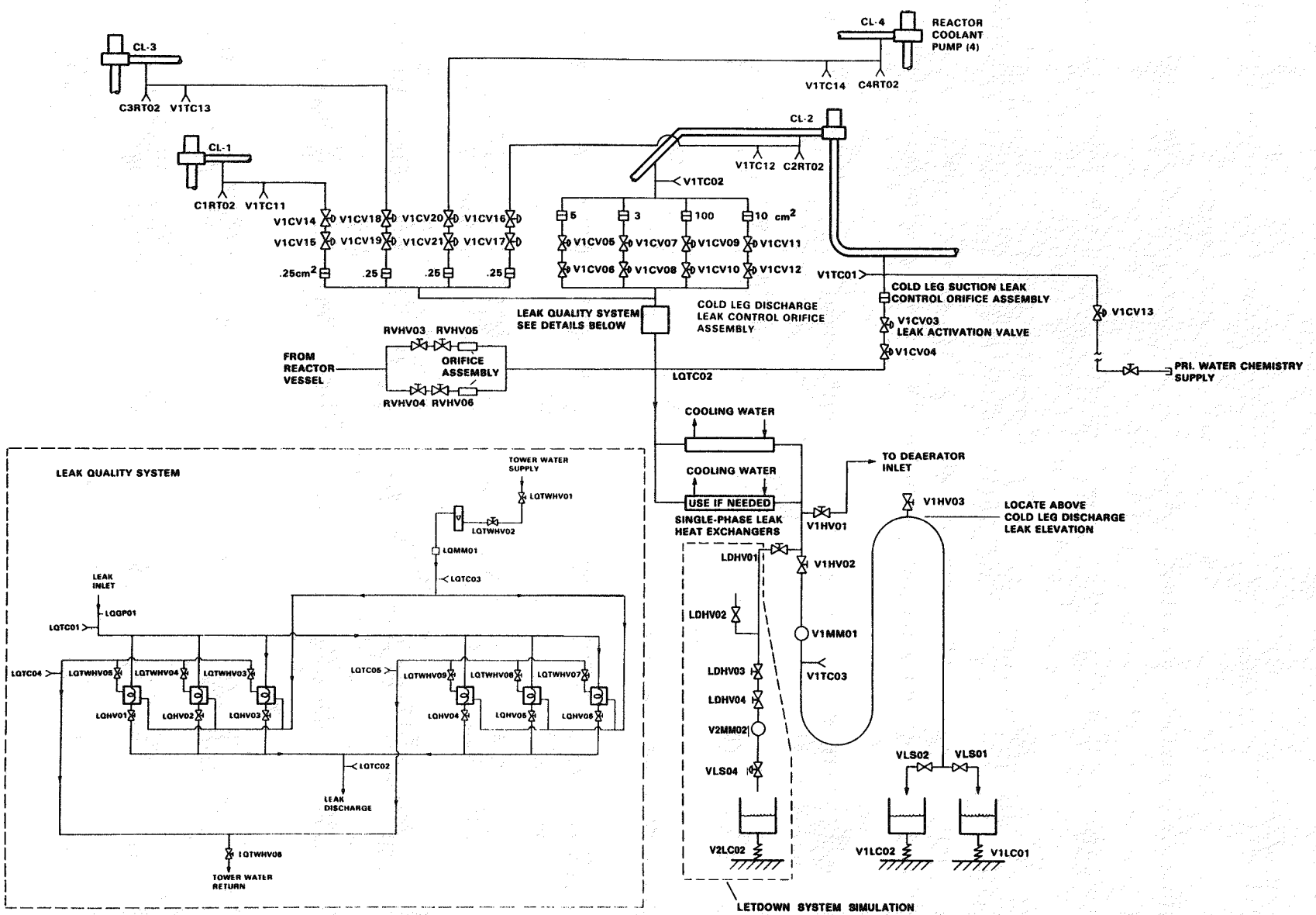

Figure 3.2 Cold Leg Leak System

For the cold leg discharge leak, the active critical orifice of the four available is indicated by limit switches and leak effluent is routed to the leak quality system. Tubing through the critical orifice to the leak quality system is insulated to maintain the energy content of leak effluent. The leak quality system is also insulated to minimize heat loss.

Fluid conditions at the cold leg discharge leak site may be single or two-phase. For single-phase conditions, leak energy content is evaluated from local reactor coolant system pressure and leak temperature. For two-phase conditions, energy content is evaluated by the leak quality system (schematic shown in Figure 3.2) by measuring the energy transferred while cooling two-phase leak fluid to slightly subcooled conditions. Six condenser coils provide the required cooling capacity.

To support the two-phase leak quality calculation, leak effluent and cooling water inlet and outlet temperatures are recorded as is leak effluent pressure at the leak quality system inlet. Leak effluent and cooling water flow rates are recorded using coriolis-type mass flow rate meters.

After the mass flow rate measurement, leak effluent is routed to one of two available weigh tanks. Limit switches define which collection tank is filling and accumulated fluid mass in each is recorded by a load cell. Integrated leak flow rate measurements are compared to the mass accumulated in the weigh tanks to confirm both flow rate and cumulative measurements.

3.2 SIMULATED VENTS

Four vent locations are simulated in the MIST reactor coolant system corresponding to plant reactor coolant system vents. These are the most likely sites for non-condensible gas accumulation in MIST and in the plant. As shown in Figure 3.3, vents are installed at each hot leg high point (HP vents), at the top of the reactor vessel upper head (UH vent), and in the pressurizer to simulate the plant power-operated relief valve (PORV). Effluent may consist of liquid, vapor, and non-condensible gas phases.

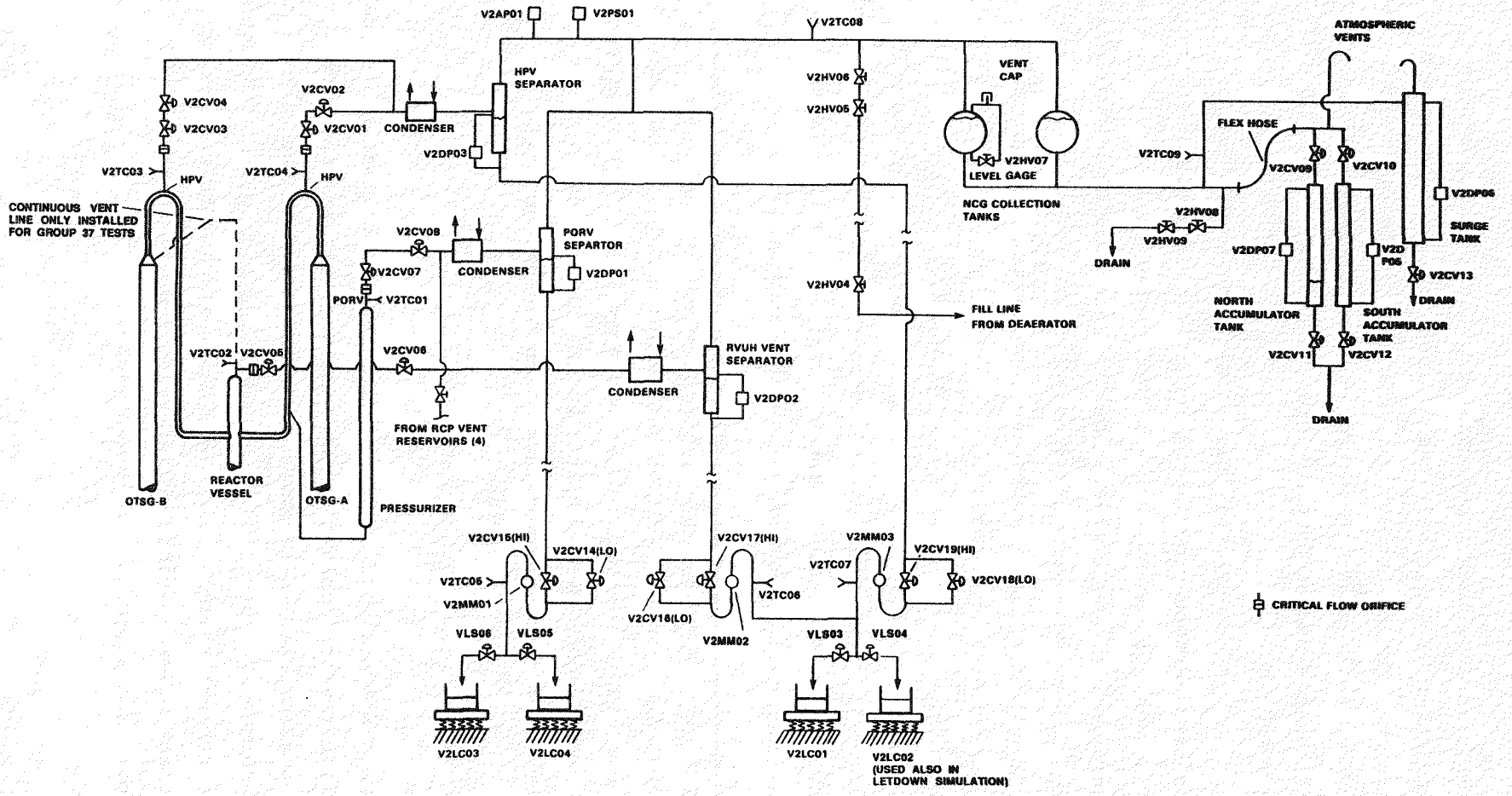

Figure 3.3 Two-Phase Venting System

The MIST hot leg high point vents are scaled to 1 cm^2 each and may be activated individually or together. The reactor vessel upper head vent is scaled to 1 cm^2. As indicated in Figure 3.3, effluent from this vent may be routed to the two-phase separation and collection system or directly to the B steam generator upper plenum (as is typical of the Davis-Besse head vent configuration). The power-operated relief valve is scaled to 10 cm^2.

Scaled vent sizes are obtained using scaled critical flow orifices installed just downstream of each vent site and orifice assemblies are similar to the leak orifice shown in Figure 3.1. Orifices for the vent sites are scaled the same as leak site orifices. Remotely actuated, sealed stem valve pairs ensure leak tightness and allow selective actuation from the control room. Each valve pair isolates an orifice assembly from reactor coolant system pressure, allowing replacement of the orifice assembly without loop shutdown.

3.2.1 Two-Phase Vent Separation and Collection

Two-phase separation systems are associated with each vent site. These systems cool the vent effluent and separate undissolved non-condensible gases to allow separate measurements of fluid and non-condensible gas flows. The two-phase vent system hardware is shown in Figure 3.3. As indicated, three separation systems are provided: one for the reactor vessel upper head vent, one for the hot leg high point vents, and one for the power-operated relief valve.

Additional primary vent sites are associated with each reactor coolant pump. These were installed to allow removal of non-condensible gas trapped in the pump impeller cavities. Effluent from the pump vents is routed to the separator nominally used for the power-operated relief valve effluent. The connection between the reactor coolant pumps and the two-phase venting system are shown in Figure 3.4. As indicated, each pump has a vent reservoir in the rotor-cavity cooling circuit. Barton differential pressure gauges are used to detect gas being collected in each reservoir, indicating the need to employ the two-phase venting system.

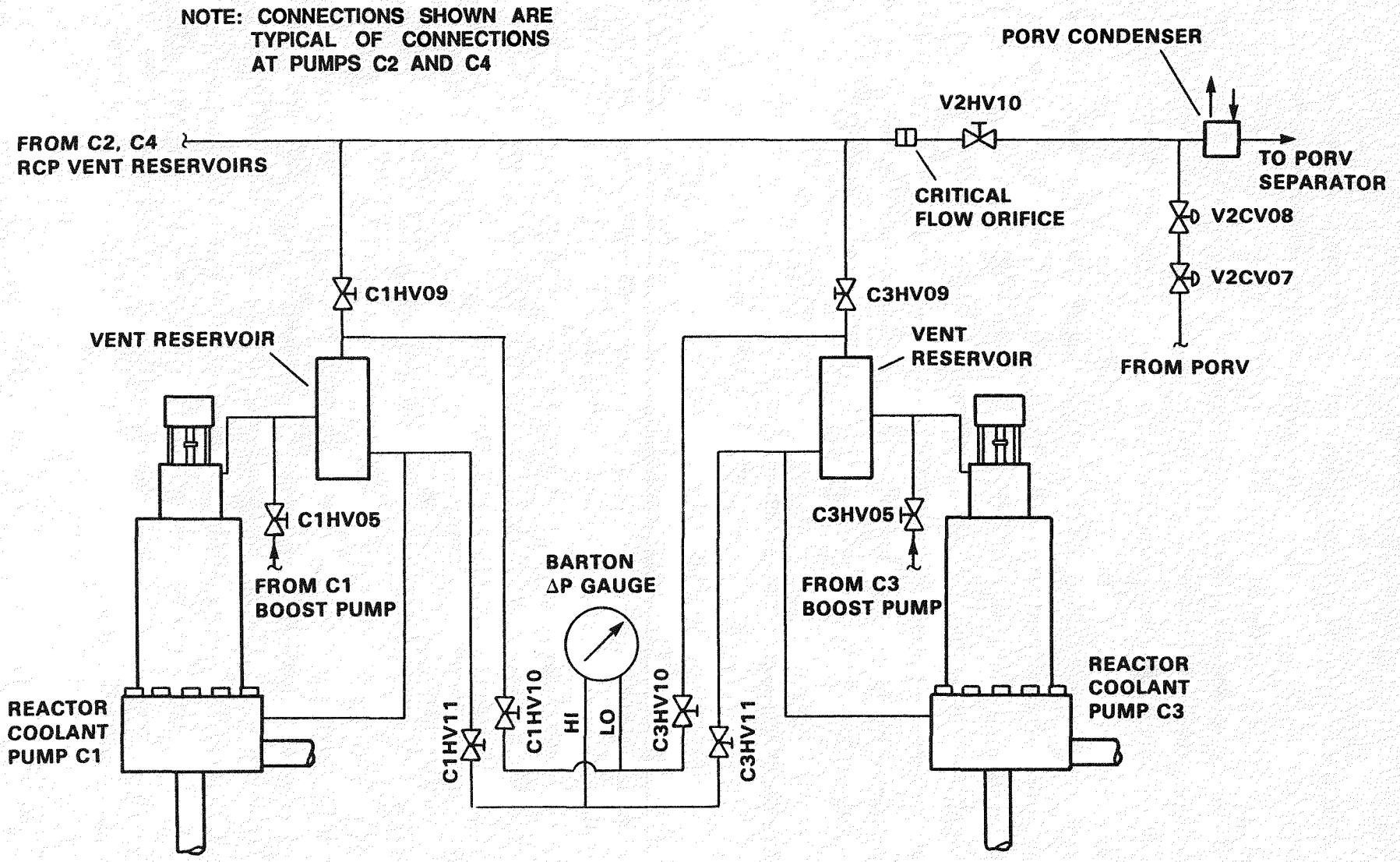

Figure 3.4 Reactor Coolant Pump Connections to Two-Phase Venting System

MIST two-phase separation systems operate as follows. Vent effluent, possibly consisting of liquid, vapor, and non-condensible gas phases, is cooled until only liquid and non-condensible gas phases remain. These phases are then separated using a cyclone-type separator. A constant liquid level is maintained in the separators, allowing liquid mass flow rate measurements downstream. Gas flow from the cyclone separators is combined and routed to a pair of collection tanks.

Combined, accumulated non-condensible gas flow is measured by displacing water from the collection tanks into one of two available accumulation tanks. As a tank fills, water level is recorded and related to collected gas volume. When one tank is filled, displaced water is routed to the second tank while the first tank is drained, allowing a continuous measurement of collected volume. A surge tank provides an alternate reservoir for displaced water when collection rates result in water flows exceeding the normal capacity of connecting lines.

The final step in the non-condensible gas collection process requires a manual adjustment of the collection tank spillover elevation until final header pressure equals initial header pressure. This ensures that the volume of water in the accumulation tanks equals the volume of non-condensible gas removed from the reactor coolant system.

3.2.2 Vent Flow Instrumentation

Two-phase venting system instrumentation is indicated in Figure 3.3. Ten thermocouples, seven differential pressure transmitters, six limit switches, four load cells, three coriolis-type mass flow meters, and an absolute pressure transmitter provide the measurements required to compute reactor coolant system mass and energy closure. Four differential pressure transmitters and one fluid thermocouple were added to the two-phase system as part of the continuous vent line system during the Group 37 tests. One load cell was removed from the MIST two-phase venting system during the natural circulation tests.

Fluid thermocouples define effluent temperature at each vent location prior to an isenthalpic expansion across a critical leak flow control orifice. Additional thermocouples define fluid temperatures at each coriolis-type mass flow rate meter, at the non-condensible gas collection tanks, and at the accumulation tanks. All two-phase vent thermocouples are 0.063-inch, ungrounded, Type J with a time constant of approximately 5 seconds.

Differential pressure transmitters are used to define fluid levels in each two-phase vent separator, in each accumulation tank, and in the surge tank. Separator transmitter differential pressure signals provide input for automatic separator level control. Differential pressure measurements in the accumulation and surge tanks, along with limit switches which define which accumulation tank is filling, are used to compute the volume of non-condensible gas removed from the reactor coolant system.

Pressure at each leak site is evaluated using reactor coolant system pressure and differential pressure transmitters. Pressure at the non-condensible gas collection tanks is recorded using an absolute pressure transmitter.

Liquid vent effluent flow rates are recorded using coriolis mass flow rate meters. Individual flow rate measurements are recorded for the combined hot leg high point vents, the reactor vessel upper head vent, and the power-operated relief valve.

After the mass flow rate measurement, each separate vent flow is routed to a weigh tank pair. Limit switches define which weigh tank of each pair is filling and accumulated fluid mass in each tank is recorded by a load cell. Integrated vent flow rate measurements are compared to the mass accumulated in the weigh tanks cells to confirm both flow rate and cumulative measurements.

3.3 GUARD HEATING SYSTEM

The reduced scale of the MIST facility, and similar SBLOCA facilities, increases the impact of heat loss in comparison to the plant. The MIST facility is insulated to offset this influence, employing both passive and active insulation types. Passive insulation is provided by standard fibrous

material. Active insulation, referred to as guard heating, offsets heat loss by a carefully controlled heat input at the pipe boundary.

The MIST reactor coolant system is fully insulated using passive and active insulation. However, necessary penetrations and connections result in insulation discontinuities and local heat losses. Insulation discontinuities are present at flanges, instrument penetrations, reactor vessel vent valves, hot leg viewports, reactor coolant pumps, pipe connections, and loop structural supports. Heat losses at most of these sites are offset by biasing guard heater power to provide an equivalent net heat input between discontinuities. Larger heat sinks at cooling jackets on the pumps, gamma densitometers, and cooled thermocouple are not offset by biasing the guard heaters. These losses are estimated to be 0.57% of scaled core power at typical test initial conditions (refer to the discussion in Section 6.6) and are offset by augmenting core power.

3.3.1 Guard Heating System Design and Operation

The reactor coolant system is divided into 40 zones for guard heater control. Additional zones are designated for the pressurizer spray line and for the continuous vent line for Davis-Besse tests. All zones are independently controlled using silicon-controlled rectifiers (SCRs). Control measurements are located near the midline of each zone.

The MIST guard heater and insulation arrangement is shown in Figure 3.5. One inch of passive insulation separates lagging material from the pipe wall, with guard heater tapes wrapped around the lagging. Several inches of additional passive insulation outside the guard heater tape reduce heat loss and required power. Thermocouples are installed on the pipe wall and in the control layer insulation. The thermocouple in the insulation is rigidly supported by the stainless steel lagging. The temperature difference between these thermocouples, along with wall metal temperature, provide the control basis for most guard heater zones.

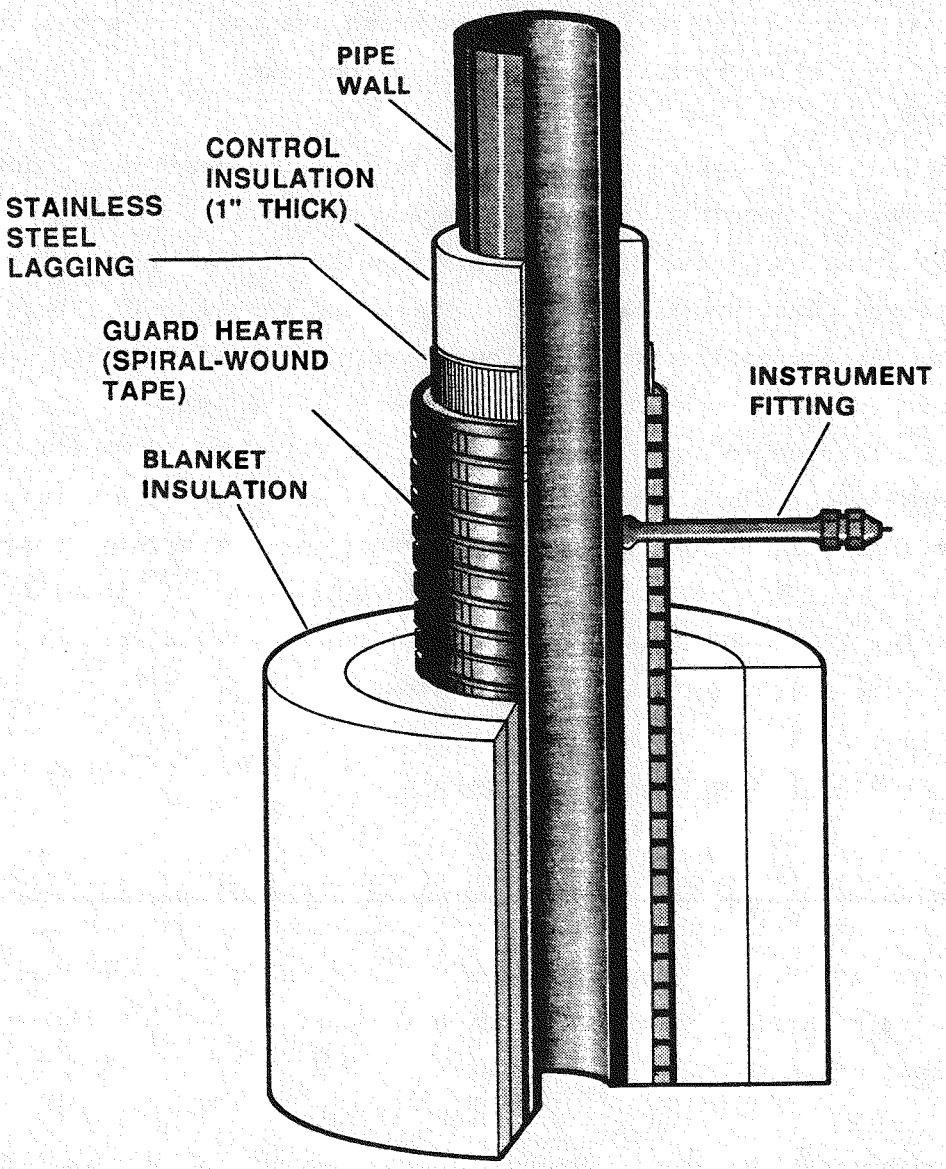

Figure 3.5 Guard Heater Arrangement

Three methods of guard heater control are employed during normal MIST operation: CASCADE, AUTOMATIC, and MANUAL. CASCADE is the preferred control mode, employed for most zones. A variation called TRACK is used in place of CASCADE mode when control layer insulation thermocouples fail. AUTOMATIC and MANUAL modes are used only where complicated zone geometry or dominating local heat losses make CASCADE control ineffective. Control modes specified for each guard heater zone are summarized in Section 6 (Table 6.12) along with the control functions.

The relationship between guard heater power, differential temperature, and metal temperature is different for each control mode. For zones in CASCADE, the guard heater power is controlled to maintain a differential temperature, which varies as a function of wall metal temperature to account for temperature dependent heat loss. The differential temperature setpoint functions were determined from characterization tests at elevated loop temperatures, as described later in Section 6.5. Over the duration of the test program, some of the control layer insulation thermocouples failed. When this occurred, the guard heater power control was switched to TRACK mode. In this mode, the guard heater power is controlled strictly as a function of wall metal temperature. These control functions were also determined from the elevated temperature characterization test results. In the TRACK mode, the guard heater control is slightly less responsive to changing conditions inside the reactor coolant system, but was evaluated to be an acceptable control method. Simple replacement of the failed thermocouple was not feasible, since the characterization results indicated that the control setpoint (for CASCADE differential temperature based control) was sensitive to the thermocouples installation. Replacing the thermocouples would have also required repeating the characterization in order to generate a new control function.

In AUTOMATIC mode, guard heater power is controlled to maintain a constant differential temperature which is independent of metal temperature. In MANUAL mode, guard heater power is directly controlled by operator intervention, and was generally used only during facility startup and shutdown.

3.3.2 Thermal Analysis and Time Response

The guard heating system and control method was designed based on the results of a steady-state and transient thermal analysis of a typical pipe section in the reactor coolant system[12]. Specifically, the steady-state analysis examined the influence of local heat losses at the instrument protrusions through the insulation system. These local heat losses prevent the use of a simple zero temperature gradient control method. That is, a slight net heat addition over the length of the pipe is necessary to compensate for the local heat loss at the instrument penetrations. As the loop changes in temperature and conditions, the heat lost through the fittings changes, and thus the required compensating heat input changes.

The steady-state thermal analysis examined the heat loss through a typical fitting at several fluid temperatures and fluid conditions on the inside surface of the pipe. The heat loss was found to be a strong function of fluid temperature, but only weakly dependent on the fluid condition (i.e., steam, water, boiling, or condensing). The control feedback signal for guard heater power is the differential temperature measurement across the control layer insulation. Based on the results of the thermal analysis, the heat addition to compensate local losses was provided by applying a non-zero setpoint for the differential temperature (also referred to as "bias"), which was varied as a function of temperature. The outside wall temperature of the pipe was used, based on installation considerations and the results of a transient thermal analysis.

The control setpoint functions could not be obtained from the thermal analysis. Rather, characterization tests were performed to experimentally determine the differential temperature setpoint for each of the guard heater control zones, as described later in Section 6.5.

The transient thermal analysis found that the outside surface temperature of the pipe does not significantly lag behind the inside surface temperature. When the pipe is filled with steam, the convective resistance at the pipe's inside surface controls the heat transfer, and the temperature difference across the pipe wall thickness is negligible. When the pipe is water-filled and the loop temperature undergoes a rapid change, the outer pipe wall temperature lags behind the inner by about 6 seconds during the relatively severe temperature transient analyzed. The control thermocouple was placed on the outside surface of the pipe wall. Based on the transient analysis, the response of the guard heater system was evaluated to be adequate (for example, in deactivating the heaters in response to a sudden fluid temperature decrease) employing the external surface thermocouple.

The guard heaters and all control measurements are outside the pipe. Thus effectively, the system imposes a controlled boundary condition outside the pipe, not inside it. During transient operation of the loop, the guard heaters operate to effectively force all the stored heat from the pipe wall to be exchanged within the pipe. The heat gained or lost by the fluid due to

heat storage in the pipe wall represents 97 to 99% of the total, depending on the rate of heatup or cooldown. The remaining 1 to 3% of the heat added or lost is due to the guard heater response, and heat stored in the control layer insulation.

3.4 EMERGENCY CORE COOLING SYSTEMS

The emergency core cooling system (ECCS) simulation includes high pressure injection (HPI), core flood, and low pressure injection (LPI) systems. Ideal scaling for these boundary systems requires model flow rates which are reduced from plant-typical by power and volume scale factors. Power scaling results in appropriate modeling of the heat removal capacity for these ECCS streams. Volume scaling promotes appropriate modeling of the loop refill sequence and timing. These factors are not equivalent for MIST. However, the impact of compromising either is readily code modelable. MIST ECCS flows were power-scaled (1/817) to provide the appropriate core heat removal capability. This approach is expected to be more conservative than volume scaling of ECCS flows.

3.4.1 High Pressure Injection

The MIST HPI system schematic is presented in Figure 3.6. Various plant-typical HPI configurations may be simulated by a branched flow network which allows injection into any combination of cold leg discharge pipes. Injection nozzles are located in the side of each discharge pipe, at mid-length in the sloping run. The nozzles are designed to preserve the ratio of injection flow momentum to cold leg flow momentum in order to preserve plant-typical mixing phenomena and stratification.

Similar to the plant, MIST HPI flow is delivered to the reactor coolant system from a single header. Therefore, differences in fluid conditions between cold legs may lead to an imbalance in resulting injection flows. To model this influence, loss coefficients for the MIST injection branches are accurately balanced using precision needle valves which are set to preserve plant-typical resistances between the header and injection points.

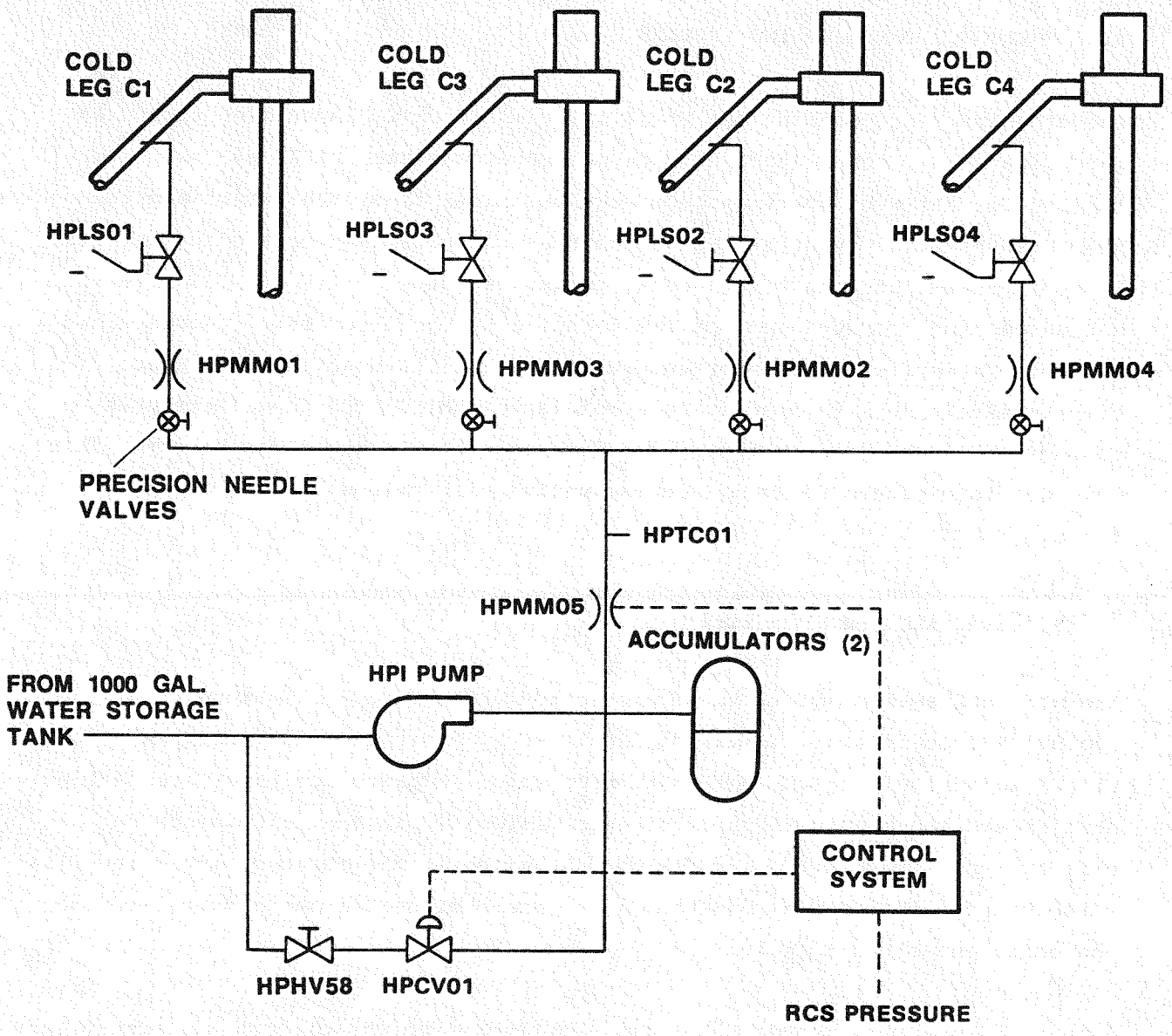

Figure 3.6 High-Pressure Injection System

Injection fluid is chemically treated prior to storage in a 1000-gallon reservoir. The stored water is deionized, deaerated, chemically adjusted to match MIST reactor coolant system pH and electrical conductivity, and saturated with non-condensible gas. This fluid feeds both the MIST HPI and LPI systems.

HPI flow is delivered to the MIST reactor coolant system by a positive displacement pump. A bypass circuit allows the simulation of plant head-flow characteristics by programmed control of the HPI bypass valve position. Available MIST control functions for total HPI flow rate as a function of reactor coolant system pressure are shown in Figure 3.7.

The positive displacement pump permits accurate control of the HPI flow, but provides undesirable HPI flow and pressure oscillations. These oscillations are dampened by a set of bladder accumulators. However, the accumulators delay the delivery of injection flow to the reactor coolant system. To minimize this delay, the HPI pump is started with full bypass flow prior to transient test initiation. With the bypass valve fully open, the HPI system pressurizes to about 900 psia. Upon HPI activation, the bypass valve rapidly closes and the system pressure rises. HPI flow is typically delivered within 10 to 15 seconds, when HPI system pressure reaches reactor coolant system pressure.

The predominate HPI control mode for MIST transient tests is modeled after the ATOG response to changes in plant subcooling margin (SCM). The subcooling margin is evaluated at the core outlet. For MIST, full head-flow HPI is activated when SCM decreases below 50°F. HPI begins to automatically throttle when SCM increases above 70°F, with the required fraction of full head-flow linearly decreasing to zero at 80°F SCM. In actual practice, MIST HPI flow is still delivered at SCM above 80°F if the reactor coolant system pressure is lower than the HPI system pressure with the bypass valve full open. Therefore, test procedures generally instruct the loop operator to manually isolate the HPI system if SCM continues to increase and reaches 100°F.

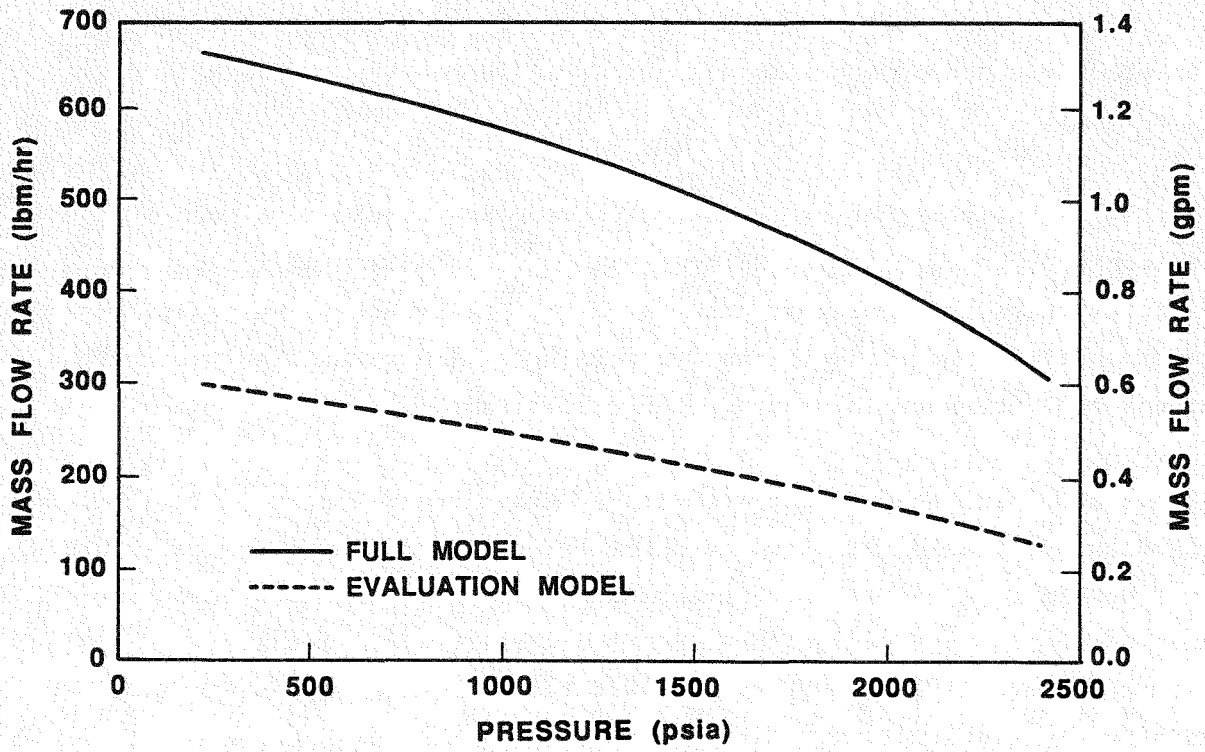

PRESSURE (psia)	MODEL:	MASS FLOW RATE (lbm/hr) FULL	EVALUATION
215		666	302
415		644	289
615		622	275
815		598	262
1015		573	248
1215		547	232
1415		519	217
1615		486	201
1815		449	185
2015		413	168
2215		364	148
2415		313	129

Figure 3.7 High-Pressure Injection Head-Flow Control Functions

The HPI system is instrumented to record individual and total injection flow rates and the temperature of the injected fluid. A differential pressure measurement on the storage reservoir indicates the available fluid supply and limit switches indicate which HPI branches are active. Instrument designations are listed in Figure 3.6. This data are recorded to the data acquisition system.

3.4.2 Core Flood System

The core flood tank is the central feature of a passive system which begins to replace reactor vessel inventory when the reactor coolant system pressure decreases to 600 psia. A schematic of the MIST core flood system is presented in Figure 3.8.

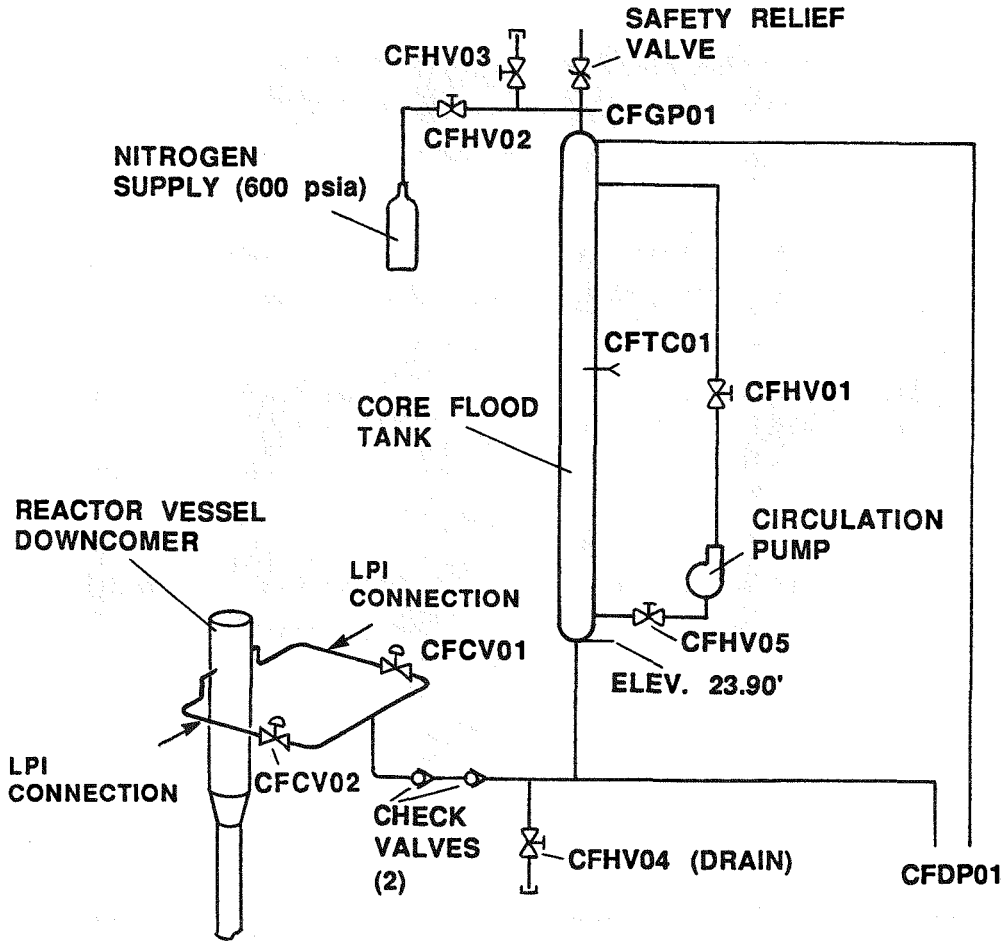

Figure 3.8 Core Flood System

In MIST operation, isolation valves open, with check valves left to prevent reverse flow, when reactor coolant system pressure decreases to approximately 650 psia. After this time, core flood inventory is naturally driven into the reactor coolant system as long as primary pressure is lower than core flood tank pressure and unless ATOG procedure requires manual isolation of the system. Barring manual isolation or primary system repressurization, core flood tank inventory is exhausted at about 165 psia and the isolation valves close automatically.

Fluid for the core flood system is chemically treated prior to filling the tank. Similar to the HPI and LPI fluids, core flood tank inventory is initially deionized, deaerated, and chemically adjusted to match MIST reactor coolant system pH and electrical conductivity. Core flood tank fluid is supplied to the reactor coolant system at ambient temperature.

The two plant typical core flood tanks are simulated in MIST by a single tank. The MIST core flood tank is 24 feet - 10 inches tall and fabricated from 5-inch, schedule 40 pipe. The tank volume of 3.45 cubic feet and initial inventory of 19 gallons are power scaled to provide plant-typical core cooling capacity. The initial core flood tank inventory is pressurized to 600 psia using nitrogen overgas, after which the nitrogen supply is isolated. A circulation pump is operated for several hours prior to each test withdrawing liquid from the bottom of the core flood tank and discharging into the gas space at the top of the tank, to ensure that the liquid inventory is saturated with nitrogen.

The core flood surge line connects the core flood tank to the upper reactor vessel downcomer. The tank is isolated from the reactor coolant system by remotely actuated valves, one in each header branch as shown in Figure 3.9, and by two check valves in series in the common surge line. As indicated in the figure, the header design at the downcomer prevents atypical circulation of flow between downcomer quadrants. To accomplish this, the header piping is located 3 inches below the injection point to provide a water seal for periods when the core flood tank is connected to the reactor coolant system. When the tank is isolated from the reactor coolant system, valves in the header close

the header piping to potential flow. The surge line is fabricated from 1-inch, schedule 80 pipe to preserve plant typical irrecoverable loss coefficients. Nozzles at the reactor vessel downcomer are designed to preserve the plant ratio of injection fluid momentum to downcomer fluid momentum in order to preserve plant-typical mixing of the fluid streams.

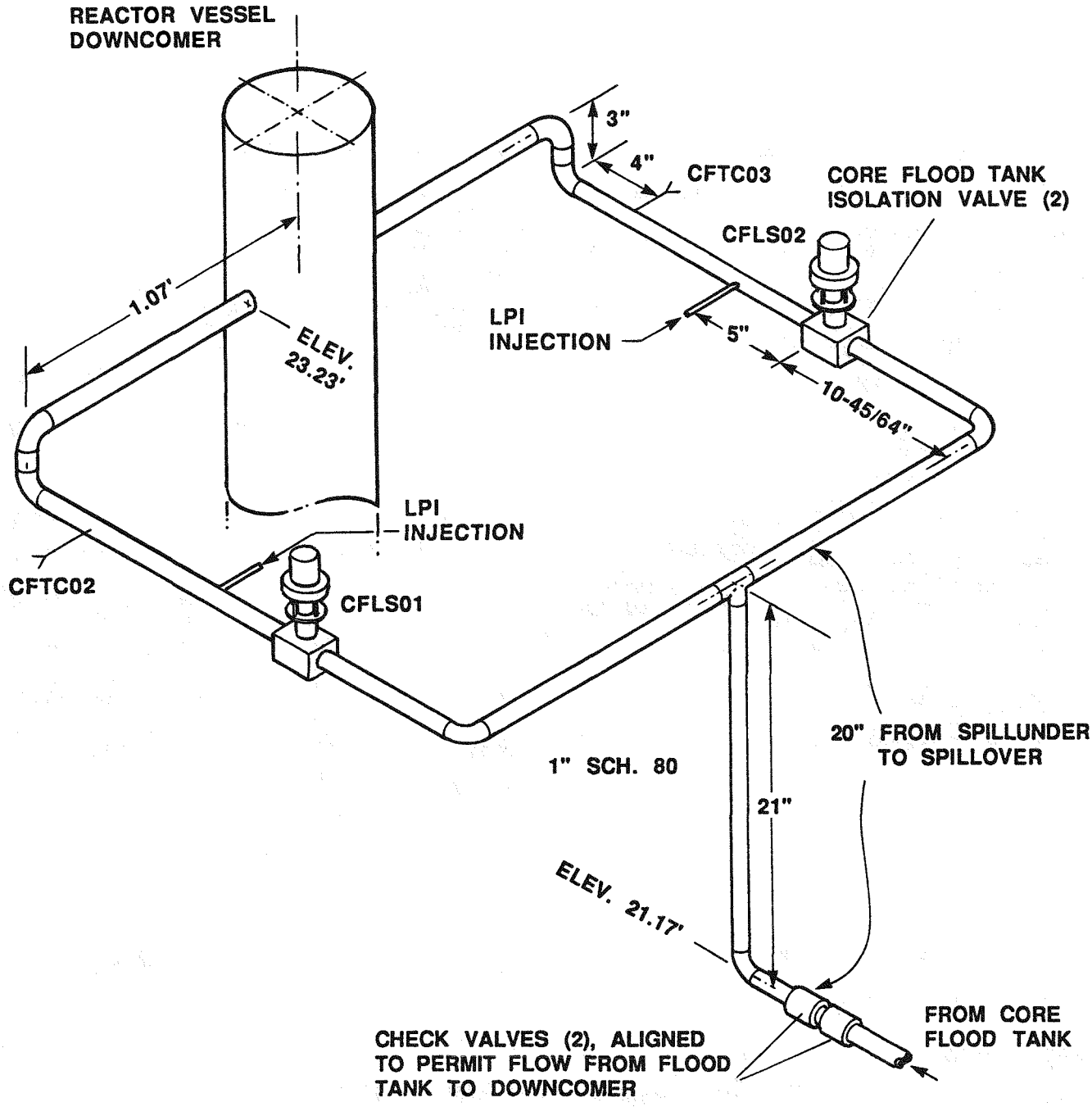

Figure 3.9 Core Flood Surge Line Detail

The MIST core flood system is instrumented to record tank pressure and temperature. Tank inventory is indicated by a differential pressure measurement on the core flood tank. Limit switches indicate when the surge line isolation valves open, with flow to the reactor coolant system confirmed by fluid temperature measurements and pressure differences. MIST core flood instrument locations are shown on Figures 3.8 and 3.9.

3.4.3 Low Pressure Injection System

The LPI system schematic is presented in Figure 3.10. This figure also illustrates LPI system valve status at transient test initiation. The MIST injection points for LPI fluid are in the core flood surge line nozzles which empty into the upper reactor vessel downcomer. The LPI system is plant-typically designed to operate at reactor coolant system pressures below 200 psia so both core flood and LPI may be active, using the same injection nozzles, at the same time.

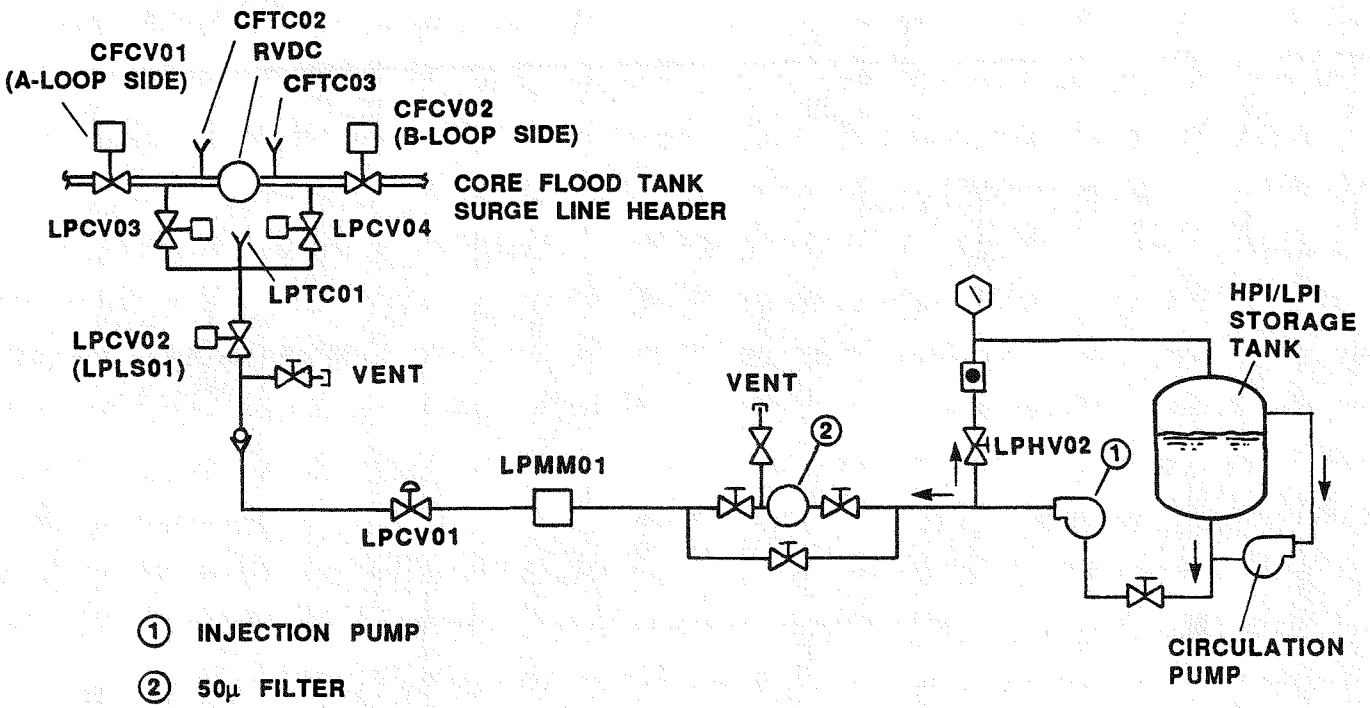

Figure 3.10 Low-Pressure Injection System

LPI fluid is supplied from the same large storage tank and has the same chemical properties as HPI fluid. Flow is delivered to the reactor coolant system by a centrifugal pump. A bypass circuit accommodates full pump output, allowing startup prior to required use. The pump is automatically started in response to a pressure signal at approximately 250 psia. This automatic startup limits the operation time for LPI pump and the heat up of storage tank inventory.

LPI system isolation valves open at approximately 203 psia, in preparation for head-flow operation. The plant-typical head-flow characteristic is simulated by programmed control of LPCV01 (see Figure 3.10). The MIST control function for LPI flow rate as a function of reactor coolant system pressure is shown in Figure 3.11.

The LPI system is instrumented to record total injection flow rate and the temperature of the injected fluid. A limit switch confirms the activation of the LPI system to the data acquisition system.

3.5 STEAM GENERATOR SECONDARY SYSTEM

The secondary loop in the MIST facility is limited to providing the steam generators secondary inventory and those fluid boundary conditions which impact SBLOCA phenomena. This includes steam generator secondary level control, auxiliary feedwater, main feedwater, and controlled cooldown (50 to 100°F/hr) or depressurization (50 psi/min). The secondary loop is a closed circulation system, schematically shown in Figure 3.12.

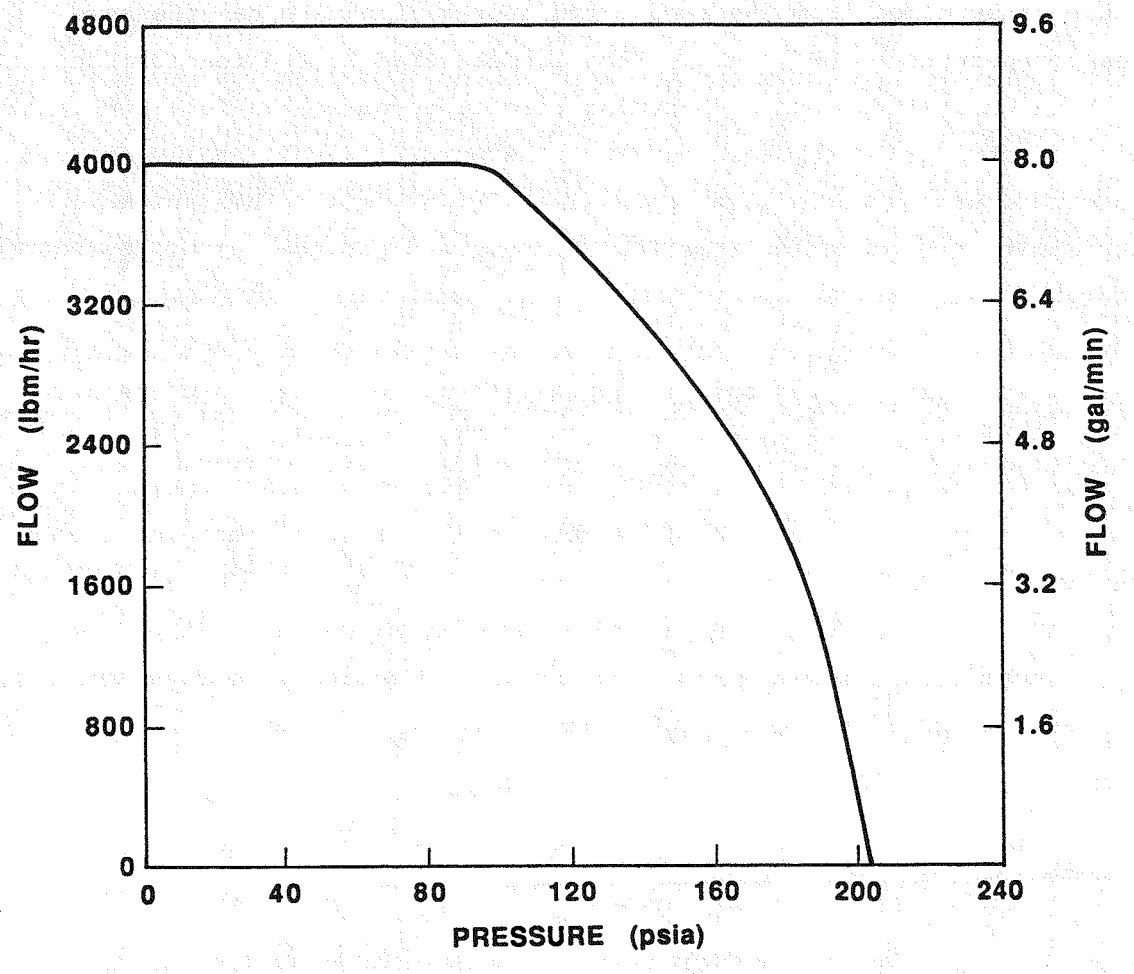

PRESSURE (psig)	MASS FLOW RATE (lbm/hr)
0	4000
85	4000
90	3835
100	3639
110	3420
120	3200
130	2962
140	2723
150	2430
160	2101
165	1910
170	1649
175	1392
180	977
185	489
188	0
200	0

Figure 3.11 Low-Pressure Injection System Head-Flow Characteristic

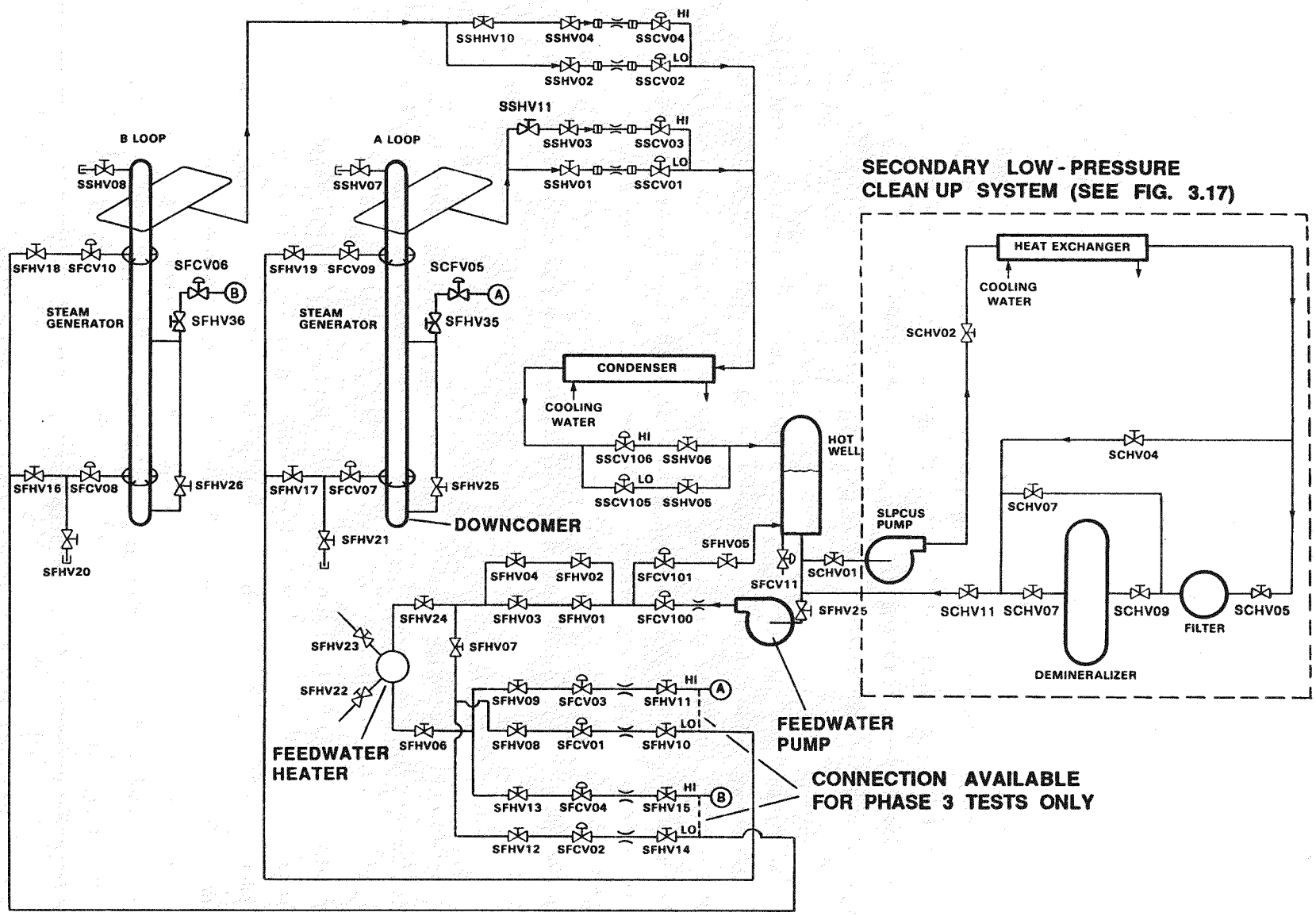

Figure 3.12 Secondary System

3.5.1 Feedwater Circuit

Referring to Figure 3.12, feedwater flow (main or auxiliary) is provided by a high-speed centrifugal feedwater pump. The feedwater pump draws from the secondary loop hot well which is maintained at approximately 30 psia, and pumps approximately 20 gpm at a discharge pressure of 1620 psia. The feedwater flow can be routed through a feedwater heater to the feedwater injection circuits, or directly back to the hot well through a bypass branch. With this arrangement, the pump is operated at a single speed near its best efficiency point despite varying feedwater requirements during a test. The secondary low pressure clean-up system (SLPCUS) is also connected to the hot well. This system, discussed later in Section 3.7.2, removes heat energy input from the feedwater pump and filters the secondary loop inventory.

The feedwater heater was used during some of the Phase 4 tests to provide main feedwater to the steam generator downcomer at a plant-typical temperature of approximately 460°F. The feedwater heaters were not energized for any Phase 3 tests. Downstream of the feedwater heater vessel, flow splits between the A and B steam generator feedwater injection circuits. Feedwater flow can be routed to the steam generator's downcomer (for main feedwater simulation), low auxiliary feedwater injection nozzles, or high auxiliary feedwater injection nozzles.

The steam generators secondary inventory can be controlled automatically, or by the operator. Two modes of automatic inventory control were available: constant level control or band level control. In the constant level control mode, feedwater flow is continuously adjusted (automatically) to maintain a preset water level in the steam generators secondary side. In the band control mode, two water level setpoints are preset in the controller. When the secondary level drops to or below the low setpoint, feedwater injection is actuated. Feedwater injection continues until the secondary level reaches the high setpoint. Feedwater injection is then halted, and the secondary level may begin dropping due to steaming. Feedwater injection is re-initiated when the secondary level drops to the low setpoint.

During the band level control mode refill process, feedwater flow rate can be controlled automatically to provide a preset constant rate of feed (constant rate of refill) or can be controlled automatically to provide scaled feedwater injection flow rates as a function of steam generator pressure. The latter method was used most frequently during tests to simulate a plant feedwater string head-flow characteristic. The auxiliary feedwater head-flow characteristic employed to simulate the plant characteristic was shown in Figure 2.32. The control system used to provide steam generator level and feedwater head-flow control is described in Section 4.5.

Feedwater flow rate was measured in each feedwater injection circuit. In Figure 3.12, the main feedwater injection circuit to each steam generator is denoted as "high", and the auxiliary feedwater circuit to each steam generator is denoted as "low" reflecting the flow (and measurement) capacity of the two circuits. The capacities of the high and low circuits were about 3210 lbm/hr and 875 lbm/hr, respectively. Also as noted in Figure 3.12, a connection that enabled the high flow circuit to be used to meter auxiliary feedwater flow was available for Phase 3 tests (only). The high circuit was rarely used to meter auxiliary feedwater flow, and was later dedicated to controlling and metering main feedwater flow for Phase 4 testing.

Figure 3.13 provides an indication of the instrumentation placement for each steam generator's feedwater injection circuitry. The flow meters in the high and low flow circuits were sharp-edged orifices. The low flow circuit used three differential pressure measurements (0-30 and 0-150 inches of water, and 0-100 psi) to span the flow rate measurement range. The low and middle range differential pressure transmitters provided flow rate measurements up to about 90 and 204 lbm/hr, respectively. Limit switches were installed on the manifold valves to indicate whether the low and middle range transmitters were in service. A limit switch was also installed on the low flow circuit control valve to indicate when the valve was fully closed or fully open. The high flow circuit employed a single differential pressure measurement. Feedwater temperature measurements were provided at each orifice flow meter, and at the high auxiliary feedwater inlet and main feedwater connection to the steam generator downcomer.

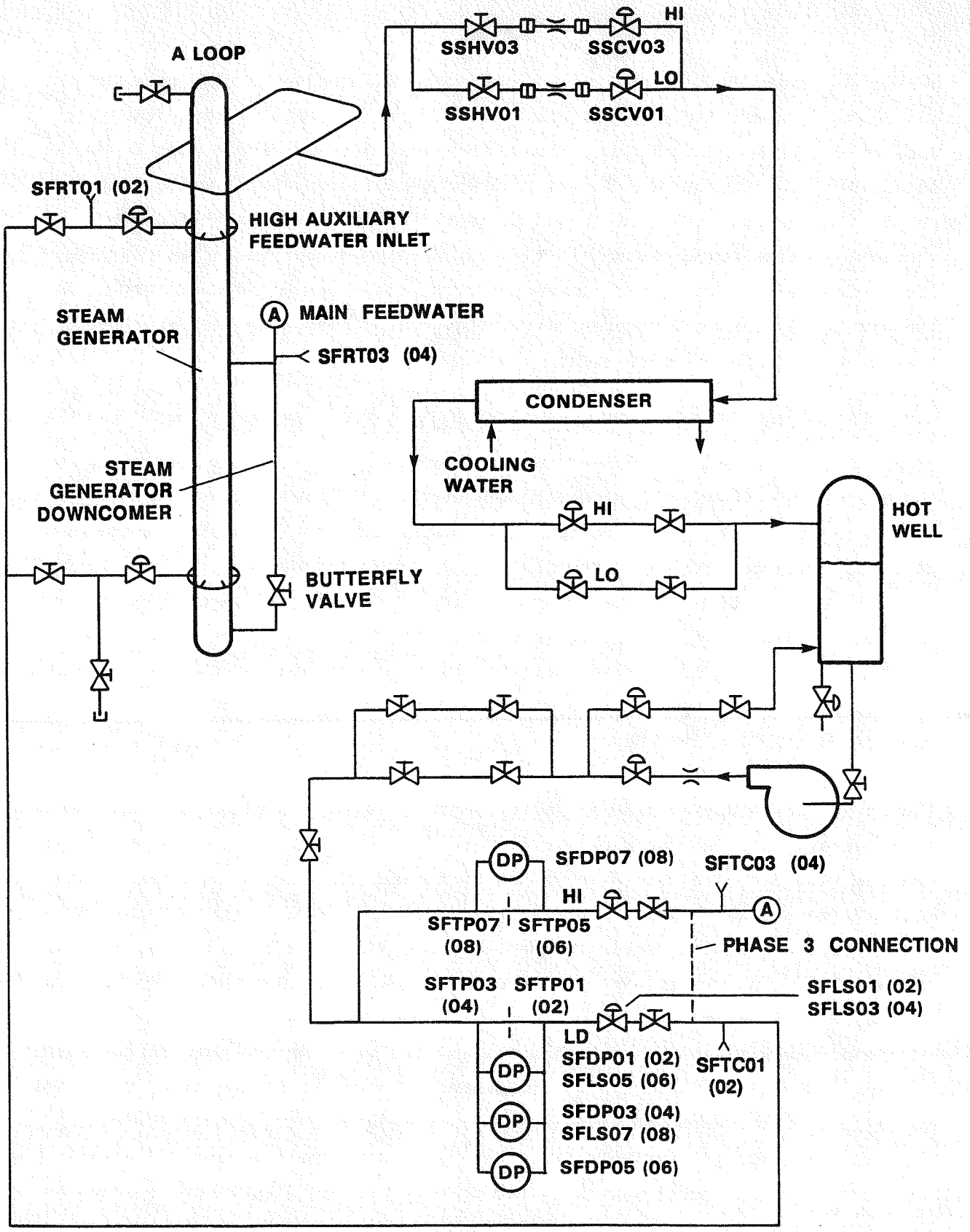

NOTE: INSTRUMENTS AND PENETRATIONS ASSOCIATED WITH STEAM GENERATOR B ARE SHOWN IN PARENTHESES

Figure 3.13 Feedwater Circuit Instrumentation

3.5.2 Steam Circuit

Steam flow from each steam generator is controlled individually. Each steam generator's steam flow control contains a high-flow and low-flow control valve. The high-flow control valve's range is sufficient for most testing requirements, and the low-flow control valve is mostly for the loop operator's use. Steam flow is controlled automatically with a controller to maintain a constant setpoint (such as constant steam pressure), programmed controller (for controlled cooldown or depressurization rates), or controlled manually by the loop operator. Steam pressure control is described later in Section 4.6.

Downstream of the flow control circuits, flow from the two steam circuits is brought together and condensed, then returned to the secondary loop hot well. The secondary loop condenser has sufficient capacity to condense steam flow corresponding to steady-state loop operation at 10% core power (330 kW). The steam circuit is capable of supporting limited blowdown testing. The maximum capacity of the circuit was found to be approximately 50 psi/min, although this varies with conditions in the steam generator. The steam circuit is not capable of simulating the full capacity of the plant's main steam safety valves.

Two parallel circuits, designated the low and high flow circuits, were used to measure the steam flow rate from each steam generator. The parallel circuit arrangement is illustrated in Figure 3.14. The capacities of the low and high circuits were approximately 890 and 975 lbm/hr, respectively, for saturated vapor at 1000 psia. These flow rates correspond to approximately 12.9% and 14.1% of scaled full-power facility operation.

Steam flow measurements were made using sharp-edged flow orifice meters. The low flow circuit used three differential pressure measurements (0-30 and 0-150 inches of water, and 0-100 psi) to span the flow rate measurement range. Limit switches indicated whether the low and middle range differential pressure transmitters were out of service. The low and middle range differential pressure transmitters provided flow rate measurements up to approximately 92 and 209 lbm/hr, respectively, for saturated vapor at 1000 psia.

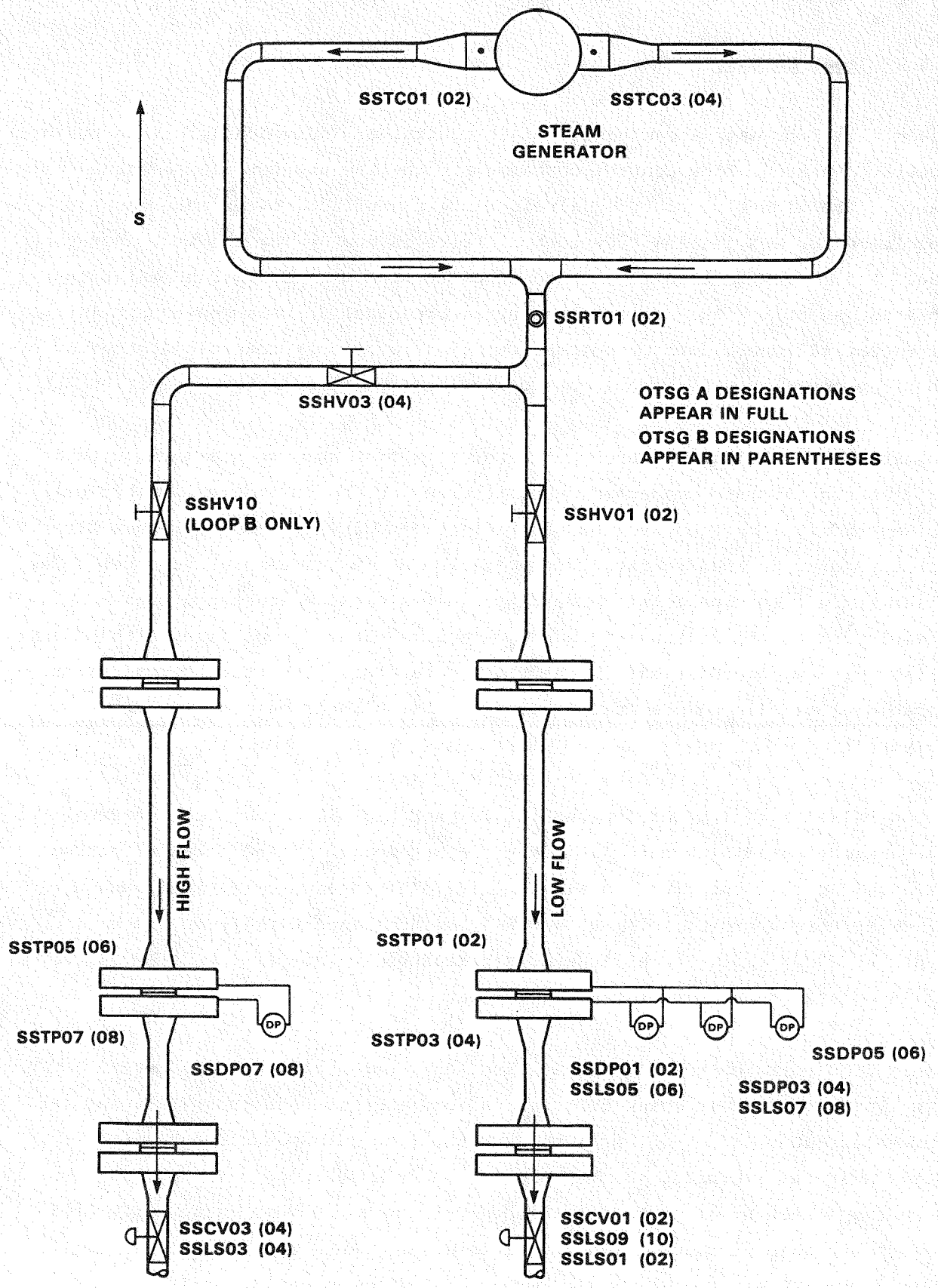

Figure 3.14 Steam Generator Steam Line Instrumentation

Limit switches were also used to indicate when the low flow circuit control valve was fully closed (SSLS01-02 for the A and B steam generators, respectively) and fully opened (SSLS09-10). Limit switches on the high flow circuit control valve for each steam generator indicated when the valve was closed.

Steam outlet temperatures were measured immediately at the steam generator outlet nozzles with thermocouples, as indicated in Figure 3.14. The thermocouples were 1/16-inch diameter. By positioning these relatively fast-responding thermocouples as close to the steam generator outlet as possible, the presence of entrained water droplets in the steam flow was periodically indicated by fluctuating temperature measurements between saturation and superheater. In addition, the thermocouples located in the two outlet nozzles of each steam generator could be used to assess thermal asymmetries at the outlet plane of the steam generator. Resistance temperature detectors were used further downstream in the steam lines to measure the fluid temperature just prior to the orifice meters.

3.6 NON-CONDENSIBLE GAS ADDITION SYSTEM

The MIST non-condensible gas (NCG) addition system is employed to investigate the impact of NCG on abnormal operating transients. Generation and accumulation of NCG in the MIST reactor coolant system is simulated using the network of vessels, valves, and injection sites shown in Figure 3.15.

In MIST operation, the gas addition system is configured to include an appropriate set of the five available reservoirs shown in Figure 3.15 and pressurized to approximately 3000 psia. The selection of included reservoirs depends on the quantity of NCG to be added and the maximum expected MIST reactor coolant system pressure. The gas addition system is initially charged using commercial 3750 psia gas bottles. Gas species available for injection include nitrogen and helium.

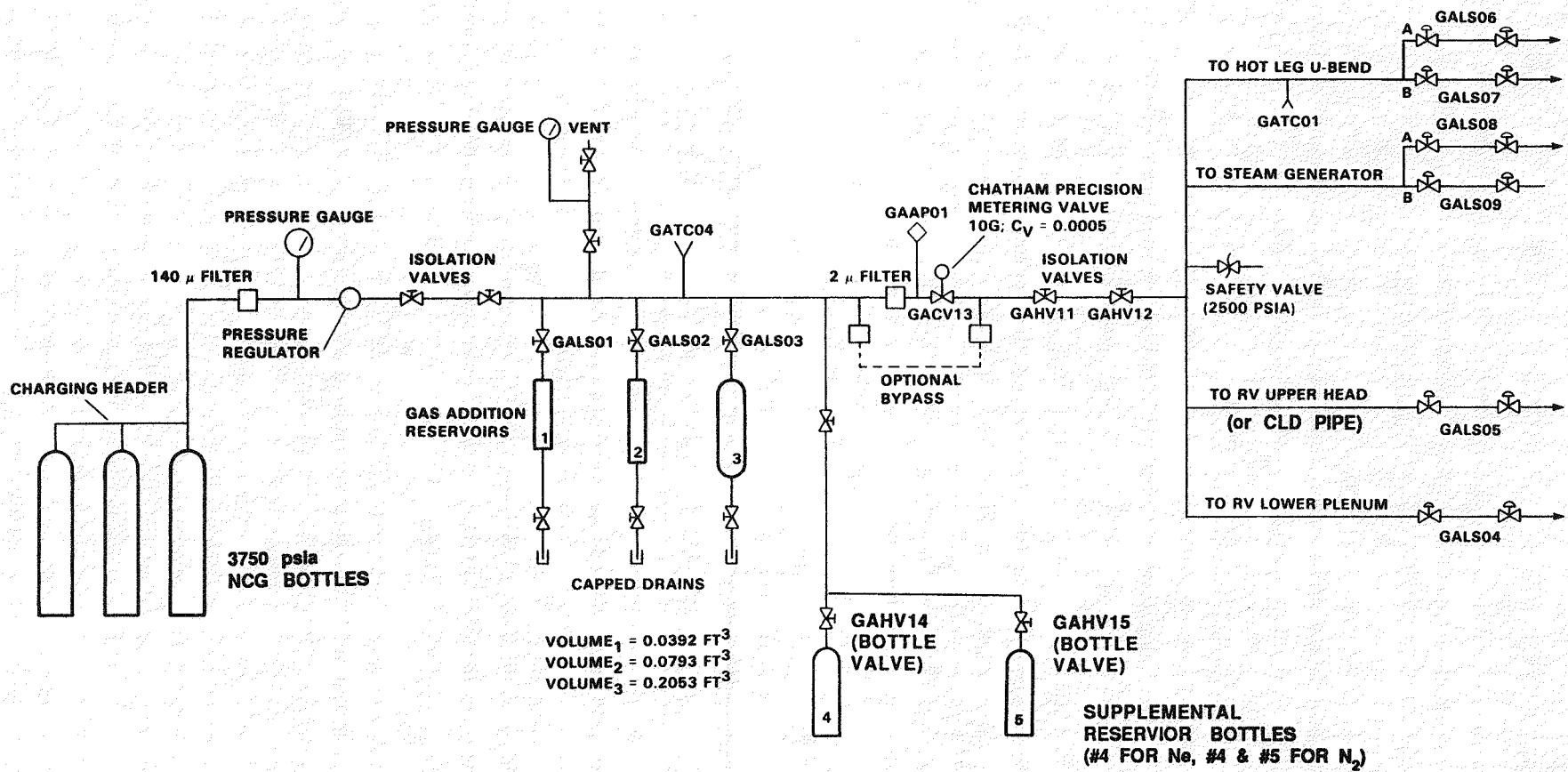

Figure 3.15 Non-Condensible Gas Addition System

Six gas addition sites are installed in the MIST reactor coolant system: the reactor vessel lower plenum, the reactor vessel top head, the primary inlet of both steam generators, and both hot leg U-bends. Gas addition system tubing may also be routed to an existing fitting at a reactor coolant pump discharge, if required. Gas addition can be controlled to be continuous at a specified rate, or added in batch quantities. Non-condensible gas generation during a Zircalloy-water reaction is simulated by continuous gas addition at the reactor vessel lower plenum site. Gas introduction by incoming ECCS streams is also simulated by ensuring that fluid in the HPI/LPI supply tank and core flood tank is saturated with dissolved nitrogen gas.

Batch NCG addition is used for phenomenological study of the effects on primary loop circulation and refill and on primary to secondary heat transfer across steam generator tubes. Batch addition is preferred for these studies to obtain selected NCG placement and thus minimize the amount removed through the simulated leaks.

Continuous and approximately constant gas addition rates are achieved by manually adjusting the precision metering valve and allowing the gas addition system pressure to decay according to a predetermined schedule. Batch gas addition is achieved by immediate blowdown to reactor coolant system pressure. In either case, NCG is preheated to at least 95% of the local fluid temperature by routing the gas injection tubing under the passive loop insulation, near the guard heaters just prior to the injection point in the reactor coolant system.

Gas addition system instrumentation is included on Figure 3.15. System pressure is recorded immediately upstream of the precision metering valve. System temperature is recorded in the common header connecting the reservoirs. Ambient temperatures are recorded at the hot leg U-bend elevation and near the reactor vessel upper and lower plenum elevations. Limit switches at each addition site indicate which injection site is active. Isolation of any of the three permanent gas reservoirs is also recorded.

3.7 WATER CHEMISTRY CONTROL

MIST facility water chemistry and cleanup systems include facility and secondary low-pressure cleanup systems and a primary loop in-line filter. These systems are described in this section. Water chemistry specifications imposed before the start of each test are listed in Table 3.1.

Table 3.1

FACILITY WATER CHEMISTRY SPECIFICATIONS

HPI/LPI SUPPLY TANK

Parameter	Specification
pH, NH_4OH adjusted	9.5 - 10.2*
Specific Conductivity	45-55 μmho/cm
Hydrazine, as N_2H_4	Residual (~20 ppb)
Dissolved Oxygen, as O_2 (Max)	100 ppb
Total Gas, as std cc/kg H_2O	<60
Copper, as Cu** (Max)	10 ppb
Nickel, as Ni** (Max)	10 ppb

* The pH is adjusted to this range to provide conductivity level required for conductivity probe(s) monitoring data.

** Required because the Elliott tank is of Monel structure.

PRIMARY LOOP INVENTORY

Parameter	Specification
pH, NH_4OH adjusted	9.5 - 10.2
Specific Conductivity	~45μS/cm
Hydrazine, as N_2H_4	Residual (~20 ppb)
Dissolved Oxygen, as O_2 (Max)	100 ppb
Chloride, as Cl^- (Max)	100 ppb
Fluoride, as F^- (Max)	100 ppb
Sulfur, as $SO_4^=$ (Max)	100 ppb
Total Gas, as std cc/kg H_2O	<60

Table 3.1 (Continued)

FACILITY WATER CHEMISTRY SPECIFICATIONS

SECONDARY WATER

Parameter	Specification
pH, NH_4OH adjusted	9.5 - 10.2*
Specific Conductivity	45-50 μmho/cm
Hydrazine, as N_2H_4	Residual (~20 ppb)
Cation Conductivity (Max)	0.2μS/cm**
Dissolved Oxygen, as O_2 (Max)	5 ppb
Total Solids (Max)***	50 ppb
Total Silica, as SiO_2 (Max)	20 ppb
Sodium, as Na (Max)	3 ppb
Chloride, as Cl^- (Max)	5 ppb
Total Sulfur, as $SO_4^=$	10 ppb
Fluoride, as F^- (Max)	10 ppb
Suspended Solids (Max)	2 ppb
Total Iron, as Fe (Max)	10 ppb

* The pH is adjusted to this range to provide a conductivity level required for conductivity probe(s) monitoring data.

** Cation conductivity indicates the major anion contaminants present, which are generally due to chloride, fluoride, and sulfate. These specification levels are theoretically equal to a cation conductivity of ~0.35μS/cm.

*** The sum of the individual species must be equal to or less than 50 ppb, to meet the total solids specification.

3.7.1 Facility Low-Pressure Cleanup System

The facility low-pressure cleanup system produces high-purity, deaerated water for the primary and secondary coolant loops, the core flood tank, and the HPI/LPI reservoir. The system is also used, when required, to remove non-condensible gases from the reactor coolant system. A system schematic is presented in Figure 3.16.

Partially demineralized water is supplied to the low-pressure cleanup system for further mineral polishing and vacuum deaeration. Mineral species which are monitored for facility protection include fluorides, chlorides, and silica. The deaerator processes 3 gallons per minute of demineralized water at 0.1 atmosphere and 110°F with total gas in the outlet stream reduced to less than 10 parts per billion. Demineralized, deaerated water is supplied to the facility using the HPI or LPI system pumps or by a small injection pump. This water may also be routed to the 1000-gallon HPI/LPI storage tank.

Chemical additions are made to the primary and secondary coolant loops, to the HPI/LPI storage tank, and to the core flood tank using the small injection pump. Water electrical conductivity and pH are established in this manner to control loop corrosion and to facilitate operation of water conductivity probes installed for phase detection in the reactor coolant system.

3.7.2 Secondary Low-Pressure Cleanup System

The secondary low-pressure cleanup system performs two functions — the removal of heat added to secondary loop inventory by the feedwater pump, and the removal of dissolved and suspended impurities from the secondary fluid. The system schematic is presented in Figure 3.17.

The secondary cleanup system circulates approximately 20 gallons per minute from the secondary's hot well, through a counterflow heat exchanger, and back to the hot well. The heat exchanger is designed to maintain the hot well fluid temperature at approximately 120°F by removing energy added to the secondary by the feedwater pump.

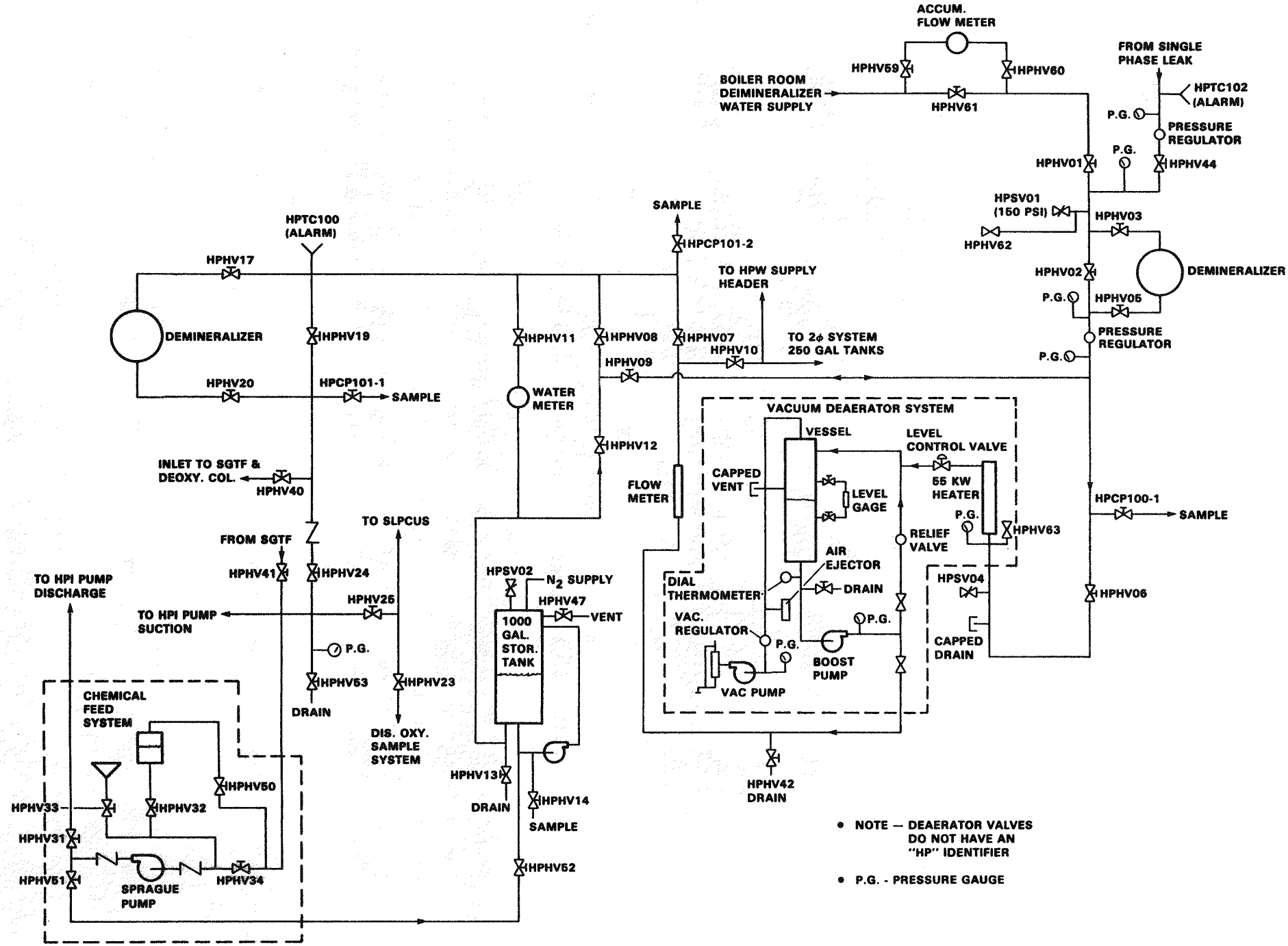

Figure 3.16 Facility Water Supply and Cleanup System

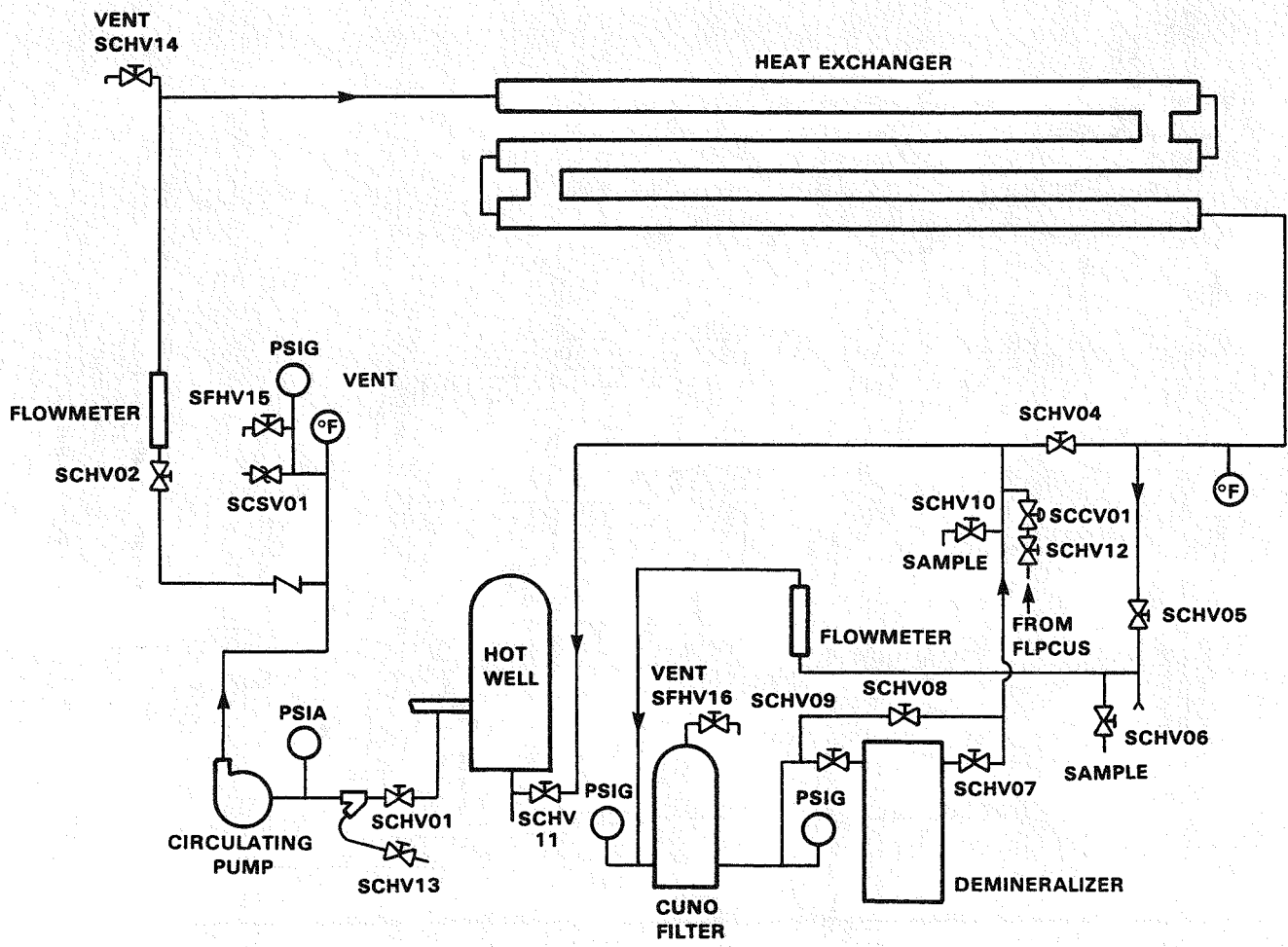

Figure 3.17 Secondary Low-Pressure Cleanup System

Secondary cleanup system flow is divided downstream of the heat exchanger outlet, with approximately 4 gallons per minute routed to purification hardware and the balance returned directly to the hot well. Suspended particles are removed from the clean-up stream by a 5-micron filter. Soluble contaminants are removed by an NH_4OH resin demineralizer. The cleanup stream is then returned to the hot well.

3.7.3 Primary In-Line Filter

The primary in-line filter is used during facility startup and between tests whenever the concentration of suspended contaminants exceeds desired limits. When the filter circuit is activated with the reactor coolant pumps running, primary fluid is driven into the filtration circuit at approximately 2 gallons per minute. The in-line filter circuit is shown in Figure 3.18.

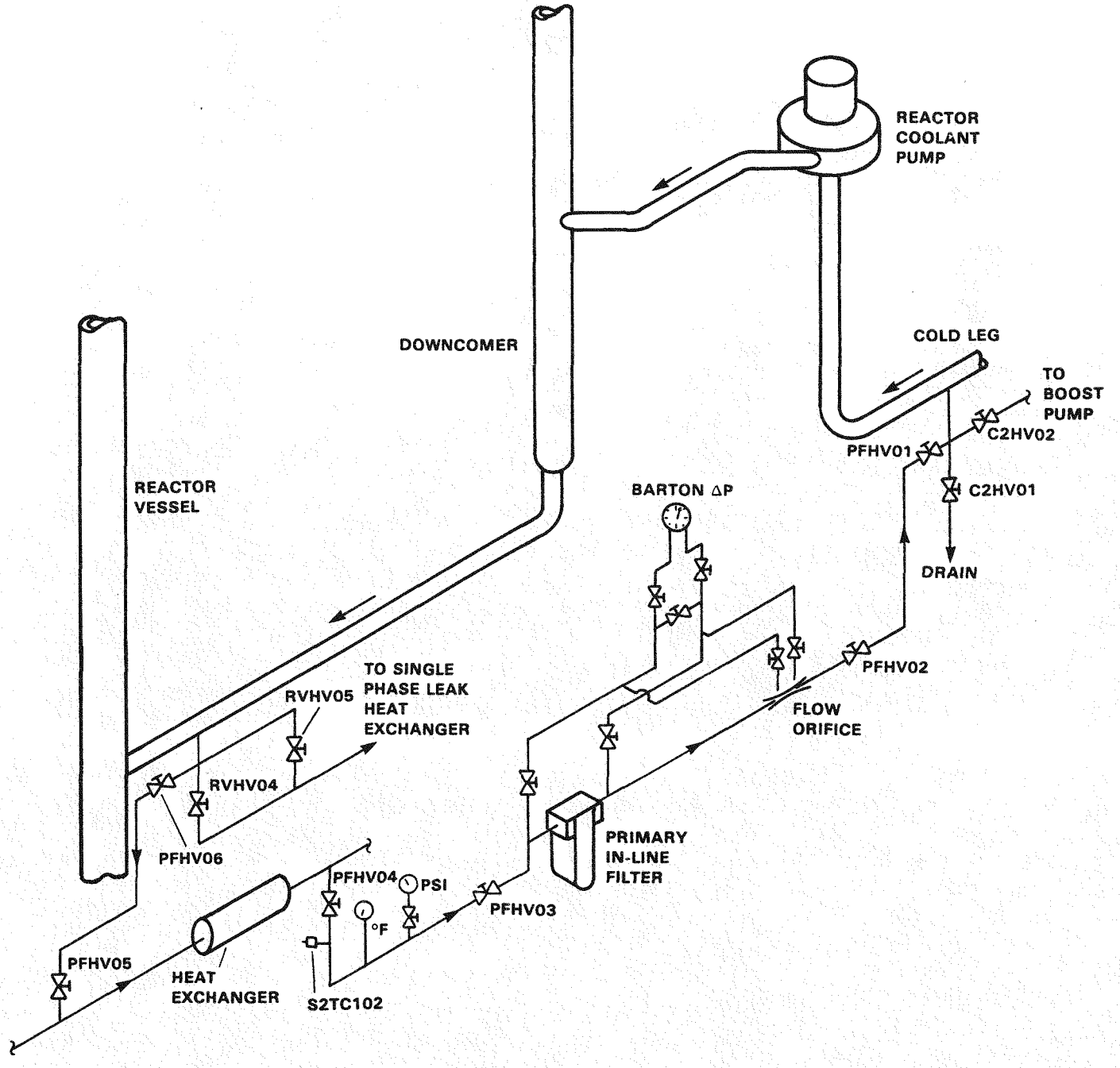

Figure 3.18 Primary In-Line Filter System

Primary inventory enters the filter circuit from a reactor vessel drain connection and is routed first to the single-phase leak system heat exchangers for cooling. Reduced temperature primary fluid is then filtered and returned to the reactor coolant system in the cold leg suction. Full reactor coolant system pressure is maintained through the in-line filter circuit hardware.

Section 4

FACILITY AUTOMATIC CONTROL SYSTEMS

This section provides a description of the MIST facility automatic control system used to control the core heater power, reactor coolant pump (RCP) rampup and coastdown, reactor vessel vent valves (RVVV), high-pressure injection (HPI), steam generator level, auxiliary feedwater (AFW), steam generator pressure, guard heaters, pressurizer heaters, and low-pressure injection (LPI).

Most of the above MIST processes were controlled using proportional/integral/derivative (PID) controllers. In such a control system, a feedback signal, known as process variable (PV), is utilized to bring information back to the controller. The feedback signal is compared to a certain desired setting, known as setpoint (SP), and the difference between the two (PV and SP), which is the error signal, is feed to the PID controller. Based on the magnitude and the rate of change of the error signal, the PID controller makes the needed adjustment to the process in order to reduce the error signal to zero. The four distinct process control modes that were used in MIST were:

- **Manual** — The PID controller is bypassed, and the controller output, or process, is manually controlled.
- **Track** — The PID controller is bypassed, and the system output is a function of a certain variable in the process.
- **Automatic** — The PID controller is controlling the process, and the setpoint is constant.
- **Cascade** — The PID controller is controlling the process, but the setpoint is changing as a function of a certain variable in the process.

4.1 CORE POWER CONTROL

Power to the reactor vessel bundle was controlled using a PID controller. A block diagram illustrating the MIST core simulation power control circuit is shown in Figure 4.1. The core power control is based on voltage and current measurements (RVVM01 and RVAM01). The voltage and current signals are conditioned and multiplied, providing a feedback signal to a PID controller. This feedback signal, referred to as the process variable (PV), is then compared to the control setpoint (SP). The output of the PID controller is based on the difference between the process variable and the setpoint. The output signal is converted to a voltage source which is then applied across the core heater rods. As the voltage source is varied, the current through the core bundle is affected. The current and the voltage are measured and fed back to the controller, completing the closed loop circuit.

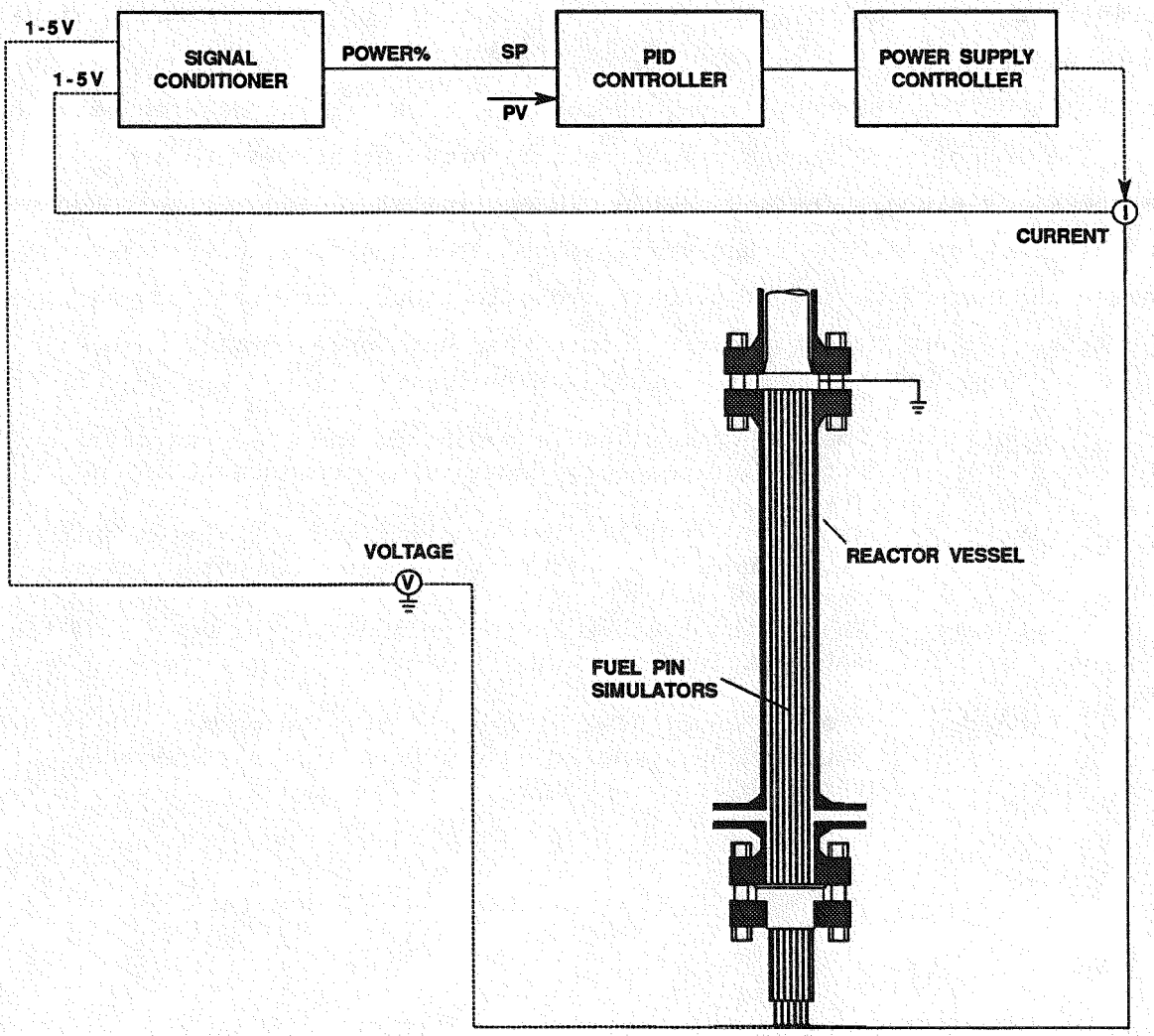

Figure 4.1 Reactor Vessel Core Power Control

The voltage and current feedback signals to the core power controller can each vary from 1 to 5 volts corresponding to 0 to 150 volts supplied to the fuel pin simulators, and 0 to 2500 amperes (total), respectively. In the controller conditioner, these analog signals are converted to percent of span. The 1 to 5 volt signal is spanned to correspond to 0 to 100% (as percent of 150 volts), whereas the current signal is spanned so it corresponds to 0 to 113.64% (as percent of 2200 amperes). Then, the power input signal can vary from 0 to 100% corresponding to 0 to 330 kW. The arithmetic operations within the controller, such as the summation and multiplication blocks, are based on the incoming signals in percent of span.

The output of the control system conditioner is given by the following expression:

$$W = IP*VP/100 \qquad (4\text{-}1)$$

where:

W = Core power (%)

IP = 100%*(R)*(I-1)/4

VP = 100%*(V-1)/4

R = Ratio of current range over span = 2500/2200 = 1.1364

I = Current through core bundle (1 to 5 volts)

V = Voltage across core bundle (1 to 5 volts)

The output of the control system conditioner is the process variable in percent. This signal is an input to the PID controller. The PID controller provides proportional, integral, and derivative (rate) control action based on the difference between PV and SP. The process variable is defined in Eq. 4-1. SP depends on the control mode (automatic or cascade). The automatic control mode is the steady-state operating mode during which SP is constant as indicated in Eq. 4-2. The cascade control mode is the transient operating mode, during which the setpoint is varying with time according to the core power decay curve. SP during the cascade mode is defined in Eq. 4-3.

a) Automatic Control Mode

$$SP = (P + P_C)*10 \qquad (4\text{-}2)$$

where P is the percent scaled power which is defined in the test procedures and the constant P_C is the power to compensate for heat losses. The value of P_C was test specific; equal to either 0.4% or 0.57% of full-scaled power. Full (100%) scaled power = 3.3 MW.

b) Cascade Control Mode

$$SP = P(t) \qquad (4\text{-}3)$$

where the function P(t) is the core power decay ramp used by the core power controller to produce a power setpoint at a given time. P(t) is a piecewise linear approximation of the ANS core power decay curve. The deviation between P(t) and the actual decay curve is below the instruments uncertainties.

The approximation of the core power decay curve is necessary since all of the MIST controllers utilize piecewise linear functions. The P(t) function is provided in the MIST test procedures. In the test procedure specifications, the power setpoint has already been compensated for for heat losses, and normalized to 330 kW (10% scaled power).

The PID output is based on the following equation:

$$\text{Output}(\%) = S5*\left[S6*(S2-S1) + S7*\int_0^{\Delta t} (S2-S1)\,dt + S8*\frac{d(S2-S1)}{dt}\right] \qquad (4\text{-}4)$$

where:

S5 is gain multiplier

S6 is proportional constant

S7 is integral constant (1/minute)

S8 is derivative constant (minute)

S2-S1 is the difference signal, also known as error signal, where S1 is the process variable and S2 is the setpoint

Δt is the processor update time, 0.25 second

The PID constants (S5, S6, S7, and S8) for the core power controller are:

S5 = 1

S6 = 2 for core power less than 3.5% scaled power;
1 for core power greater than 3.5% scaled power

S7 = 9

S8 = 0

The output of the PID controller is a 4 to 20 mA signal. At 4 mA, output from the PID controller results in zero volts across the core heaters; a 20 mA output from the controller results in 150 volts across the core heaters.

4.2 REACTOR COOLANT PUMP RAMPUP AND COASTDOWN CONTROL

A block diagram illustrating the MIST reactor coolant pump (RCP) speed control circuit is shown in Figure 4.2. This open control loop system does not require any feedback information from the process. The pump speed is controlled by forcing the controller to track a desired setpoint. Therefore, in this track control mode, the controller input is equal to the output. When the reactor coolant pump is started, the speed setpoint increases (rampup) according to Eq. 4-5; when the pump is turned off, the speed setpoint decreases (coastdown) according to Eq. 4-6.

$$SP = (6.667*t)*K \quad (4\text{-}5)$$

$$SP = S(t)*K \quad (4\text{-}6)$$

where:

t = Elapsed time from the pump startup in seconds. The coefficient (6.667) is the speed rate of increase.

K = Values are 0.975, 0.990, 0.994, and 0.978 for reactor coolant pumps C1, C2, C3, and C4, respectively. These coefficients force the pumps to produce equal flow rates through the cold legs when the pumps are running at maximum speed.

S(t) = Piecewise linear approximation of the pump speed coastdown ramp. This function provide a speed setpoint (%) at a certain time (sec) from the pump shutoff time. The S(t) function is provided in the MIST test procedures, in which the speed setpoint has been normalized to the pump maximum speed (3540 rpm).

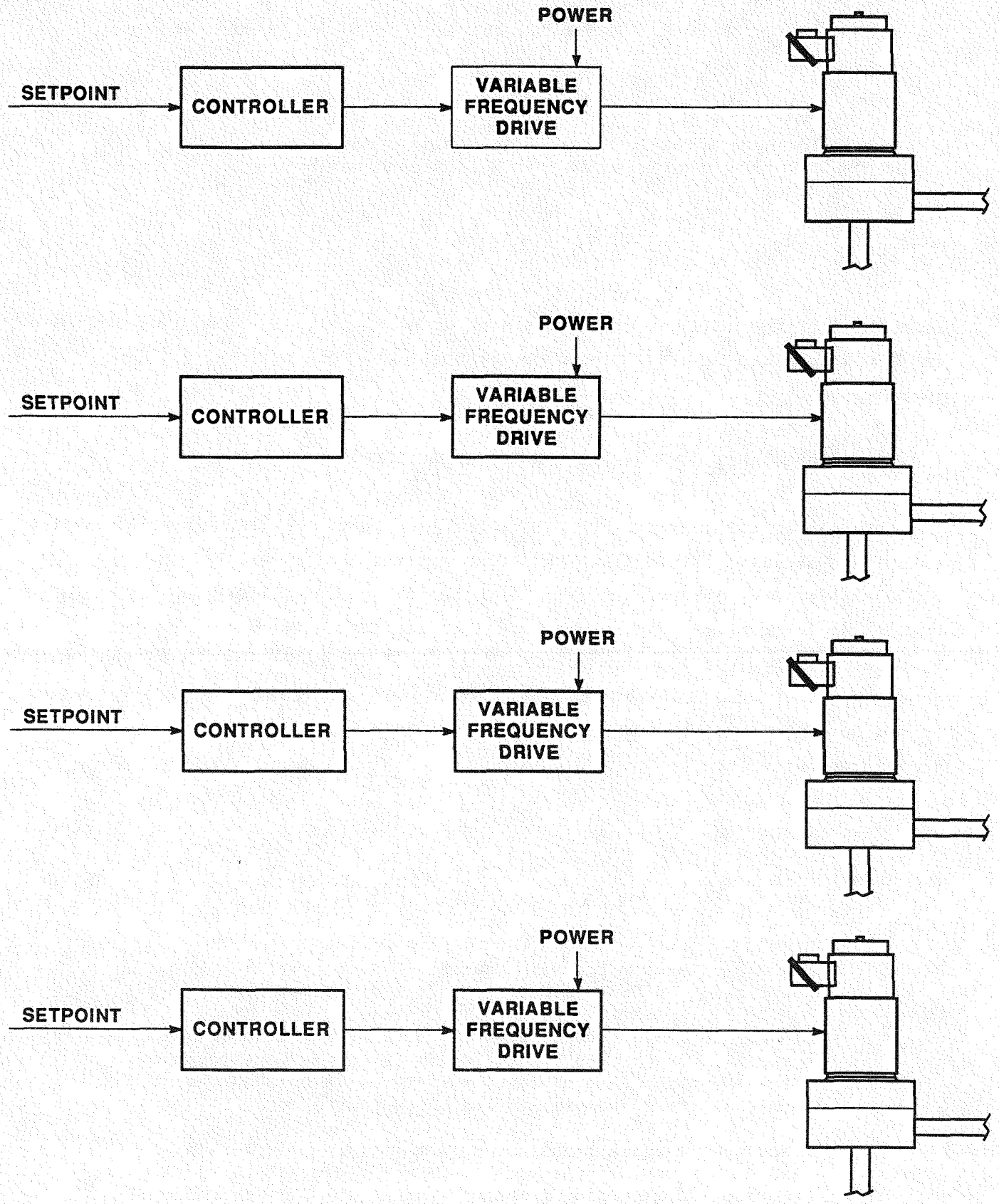

Figure 4.2 Reactor Coolant Pump Control

The controller output is a 4 to 20 mA signal that feeds into a variable frequency drive. Consequently, the variable frequency drive supplies an equivalent 0 to 60 Hz control signal to the reactor coolant pump. A 20 mA signal from the controller would command the pump to run at 100% of maximum speed; a 4 mA signal would cause the pump to stop rotating.

4.3 REACTOR VESSEL VENT VALVES CONTROL

The actuation of the reactor vessel vent valves (RVVVs) was controlled using a logic controller which uses a sequence of true/false logic blocks in order to open or close the valves, as indicated in Figure 4.3. These four control systems are similarly structured, and each system is independent of the others. The RVVV actuation is based on the pressure difference (RVDP06, RVDP07, RVDP08, and RVDP09) between the reactor vessel and a reactor vessel downcomer quadrants. Each of these differential pressure measurements is conditioned and converted to a percentage of the full range of the differential pressure transmitters. The conditioned signal, known as process variable (PV), is routed to a logic controller. At this controller, PV is compared to two setpoints — high (0.125 psi) and low (0.04 psi). When PV is equal to or larger than the high setpoint, the controller output is set to logic "1"; when the process variable is equal to or lower than the low setpoint, the controller output is set to logic "0". The logic "1" or "0" closes or opens a contact relay which either connects or disconnects power to the valve solenoid. The vent valve is normally closed, and opens when the solenoid is energized.

The differential pressure signals (RVDP06, RVDP07, RVDP08, and RVDP09) to the RVVV controller vary from 1 to 5 volts corresponding to the calibrated range of the transmitters which is -4 to 26 inches water. In the controller conditioner, the 1- to 5-volt signal is spanned to correspond to 0 to 100% of the full range of differential pressure transmitters.

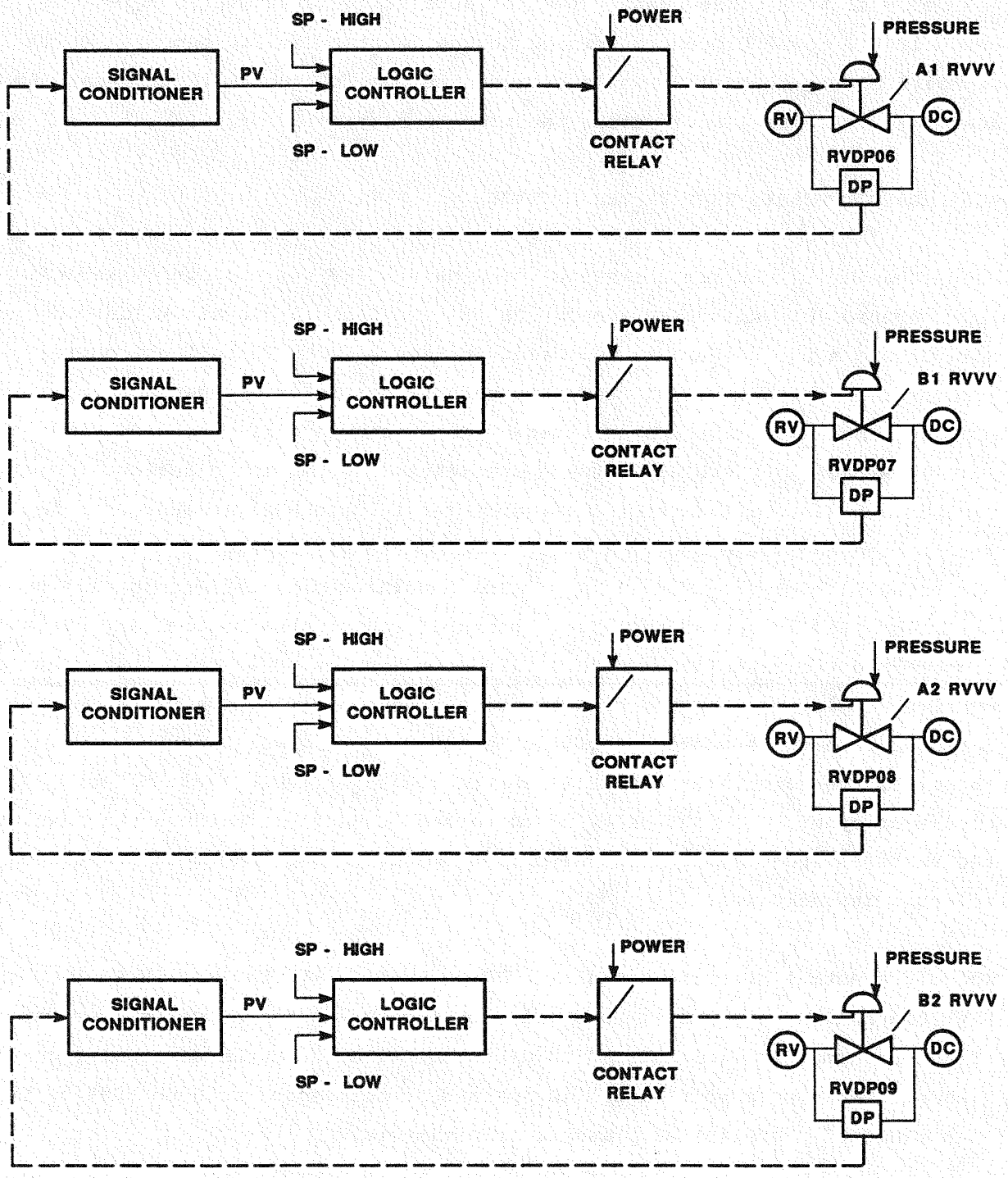

Figure 4.3 Reactor Vessel Vent Valve Control

The output of the signal conditioner (%), which is the process variable, is given by the following expression:

$$PV = 100\%*(V-1)/4 \qquad (4\text{-}7)$$

where V is the differential pressure transmitter signal (1 to 5 volts).

The high and low setpoints for each of the vent valves are presented in Table 4.1.

Table 4.1

REACTOR VESSEL VENT VALVE ACTUATION SETPOINTS

Valve	Open %	Close %
C1	23.344*	15.859
C2	23.219	15.844
C3	23.063	16.125
C4	22.688	15.797

* The value for this setpoint was 22.0 prior to July 30, 1986.

All values are % of differential transmitter span.

4.4 HIGH-PRESSURE INJECTION CONTROL

The high-pressure injection of emergency coolant into the cold legs was controlled using a PID controller. A block diagram illustrating the MIST high-pressure injection (HPI) control system is shown in Figure 4.4. This HPI control is based on the mass flow rate measurement (HPMM05) using the Micro Motion mass flowmeter. The automatic controller system controls total HPI flow rate. The division of the total flow among the four cold leg HPI nozzles is controlled manually with precision metering valves. The output of the Micro Motion meter is a 4 to 20 mA signal, resulting in a 1- to 5-volt control signal. This 1- to 5-volt process variable is conditioned before being supplied to the PID controller. The output of the PID controller is based on the difference between the process variable and the setpoint. This output is converted to a pneumatic control signal that varies the air pressure to the

valve actuator for the HPI bypass control valve (HPCV01). The control valve is proportionally opened or closed as the air pressure is varied. As the position of the HPI control valve is changed, the mass flow rate to the cold legs is changed, thus providing a feedback signal to the controller.

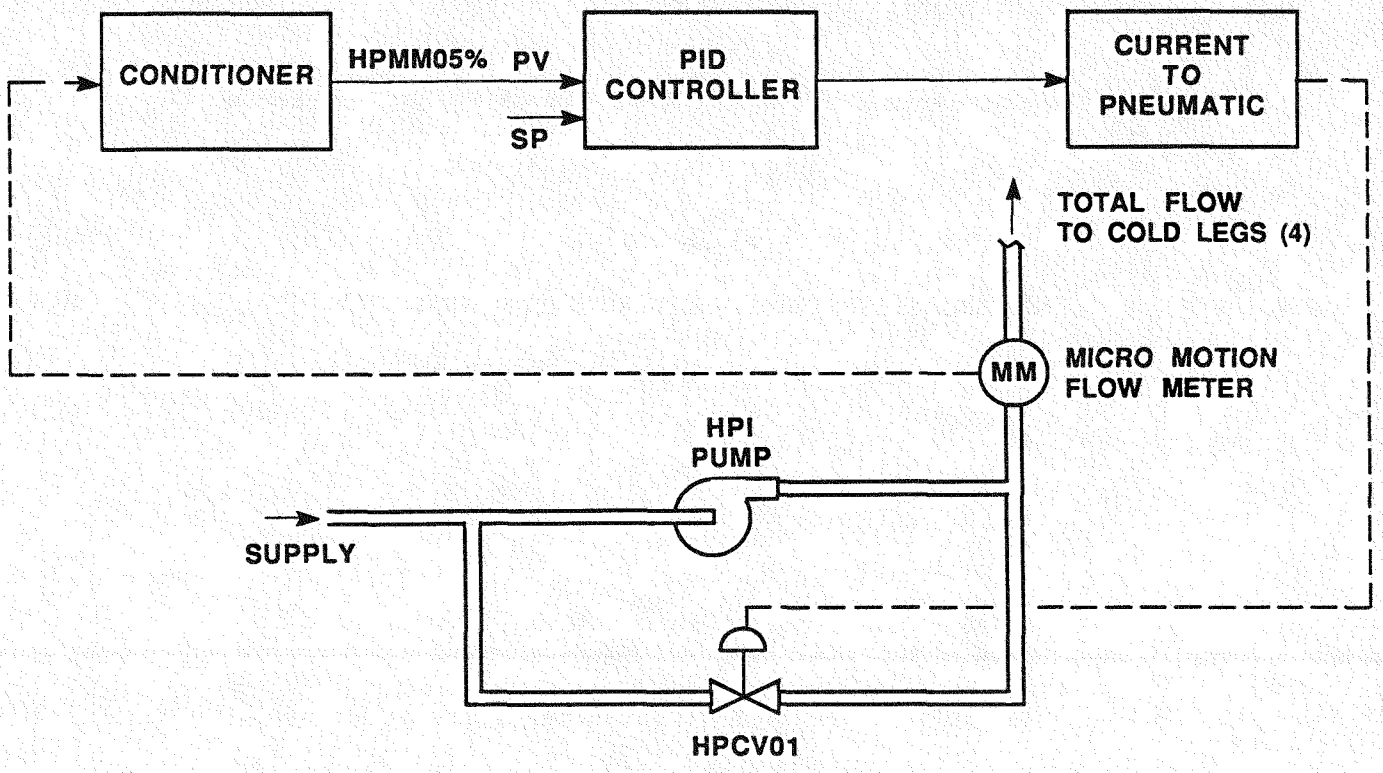

Figure 4.4 High-Pressure Injection Control

In the HPI control conditioner, the 1- to 5-volt feedback signal is converted to 0 to 100% of the calibrated span of the Micro Motion flowmeter. For example, the mass flow rate feedback signal of 1 to 5 volts corresponds to 0 to 1.56 gpm.

The output of the high-pressure injection PID controller was based on the following equation:

$$\text{Output}(\%) = S5*\left[S6*(S1-S2) + S7*\int_{o}^{\Delta t}(S1-S2)dt + S8*\frac{d(S1-S2)}{dt}\right] \qquad (4\text{-}8)$$

where:

S5 is gain multiplier

S6 is proportional constant

S7 is integral constant (1/minute)

S8 is derivative constant (minute)

S1-S2 is the difference signal, also known as error signal, where S1 is the process variable and S2 is the setpoint

Δt is the processor update time, 0.25 second

The PID constants (S5, S6, S7, and S8) for the HPI control are:

S5 = 1

S6 = 0.9

S7 = 5

S8 = 0

the process variable (S1), the mass flow rate feedback signal, is given by:

$$PV = 100\%*(V-1)/4 \qquad (4\text{-}9)$$

where V is the mass flow rate signal (1 to 5 volts).

The mass flow rate setpoint (S2) depends on the control mode (automatic or cascade). In the automatic control mode, the setpoint is constant as indicated in Eq. 4-10. In the cascade control mode, the setpoint is a function of pressure and the loop subcooling temperature (T). The loop subcooling temperature is the difference between the primary loop saturation temperature (T_{sat}) and the core exit temperature (RVTC15). The setpoint during the cascade mode is defined in Eqs. 4-11 and 4-12.

a) **Automatic Control Mode**

$$SP = (M/1.56)*100\% \quad (4\text{-}10)$$

where M is the mass flow rate (gpm), which is defined in the test procedures.

b) **Cascade Control Mode**

1) If subcooling < T, then:

$$SP = M(p) \quad (4\text{-}11)$$

where M(p) is the piecewise linear approximation of the HPI head-flow curve. This function provides a mass flow setpoint (%) at a given primary loop pressure, p (%). The M(p) function is provided in the MIST test procedures, in which the flow rate setpoint is normalized by the maximum HPI flow rate (1.56 gpm). The allowable subcooling temperature (T) is also given in the test procedures.

2) If subcooling > T, then:

$$SP = M(p)*(1-0.1*(T-T_{sat})) \quad (4\text{-}12)$$

The PID output was 4 - 20 mA. The HPI control valve, HPCV01, is normally open. Thus, air is required to close this valve. A 4 mA output from the controller would result in the valve being open, allowing all the HPI mass flow to recirculate. A 20 mA signal from the controller would signal the valve to be fully closed, thus forcing all of the HPI mass flow to be pumped into the loop. The valve is proportionally closed with outputs between 4 to 20 mA. The HPI bypass valve is an Annin Series 94 control valve with a flow coefficient (full open) of 0.1. The flow coefficient is linear with percentage of opening.

4.5 AUXILIARY FEEDWATER CONTROL

The auxiliary feedwater to the A and B steam generators is regulated by control valves SFCV01 and SFCV02, respectively. These valves are controlled by two separate controllers — constant level and head-flow feedwater. The constant and the head-flow feedwater controllers are independent; they both control the feedwater control valves, but one at the time. The constant level controller maintains the steam generator level at a constant elevation without any feedwater flow compensation, while the head-flow feedwater controller

maintains the auxiliary feedwater flow at the desired setting regardless of the water level. The head-flow feedwater control system is normally used during steam generator refill, and during the steam generator band level control. The band level control does not directly control the feedwater valves; however, it actuates pneumatic isolation valves downstream of the feedwater valves. In summary, there are three distinctive auxiliary feedwater controls used in MIST:

1) Steam generator constant level control
2) Head-flow feedwater flow control
3) Steam generator band level control

4.5.1 Constant Steam Generator Level Control

The water level in the steam generator secondary is controlled using a PID controller which regulates the auxiliary feedwater valves. The MIST steam generator A and B level control circuits are shown in Figure 4.5.

The steam generator constant level control function is based on differential pressure and gauge pressure measurements in each loop (S1DP01 and S1GP01 for the A loop; S2DP01 and S2GP01 for the B loop). The pressure and differential pressure measurements are conditioned to provide a signal proportional to the steam generator level. The conditioned signal, referred to as the process variable (PV), is supplied to the PID controller where it is compared to the control setpoint (SP). The output of the PID controller is based on the difference between the process variable and the setpoint. The output signal is converted to a pneumatic control signal, which varies the air pressure to the valve actuator for the feedwater control valve (SFCV01 and SFCV02 for the A and B steam generators). The control valve is proportionally opened or closed as the air pressure is varied. As the position of the feedwater control valve is varied, the water level in the steam generator, sensed by the differential pressure transmitter (S1DP01 and S2DP01) is affected. This provides the feedback signal to the controller, completing the closed loop control circuit.

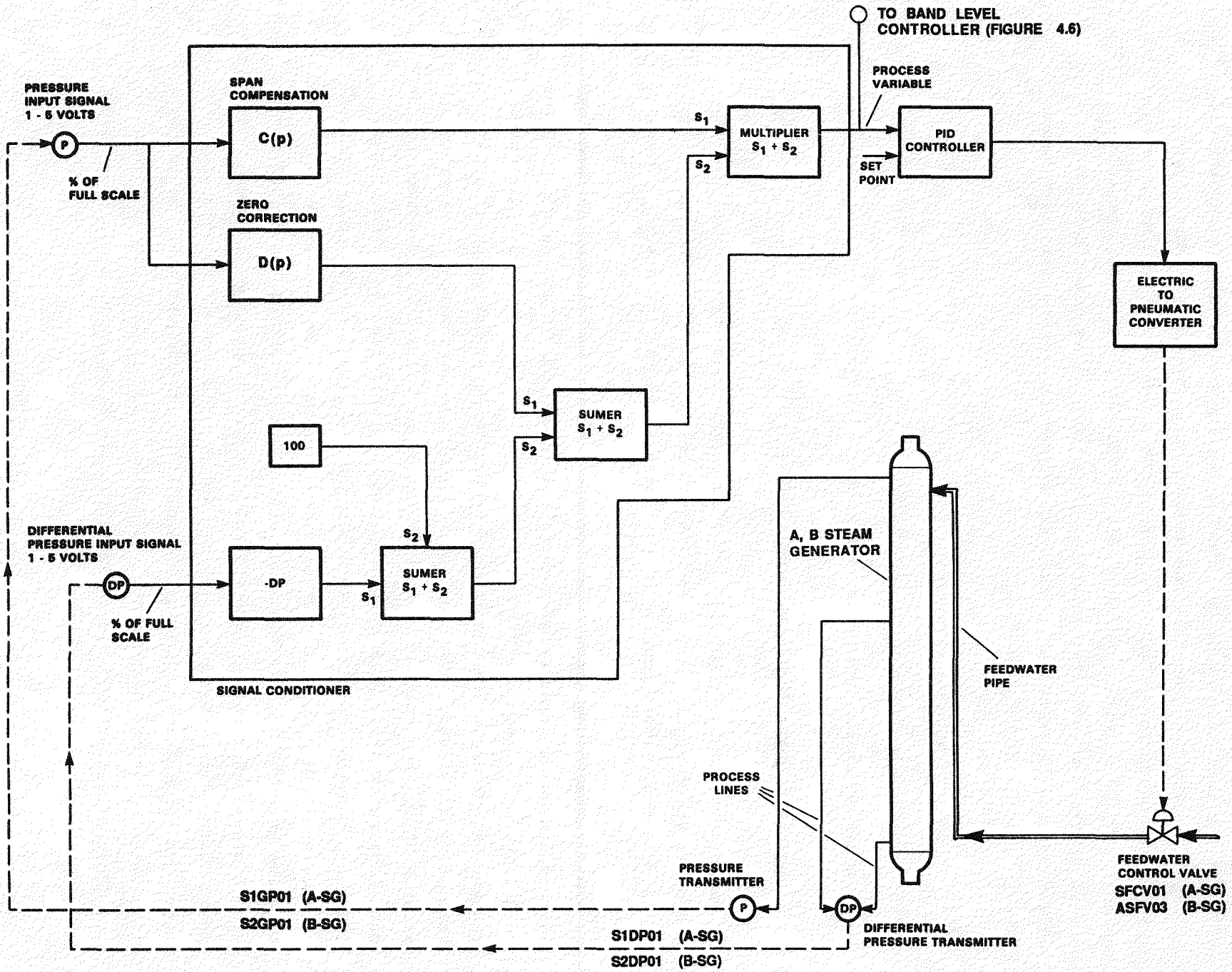

Figure 4.5 Steam Generator Constant Level Control

The analog signals (S1DP01, S1GP01, S2DP01, and S2GP01) can vary from 1 to 5 volts. These signals are proportional to the calibrated span of the transmitter which is 0 to 630 inches water for S1DP01 and S2DP01, and 0 to 1500 psig for S1GP01 and S2GP01. In the control conditioner of each loop, each feedback signal from the transmitters is converted to percentage of span of the transmitter. After conversion, the 1- to 5-volt signal corresponds to 0 to 100% for S1GP01 and S2GP01, 0 to 100.7% for S1DP01, and 0 to 101.1% for S2DP01.

Signal conditioner output (%) is given by the following expressions:

$$PV = D(p)*[B-(A+C(p)] \quad (4\text{-}13)$$

$$A = 100\%*(R)*(V-1)/4 \quad (4\text{-}14)$$

where:

A = Transmitter signal percentage

R = Ratio of transmitter range over span = 1.007 for S1DP01, 1.011 for S2DP01, and 1.0 for S1GP01 and S2GP01.

V = Transmitter signal (1 to 5 volts)

B = Bias fixed at zero operating conditions = 100%

C(p) and D(p) are the zero correction and span compensation factors, respectively. In order to obtain a signal proportional to the fluid level in the generator, these two factors need to be applied to the differential pressure signal to compensate for the density variation with pressure. The values for these two factors are listed in Table 4.2.

The conditioner output is the process variable (%). This signal is an input to the PID controller. The PID controller provides proportional, integral, and derivative (rate) control action based on the difference between the process variable (PV) and the setpoint (SP). The process variable is defined in Eq. 4-13 and the setpoint is defined in Eq. 4-15. The PID output is 4 to 20 mA. The feedwater control valves, SFCV01 and SFCV02, are normally open, so air is required to close these valves. A 4 mA output from the controller results in the valves being open; a 20 mA signal from the controller signals the valves to be fully closed. The valve is proportionally closed with

outputs between 4 to 20 mA. Both feedwater control valves are Annin Series 94 control valves with a flow coefficient (full open) of 0.075. The flow coefficient varies linearly with percent opening.

Table 4.2

SPAN AND ZERO CORRECTION FUNCTIONS FOR STEAM GENERATOR LEVEL

Percent of 1500 psig	Zero Correction C(p)	Span Compensation D(p)
0	0	1.000
2.35	0.184	1.078
5.69	0.300	1.110
12.35	0.639	1.155
19.02	0.916	1.191
32.35	1.543	1.257
39.02	1.898	1.271
59.02	2.954	1.381
79.02	4.053	1.482
99.02	5.352	1.597

$$SP = L/S*100\% \qquad (4\text{-}15)$$

where:

L = Level setpoint in inches relative to the secondary face of the lower tubesheet. The level setpoints are defined in the test-specific procedures.

S = Difference in pressure taps, which is 625.6 inches water for S1DP01 and 623.4 inches water for S2DP01.

The PID output is a function of the difference between the process variable (PV) and the setpoint (SP) as indicated by Eq. 4-4.

The level control PID constants (S5, S6, S7, and S8) are:

S5 = 1 (Steam Generator A) — S5 = 1 (Steam Generator B)
S6 = 4 (Steam Generator A) — S6 = 3.5 (Steam Generator B)
S7 = 2 (Steam Generator A) — S7 = 1.5 (Steam Generator B)
S8 = 0 (Steam Generator A) — S8 = 0 (Steam Generator B)

The PID output is 4 - 20 mA. The feedwater control valves, SFCV01 and SFCV02, are normally open, so air is required to close these valves. A 4 mA output from the controller results in the valves being open; a 20 mA signal from the controller signals the valves to be fully closed. The valve is proportionally closed with outputs between 4 to 20 mA. Both feedwater control valves are Annin Series 94 control valves with a flow coefficient (full open) of 0.075. The flow coefficient varies linearly with percent opening.

4.5.2 Head-Flow Feedwater Control

The head-flow feedwater control regulates the feedwater control valves (SFCV01 and SFCV02 for A and B steam generators, respectively) in order to produce the desired auxiliary feedwater flow into the generators. The feedwater flow is normally used during the steam generator refill during the early stages of a transient. It is also used during the band level control mode.

The auxiliary feedwater mass flow rate is controlled using a PID controller. This feedwater flow control system is based on differential pressure measurement (SFDP05 in the A loop; SFDP06 in the B loop). The output signal from the transmitter is a 4 to 20 mA signal, resulting in a 1- to 5-volt control signal. This 1- to 5-volt process variable is conditioned before being supplied to the PID controller for the band level control. The output of the PID controller is based on the difference between the process variable (PV) and the the setpoint (SP). Each of the PID controller outputs is converted to a pneumatic control signal, which varies the air pressure to the valve actuator for the feedwater control valve (SFCV01 and SFCV02 for the A and B generators, respectively). The control valve is proportionally opened or closed as the air pressure is varied. As the position of the feedwater control valve is changed, the mass flow rate to the generator is changed; this provides a feedback signal to the controller.

The 1- to 5-volt flow signal to the band level control conditioner is proportional to the transmitter calibrated span, which is 0 to 0.2456 lbm/sec for SFDP05, and 0 to 0.2467 lbm/sec for SFDP06. Once in the controller, the analog flow signal is converted to percent of span. Thus, the 1- to 5-volt signal corresponds to 0 to 100%.

The output of each of the PID controller is based on the expression in Eq. 4-8. The process variable is the mass flow rate signal and is given by Eq. 4-16.

$$PV = 10*SQRT(100\%*(V-1)/4) \quad (4\text{-}16)$$

where V is the differential pressure signal (1 to 5 volts).

The setpoint depends on the control mode (automatic or cascade). In the automatic control mode, the setpoint is constant as indicated in Eq. 4-17; whereas in the cascade control mode, the setpoint is a function of pressure as indicated in Eq. 4-18.

a) Automatic Control Mode

$$SP = (M/C)*100\% \quad (4\text{-}17)$$

where:

M = Mass flow rate (lbm/sec), which is defined in the test-specific procedures.

C = 0.2456 and 0.2467 lb/sec for the A and B steam generator, respectively. These values are the maximum flow across the orifice flowmeters (SFOR05 and SFOR06).

b) Cascade Control Mode

$$SP = M(p) \quad (4\text{-}18)$$

where M(p) is the piecewise linear approximation of the AFW head-flow curve. This function provides a mass flow rate setpoint at a given steam generator secondary pressure. M(p) is provided in MIST test procedures, in which the mass flow rate setpoint is normalized to the maximum AFW flow across the calibrated orifices.

The PID constants (S5, S6, S7, and S8) referred to in Eq. 4-8 for steam generator A and B controllers are identical. They are:

S5 = 1

S6 = 0.5

S7 = 10

S8 = 0

It should be mentioned that in preparation for Phase 4, a main feedwater system was added for supplying feedwater into the generator through the steam generator downcomer. This system utilized the same control scheme as the auxiliary feedwater control, except main feedwater valves SFCV03 and SFCV04 were used for throttling the main feed water flow into the A and B generators, respectively.

4.5.3 Band Level Control

As mentioned earlier, the band level controller maintains the steam generator secondary water level between two desired elevations using head-flow feedwater. As illustrated in Figure 4.6, the band level controller controls the actuation of feedwater pneumatic isolation valves SFCV09 and SFCV10 for the A and B steam generators, respectively. When the water level reaches the high level setpoint, the controller causes the feedwater isolation valve to close. With the absence of feedwater, as the water level decreases below the low level setpoint, the controller causes the feedwater valve to open allowing the generator to fill. During this fill period, the auxiliary feedwater flow is controlled by the auxiliary feedwater flow controller. The high and low level setpoints are normally given in the test procedure.

4.6 STEAM PRESSURE CONTROL

The steam generator secondary pressure was controlled using a PID controller. The steam pressure control systems for the A and B steam generator are presented in Figure 4.7. Both control systems are based on steam generator secondary pressure measurements (S1GP01 in the A loop; S2GP01 in the B loop). The output signal from the transmitter is a 4 to 20 mA signal, resulting in a 1- to 5-volt control signal. This 1- to 5-volt process variable is conditioned, then provided to the steam generator pressure PID controller. The output of the PID controller is based on the difference between the process variable (PV) and the setpoint (SP). Each of the PID outputs is converted to a pneumatic control signal that varies the air pressure to the valve actuator for the steam pressure control valve (SSCV01 and SSCV02 for the A and B generators, respectively). The control valve is proportionally opened or

closed as the air pressure is varied. As the position of the steam flow control valve is changed, the steam generator pressure is changed, thereby providing the feedback signal to the controller.

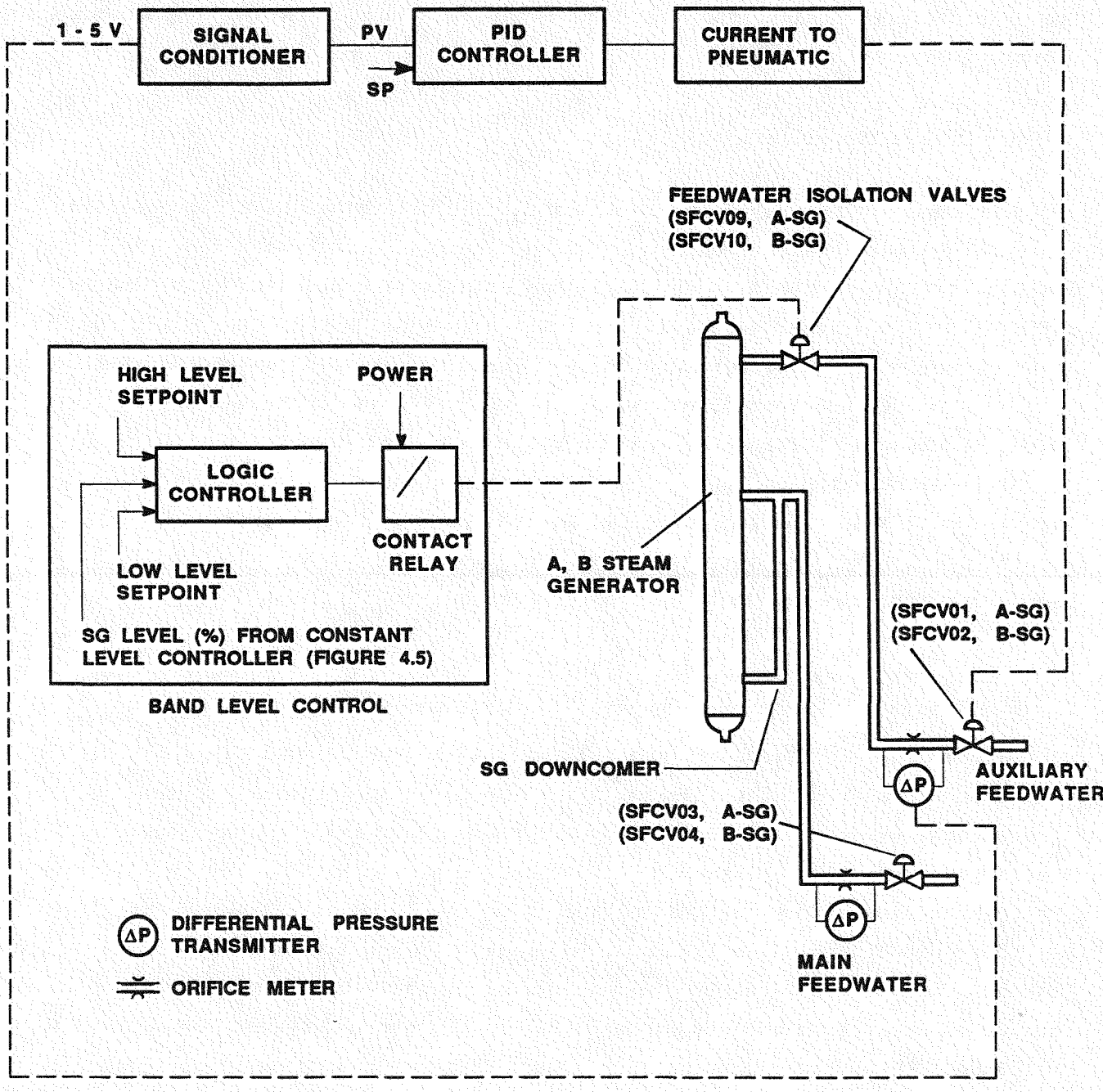

Figure 4.6 Auxiliary Feedwater Band Level Control

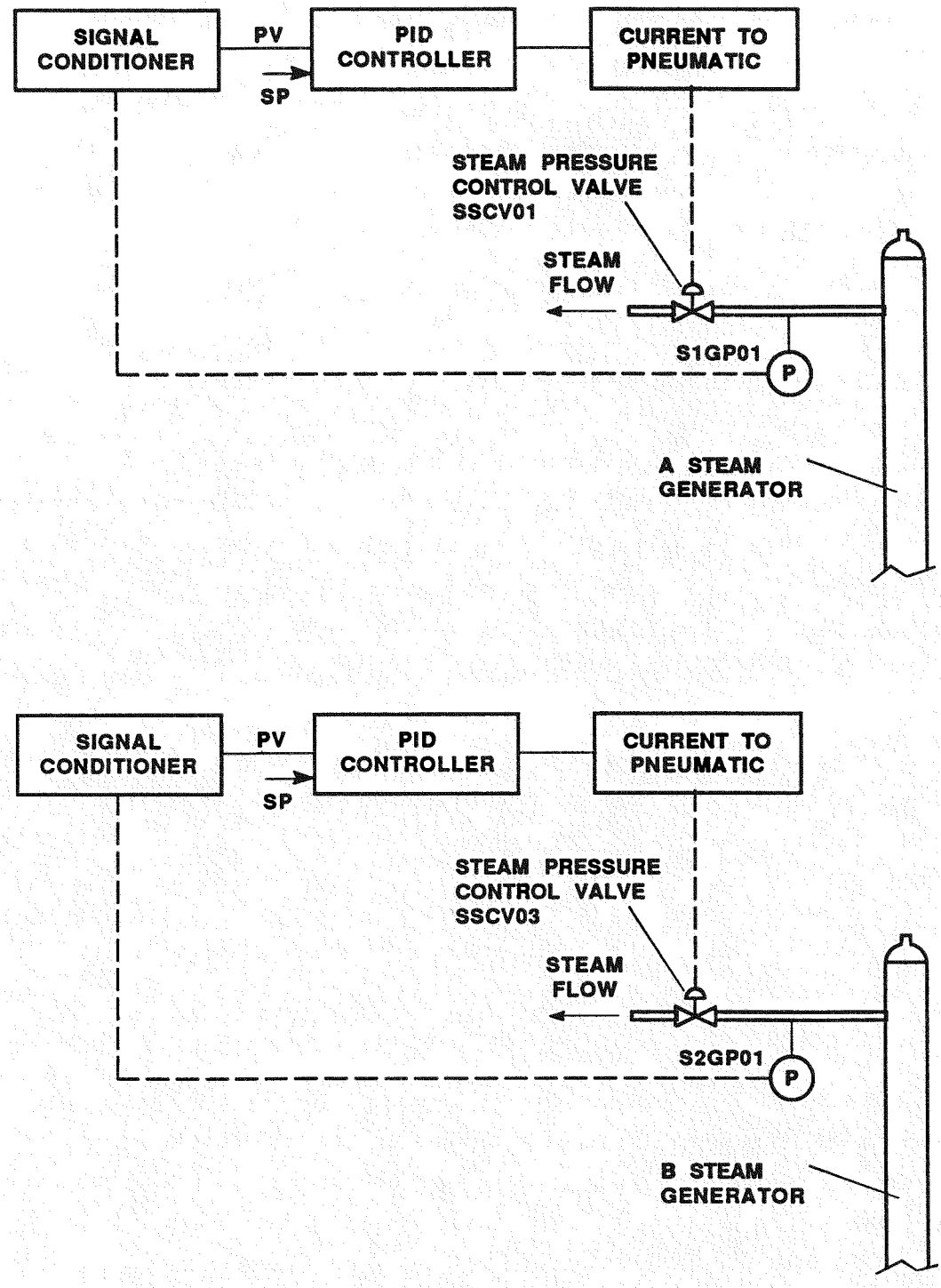

Figure 4.7 Steam Pressure Control

The 1- to 5-volt signal to the steam pressure control conditioner is proportional to the gauge pressure transmitter calibrated span of 0 to 1500 psig for both generators. The conditioner converts the 1- to 5-volt signal to percent of transmitter span. Thus, the 1- to 5-volt signal corresponds to 0 to 100%.

The output of each of the steam generator controllers is based on the expression in Eq. 4-8. The process variable is the steam generator pressure, and is given by Eq. 4-19.

$$PV = (100\%*(V-1)/4) \tag{4-19}$$

where V is the differential pressure signal (1 to 5 volts).

Each steam pressure control valve is a normally open valve. A 1-volt output from the PID controller signals the valve to open, while 5 volts signals the valve to close. The valve is proportionally closed with outputs between 1 to 5 volts. Both of the steam pressure control valves are Annin Series 94 control valves with a flow coefficient (full open) of 1.0. The valve's flow coefficient varies linearly with percent opening.

The PID constants (S5 ,S6, S7, and S8) referred to in Eq. 4-8 for the A and B steam generator steam pressure controllers are:

$S5 = 1$

$S6 = 5$

$S7 = 2.75$

$S8 = 0$

The dynamics of the control setpoint depend on the operating control mode (automatic or cascade). During the automatic control mode, the setpoint is constant, and it is equal to:

$$SP = P/1500*100\% \tag{4-20}$$

where P is the steam generator secondary pressure (psig). Initial setpoint is provided in the test procedures.

During the cascade control mode, the control setpoint (desired steam generator pressure) can vary according to the two types of pressure controls:

1) Automatic depressurization

2) ATOG depressurization

4.6.1 Automatic Depressurization Control

The automatic depressurization consists of depressurizing the secondary steam generator pressure at a desired rate, i.e., 50 psi/min. During this control mode, the setpoint (desired pressure) decreases at the rate specified in the technical procedure. The pressure setpoint is expressed as:

$$SP = P(t)/1500*100\% \qquad (4\text{-}21)$$

where P(t) is the saturation pressure (psig) as a function of time. This function is normally specified in the technical procedure.

4.6.2 ATOG Depressurization Control

The ATOG steam generator depressurization is used to control the primary system subcooling (DT) which is defined as the difference between the core outlet temperature, and the individual or the maximum of the two steam generator secondary saturation temperatures. The dynamics of the steam generator pressure setpoints vary according to the following ranges of the primary system subcooling:

1) **DT ≥ 50°F**

   If the DT is greater than or equal to 50°F, the secondary steam pressure control setpoint is to remain constant. The setpoint is then equal to the current steam generator pressure (see Eq. 4-20).

2) **0 < DT < 50°F**

   If the DT is less than 50°F but greater than 0°F, a cooldown rate of 100°F/hr is imposed on the secondary pressure setpoints and maintained until the DT increases to 50°F at which time constant pressure control is invoked. The setpoint is evaluated according to Eq. 4-22:

$$SP = [Pi*SAT(Ti-100/3600*N)]/1500*100\% \quad (4\text{-}22)$$

where:

Pi = Steam generator pressure (psig) of last cycle

Ti = Saturation temperature (°F) equivalent to Pi

SAT = Saturation pressure as a function of temperature

N = Number of executions per second (cycle/sec)

3) **DT ≤ 0°F**

If the DT is less than or equal to 0°F, a secondary depressurization rate of 50 psi/min is to be imposed on the secondary pressure setpoints and maintained until the DT increases to 50°F. The setpoint is evaluated according to Eq. 4-23.

$$SP = (Pi-50/60*N)/1500*100\% \quad (4\text{-}23)$$

4.7 GUARD HEATER CONTROL

The heat addition to the loop in order to compensate for heat losses was achieved using a guard heating system. The power to the guard heaters was controlled using a PID controller. A diagram illustrating the MIST guard heater control system is shown in Figure 4.8. Guard heater power control is based on the temperature difference between the vessel metal temperature and a point in the control insulation. The differential temperature signal (-20 to 80 mV) from the thermocouple pair is converted from millivolts to °F, then supplied to the guard heater PID controller.

The process variable (PV) signal is converted to °F as follows:

$$PV(°F) = PV(mvolts) * 32.25\ °F/mvolts \quad (4\text{-}24)$$

The output of the PID controller, a 4- to 20-mA signal, is based on the difference between the process variable (PV) and the the setpoint (SP). This output is supplied to a silicon-controlled rectifier (SCR) which provides power to the guard heaters. The output of the SCR is proportional to the 4- to 20-mA signal. As the power to the guard heater changes, the vessel and the insulation temperatures are affected, providing a feedback signal to the controller.

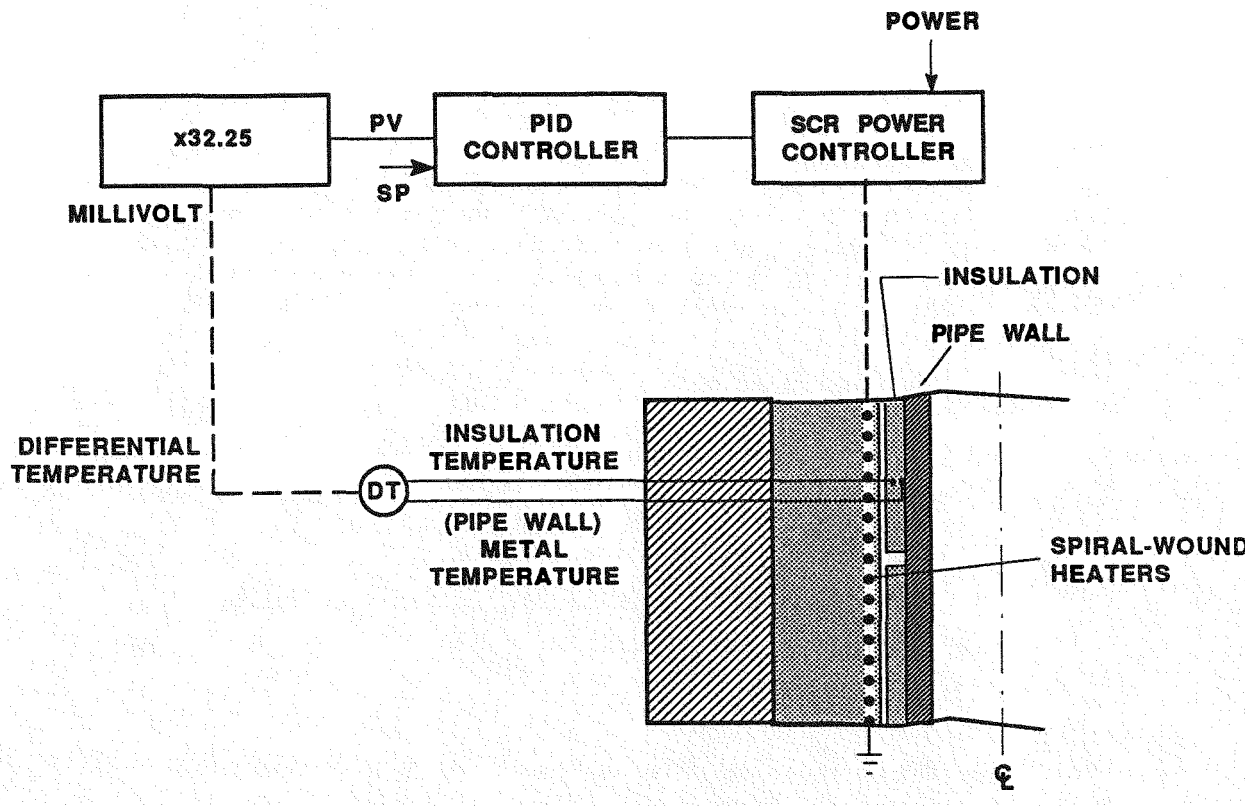

Figure 4.8 Guard Heater Control

The output of the PID controller (% power) varies with the control operation mode:

a) **Automatic or Cascade Mode**

The output in this control mode is given in Eq. 4-8. The setpoint (SP) is given as:

Auto Mode

SP = DT (°F)

(a constant dialed into control station by the operator)

Cascade Mode

SP = DT(T)

where DT is the differential temperature setpoint as a function of temperature, given in Table 6.12 (Section 6).

b) Track Mode

Output(%) = Power(T)

where Power(T) is guard heater power (%) as a function of vessel metal temperature. Only few guard heater zones were operating in Track control mode since their differential temperature thermocouples were broken. The zones operating in Track mode and their corresponding power functions are listed in Table 6.12.

The PID constants (S5, S6, S7, and S8) referred to in Eq. 4-8 for the guard heater controller of the various zones in the loop are the same, except for the zones noted below:

	All Zones	Zones 8, 13, 22, 27, and 42
S5 =	1	1
S6 =	2	15
S7 =	1	0
S8 =	0	0

4.8 PRESSURIZER HEATER CONTROL

The pressurizer heater control maintains the primary loop at a desired pressure, and also denergizes the heaters when the fluid level in the pressurizer drops sufficiently to begin exposing the heaters to steam. Two feedback signals are used in this control system: gauge pressure (PZGP01) and differential pressure (PZDP02). These two signals are conditioned to provide two process variables: the fluid level in the pressurizer and the pressurizer pressure. The fluid level process variable is provided to a logic block. In this block, the level process variable is compared to the pressurizer uppermost heater elevation. As soon as the pressurizer level is equal or below the upper heater elevation, the logic block output is set to "1". This Boolean signal trips the power to the heaters. The second process variable, gauge pressure, is supplied to a PID controller where it is compared to a pressure setpoint. The output of the PID controller, which is 4 to 20 mA, is based on the difference between the process variable (PV) and the the setpoint (SP). This output is supplied to a silicon-controlled rectifier (SCR) which provides power to the pressurizer heaters. The output of the SCR is proportional to

the 4- to 20-mA signal. As the power to the pressurizer heaters changes, the loop pressure is affected, providing a feedback signal to the controller. A diagram illustrating this circuit is shown in Figure 4.9.

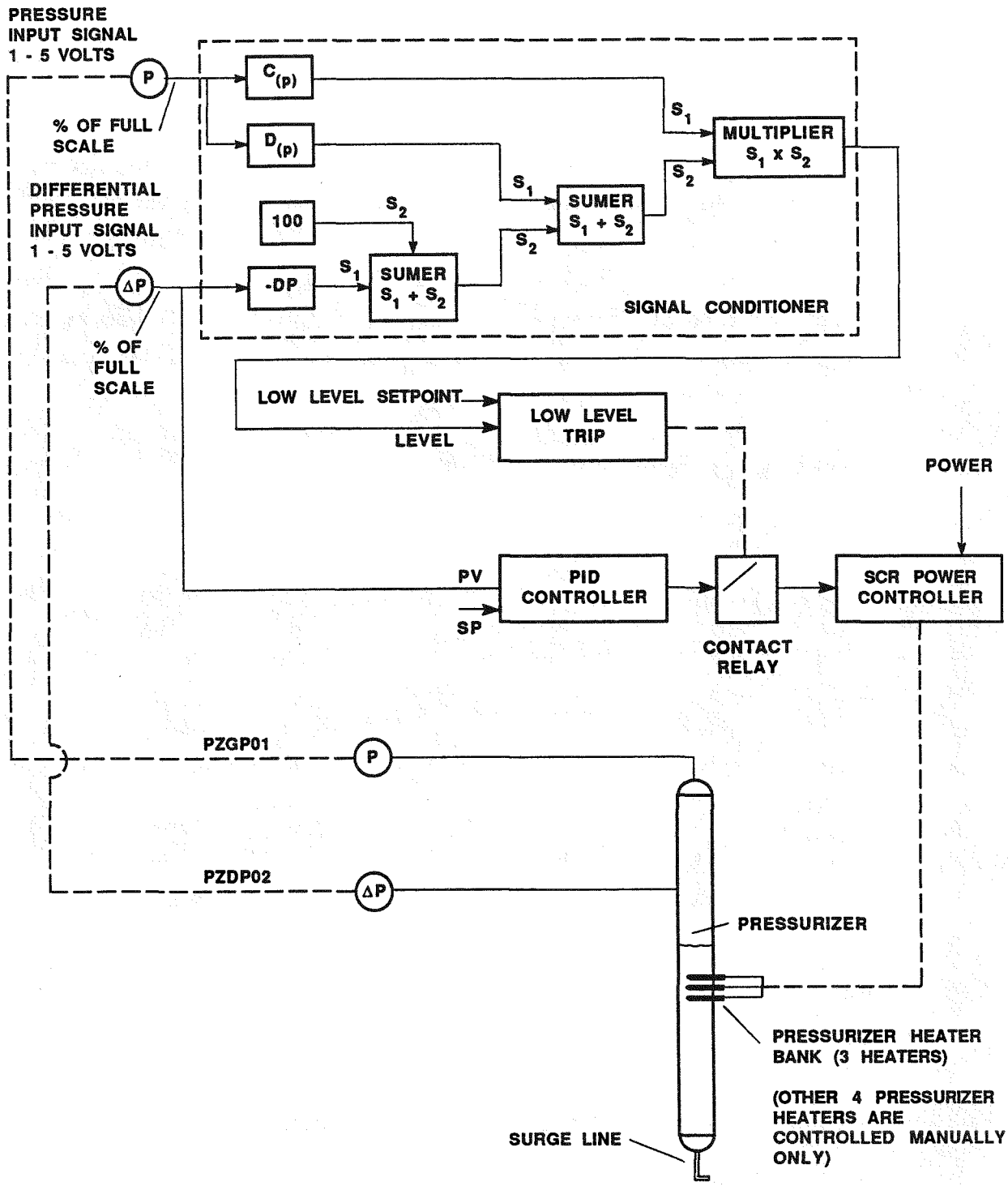

Figure 4.9 Pressurizer Pressure Control

The analog signals (PZDP02 and PZGP01) can vary from 1 to 5 volts. These signals are proportional to the calibrated span of the transmitter which is 0 to 150 inches water for PZDP02, and 0 to 2500 psig for PZGP01. In the control signal conditioner of each loop, the feedback signal from the transmitters is converted to percent of transmitter span. The 1- to 5-volt signal is converted and spanned to correspond to 0 to 117.97% for PZDP02, and 0 to 100% for PZGP01.

The output of the pressurizer heaters PID controller is based on the expression in Eq. 4-4. The pressurizer level process variable is given by Eqs. 4-13 and 4-14, with R equal to 1.1797; the C(p) and D(p) functions are given in Table 4.3. The pressure process variable is given below by Eq. 4-25. The upper heater elevation at which pressurizer heater power is tripped is 13.359% (percent of differential transmitter span). The gauge pressure setpoint is constant as expressed by Eq. 4-26.

$$PV = 100\%*(V-1)/4 \qquad (4\text{-}25)$$

where V is the gauge pressure signal (1 to 5 volts).

$$SP = (P/2500)*100\% \qquad (4\text{-}26)$$

with P being the desired operating loop pressure (psig). This is given in the MIST test procedures.

The PID constants (S5, S6, S7, and S8 in Eq. 4-4) for the pressurizer heater controller are:

S5 = 1

S6 = 32

S7 = 15

S8 = 0

Table 4.3

SPAN AND ZERO CORRECTION FUNCTIONS FOR PRESSURIZER LEVEL

Percent of 2500 psig	Zero Correction C(p)	Span Compensation D(p)
0	0	1
19.4	1.543	1.256
39.375	3.285	1.412
59.375	5.352	1.596
79.375	7.891	1.850
99.375	11.516	2.277

4.9 LOW-PRESSURE INJECTION CONTROL

In MIST Phase 4, a low-pressure injection (LPI) system was added to the emergency cooling control system of the MIST facility. This LPI system provided coolant flow into the downcomer at pressures lower than 200 psig. The low-pressure injection control scheme is similar to that of the high-pressure injection system. It uses a PID controller to control the LPI control valve (LPCV01), as indicated in Figure 4.10.

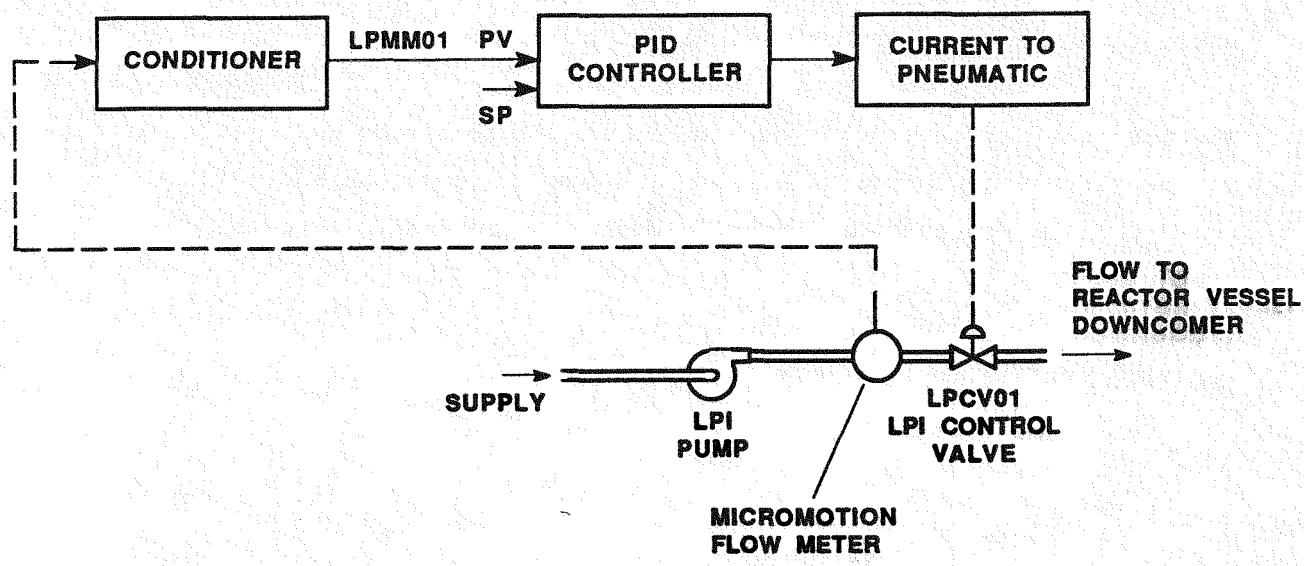

Figure 4.10 Low-Pressure Injection Control

The LPI control is based on the mass flow rate measurement (LPMM01) using the Micro Motion mass flowmeter. The output of the Micro Motion meter is a 4- to 20-mA signal, resulting in a 1- to 5-volt control signal. This 1- to 5-volt process variable is conditioned before it is routed to the PID controller. The output of the PID controller is based on the difference between the process variable (PV) and the setpoint (SP). This output is converted to a pneumatic control signal, which varies the air pressure to the valve actuator for the LPI control valve (LPCV01). The control valve is proportionally opened or closed as the air pressure is varied. As the position of the LPI control valve is changed, the mass flow rate to the cold legs is changed thus providing a feedback signal to the controller.

In the LPI control condition, the 1- to 5-volt feedback signal is converted to 0 to 100% of the calibrated span of the Micro Motion meter. For example, the mass flow rate feedback signal of 1 to 5 volts corresponds to 0 to 9 gpm.

The output of the low pressure injection PID controller was based on Eq. 4-4. The process variable, the mass flow rate signal, is given by:

$$PV = 100\%*(V-1)/4 \qquad (4\text{-}27)$$

where V is the mass flow rate signal (1 to 5 volts).

The mass flow rate setpoint depends on the control mode (automatic or cascade) in the automatic control mode. The setpoint is constant as indicated in Eq. 4-28. In the cascade control mode, the setpoint is a function of pressure.

a) **Automatic Control Mode**

$$SP = (M/9)*100\% \qquad (4\text{-}28)$$

where M is the mass flow rate (gpm), which is defined in the test procedures.

b) **Cascade Control Mode**

$$SP = M(P)/9*100\% \quad (4\text{-}29)$$

where M(p) is a piecewise linear approximation of the LPI head-flow curve. This function provides a mass flow setpoint (%) at a given primary loop pressure (%). The M(p) function is provided in the MIST test procedures, where the flow rate setpoint is already been normalized by the maximum LPI flow rate (9 gpm).

The PID output was 4 to 20 mA. The LPI control valve, HPCV01, is normally open, so air is required to close it. A 4-mA output from the controller would result in the valve being open allowing the LPI mass flow into the reactor vessel downcomer. A 20-mA signal from the controller would signal the valve to be fully closed. The LPI bypass valve is a Masonelian Micropak control valve with a flow coefficient (full open) of 0.6.

The PID constants (S5, S6, S7, and S8) of the LPI controller were:

S5 = 1

S6 = 0.5

S7 = 3

S8 = 0

Section 5

DATA ACQUISITION SYSTEM

5.1 DATA ACQUISITION AND DATA PROCESSING HARDWARE

The hardware configuration for the MIST data acquisition system was structured according to the system requirements defined in Reference 1. A hardware specification was also presented in Reference 1. No major modifications to this initial hardware configuration were needed to complete the MIST test program. An overview of the data acquisition system, supporting computers and storage devices, communication paths, and data display terminals is presented.

5.1.1 Data Acquisition Hardware

The Analogic ANDS5400 data acquisition system served as the front end hardware, acquiring and digitizing signals from the complete scope of MIST instrumentation. Analog-to-digital conversion rates of about 10 kHz with a precision of 16 bits, including sign, were performed using this hardware. The hardware accepted input from analog voltage, frequency, and digital sources. Figure 5.1 shows a schematic of the Analogic hardware configuration with interface to the VAX 11/750 computer. Details of the hardware configuration are described in the remainder of this section.

Selection of the Analogic analog voltage card type was dependent upon the full-scale output of the instrument and the filter characteristic of the voltage card. As indicated in Table 5.1, low level analog voltage inputs from thermocouples, for example, were acquired on an AC4052 card with an accuracy of ±0.040 mV and a sensitivity of 0.0012 mV. Correspondingly, a high level voltage input signal up to 10 V was acquired on the AC4060 card at an accuracy of ±5 mV and a sensitivity of 0.31 mV. For these two card types plus the AC4057 (±1.25 V full-scale), the filter bandwidth was specified as 5 Hz, resulting in an additional error of ±0.05% full-scale at 0.12 Hz. For analog

signals with frequency content greater than 0.12 Hz, the attenuation error caused by the filter increased to approximately 30% at 5 Hz.

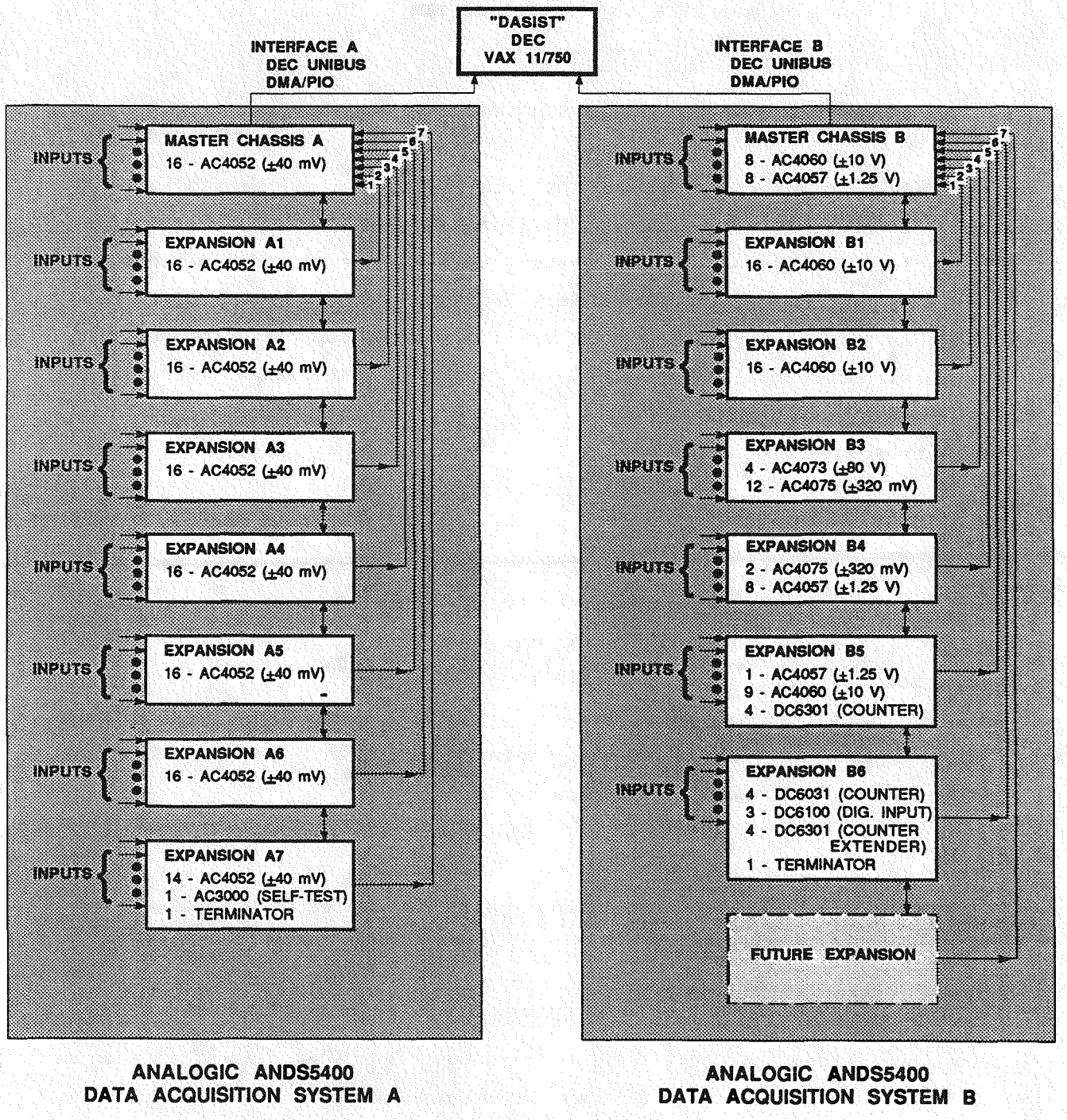

Figure 5.1 Analogic Data Acquisition System Configuration

Table 5.1

ANALOG VOLTAGE CARD TYPES FOR THE DATA ACQUISITION SYSTEM

Card Type	Full-Scale Input	Sensitivity (mV)	Accuracy (mV)	Filter Bandwidth	Typical Inputs
AC4052	±40 mV	0.0012	±0.040	5 Hz	Thermocouple
AC4057	±1.25 V	0.038	±0.625	5 Hz	Resistance temperature detector
AC4060	±10.0 V	0.305	±5.0	5 Hz	4-20 mA transmitter outputs such as pressure and differential pressure
AC4073	±80 mV	0.0024	±0.112	100 Hz	Low level inputs (thermocouple) for high-speed data acquisition
AC4075	±320 mV	0.0098	±0.448	100 Hz	High level inputs (transmitters) for high-speed data acquisition

NOTE: Specifications are for Analogic ANDS5400 Data Acquisition System

Two other voltage card types — AC4073 and AC4075 — were used in the data acquisition system where additional frequency response was needed. These cards had a bandwidth of 100 Hz and were primarily used for the conductivity probes, reactor vessel vent valve differential pressure measurements, and reactor coolant pump power measurements.

Frequency was measured using the Analogic DC6301 counter-timer card in frequency mode. An accumulation time of 10 seconds was used to measure the frequency output of the turbine meters. The accuracy of the measured frequency using these cards was conservatively specified as ±0.1 Hz for frequency inputs from 1 to 100 Hz and ±0.1% of the reading for inputs of 100 to 5000 Hz. In the count mode of operation, the DC6301 card experienced no measurement error with input frequencies to 30 kHz, which corresponds to pump full speed.

Digital inputs were measured with the DC6100 card which accepted 32 inputs on a single voltage card. No error was associated with this measurement.

5.1.2 Computer and Peripheral Hardware

Figure 5.2 shows a schematic of the hardware configuration for the VAX 11/750 computers used for data acquisition, real-time data display to the test operators, and post-test data processing. The block diagram shows two VAX 11/750 computers, referred to as the "DASIST" and "MIST" nodes of the network. The primary function of the DASIST computer was to support data acquisition and data display to the test operators in real-time operation. When data acquisition was not required, this computer was used to support post-test data processing activities. The function of the MIST computer was strictly associated with post-test data processing activities. The following discussion summarizes the major computer hardware components and functions of each for the MIST data acquisition and data processing system.

DASIST Node. The VAX 11/750 associated with the DASIST node was configured with 8 megabytes of memory, a floating point processor, and operated under VMS version 4.1. A single 456-megabyte RA81 fixed-media disk drive stored the operating system, source code executables, and served as the data storage device. A second disk drive, a 205-megabyte removable-media RA60, was dual ported to the DASIST and MIST nodes. This disk stored the source code and provided a removable media for weekly software and data backups of both nodes.

Test data was acquired through the Analogic hardware, as shown, with communication provided by the DEC DMA/PIO unibus interface. The Bailey NETWORK90 control system provided data input to the VAX over a serial interface, at a communication speed of 19,200 baud.

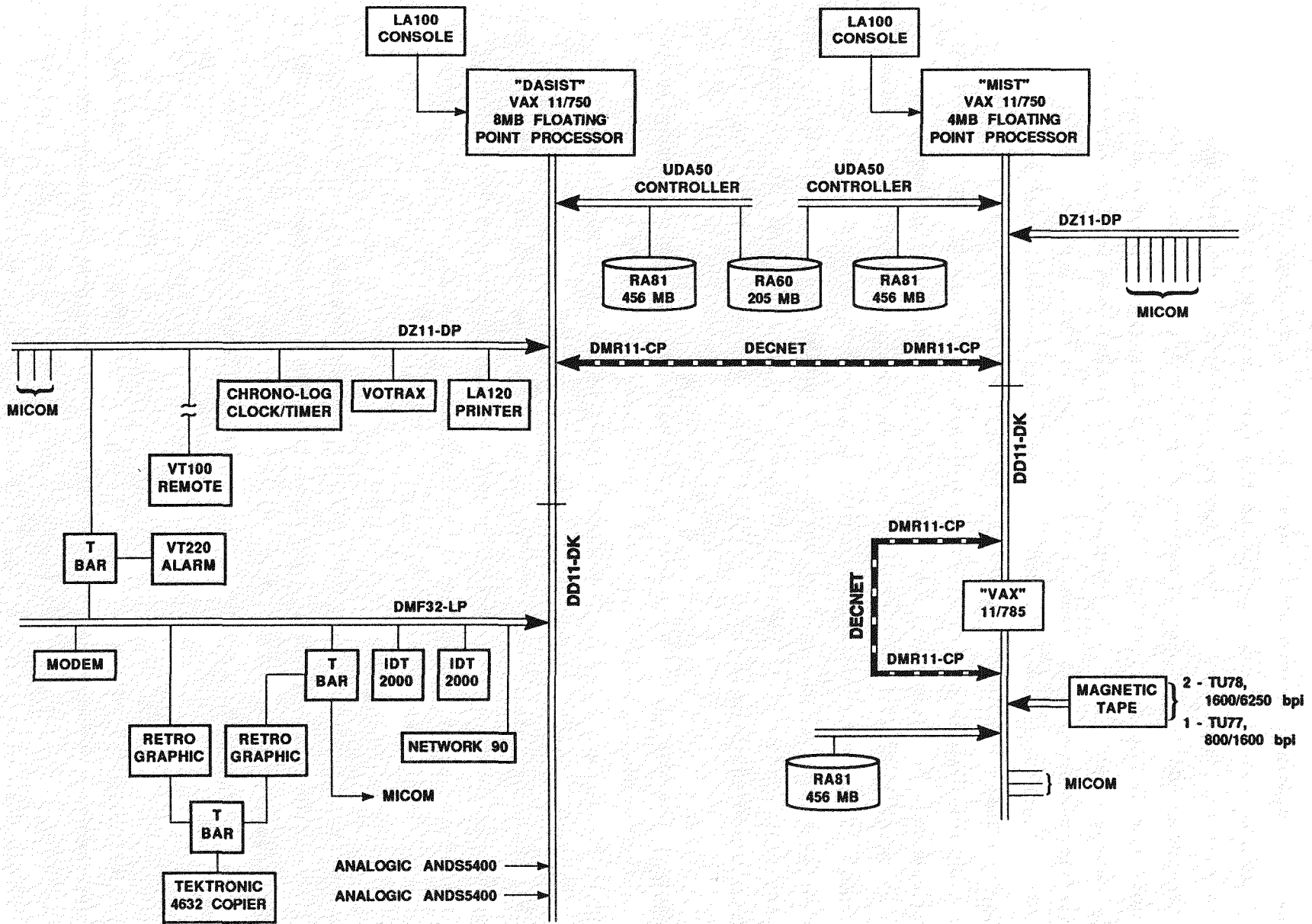

Figure 5.2 MIST Data Acquisition and Data Processing Program

A number of peripherals were attached to the DASIST computer. The Chrono-Log clock/timer was synchronized in time to the computer via the RS-232 interface and provided the time input to the viewport video displays. Two Industrial Data Terminal 2000 color graphic terminals provided a real-time display of test measurements on a schematic of the MIST facility and the simulated plant safety parameter display. A Votrax speech synthesizer was used to output voice alarm messages to the test operators. Two DEC VT131 video terminals with Retro-Graphic upgrade provided 800 x 480 graphics resolution for data display. A Tektronix 4632 video hard copy unit was connected to either of these graphics terminals through a two-way data switch. A DEC VT220 terminal in the control room was used to display data lists and alarm messages. A "remote" VT100 terminal was used to support calibration activities associated with the Analogic data acquisition system in the control room and was used remotely from the control room to support test activities. A DEC LA120 hardcopy printer served as the control room printer device and was shared by the DASIST and MIST computers.

MIST Node. The VAX 11/750 associated with the MIST node was configured with 4 megabytes of memory, a floating point processor, and operated under VMS version 4.1. A single 456-megabyte RA81 fixed-media disk drive stored the operating system, source code executables, and served as the data storage device. Most communication activities to this computer were from terminals remote to the test facility control room. Communications were routed through the Micom intelligent port selector, which services the Alliance Research Center's computer network.

Communication between the MIST and DASIST computers was supported by the DECnet communication software, supporting data transfer between computers at a 1 megabit/sec rate. In addition, a DECnet link to the VAX 11/785 computer servicing the research center provided a similar high-speed data transfer capability.

Support Hardware. Hardware shown on Figure 5.2 that performed data archival to tape used the research center's VAX 11/785. A single 456-megabyte RA81 disk drive was part of the MIST hardware and served as a data buffer to the tape drives connected to the 11/785, and a storage media for data sets

actively being used. Three tape drives were available, two DEC TU78 drives with read/write densities of 1600 and 6250 bpi, and a TU77 drive with a read/write density of 800 and 1600 bpi.

5.2 SOFTWARE OVERVIEW

The software developed for the MIST test program was extensive, encompassing real-time data acquisition, data display to the test operators, and post-test data processing and qualification activities. The software overview presented herein is not intended to provide a comprehensive description of the MIST software, but rather present a global overview of its function and architecture. A detailed description of the software associated with data acquisition, data storage to disk, the conversion of the raw data to engineering units, data qualification, and data archival to magnetic tape is contained in the Quality Assurance documentation prepared for this software. These documents are maintained on file by B&W. A detailed discussion, however, is presented in this section regarding the format and contents of the engineering data distributed outside of B&W. This discussion is of particular importance to the end users of the data, providing the necessary support documentation to define the contents of the data tapes.

The remainder of this section presents an overview of the real-time and post-test data processing software, and concludes with a detailed discussion of the contents of the engineering data tapes distributed outside of B&W.

5.2.1 Real-Time Data Acquisition Software

The data acquisition software was designed to implement VAX/VMS system service features to efficiently utilize the VAX 11/750 as a real-time system. As illustrated in Figure 5.3, the software architecture was designed around a central data base, referred to as the "global common". This central data base contained all of the parameters necessary to control the flow of data from each instrument, through the data acquisition hardware, to the computer disk. In addition, this data base contained the parameters required to convert the raw data to engineering units for each data base instrument and derived quantity. Two modules directly interfaced with the global common. UPDSYS

allowed dynamic update of the system control features of the data base, such as the definition of the test title, acquisition rates for each of the four raw data files acquired, data storage to disk specifications, and alarm module specifications. The second module, UPDVTB, provided the means to update the data acquisition control and data processing parameters associated with each data base entry or VTAB. The data base entries consisted of both instrument and derived quantity values.

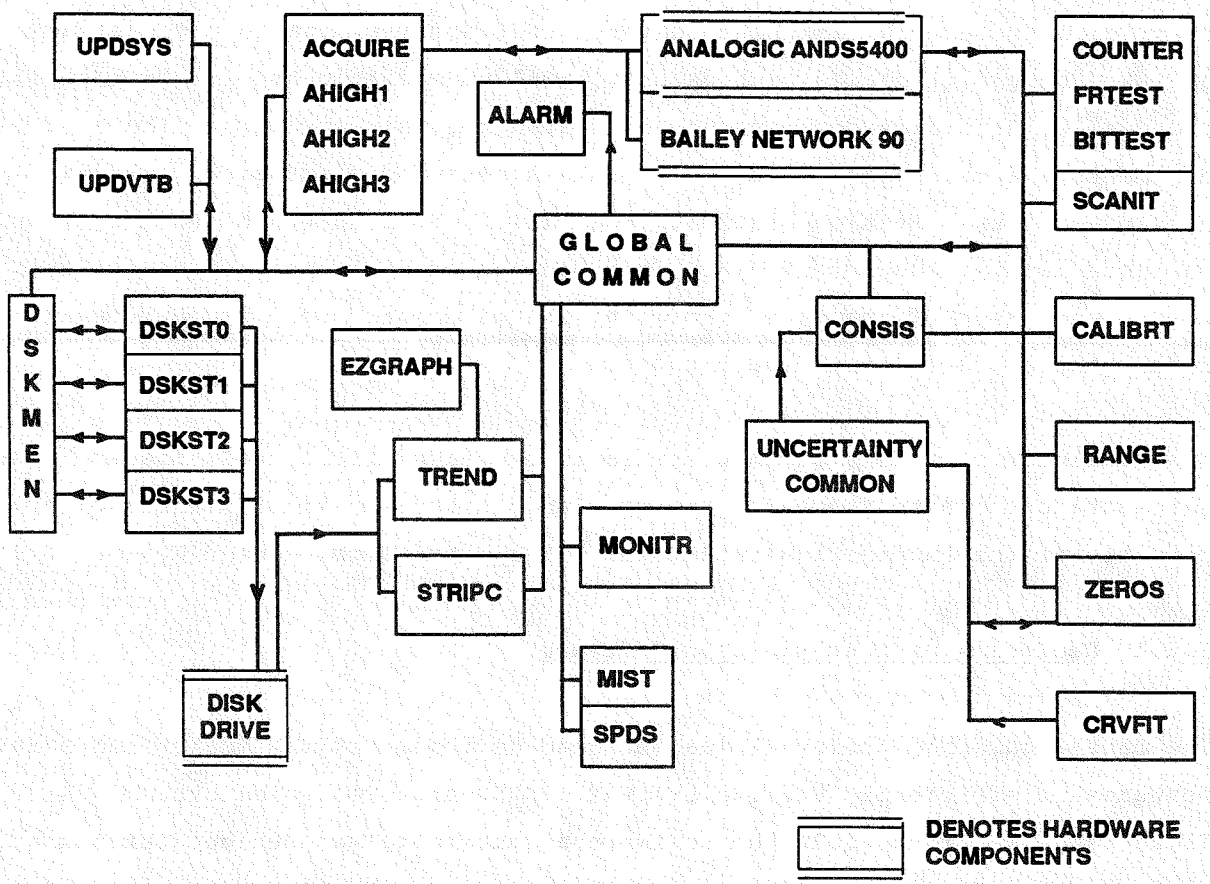

Figure 5.3 Real-Time Software for Data Acquisition and Test Support

As Figure 5.3 illustrates, four modules were responsible for data acquisition, communicating with the Analogic ANDS5400 hardware and depositing the raw data to the global common for access by the disk storage, data display routines, and other utility programs. The ACQUIRE module, responsible for acquisition of all data base instrument readings, provided "low speed" data acquisition at a minimum scan interval of 5 seconds. The high-speed data acquisition modules — AHIGH1, AHIGH2, and AHIGH3 — provided acquisition at a minimum scan interval of 0.1 second for selected instruments. In particular, AHIGH1 scanned the conductivity probes and the reactor vessel vent valve differential pressure transmitters. The AHIGH2 module scanned all of the valve and differential pressure transmitter limit switches, and AHIGH3 obtained information on the reactor coolant pumps during pump "bump" operation.

Associated with each of the acquisition modules was a module to move the acquired data from the global common to the computer disk. As shown in Figure 5.3, the low-speed module DSKST0 and the three high-speed modules DSKST1, DSKST2, and DSKST3 performed the disk storage tasks. The parent module, DSKMEN, provided functional control over each, allowing the data save rates to be independently defined and establishing the trigger for data save initiation and termination.

With the data acquired, a number of modules provided real-time display to the test operator. Program STRIPC served as a digital strip chart recorder, providing data time plots for operator selected instruments and derived quantities. The TREND module allowed "old" data written to disk to be retrieved and graphically displayed, using the Tektronix Plot 10 EZGRAPH software, either as a function of time or a function of another data base entry. The MONITR routine displayed user selected data base entries, the raw data value, and the engineering value in a table format. Finally, the modules MIST and SPDS provided real-time update to two color graphic displays. The display from the MIST module, shown in Figure 5.4, detailed the primary and secondary loops with indications of component liquid inventories, pressure and temperature distributions, and functional status of vent sites and safety systems. The SPDS module, simulating the Crystal River Plant's Safety Parameter Display System, was used by the plant-trained operator to control test performance.

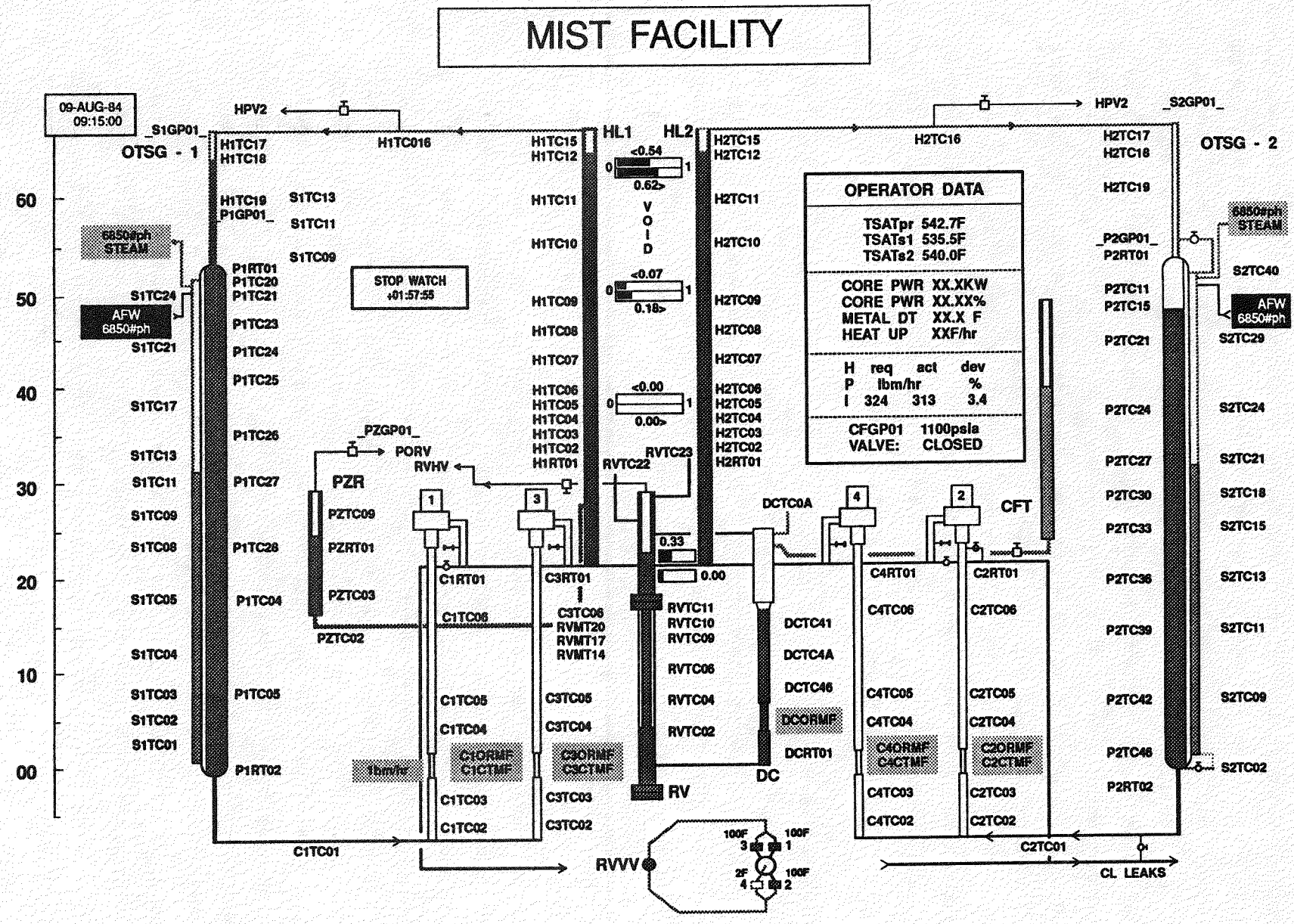

Figure 5.4 MIST Reactor Coolant System On-Line Status Display

A number of utility programs allowed the performance of the Analogic ANDS5400 data acquisition system hardware to be routinely examined. As shown on Figure 5.3, the FRTEST, BITTEST, and COUNTER interface modules to the Analogic supported the examination of frequency, digital input, and counts to the data acquisition hardware. The SCANIT module read analog voltage inputs to the Analogic and performed calibration checks on this hardware.

The in-place calibration of loop thermocouple instrumentation was supported by the CALBRT module. The CALBRT module was used to calibrate the thermocouples against the resistance temperature detector standards for the thermocouples in the primary and secondary flow loops. The CRVFIT modules performed polynomial curve fitting of the acquired calibration data from the thermocouples and all other MIST instruments, updating the conversion coefficients in both the global common and the "uncertainty common" data base. The latter data base contained the instrument performance specifications required to support the detailed measurement uncertainty analyses. The ZEROS module acquired transmitter zero readings, compared the acquired zero reading to the expected reading based on a real-time uncertainty analysis, and provided diagnostics to the test operator. This program also updated the uncertainty data base. Real-time data qualification checks were performed using the RANGE and CONSIS modules. RANGE compared the instrument signal output to the expected range of output values, providing diagnostic messages if an out of range reading was encountered. The CONSIS module tested most of the instruments in the primary and secondary loops using either neighboring instruments for assessment of measurement consistency or comparing the instrument measurement to a best-estimate calculation to determine if the measurement was as expected. In each instance, a real-time computation of the measurement and/or algorithm uncertainty was made and served as the standard for acceptable consistency.

5.2.2 Post-Test Data Processing Software

The post-test data processing software performed the conversion of raw data to engineering data, the computer automated data qualification checks, and provided tape archival and retrieval capability. A schematic summarizing these software modules is shown in Figure 5.5.

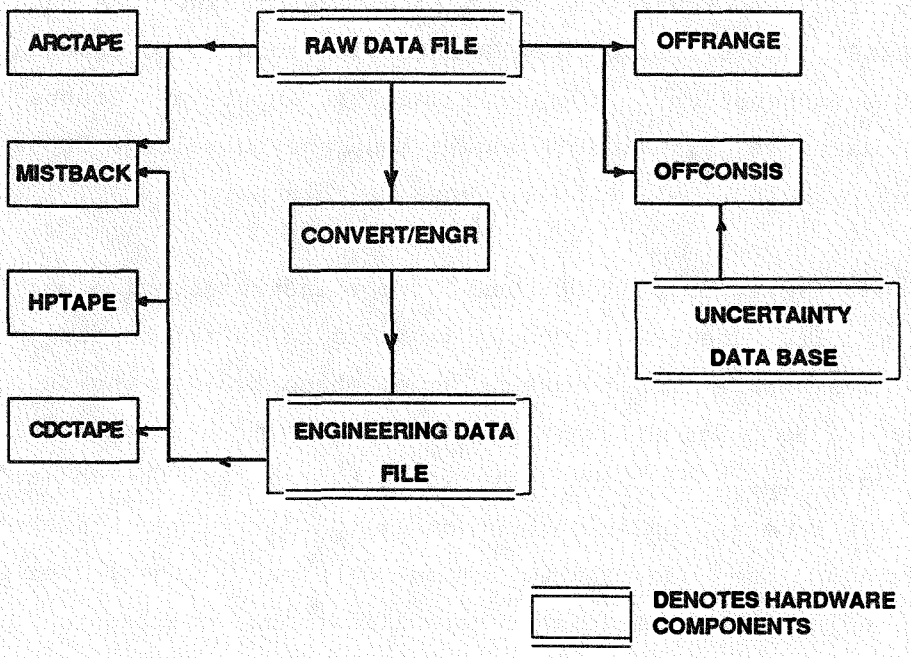

Figure 5.5 Post-Test Data Processing Software

The CONVERT/ENGR routine performed the raw to engineering data conversion, thus creating the engineering data file from the raw file. The OFFRANGE module performed a range check on all of the acquired raw data values, checking each data point against the expected range and providing diagnostics if out-of-range values were detected. The OFFCONSIS code performed a series of data consistency and automatic control system checks to examine most of the instrument readings for consistency, using neighbor measurements and/or computed values. The data consistency was evaluated using the instrument measurement specifications defined in the uncertainty data base as illustrated by the figure. For reference, the output from both the OFFRANGE and OFFCONSIS programs was included in the test immediate reports. Archival of the raw data files, and the test engineering and header files in binary format was performed using the tape modules MISTBACK, HPTAPE, and CDCTAPE depending upon the computer system accessing the tape. ARCTAPE produced an ASCII format tape of the header and engineering data files for archival.

5.2.3 Engineering Data Tape Contents

Each MIST test data set consisted of two ASCII files, referred to as the header file and the time-sequenced engineering data file. The header and engineering data files were supplied to users outside of B&W on magnetic tape. The format of the tapes were non-labelled, ASCII, 1600 bpi, 80-byte records, and 2560-byte blocks. The multi-volume tape set for each test consisted of the header and engineering tape files of the name testidANM.Enz or testid.HDz, where:

testid - Six alpha-numeric character test identifier such as 3109AA or 311000

A - Denotes an ASCII tape format

N,M - Tape sequential volume number (N) out of the total tapes (M) for the test

.Enz - Denotes the revision (z) of the n^{th} engineering (En) data file, where n=0, 1, 2, or 3 for the low-speed, high-speed 1, high-speed 2, and high-speed 3 files, respectively

.HDz - Denotes the revision (z) of the header (HD) file

The format and attributes of the engineering data and header files are discussed in the following paragraphs.

5.2.3.1 Engineering Data File. The engineering data file was time-ordered, with each time scan of data consisting of a single time entry followed by the engineering value for each of the data base entries or VTABs. The number of VTABs, NVTAB, associated with each test is defined in the header file discussed in Section 5.2.3.2. The first line of each file identifies the name of the file, testid.HDz or testid.ANM.Enz, as defined above. The engineering file data format for subsequent time scans is given by:

FORMAT (F11.5,2X,5E13.7,2X) - Time in minutes, first five engineering data values

FORMAT (6E13.7,2X) - Next six engineering data values,

:
:

FORMAT (6E13.7,2X) - Six engineering data values preceding the last record of the time set

FORMAT (6E13.7,2X) - Last record of the engineering data set where only NVTAB total entries are valid

5.2.3.2 Header File. The header file defines the test identifier, the data base configuration for the test data set, and documents the historical changes to the data base beginning with the initial raw-to-engineering data conversion. Specifically, the header file defines the instrument and derived quantity VTABs in the data set, the data acquisition system control parameters for each instrument VTAB, the raw data to engineering data conversion attributes, and the order of the VTABs in the engineering data file for each time scan. A detailed description of the header file follows.

5.2.3.2.1 General Format. The header file is subdivided into seven sections. These sections define:

1) Project attributes
2) Test title
3) Zero time
4) Comments to document the header and data base revisions
5) VTAB data base
6) Updates
7) Summary information

The beginning of each section is defined by a character entry in column 1 of the data record. Subsequent entries to the section have a blank in the first column. Table 5.2 shows a sample header file extracted from the Test 350800 and will be used to discuss the contents of each section.

Table 5.2

SAMPLE DATA TAPE HEADER FILE

```
        1         2         3         4         5         6         7         8
12345678901234567890123456789012345678901234567890123456789012345678901234567890
---- This ruler is shown for reference only.  It is not a part of the header. ----

P 24-OCT-1986 04:13:00.54
 350800
 1191  881
   22   22
   80   80
    0    0
T GROUP 35 SERIES - NITROGEN AS NCG SPECIES; HPV VENTING REMOVAL OF NCG; CLS LEA
Z ZERO TIME: 24-OCT-1986 04:35:05.68
  TRIGGER VTAB: V1LS03
  TRIGGER VALUE: 0.5
C *** COMMENT SECTION ***
  Enter comments after this point.


      The following VTAB names were marked NOREAD for this data conversion:

      C1TM01 C2TM01 C3TM01 C4TM01 H1MS01 H1MS02 H1MS03 H2MS01 H2MS02 H2MS03
      P1TC06 P1TC07 P1TC08 HVDT01 HVMT01 HVWM01 C4DT03 PZDT03 DCTC03 PZWM03

  The following descriptors were changed by FIXDESC on  2-FEB-87  13:03:25 :
      HVDT01    CVL GUARD HEATER CONTROL DT       41.35'
      HVMT01    CVL GUARD HEATER METAL TEMP       41.35'
      HVWM01    CVL GUARD HEATER POWER

  ***************   MIST Data Base Revisions Log   ****************************
```

Table 5.2 (Continued)

SAMPLE DATA TAPE HEADER FILE

```
 Rev    Date  Init Review          Description of Changes
 No.
---- --------- ---- ---- ------------------------------------------------------------

 001 02-Feb-87 JEB MTC Set PZWM04 to zero (with update) at 04:36:44

                      Fix references for RVOR's :   (& set RVOR01-07 to READ)
                       RVOR01,03:
                           RVGP01 RVTC21 RVTC19 RVTC19 RVDP06 RVDP08 RVVF04
                       RVOR02,04:
                           RVGP01 RVTC21 RVTC18 RVTC20 RVDP07 RVDP09 RVVF04

                      Add V1LC30: Leak flow rate based on weigh tanks. Reduc46
                        Nvtabs = Nvtabs + 1

  *** END OF COMMENT SECTION ***

D
      C1TM01 0 0 1 00 2 016 06 001 6 01 TURBINE IN PUMP SUCTION - LOOP A1  23.15
  00000  0.000000E+00  0.000000E+00  0.000000E+00  0.000000E+00  0.000000E+00
      1  0.000000E+00  0.000000E+00  0.000000E+00  0.000000E+00  0.000000E+00
 RVGP01 C1RT01
      C2MT03 1 0 0 00 1 001 02 001 1 03 PIPE OD TEMPERATURE ZONE 3-LOOP B1 23.45
  00008  0.000000E+00  0.000000E+00  0.000000E+00  0.000000E+00  0.000000E+00
      0  0.000000E+00  0.000000E+00  0.000000E+00  0.000000E+00  0.000000E+00
  .
  .
  .
  .    Entries deleted to minimize the length of this sample header.
  .

U 24-OCT-1986 04:36:44.00
      PZWM04 1 0 0 00 3 004 08 035 2 02 PRESSURIZER MAIN HEATER POWER
  00008  0.000000E+00  0.000000E+00  0.000000E+00  0.000000E+00  0.000000E+00
      0  0.000000E+00  0.000000E+00  0.000000E+00  0.000000E+00  0.000000E+00

S 24-OCT-1986 16:06:58.20
 THE FOLLOWING ARE THE NUMBER OF SCANS RECORDED FOR LOW, H1, H2, H3:
    6410   93558    1708       0
```

Project Attributes. A "P" in a column one denotes the project and is the first section in each header. The first record of the project defines the project stamp, date, and time of the header creation. The second record defines the six-character test identifier. The third record defines the total number of VTABs in the header and the number of instrument VTABs. Records four through six define the number of VTABs and instrument VTABs in the high-speed 1, 2, and 3 data files, respectively.

Test Title. A "T" in column one denotes the test title and is the second section in the header file. The title field is a maximum of 80 characters in length.

Zero Time. A "Z" in column one denotes the test zero time. The second and third lines indicate (if applicable) the VTAB used as the trigger for determining the zero time and the trigger value. The zero time is the third section in the header file. In the sample header shown in Table 5.2, the zero time was determined to be time 04:35:05.68 based on the valve limit switch V1LS03 crossing a value of 0.5.

Comment. A "C" in column one denotes the comment section and is the fourth section in each header. As shown in the sample header of Table 5.2, the comment section defines several data entries useful for test documentation. The list of VTABs is identified that did not acquire data (NOREAD) during test performance and those VTABs that were set for no raw-to-engineering data conversion as a result of post-test data qualification findings. Changes to the VTAB descriptors are noted. The historical record of revisions to the header file that effect raw-to-engineering data conversions are defined. Any general comments regarding test performance are noted.

Data Base. A "D" in column one denotes the start of the data base list of VTABs (instrument and derived quantities) and is the fifth section in each header. This data base defines all of the information needed to control the data acquisition system and to acquire the raw data for each instrument VTAB. The parameters required to control the conversion of the acquired raw data to engineering data are defined. A detailed discussion of the information contained in this data base is presented in Section 5.2.3.2.2.

Updates. A "U" in column one denotes an update to a VTAB in the data base and follows the data base section. The first record of the update contains the update stamp followed by a date and time identifier of the update. The remaining information of each update includes the ASCII dump of the VTAB record in the data base, including the change associated with the update. A separate "U" stamp appears for each VTAB update.

Summary. A "S" in column one denotes the summary record and is the last section in each header file. The first record contains the "S" stamp, and the date and time stamp that the record was written. The following two records contain a data definition and the number of acquired time scans of data for the low speed and each of the three high-speed raw data files. For reference, the first high-speed file contained instrument data for the conductivity probes and reactor vessel vent valve differential pressures. The second high-speed file recorded changes to the limit switches denoting times of valve actuations. The third high-speed file was used to acquire pump "bump" detailed measurements.

5.2.3.2.2 Data Base Format. The entries for each of the VTABs contained in the header file test data base document the data acquisition system, data base configuration, and the raw data to engineering conversion parameters. The VTAB order in the data base also defines the order of the engineering data file entries for each time scan. Since the data base information is important for all users of the data base, a detailed definition of its contents is presented.

Data Base Entry. A sample entry for VTAB C1TM01, the A1 cold leg turbine meter, is shown here for reference.

```
   C1TM01 0 0 1 00 2 016 06 001 6 01 TURBINE IN PUMP SECTION - LOOP A1 23.15
 00000  0.000000E+00  0.000000E+00  0.000000E+00  0.000000E+00  0.000000E+00
 00000  0.000000E+00  0.000000E+00  0.000000E+00  0.000000E+00  0.000000E+00
 RVGP01 C1RT01

   a1a2a3 b c d ee f ggg hh iii j kk [*************** desc ***************]
 mmmmm  [    con1   ] [   con2   ] [   con3   ] [   con4   ] [   con5   ]
 nnnn   [    con6   ] [   con7   ] [   con8   ] [   con9   ] [   con10  ]
 [ref1] [ref2] [ref3 [ref4] [ref5] [ref6] [ref7] [ref8]
```

The entries associated with each record are defined below.

Field	Format	Description
a1a2a3	A6	VTAB identifier where a1, a2, and a3 define the MIST subsystem, instrument type, and instrument number, respectively.
b	I1	NOREAD/READ (0/1) byte. A NOREAD status indicates that: 1) raw data was not acquired, and/or 2) no engineering data was converted for the initial time scan of the data set. In the latter instance, an UPDATE record in the HEADER file could be used to reset this value to READ, thereby initiating raw to engineering data conversion.
c	I1	Raw file pointer. The pointer defines which of the high-speed files the raw data is to be written to in addition to the low-speed data file. Acceptable values are: 0 - low-speed file only 1 - low- and high-speed 1 files 2 - low- and high-speed 2 files 3 - low- and high-speed 3 files
d	I1	Reference VTAB pointer. If the raw value to engineering value conversion requires other VTABs for supporting information, d = 1. Otherwise, no references are needed and d = 0.
ee	I2	Not used
f	I1	Not used
ggg	I3	Reduction type for the raw data to engineering conversion. The valid reduction types are defined in Table 5.3.
hh	I2	Engineering units code. The following units are defined in the data base:

Units Code	Units	Comments
1	volt	electrical volts
2	deg F	degrees Fahrenheit
3	psia	pressure, absolute
4	psig	pressure, gauge
5	gpm	gallons per minute
6	lbm/hr	pound mass per hour
7	psi	pounds per square inch
8	kwatt	kilowatt
9	Btu/hr	Btu per hour

Field	Format	Description

Units Code	Units	Comments
10	counts	digital counts
11	opn/cl	open/close (0/1)
12	lbm	pound mass
13	ft	feet
14	amps	electrical amperes
15	gal	gallons
16	cl/opn	close/open (0/1)
17	hz	frequency, hertz
18	scf/m	standard cubic feet per minute
19	%	percent
20	scf	standard cubic feet
21	rpm	revolutions per minute
22	Btu/lb	Btu per pound
23	lbm/ft^3	pound per cubic foot
24		blank designates no units
25	out/in	out/in (0/1) to designate a differential pressure transmitter out or in service
26	fc/nfc	full close/not full close (0/1) to designate valve position either full closed or in transition
27	nfo/fo	not full open/full open (0/1) to designate valve position either full open or in transition

iii I3 Defines the Analogic channel number or the NETWORK90 block number

j I1 Defines the Bailey NETWORK90 PCU number or the Analogic data acquisition system voltage card type where:

Value	Descriptor
0	denotes derived quantity

Analogic Card Type

1	±0.040 volt
2	±1.25 volts
3	±10.0 volts
4	digital (1/0)
5	counter
6	frequency
7	±0.080 volt
8	±0.320 volt

Field	Format	Description
kk	I2	Gain code which is Bailey NETWORK90 or Analogic card dependent according to the following: **Bailey NETWORK90** – the gain defines the module number **Analogic Card** –

Type	Gain Code
0	Not applicable
1,2,3,7,8	1 - card gain of 1 2 - card gain of 2 4 - card gain of 4 8 - card gain of 8
4	0-15; bit number
5	Not applicable
6	4 - 600 sec Gate Time 5 - 3600 sec Gate Time 6 - 60 sec Gate Time 7 - 100 sec Gate Time 8 - 10 sec Gate Time 9 - 1 sec Gate Time 10 - 1E-1 sec Gate Time 11 - 1E-2 sec Gate Time 12 - 1E-3 sec Gate Time 13 - 1E-4 sec Gate Time 14 - 1E-5 sec Gate Time 15 - 1E-6 sec Gate Time

desc	A40	VTAB descriptor, limited to 40 characters
mmmmmm	I6	Coded value defining the Analogic channel options, the Bailey NETWORK90 attributes, and math error status according to the following:

Bit	Description
0	bit 0 of the two bit indicator of the Analogic chassis number
1	bit 1 of the two bit indicator
2,4,6-15	not used
3	enable VTAB input from the NETWORK90 hardware
5	real-time engineering math error status

Field	Format	Description
nnnnnn	I6	Conversion error code defining raw data to engineering data conversion error(s). The presence of a non-zero value indicates at least one conversion error in the processed engineering data set. The integer value is bit packed (each of 16 bits define an error type). The error types are defined in Table 5.4 along with the error value, the bit number of the error, a description of the error, and the engineering reduction type(s) to which this error is applicable. Note that an error code equal to 0 does not assure that data conversion errors are absent. Not all of the conversion errors trigger the error code. However, the magnitudes of all possible error values are defined in the error value list.
con1-10	E13.6	Reference constants required for the raw-to-engineering data conversion. Table 5.3 defines the constants for each reduction type.
ref1-8	A6	Reference VTABs required for the raw-to-engineering data conversion. Table 5.3 defines the references for each reduction type.

Table 5.3

ENGINEERING DATA REDUCTION TYPES, REFERENCE VTABS, AND CONVERSION CONSTANTS

Reduction Type	Description	Conversion Constants	Reference VTABs
1	Engineering value equal to raw data value	none required	1) Metal temperature for differential temperature VTABs only
2	Resistance temperature detector (RTD) with calibration	1) RTD resistance at 32°F (ohms) 2) Temperature coefficient (C^{-1}) 3) RTD constant 4) Resistance of circuit resistor (ohms)	1) Reference voltage
3	Reduction equation = $C_1 + C_2*\Delta + C_3*\Delta^2 + C_4*\Delta^3$ where $\Delta = V-V_{ref}$. Examples include a transmitter with a "zero" voltage, V_{ref}.	1) Constant, C_1 2) Constant, C_2 3) Constant, C_3 4) Constant, C_4 5) Constant, V_{ref}	none required
4	Reduction equation = $C_1 + C_2*V + C_3*V^2 + C_4*V^3 + C_5*V^4$ General 4^{th} order polynomial.	1) Constant, C_1 2) Constant, C_2 3) Constant, C_3 4) Constant, C_4 5) Constant, C_5	none required
5	Reduction equation for an uncalibrated Type J thermocouple (iron-constantan). Reference junction: 150°F, Fit range: $32 \leq T(F) \leq 2000$	none required	none required
6	Reduction equation for an uncalibrated Type K thermocouple (chromel-alumel). Reference junction: 150°F, Fit range: $32 \leq T(F) \leq 2000$	none required	none required

Table 5.3 (Continued)

ENGINEERING DATA REDUCTION TYPES, REFERENCE VTABS, AND CONVERSION CONSTANTS

Reduction Type	Description	Conversion Constants	Reference VTABs
7	Reduction equation = C_0 [(C_1 + C_2*Δ + C_3*Δ^2) (1-C_4*P)] + (Lρ/144) where Δ = V-V_{ref}. Differential pressure transmitter corrected for zero shift, span, and reference leg.	1) Constant, C_1 2) Constant, C_2 3) Constant, C_3 4) Pressure effect on span C_4, 5) Constant, V_{ref} (volt) 6) Pressure effect on zero, C_1 of linear fit 7) Pressure effect on zero, C_2 of linear fit 8) Pressure at zero, psia 9) Reference leg height, L (ft). 10) Material type code: 1-stainless steel 2-carbon steel 3-Inconel 600	1) Pressure 2) Reference leg temperature 3) Fluid temperature
8	Reduction equation for the turbine meter (general). Reduction equation = C_1 + C_2*R + C_3*R^2 + C_4*R^3 + C_5*R^4	1-5) Curve fit constants C_1-C_4 for forward flow. 6-10) Flow direction constants C_6-C_{10} for reverse flow.	1) Pressure 2) Fluid temperature 3) Flow direction limit switch
9	Pressure transmitter corrected for reference leg. Reduction equation = (C_1 + C_2*Δ + C_3*Δ^2 + C_4*Δ^3) - Lρ/144 where Δ = V-V_{ref}.	1) Constant, C_1 2) Constant, C_2 3) Constant, C_3 4) Constant, C_4 5) Constant, V_{ref} 6) Reference leg length, L (ft)	1) Reference leg temperature
10	Reduction equation for adding composite venturis	none required	1) Composite venturi 1 2) Composite venturi 2

Table 5.3 (Continued)

ENGINEERING DATA REDUCTION TYPES, REFERENCE VTABS, AND CONVERSION CONSTANTS

Reduction Type	Description	Conversion Constants	Reference VTABs
11	Reduction equation for adding RVVV lines	none required	1) RVVV line 1 2) RVVV line 2
12	Reduction equation for adding tachometer counter-extender cards	none required	1) Counter card 2) Extender card
13	Saturation temperature based on pressure measurement	none required	1) Pressure
14	Feedwater temperature for OTIS test (not used for MIST)	none required	1) Temperature 1 2) Temperature 2 3) Temperature 3
15	Chordal average density from gamma densitometer	1) Constant A 2) Constant B (see Alliance Research Center document QA120 for a definition of these constants.)	none required
16	Turbine meter mass flow using densitometer density	Same constants as reduction type 8	1) Pressure 2) Fluid temperature 3) Densitometer density 4) Flow direction limit switch
17	Reduction equation for adding RVVV line pairs	none required	1) RVVV branch 1 2) RVVV branch 2
18	Cold leg liquid and total fluid mass	none required	1) Suction liquid and fluid mass 2) Discharge liquid and fluid mass
19	Hot leg liquid and total fluid mass	none required	1) Riser liquid and fluid mass 2) Stub liquid and fluid mass

Table 5.3 (Continued)

ENGINEERING DATA REDUCTION TYPES, REFERENCE VTABS, AND CONVERSION CONSTANTS

Reduction Type	Description	Conversion Constants	Reference VTABs
20	Gas discharged into the two-phase venting system	none required	1) Pressure 2) Temperature 3) V2DP04 4) V2DP05 5) V2DP06
21	Orifice flowmeter	1) Orifice diameter (in) 2) Pipe diameter (in) 3) Orifice material 1-stainless steel 2-carbon steel 3-Inconel 600 4) Pipe material (code type as above)	1) Pressure 2) Fluid temperature 3) Differential pressure
22	Venturi flowmeter	1) Throat diameter (in) 2) Pipe diameter (in) 3) Flow direction 0-up flow 1-down flow	1) Pressure 2) Fluid temperature 3) Differential pressure 4) Reference leg temperature
23	Composite orifice flow rate	none required	1) Low flow rate 2) Mid flow rate 3) High flow rate 4) High flow rate (high circuit) 5) Low circuit valve limit switch 6) Low range DP limit switch 7) Mid range DP limit switch 8) High circuit valve limit switch

Table 5.3 (Continued)

ENGINEERING DATA REDUCTION TYPES, REFERENCE VTABS, AND CONVERSION CONSTANTS

Reduction Type	Description	Conversion Constants	Reference VTABs
24	Composite venturi flow rate	none required	1) Low flow rate 2) Mid flow rate 3) High flow rate 4) Reverse flow rate 5) Low range DP 6) Mid range DP 7) High range DP 8) Reverse DP
25	Pitot tube mass flow rate	1) Flow area (ft^2)	1) Pressure 2) Fluid temperature 3) Differential pressure
26	Integration of Micro Motion mass flowmeters HPI, PORV, HPV, RVHV, single-phase leak	none required	1) Flow rate
27	RVVV mass flow rate	none required	1) Pressure 2) RVTC21 3) RVTC20 or (19) 4) RVTC18 or (17) 5) RVDP09 or (08) 6) RVDP07 or (06)
28	Void fraction from a conductivity probe	1-4) Liquid curve fit constants 5) Vapor voltage (volt)	1) Fluid temperature 2) Conductivity probe voltage
29	Primary loop mass closure based on boundary flows	none required	1) HPMM25 2) V1MM21 3) V2MM21 4) V2MM23 5) V2MM22 6) PSLK21 7) PLML20
30	Primary-to-secondary tube leak flow rate	none required	none required

Table 5.3 (Continued)

ENGINEERING DATA REDUCTION TYPES, REFERENCE VTABS, AND CONVERSION CONSTANTS

Reduction Type	Description	Conversion Constants	Reference VTABs
31	Secondary loop mass closure based on boundary flows	none required	1) SFOR30 2) SFOR31 3) SSOR30 4) SSOR31 5) PSLK21 6) SLML20
32	Leak enthalpy measurement	none required	1) LQTC01 2) LQTCO2 3) LQTC03 4) LQTC04 5) LQMM01 6) V1MM01 7) LQGP01 8) V1LS20
33	Composite limit switch for single-phase leak	none required	1-8) limit switch references
34	Power derived from current and voltage measurements	1) not used 2) not used 3) core resistance (ohms)	1) Current shunt voltage drop 2) Core voltage
35	Guard heater power	1) Heater full power (kW)	none required
36	Void fraction from a differential pressure measurement	none required	1) Pressure 2) Fluid temperature 3) Differential pressure
37	Gas addition flow rate	1) Gas addition system volume (ft^3)	1) Gas add pressure 2) Fluid temperature 3) Limit switch
38	Accumulated gas addition	1) Gas addition system volume (ft^3)	1) Gas add pressure 2) Fluid temperature 3) Limit switch

Table 5.3 (Continued)

ENGINEERING DATA REDUCTION TYPES, REFERENCE VTABS, AND CONVERSION CONSTANTS

Reduction Type	Description	Conversion Constants	Reference VTABs
39	Monitor core temperature for operational safety	none required	none required
40	Pump speed	none required	1) CnTA03 (n-1,2,3,4)
41	Composite weigh tank	none required	none required
42	Integration of secondary-side boundary mass flow rates	none required	1) Composite flow rate References 2 and 3 needed for main feedwater tests only 2) Flow rate (SFOR07 or 08) 3) Valve limit switch (S1LS03 or S2LS05)
43	Subcooled margin (temperature 1 - temperature 2)	none required	1) Temperature 1 (saturation) 2) Temperature 2
44	Conductivity probe not dry/dry indication	none required	1) Conductivity probe voltage 2) Upstream temperature 3) Downstream temperature 4) Pressure 5) Void fraction from a differential pressure
45	Composite of CnAM01 raw voltages (maximum of the four)	none required	none required
46	Flow rate based on weigh tanks	1) Time period for flow rate derivative (sec)	1) Composite load cell

Table 5.3 (Continued)

ENGINEERING DATA REDUCTION TYPES, REFERENCE VTABS, AND CONVERSION CONSTANTS

Reduction Type	Description	Conversion Constants	Reference VTABs
50	Cross-sectional averaged density and void fraction from the densitometer	1) Pipe size code 1-2.5 inch sch 80 2-2.0 inch sch 80 2) Void model type 0-homogeneous or stratified flow 1-stratified only	1) Pressure 2) Temperature 3) Densitometer (angled beam) 4) Densitometer (diametral beam)
51	Cooled thermocouple	1) Curve fit constant 2) Curve fit constant 3) Curve fit constant 4) Curve fit constant 5) Curve fit constant 6) Curve fit constant	1) Pressure 2) Upstream wall temperature 3) Coolant temperature 4) Fluid temperature
52	Primary-to-secondary tube leak flow rate using PLML20	none required	1) HPMM25 2) V1LC20 3) V2LC20 4) V2LC21 5) PLML20
53	Cold leg A1 suction level and mass with pumps on	none required	none required
54	Cold leg A1 discharge level and mass with pumps on	none required	none required
55	Cold leg A2 suction level and mass with pumps on	none required	none required
56	Cold leg A2 discharge level and mass with pumps on	none required	none required
57	Cold leg B1 suction level and mass with pumps on	none required	none required
58	Cold leg B1 discharge level and mass with pumps on	none required	none required

Table 5.3 (Continued)

ENGINEERING DATA REDUCTION TYPES, REFERENCE VTABS, AND CONVERSION CONSTANTS

Reduction Type	Description	Conversion Constants	Reference VTABs
60	Steam generator B level (secondary side) and mass	none required	none required
61	Steam generator A level (secondary side) and mass	none required	none required
62	Steam generator A downcomer level (secondary side) and mass	none required	none required
63	Steam generator B downcomer level (secondary side) and mass	none required	none required
64	Steam generator B level (primary side) and mass	none required	none required
65	Steam generator A level (primary side) and mass	none required	none required
66	Reactor vessel level and mass	none required	none required
67	Downcomer level and mass	none required	none required
68	Pressurizer level and mass	none required	none required
69	Core flood tank level and mass	none required	none required
70	Hot leg A riser level and mass	none required	none required
71	Hot leg A stub level and mass	none required	none required
72	Hot leg B riser level and mass	none required	none required

Table 5.3 (Continued)

ENGINEERING DATA REDUCTION TYPES, REFERENCE VTABS, AND CONVERSION CONSTANTS

Reduction Type	Description	Conversion Constants	Reference VTABs
73	Hot leg B stub level and mass	none required	none required
74	Cold leg A1 and A2 stub (steam generator discharge) level and mass	none required	none required
75	Cold leg A1 (suction) level and mass	none required	none required
76	Cold leg A1 (discharge) level and mass	none required	none required
77	Cold leg A2 (suction) level and mass	none required	none required
78	Cold leg A2 (discharge) level and mass	none required	none required
79	Cold leg B1 and B2 stub (steam generator discharge) level and mass	none required	none required
80	Cold leg B1 (suction) level and mass	none required	none required
81	Cold leg B1 (discharge) level and mass	none required	none required
82	Cold leg B2 (suction) level and mass	none required	none required
83	Cold leg B2 (discharge) level and mass	none required	none required
84	HPI supply tank level and mass	none required	none required
85	Davis-Besse vent line level and mass	none required	none required

Table 5.3 (Continued)

ENGINEERING DATA REDUCTION TYPES, REFERENCE VTABS, AND CONVERSION CONSTANTS

Reduction Type	Description	Conversion Constants	Reference VTABs
86	Davis-Besse orifice flow rate calculation	1) Orifice diameter (in) 2) Pipe diameter (in) 3) Orifice material type 1-stainless steel 2-carbon steel 3-Inconel 600 4) Pipe material type (type codes above)	1) Pressure 2) Fluid temperature 3) Differential pressure 4) Void fraction from differential pressure 5) HVLV20
87	Davis-Besse composite orifice	none required	1) Low flow rate 2) High flow rate
88	Cold leg B2 suction level and mass with pumps on	none required	none required
89	Cold leg B2 discharge level and mass with pumps on	none required	none required
90	Summation of primary loop mass based on levels	none required	none required
91	Summation of secondary loop mass based on levels	none required	1) S1MS20 2) S2MS20 3) S1MS21 4) S2MS21
92	Primary loop mass closure based on boundary flows using load cells	none required	1) HPMM25 2) V1LC20 3) V2LC20 4) V2LC21 5) PSLK21 6) PLML20
99	RVVV composite limit switch	none required	1-8) Limit switches

Table 5.4

ENGINEERING DATA ERROR CODES

Error Code	Bit Number	Reduction Type	Error Value	Error Code Descriptor
1	0	All	1.95E-10	VTAB marked to NOREAD.
2	1	2,7-9,12,13,16 20-22,24-28, 30-32,34,36-42, 44,50,51,86	1.90E-10	Error in reference VTAB.
		53-58,60-85, 88,89	WARNING*	Level below the bottom of the component.
		54,56,58,69, 85,89	1.10E-10	Insufficient instruments to perform the calculation.
4	2	5	31.9	Temperature below curve fit range for Type J thermocouples.
		6	29.9	Temperature below curve fit range for Type K thermocouples.
		53-58,60-85, 88,89	WARNING*	Level above the top of the component.
8	3	5	900.1	Temperature above curve fit range for Type J thermocouples.
		6	1897.0	Temperature above curve fit range for Type K thermocouples.
		32	1.10E-10	Leak temperature derived from leak enthalpy measurement does not agree with measured to within ±10°F.
		30,53,55,57 60-68,70-84,88	1.10E-10	Insufficient instruments to perform calculation.
16	4	7	1.85E-10	Open limit switch on a differential pressure transmitter signifying the transmitter is in the zero mode.
		53,55,57,60-68 70-83,88	WARNING*	Level calculation does not converge.

Table 5.4 (Continued)

ENGINEERING DATA ERROR CODES

Error Code	Bit Number	Reduction Type	Error Value	Error Code Descriptor
32	5	7-9,13,14,16, 20-22,25-32,34 36-38,40-42,44, 46,50,52,86,91, 92	1.80E-10	Error in reference VTAB.
64	6	ENGR, 7-14, 16-34,36-38, 40-42,44,46, 50-52,86,87,91, 92	1.75E-10	Invalid reduction type.
128	7	26,40,42	1.70E-10	Error in VTAB name.
256	8	21,22,27,86	1.25E-10	Flowmeter Reynolds number outside the calibration curve fit range.
512	9	7	1.60E-10	Differential pressure transmitter over-ranged low.
		27	WARNING*	Reactor vessel vent valve flow Reynolds number outside the calibration curve fit range.
1024	10	7	1.55E-10	Differential pressure transmitter over-ranged high.
2048	11	21,22,27,30,86	1.45E-10	No convergence in mass flow rate.
4096	12	23,24,87	1.40E-10	Invalid composite mass flow rate.
8192	13	26,40-42	1.35E-10	Invalid VTAB location number.
16384	14	Not Used	1.30E-10	---
32768	15	All	1.50E-10	Arithmetic error.
---**	--	27	1.30E-10	Two-phase conditions indicated in the reactor vessel vent valve circuit. Flow rate calculation aborted.

Table 5.4 (Continued)

ENGINEERING DATA ERROR CODES

Error Code	Bit Number	Reduction Type	Error Value	Error Code Descriptor
---**	--	27	1.15E-10	Reactor vessel vent valve not full open or full closed. Flow rate calculation aborted.
---**	--	32	1.05E-10	Leak enthalpy calculation aborted. Either the leak flow rate is too low (less than 30 lbm/hr) or the leak is not activated.

---

* WARNING: The warning message is written to the B&W raw-to-engineering data conversion log file. An error value is not written to the engineering data file. Instead, the computed value is written to the data file.

** An error value is written to the engineering data file but the error code is not toggled since these errors are not indicative of raw-to-engineering data conversion errors.

Section 6

CHARACTERIZATION TEST RESULTS

MIST characterization testing verified the facility design, instrument performance, control system functionality and tuning, and hardware operation. These tests also provided MIST operators with the experience necessary for performance of subsequent transient tests. The following characterization results are discussed in this report:

- Primary and Secondary System Volume
- Primary Loop Irrecoverable Pressure Drop
- Reactor Vessel Vent Valve Performance
- Reactor Coolant Pump Performance
- Guard Heater Performance
- Loop Heat Loss Without Guard Heaters
- Leak Enthalpy System Performance

A detailed account of MIST Characterization testing is reported in Reference 7.

6.1 PRIMARY AND SECONDARY SYSTEM VOLUME

MIST facility component volumes versus elevation are an important input to computer models used to predict small break loss-of-coolant accident (SBLOCA) transient response. Volume versus elevation functions were developed by calculation and verified by controlled drains of loop inventory into weigh tanks. Component levels were based on differential pressure measurements. All drains were executed with loop inventory at ambient conditions.

In several instances, combined component volumes versus elevations were obtained since individual components could not be isolated. For example, the

A- and B-loop hot leg risers and stubs drain equally as level is reduced from the U-bend to the steam generator primary inlets. The steam generator primaries and hot leg risers drain together until the primary level reaches the top of the reactor vessel when the reactor vessel begins to drain also. Similar interactions occur throughout the primary system drain (see Figure 6.1). Individual drains were executed for the pressurizer, the core flood tank, and each steam generator secondary.

Calculated volumes from the data analysis program were benchmarked against the data obtained in these characterization tests. Good agreement was noted and individual component volume versus elevation functions based on the benchmarked calculations are reported in Table 6.1 for use by code analysts. All volumes are expressed in cubic feet and all levels are in feet relative to the secondary face of the steam generator lower tube sheet. Note that volume functions for portions of the cold legs are listed separately for tests with and without pump operation. As described earlier in Section 2.5.3 (Cold Leg Instrumentation), the differential pressure tap locations were moved for pumps running tests.

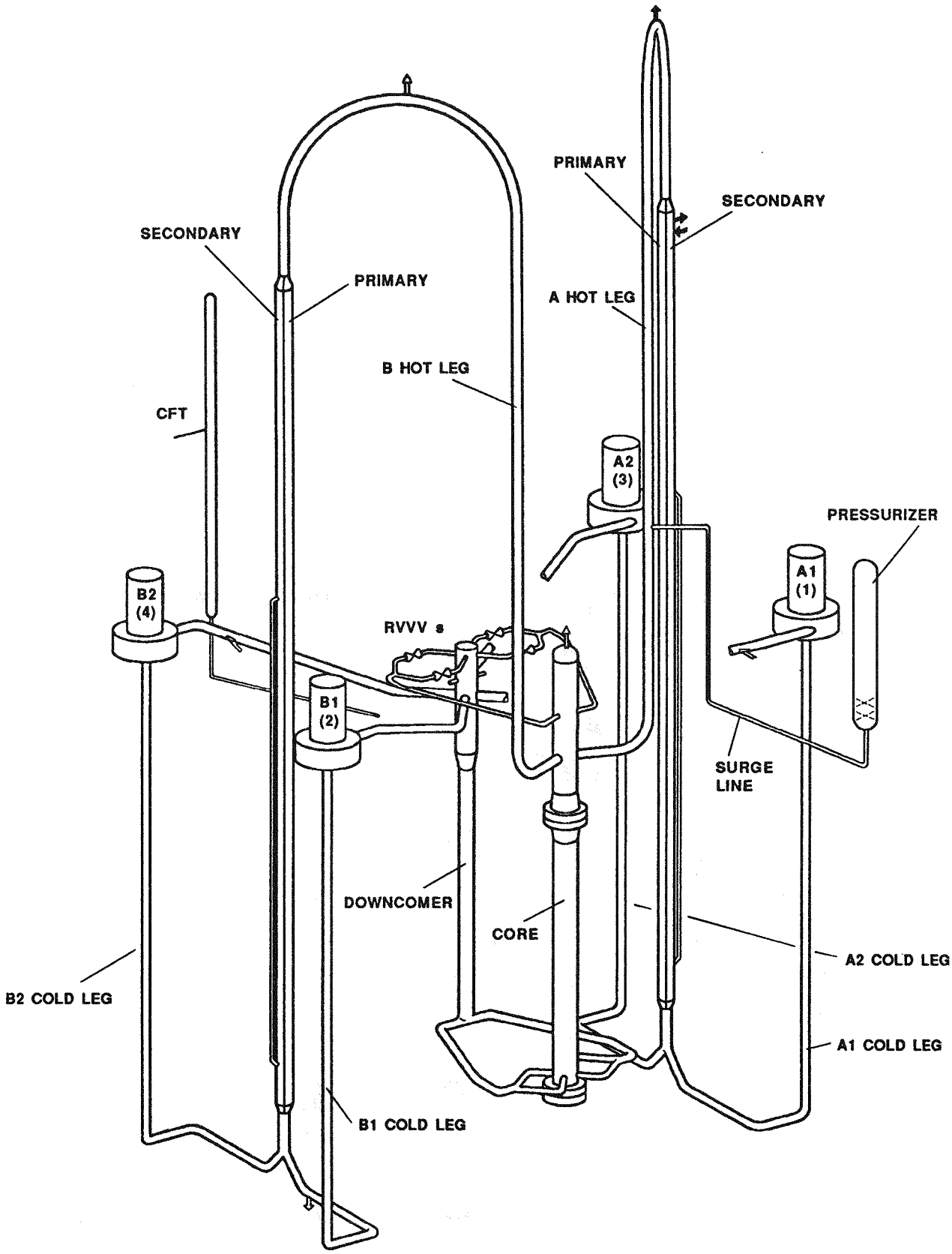

Figure 6.1 MIST Primary Loop Configuration

Table 6.1

COMPONENT VOLUME VERSUS LEVEL FUNCTIONS

MIST Component	Level Range	Volume Versus Level Function
SG-A Secondary	(0.00′ to 52.14′)	VOL = 0.05264 x (S1LV - 0.00) [ft^3]
• Subtract 0.00378 ft^3 for each submerged tube support plate.		
SG-B Secondary	(0.00′ to 51.95′)	VOL = 0.05264 x (S2LV - 0.00) [ft^3]
• Subtract 0.00378 ft^3 for each submerged tube support plate.		
• Add 0.00842 ft^3 to account for volume above upper DP tap.		
SG-A Downcomer VOL[ft^3]	(0.447′ to 0.553′)	VOL = 0.0471
	(0.553′ to 0.656′)	VOL = 0.0471 + 0.01068 x (S1LV - 0.553)
	(0.656′ to 0.948′)	VOL = 0.0482 + 0.01678 x (S1LV - 0.656)
	(0.948′ to 31.50′)	VOL = 0.0531 + 0.02463 x (S1LV - 0.948)
	(31.50′ to 31.75′)	VOL = 0.8047 + 0.02260 x (S1LV - 31.50)
	(31.75′ to 32.00′)	VOL = 0.8113 + 0.02047 x (S1LV - 31.75)
	(32.00′ to 32.16′)	VOL = 0.8880
SG-B Downcomer VOL[ft^3]	(0.447′ to 0.553′)	VOL = 0.0471
	(0.553′ to 0.656′)	VOL = 0.0471 + 0.01068 x (S2LV - 0.553)
	(0.656′ to 0.948′)	VOL = 0.0482 + 0.01678 x (S2LV - 0.656)
	(0.948′ to 31.50′)	VOL = 0.0531 + 0.02463 x (S2LV - 0.948)
	(31.50′ to 31.75′)	VOL = 0.8047 + 0.02260 x (S2LV - 31.50)
	(31.75′ to 32.00′)	VOL = 0.8113 + 0.02047 x (S2LV - 31.75)
	(32.00′ to 32.16′)	VOL = 0.8880
SG-A Primary VOL[ft^3]	(-3.15′ to -2.46′)	VOL = 0.0295 x (P1LV + 3.15)
	(-2.46′ to -2.25′)	VOL = 0.0204 + π/3(P1LV+2.46)(R^2+0.0968R+0.0094), where R[ft] = 0.1797 + 0.3976 x (P1LV + 2.46)
	(-2.25′ to -2.00′)	VOL = 0.0333 + 0.1014 x (P1LV + 2.25)
	(-2.00′ to 52.34′)	VOL = 0.0586 + 0.03163 x (P1LV + 2.00)
	(52.34′ to 52.59′)	VOL = 1.7778 + 0.1014 x (P1LV - 52.34)
	(52.59′ to 52.80′)	VOL = 1.8032 + π/3(P1LV-52.59)(R^2+0.0968R+0.0094), where R[ft] = 0.1797 - 0.3976 x (P1LV - 52.59)
	(52.80′ to 53.10′)	VOL = 1.8093 + 0.0295 x (P1LV - 52.80)
SG-B Primary VOL[ft^3]	(-3.11′ to -2.46′)	VOL = 0.0295 x (P2LV + 3.11)
	(-2.46′ to -2.25′)	VOL = 0.0192 + π/3(P2LV+2.46)(R^2+0.0968R+0.0094), where R[ft] = 0.1797 + 0.3976 x (P2LV + 2.46)
	(-2.25′ to -2.00′)	VOL = 0.0321 + 0.1014 x (P2LV + 2.25)
	(-2.00′ to 52.37′)	VOL = 0.0574 + 0.03163 x (P2LV + 2.00)
	(52.37′ to 52.62′)	VOL = 1.7769 + 0.1014 x (P2LV - 52.37)
	(52.62′ to 52.82′)	VOL = 1.8023 + π/3(P2LV-52.62)(R^2+0.0968R+0.0094), where R[ft] = 0.1797 - 0.3976 x (P2LV - 52.62)
	(52.82′ to 53.09′)	VOL = 1.8084 + 0.0295 x (P2LV - 52.82)

Table 6.1 (Continued)

COMPONENT VOLUME VERSUS LEVEL FUNCTIONS

MIST Component	Level Range	Volume Versus Level Function
Pressurizer		Volume below lower DP tap = 0.0287 ft^3
VOL[ft^3]	(15.82′ to 17.95′)	VOL = 0.0299 + 0.0204 x (PZLV - 15.82)
	(17.95′ to 20.18′)	VOL = 0.0343 + 0.1648 x (PZLV - 17.95)
	(20.18′ to 28.98′)	VOL = 0.4018 + 0.1651 x (PZLV - 20.18)
Core Flood	(24.35′ to 49.18′)	VOL = 0.1389 x (CFLV - 24.35)
VOL[ft^3]		
Reactor Vessel		Volume below lower DP tap = 0.0183 ft^3
VOL[ft^3]	(-1.03′ to 16.73′)	VOL = 0.0183 + 0.0626 x (RVLV + 1.03)
	(16.73′ to 16.93′)	VOL = 1.1301 + 0.1650 x (RVLV - 16.73)
	(16.93′ to 17.10′)	VOL = 1.1631 + 0.0531 x (RVLV - 16.93)
	(17.10′ to 17.17′)	VOL = 1.1721 + 0.1650 x (RVLV - 17.10)
	(17.17′ to 17.42′)	VOL = 1.1837 + π/3(RVLV-17.17)(R^2+0.2233R+0.0499), where R[ft] = 0.2233 - 0.302 x (RVLV - 17.17)
	(17.42′ to 17.50′)	VOL = 1.2111 + 0.0689 x (RVLV - 17.42)
	(17.50′ to 22.73′)	VOL = 1.2166 + 0.1464 x (RVLV - 17.50)
	(22.73′ to 25.29′)	VOL = 1.9823 + 0.1481 x (RVLV - 22.73) Add 0.1091 ft^3 to account for RVVV lines
	(25.29′ to 29.00′)	VOL = 2.4705 + 0.1650 x (RVLV - 25.29) Volume above upper DP tap = 0.0493 ft^3
RV Downcomer		Volume below lower DP tap = 0.3047 ft^3
VOL[ft^3]	(1.54′ to 4.04′)	VOL = 0.3047 + 0.04587 x (DCLV - 1.54)
	(4.04′ to 5.40′)	VOL = 0.4196 + π/3(DCLV-4.04)(R^2+0.1208R+0.0146), where R[ft] = 0.1208 - 0.0538 x (DCLV - 4.04)
	(5.40′ to 6.83′)	VOL = 0.4518 + π/3(DCLV-5.40)(R^2+0.0458R+0.0021), where R[ft] = 0.0458 + 0.0538 x (DCLV - 5.40)
	(6.83′ to 16.73′)	VOL = 0.4859 + 0.04587 x (DCLV - 6.83)
	(16.73′ to 17.34′)	VOL = 0.9400 + (DCLV - 16.73) x (-0.01233 + π/3((R^2+0.12083R+0.0146)-(r^2+0.01042r+0.00011))), where R[ft] = 0.1208 + 0.2673 x (DCLV - 16.73), and r[ft] = 0.0104 + 0.2775 x (DCLV - 16.73)
	(17.34′ to 24.34′)	VOL = 0.9983 + 0.1555 x (DCLV - 17.34) Add 0.01665 ft^3 to account for RVVV lines
CL-A Stub	(-7.51′ to -7.34′)	VOL = 0.4047 x (C1LV + 7.51)
VOL[ft^3]	(-7.34′ to -6.31′)	VOL = 0.0688 + 0.0548 x (C1LV + 7.34)
	(-6.31′ to -6.19′)	VOL = 0.1252 + 0.0487 x (C1LV + 6.31)
	(-6.19′ to -3.15′)	VOL = 0.1311 + 0.0376 x (C1LV + 6.19)
CL-B Stub	(-7.52′ to -7.35′)	VOL = 0.4047 x (C1LV + 7.51)
VOL[ft^3]	(-7.35′ to -6.34′)	VOL = 0.0688 + 0.0548 x (C1LV + 7.35)
	(-6.34′ to -6.22′)	VOL = 0.1241 + 0.0487 x (C1LV + 6.34)
	(-6.22′ to -3.11′)	VOL = 0.1299 + 0.0376 x (C1LV + 6.22)

Table 6.1 (Continued)

COMPONENT VOLUME VERSUS LEVEL FUNCTIONS

MIST Component	Level Range	Volume Versus Level Function
CL-A1 Suction VOL[ft^3]	(-7.51′ to -0.51′)	VOL = 0.0205 x (C1LV + 7.51)
	(-0.51′ to 0.55′)	VOL = 0.1436 + π/3(C1LV+0.51) (R^2+0.0808R+0.00653), where R[ft] = 0.0808 - 0.0608 x (C1LV + 0.51)
Pumps off	(0.55′ to 0.60′)	VOL = 0.1526 + 0.00085 x (C1LV - 0.55)
	(0.60′ to 1.66′)	VOL = 0.1527 + π/3(C1LV-0.60) (R^2+0.0164R+0.00027), where R[ft] = 0.0164 + 0.0608 x (C1LV - 0.60)
	(1.66′ to 25.75′)	VOL = 0.1617 + 0.0205 x (C1LV - 1.66)
Pumps on	(-7.51′ to 23.46′)	VOL = 0.0205 x (C1LV + 7.51) Pipe volume above upper DP tap = 0.0469 ft^3
CL-A2 Suction VOL[ft^3]	(-7.51′ to -0.49′)	VOL = 0.0205 x (C3LV + 7.51)
	(-0.49′ to 0.57′)	VOL = 0.1439 + π/3(C3LV+0.49) (R^2+0.0808R+0.00653), where R[ft] = 0.0808 - 0.0608 x (C3LV + 0.49)
Pumps off	(0.57′ to 0.62′)	VOL = 0.1529 + 0.00085 x (C3LV - 0.57)
	(0.62′ to 1.68′)	VOL = 0.1530 + π/3(C3LV-0.62) (R^2+0.0164R+0.00027), where R[ft] = 0.0164 + 0.0608 x (C3LV - 0.62)
	(1.68′ to 25.75′)	VOL = 0.1620 + 0.0205 x (C3LV - 1.68)
Pumps on	(-7.51′ to 23.47′)	VOL = 0.0205 x (C3LV + 7.51) Pipe volume above upper DP tap = 0.0467 ft^3
CL-B1 Suction VOL[ft^3]	(-7.52′ to -0.48′)	VOL = 0.0205 x (C2LV + 7.52)
	(-0.48′ to 0.58′)	VOL = 0.1443 + π/3(C2LV+0.48) (R^2+0.0808R+0.00653), where R[ft] = 0.0808 - 0.0608 x (C2LV + 0.48)
Pumps off	(0.58′ to 0.63′)	VOL = 0.1533 + 0.00085 x (C2LV - 0.58)
	(0.63′ to 1.69′)	VOL = 0.1534 + π/3(C2LV-0.63) (R^2+0.0164R+0.00027), where R[ft] = 0.0164 + 0.0608 x (C2LV - 0.63)
	(1.69′ to 25.75′)	VOL = 0.1624 + 0.0205 x (C2LV - 1.69)
Pumps on	(-7.52′ to 23.48′)	VOL = 0.0205 x (C1LV + 7.52) Pipe volume above upper DP tap = 0.0465 ft^3
CL-B2 Suction VOL[ft^3]	(-7.52′ to -0.47′)	VOL = 0.0205 x (C4LV + 7.52)
	(-0.47′ to 0.59′)	VOL = 0.1445 + π/3(C4LV+0.51) (R^2+0.0808R+0.00653), where R[ft] = 0.0808 - 0.0608 x (C4LV + 0.47)
Pumps off	(0.59′ to 0.64′)	VOL = 0.1535 + 0.00085 x (C4LV - 0.59)
	(0.64′ to 1.70′)	VOL = 0.1536 + π/3(C4LV-0.64) (R^2+0.0164R+0.00027), where R[ft] = 0.0164 + 0.0608 x (C4LV - 0.64)
	(1.70′ to 25.75′)	VOL = 0.1626 + 0.0205 x (C4LV - 1.70)
Pumps on	(-7.52′ to 23.48′)	VOL = 0.0205 x (C4LV + 7.52) Pipe volume above upper DP tap = 0.0465 ft^3

Table 6.1 (Continued)

COMPONENT VOLUME VERSUS LEVEL FUNCTIONS

MIST Component	Level Range	Volume Versus Level Function
CL-A1 Disch. VOL[ft^3]	(21.11′ to 21.27′)	VOL = 0.8258 x $[R^2 \text{acos}\left[\frac{R-H}{R}\right] - (R-H)\sqrt{2(R)H-H^2}]$, where R = 0.0808 and H = (C1LV - 21.11)
Pumps off	(21.27′ to 25.03′)	VOL = 0.0169 + 0.02422 x (C1LV - 21.27)
	(25.03′ to 25.75′)	VOL = 0.1242 + 0.0242 x (C1LV - 25.70)
		Add 0.12 and 0.0242 ft^3 for pump volute and discharge pipe, respectively, above 25.75′
CL-A2 Disch. VOL[ft^3]	(21.11′ to 21.27′)	VOL = 0.8258 x $[R^2 \text{acos}\left[\frac{R-H}{R}\right] - (R-H)\sqrt{2(R)H-H^2}]$ where R = 0.0808 and H = (C3LV - 21.11)
Pumps off	(21.27′ to 25.72′)	VOL = 0.0169 + 0.02422 x (C3LV - 21.27)
	(25.72′ to 25.75′)	VOL = 0.1248 + 0.0242 x (C3LV - 25.72)
		Add 0.12 and 0.0242 ft^3 for pump volute and discharge pipe, respectively, above 25.75′
CL-B1 Disch. VOL[ft^3]	(21.13′ to 21.29′)	VOL = 0.8258 x $[R^2 \text{acos}\left[\frac{R-H}{R}\right] - (R-H)\sqrt{2(R)H-H^2}]$, where R = 0.0808 and H = (C2LV - 21.13)
Pumps off	(21.29′ to 25.70′)	VOL = 0.0169 + 0.02422 x (C2LV - 21.29)
	(25.70′ to 25.75′)	VOL = 0.1237 + 0.0242 x (C2LV - 25.70)
		Add 0.12 and 0.0242 ft^3 for pump volute and discharge pipe, respectively, above 25.75′
CL-B2 Disch. VOL[ft^3]	(21.14′ to 21.30′)	VOL = 0.8258 x $[R^2 \text{acos}\left[\frac{R-H}{R}\right] - (R-H)\sqrt{2(R)H-H^2}]$, where R = 0.0808 and H = (C4LV - 21.14)
Pumps off	(21.30′ to 25.70′)	VOL = 0.0169 + 0.02422 x (C3LV - 21.30)
	(25.70′ to 25.75′)	VOL = 0.1235 + 0.0242 x (C3LV - 25.70)
		Add 0.12 and 0.0242 ft^3 for pump volute and discharge pipe, respectively, above 25.75′
HL-A Riser VOL[ft^3]		Volume below lower DP tap = 0.0050 ft^3
	(20.94′ to 21.04′)	VOL = 0.0050 + 0.180 x (H1LV - 20.94)
	(21.04′ to 22.65′)	VOL = 0.0230 + 0.01579α_1 + 0.03158α_2, where $\alpha_1 = \text{acos}\left[\frac{(22.65-H1LV)}{1.5126}\right]$ [radians], and $\alpha_2 = \text{acos}\left[\frac{(22.65-H1LV)}{1.7062}\right]$ [radians]
	(22.65′ to 64.94′)	VOL = 0.0974 + 0.02943 x (H1LV - 22.65)
	(64.94′ to 66.45′)	VOL = 1.3420 + 0.01579α_1 + 0.03158α_2, where $\alpha_1 = \text{asin}\left[\frac{(H1LV-64.94)}{1.5126}\right]$ [radians], and $\alpha_2 = \text{asin}\left[\frac{(H1LV-64.94)}{1.7062}\right]$ [radians]
	(66.45′ to 66.65′)	VOL = 1.4010 + 0.1993 x (H2LV - 66.45)
		Volume above upper DP tap = 0.0056 ft^3

Table 6.1 (Continued)

COMPONENT VOLUME VERSUS LEVEL FUNCTIONS

MIST Component	Level Range	Volume Versus Level Function
HL-B Riser		Volume below lower DP tap = 0.0050 ft^3
VOL[ft^3]	(20.92′ to 21.02′)	VOL = 0.0050 + 0.180 x (H2LV - 20.92)
	(21.02′ to 22.53′)	VOL = 0.0230 + 0.01579α_1 + 0.03158α_2, where $\alpha_1 = \text{acos}\left[\frac{(22.53-H2LV)}{1.5126}\right]$ [radians], and $\alpha_2 = \text{acos}\left[\frac{(22.53-H2LV)}{1.7062}\right]$ [radians]
	(22.53′ to 64.94′)	VOL = 0.0974 + 0.02943 x (H2LV - 22.53)
	(64.94′ to 66.45′)	VOL = 1.3455 + 0.01579α_1 + 0.03158α_2, where $\alpha_1 = \text{asin}\left[\frac{(H2LV-64.94)}{1.5126}\right]$ [radians], and $\alpha_2 = \text{asin}\left[\frac{(H2LV-64.94)}{1.7062}\right]$ [radians]
	(66.45′ to 66.65′)	VOL = 1.4037 + 0.1993 x (H2LV - 66.45)
		Volume above upper DP tap = 0.0056 ft^3
HL-A Stub	(53.10′ to 64.94′)	VOL = 0.02943 x (H1LV - 53.10)
VOL[ft^3]	(64.94′ to 66.45′)	VOL = 0.3485 + 0.01579α_1 + 0.03158α_2, where $\alpha_1 = \text{asin}\left[\frac{(H1LV-64.94)}{1.5126}\right]$ [radians], and $\alpha_2 = \text{asin}\left[\frac{(H1LV-64.94)}{1.7062}\right]$ [radians]
	(66.45′ to 66.65′)	VOL = 0.4077 + 0.1993 x (H1LV - 66.45)
		Volume above upper DP tap = 0.0056 ft^3
HL-B Stub	(53.09′ to 64.94′)	VOL = 0.02943 x (H1LV - 53.09)
VOL[ft^3]	(64.94′ to 66.45′)	VOL = 0.3487 + 0.01579α_1 + 0.03158α_2, where $\alpha_1 = \text{asin}\left[\frac{(H1LV-64.94)}{1.5126}\right]$ [radians], and $\alpha_2 = \text{asin}\left[\frac{(H1LV-64.94)}{1.7062}\right]$ [radians]
	(66.45′ to 66.65′)	VOL = 0.4079 + 0.1993 x (H1LV - 66.45)
		Volume above upper DP tap = 0.0056 ft^3

Volume functions for the Elliot (HPI/LPI supply) tank are expressed as a function of differential pressure, as shown in Table 6.2.

Table 6.2

ELLIOT TANK VOLUME VERSUS DIFFERENTIAL PRESSURE FUNCTIONS

MIST Component	Volume [ft^3] Versus Differential Pressure [psid]	
Elliot tank VOL[ft^3]	$VOL = C_1 + C_2(HPDP) + C_3(HPDP)^2 + C_4(HPDP)^3 + C_5(HPDP)^4$	
	For (0.0677 < HPDP[psi] < 0.4309)	$C_1 = 166.75215$ $C_2 = -15.50653$ $C_3 = -69.48482$ $C_4 = 0.00000$ $C_5 = 0.00000$
	For (0.4309 < HPDP[psi] < 2.8778)	$C_1 = 190.60618$ $C_2 = -128.51244$ $C_3 = 82.85680$ $C_4 = -46.88855$ $C_5 = 8.86564$

NOTE: HPDP = Overall differential pressure across Elliot tank

Facility geometric symmetry and dimensional accuracy were verified for the MIST loops and components as part of the volume versus level characterization. This verification was achieved by comparing calculated levels for overlapping components during the loop drain. Hot leg riser and stub levels were compared from 53.1 to 66.7 feet. Riser and steam generator primary levels were compared between 20.9 and 53.1 feet. The reactor vessel was included in this comparison beginning at 29.0 feet; the cold leg suctions and discharges from 25.7 feet; and the downcomer from 24.3 feet. Below 20.9 feet, cold leg suction levels were compared to steam generator primary or cold leg stub levels.

Level comparisons were evaluated in terms of total expected measurement uncertainty. This includes uncertainty components due to differential pressure measurement uncertainty, the measurement of tap-to-tap displacement, and the mechanical tolerance associated with component installation. Total uncertainties for calculated levels are summarized in Table 6.3.

Table 6.3

COMPONENT LEVEL MEASUREMENT UNCERTAINTIES

VTAB	Component	Tap-to-Tap Displacement	Level Uncertainty
CFLV20	Core Flood Tank	297.94"	4.38"
C1LV21	Cold Leg A Stub	52.31"	0.46"
C2LV21	Cold Leg B Stub	52.94"	0.46"
C1LV22	Cold Leg A1 Suction	399.13"	0.47"
C2LV22	Cold Leg B1 Suction	399.25"	0.47"
C3LV22	Cold Leg A2 Suction	399.13"	0.47"
C4LV22	Cold Leg B2 Suction	399.25"	0.47"
C1LV23	Cold Leg A1 Discharge	55.69"	0.46"
C2LV23	Cold Leg B1 Discharge	55.44"	0.46"
C3LV23	Cold Leg A2 Discharge	55.69"	0.46"
C4LV23	Cold Leg B2 Discharge	55.31"	0.46"
DCLV20	Reactor Vessel Downcomer	273.63"	1.15"
H1LV21	Hot Leg A Riser	548.50"	2.03"
H2LV21	Hot Leg B Riser	548.75"	2.03"
H1LV22	Hot Leg A Stub	162.63"	1.06"
H2LV22	Hot Leg B Stub	162.75"	1.06"
PZLV20	Pressurizer	157.94"	1.06"
P1LV20	SG-A Primary	675.00"	2.09"
P2LV20	SG-B Primary	674.38"	2.10"
S1LV20	SG-A Secondary	625.69"	1.97"
S2LV20	SG-B Secondary	623.38"	1.97"
S1LV21	SG-A Downcomer	380.56"	2.21"
S2LV21	SG-B Downcomer	380.56"	2.21"

System drain rates were minimized to avoid disruption of component-to-component manometric balances and agreement was noted for most comparable level calculations. An isolated exception occurs due to differences in model reactor coolant pump seal characteristics. Asymmetric drains resulted for the cold leg suctions because positive seals were lost for the A2 and B2 pumps. This allowed the A2 and B2 pump rotor cavities to drain into the cold legs. Positive seals were maintained for the A1 and B1 pumps, thus retaining fluid in the pump rotor cavities and distorting the manometric balance between the four cold legs. With this exception noted, the checks examined loop-to-loop symmetry and dimensionally verified the facility fabrication according to design specifications, to within the accuracy of the instruments employed.

6.2 PRIMARY LOOP IRRECOVERABLE PRESSURE LOSSES

An ideal integral system plant model preserves irrecoverable pressure losses at power-scaled flow rates. However, scaling to preserve plant-typical SBLOCA phenomena requires compromise of ideal loop and component hydraulic resistances. Actual MIST hydraulic resistances were determined with the reactor coolant pumps running and with loop fluid at 2000 psia, 550°F. At the noted conditions, approximately 22% speed was required to achieve fully turbulent flow. Consequently, the hydraulic resistances determined are believed to be valid up to 100% flow. Two test points were executed: one with pump speeds matched (Trial 1) and one with cold leg flow rates matched (Trial 2) by adjusting the individual pump speeds as necessary. Similar test data was obtained during reactor coolant pump characterization, with the cold leg venturis removed (Trial 3) and turbine meters installed in each cold leg.

Reactor coolant pump hydraulic performance was not investigated as part of the MIST loop irrecoverable pressure loss characterization. Single-phase pump head-flow characteristics were determined in subsequent testing and locked-rotor resistances were determined by the pump vendor (Chempump).

Hydraulic resistances were determined for each MIST reactor coolant system component and flow path. Each resistance (K/A^2) [ft^{-4}] is computed as:

$$\frac{K}{A^2} = 2 \times g_c \left[\frac{ft\text{-}lbm}{lbf\text{-}sec^2}\right] \times 144 \left[\frac{in^2}{ft^2}\right] \times \left[3600 \frac{sec}{hr}\right]^2 \times \frac{\rho \Delta P}{m^2} \qquad (6\text{-}1)$$

where ρ is the fluid density [lbm/ft^3], ΔP is the irrecoverable pressure loss [psid], and m is the fluid mass flow rate [lbm/hr].

The hydraulic resistances determined by testing are reported in Table 6.4, along with associated uncertainties and corresponding plant resistances. The flow path corresponding to each resistance is specified by reference to points noted on Figure 6.2.

Table 6.4

SUMMARY OF COMPONENT HYDRAULIC RESISTANCES

MIST Component	Flow Path	Reference ΔP	VTABs Flow	K/A^2 (w/uncert) Trial 1,2,3	Plant K/A^2 (Scaled to MIST)
RV Downcomer	1 to 2	C2DP09	DCVN20	4851 ±237	
		DCDP02		4816 ±241	4700
		DCDP08		5128 ±293	
Reactor Core	2 to 3	RVDP01	DCVN20	4099 ±283	
		RVDP05		4118 ±296	3100
		RVDP04		3776 ±322	
		RVDP03			
Reactor Vessel	2 to 4B	RVDP01	DCVN20	5020 ±313	
		RVDP05		5031 ±325	6300
		RVDP04		5102 ±358	
		RVDP03			
		H2DP02			
		H2DP16			
Hot Leg A	4A to 5A	H1DP01	C1VN20	10357 ±1417	
		H1DP14	C3VN20	10382 ±1467	7000
			C1,3TM01	8458 ±1582	
Hot Leg B	4B to 5B	H2DP01	C2VN20	9784 ±1512	
		H2DP14	C4VN20	9898 ±1570	7000
			C2,4TM01	8418 ±1631	
OTSG A	5A to 6A	P1DP04	C1VN20	19995 ±2006	
			C3VN20	19971 ±2043	25000
			C1,3TM01	18760 ±2226	
OTSG B	5B to 6B	P2DP06	C2VN20	16506 ±1672	
			C4VN20	16481 ±1735	25000
			C2,4TM01	17022 ±1998	
Cold Leg A1	6A to 7A1	C1DP01	C1VN20	268802 ±11883	
		C1DP02		271154 ±12153	
			C1TM01	26259 ±4872	
Cold Leg A2	6A to 7A2	C3DP01	C3VN20	281873 ±11739	
		C3DP02		281369 ±11757	SEE
			C3TM01	26981 ±4079	DISCUSSION
Cold Leg B1	6B to 7B1	C2DP01	C2VN20	262899 ±10962	WHICH
		C2DP02		265289 ±11204	FOLLOWS
			C2TM01	26252 ±4083	
Cold Leg B2	6B to 7B2	C4DP01	C4VN20	257687 ±10849	
		C4DP02		256882 ±10855	
			C4TM01	26150 ±4607	

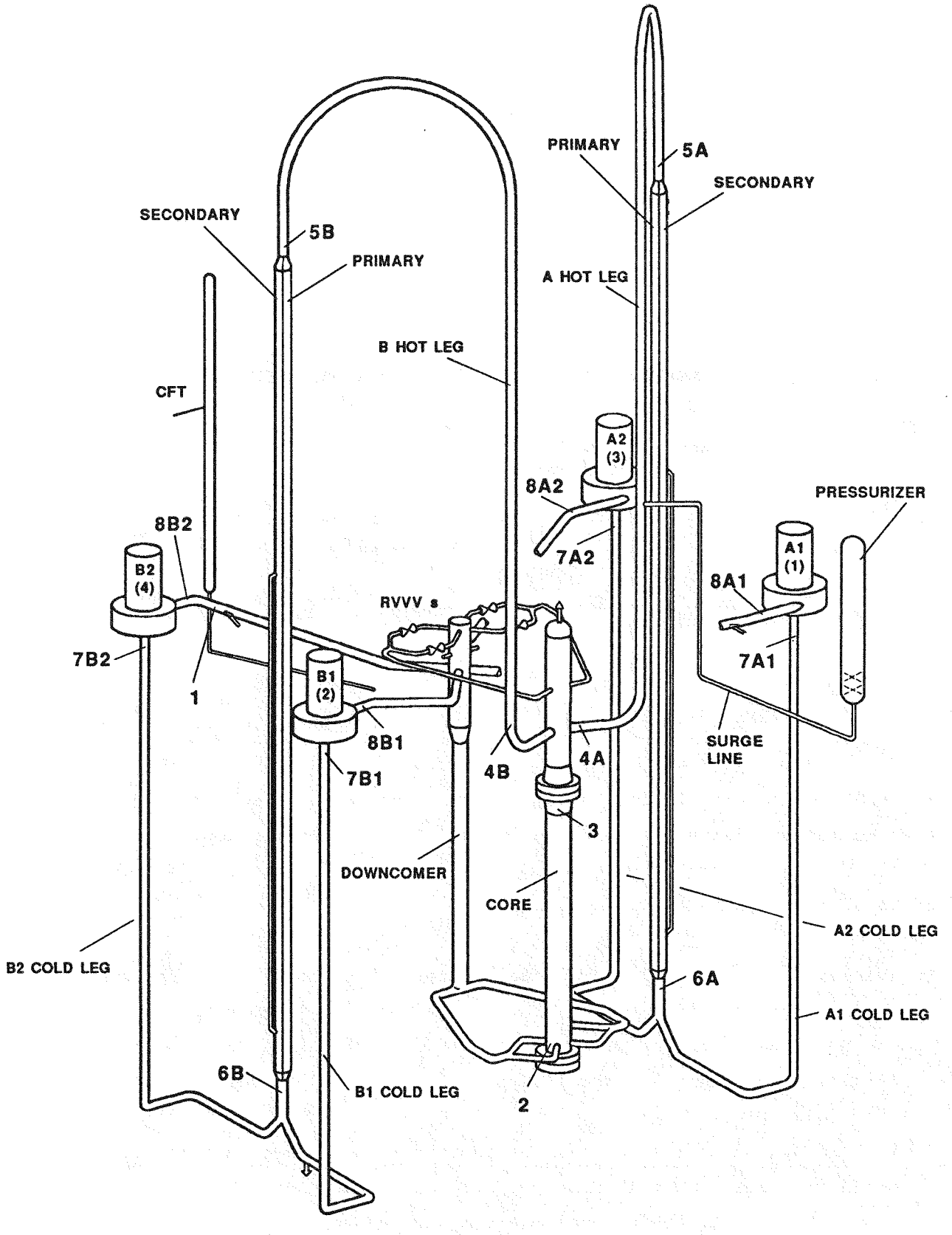

Figure 6.2 Component Identification for Reported Hydraulic Resistances

MIST reactor coolant pump locked-rotor resistances are reported in Table 6.5 as a function of scaled cold leg flow. Values at 19% and 110.6% flow are obtained from a curve fit of the remaining six points. At 100% scaled flow, MIST locked-rotor resistances (which include resistance due to pump discharge orifices) are approximately 29% of (scaled) plant locked-rotor resistances. The additional hydraulic resistance provided by the cold leg venturis and piping increases total MIST cold leg resistance to between 92% and 98% of the plant resistance.

Table 6.5

AVERAGE REACTOR COOLANT PUMP LOCKED-ROTOR RESISTANCE

Scaled Flow (%) (100% = 120 gpm)	Average Resistance for MIST Pumps [ft-4]
19.0	**326500**
24.0	243300
32.3	176200
49.0	138100
67.8	121000
83.3	114200
99.0	109200
110.6	**105900**

For MIST forced circulation tests, the cold leg venturis were replaced by turbine meters. With the venturis removed, total cold leg resistance with the reactor coolant pumps running is approximately 10% of the value with pump rotors locked and venturis installed.

At 19% scaled cold leg flow, MIST locked-rotor resistances are approximately 66% of the corresponding plant values. The additional resistance provided by the cold leg venturis and piping increases the total MIST cold leg hydraulic resistance to between 115% and 120% of the plant resistance.

Equivalent hydraulic resistances (based on flow through each cold leg) were computed for each flow path from reactor vessel outlet to reactor coolant pump suction. Equivalent resistances are computed as:

$$\left[\frac{K}{A^2}\right]_{eq_i} = \left[\frac{K}{A^2}\right]_{cl_i} + \left[\frac{K}{A^2}\right]_{hl_i} \times \left[\frac{m_{hl_i}}{m_{cl_i}}\right]^2 + \left[\frac{K}{A^2}\right]_{sg_i} \times \left[\frac{m_{sg_i}}{m_{cl_i}}\right]^2 \qquad (6\text{-}2)$$

with subscripts cl, hl, and sg referring to cold leg, hot leg and steam generator, respectively; and with i = 1,2,3,4, denoting cold leg flow loops A1, B1, A2, and B2. Cold legs A1, B1, A2, and B2 are alternatively referred to as C1, C2, C3, and C4, respectively. Equivalent hydraulic resistances for each of the four cold leg flow loops are compared in Table 6.6 for the matched pump speed and the matched flow rate trials. These resistances were specified to compare within ±9% of their mean value and met the required specification.

Table 6.6

COLD LEG FLOW LOOP EQUIVALENT HYDRAULIC RESISTANCE

MATCHED REACTOR COOLANT PUMP SPEED:

	Hydraulic Resistance [ft^{-4}]				Difference
Flow Loop	**Hot Leg**	**OTSG**	**Cold Leg**	**Equivalent**	**from mean (%)**
A1	10357	19995	268802	389053 ±15359	+7643 (+2.0)
B1	9784	16506	262899	362746 ±13909	-18664 (-4.9)
A2	10357	19995	281873	405529 ±15425	+24119 (+6.3)
B2	9784	16506	257687	368313 ±14411	-13097 (-3.4)
mean				381410 ±6526	

MATCHED COLD LEG FLOW RATE:

	Hydraulic Resistance [ft^{-4}]				Difference
Flow Loop	**Hot Leg**	**OTSG**	**Cold Leg**	**Equivalent**	**from mean (%)**
A1	10382	19971	271154	395508 ±15993	+13144 (+3.4)
B1	9898	16481	265289	371711 ±14651	-10653 (-2.8)
A2	10382	19971	281369	401022 ±15340	+18658 (+4.9)
B2	9898	16481	256882	361214 ±14265	-21150 (-5.5)
mean				382364 ±7538	

NOTE: Uncertainties are given as computed root sum square (RSS) values.

Equivalent hydraulic resistances (based on the hot leg flow rate) were computed for each flow path from reactor vessel outlet through the associated reactor coolant pumps. Equivalent resistances are computed as:

$$\left[\frac{K}{A^2}\right]_{eq_i} = \left[\frac{K}{A^2}\right]_{hl_i} + \left[\frac{K}{A^2}\right]_{sg_i} + \left[\frac{K}{A^2}\right]_{clpr_i} \qquad (6\text{-}3)$$

with cl, hl, and sg defined as above, and clpr defined as the effective resistance for parallel cold legs associated with the same hot leg flow loop. The subscript i takes the value of a or b to denote hot leg flow loops A or B. Effective resistances for parallel cold legs are computed as:

$$\left[\frac{K}{A^2}\right]_{clpr_i} = \frac{\left[\frac{K}{A^2}\right]_{cl_i1}}{\left[1 + \frac{\left[\frac{K}{A^2}\right]_{cl_i1}}{\left[\frac{K}{A^2}\right]_{cl_i2}}\right]^{1/2\ \ 2}} \qquad (6\text{-}4)$$

Equivalent hydraulic resistances for each hot leg flow loop are compared in Table 6.7 for the matched pump speed and the matched flow rate trials. These resistances were specified to compare within ±9% of their mean value and met the required specification.

Table 6.7

HOT LEG FLOW LOOP EQUIVALENT HYDRAULIC RESISTANCE

FROM TESTS WITH MATCHED REACTOR COOLANT PUMP SPEED:

	Hydraulic Resistance [ft^{-4}]				Difference
Flow Loop	**Hot Leg**	**OTSG**	**Cold Leg**	**Equivalent**	**from mean (%)**
A	10357	19995	153723	184075 ±8346	+3906 (+2.2)
B	9784	16506	149973	176263 ±8248	-3906 (-2.2)
mean				180169 ±5867	

FROM TESTS WITH MATCHED COLD LEG FLOW RATE:

	Hydraulic Resistance [ft^{-4}]				Difference
Flow Loop	**Hot Leg**	**OTSG**	**Cold Leg**	**Equivalent**	**from mean (%)**
A	10382	19971	153959	184312 ±8370	+3883 (+2.2)
B	9898	16481	150167	176546 ±8280	-3883 (-2.2)
mean				180429 ±5887	

NOTE: Uncertainties are given as computed RSS values.

6.3 REACTOR VESSEL VENT VALVE PERFORMANCE

The four MIST reactor vessel vent valves can be operated in manual or automatic modes. In the automatic mode, the vent valves can actuate independently based on the differential pressure between the reactor vessel upper head and the corresponding upper downcomer quadrant, or simultaneously when any one of the four measured differential pressures reaches a trigger value. Simultaneous vent valve operation is referred to as "ganged" control.

Nominal trigger values for automatic reactor vessel vent valve actuation are 0.125 psid to open and 0.040 psid to close. The vent valves are closed in automatic mode for differential pressures lower than 0.040 psid and open for differential pressures higher than 0.125 psid. Between 0.040 and 0.125 psid, the vent valves can be either open or closed depending on the last trigger.

Reactor vessel vent valve trigger setpoint checks were performed before and after MIST Phase 3 and 4 transient testing. Initial open and close setpoints were adjusted to within ±0.006 psi of the specified nominal values as part of MIST facility characterization. Open/close setpoints were established with the primary partially voided at conditions typical of initial loop saturation due to lost inventory. Core steam production was slowly adjusted to trigger vent valve actuations by adjusting core power. "High speed" data acquisition was utilized, with vent valve differential pressures recorded at 0.1 second intervals to determine trigger values.

Reactor vessel vent valve open/close setpoints were checked during several extended facility cold shutdown periods during MIST Phase 3 and 4 testing. Checks in July 1986 and September 1987 were performed by procedure similar to the initial characterization. Test 3600AA data was analyzed to bracket Phase 3 transient tests performed before March 1987. The September 1987 setpoint check provides closure for the balance of Phase 3 transient tests and a baseline for Phase 4 testing. Test 4SBO11 data was used to bracket Phase 4 transient tests through November 1987 and Test 4CR3T1 data was used to provide closure for the balance of Phase 4 testing. Results for all reactor vessel vent valve setpoint checks are presented in Tables 6.8 and 6.9.

Table 6.8

REACTOR VESSEL VENT VALVE OPEN SETPOINTS

		Differential Pressure Setpoints (psid)							
Valve	VTAB	04-86	07-86	03-87	09-87	11-87	12-87	Average	σ
RVVV A1	RVDP06	0.125	0.112					0.119	0.009
			0.125	0.132	0.132	0.133	0.131	0.131	0.003
RVVV B1	RVDP07	0.131	0.122	0.128	0.131	0.125	0.129	0.128	0.004
RVVV A2	RVDP08	0.129	0.122	0.123	0.127	0.128	0.129	0.126	0.003
RVVV B2	RVDP09	0.126	0.119	0.123	0.119	0.119	0.127	0.122	0.004

Table 6.9

REACTOR VESSEL VENT VALVE CLOSE SETPOINTS

		Differential Pressure Setpoints (psid)							
Valve	VTAB	04-86	07-86	03-87	09-87	11-87	12-87	Average	σ
RVVV A1	RVDP06	0.041	0.045	0.043	0.044	0.047	0.042	0.044	0.002
RVVV B1	RVDP07	0.037	0.042	0.034	0.039	0.040	0.035	0.038	0.003
RVVV A2	RVDP08	0.037	0.046	0.043	0.045	0.047	0.047	0.044	0.004
RVVV B2	RVDP09	0.041	0.045	0.043	0.042	0.041	0.043	0.043	0.002

Open setpoints for all vent valves except RVVV A1 were within 0.006 psi of the specified 0.125 psid for all Phase 3 and 4 tests. The open setpoint for the A1 valve was found to be out of tolerance in July 1986 and was readjusted as noted in the table. The setpoint drifted slightly out of tolerance again during Phase 4 testing, but no corrective action was taken.

Close setpoints for all vent valves were within the 0.040 ±0.006 psid specification except for the A1 and A2 valves late in Phase 4 testing. The noted deviations were slight and no corrective action was taken. Averages and standard deviations (σ) for opening and closing differential pressure setpoints are included to provide an indication of setpoint stability.

6.4 REACTOR COOLANT PUMP PERFORMANCE

Single-phase performance characteristics were determined for each MIST reactor coolant pump for input to computer models used to predict plant SBLOCA transient response. Pump head-flow characteristics and locked-rotor hydraulic

resistances to forward and reverse flow were determined at the vendor prior to installation at the MIST facility and verified later in-loop. Plant-typical pump spinup and coastdown characteristics were developed, incorporated into Network 90 control logic, and verified as part of reactor coolant pump performance characterization.

The nominal rated speed for the MIST reactor coolant pumps was 3450 rpm. The design operating point at rated speed was 340 feet of head at 120 gpm with discharge orifices installed. Actual pump speed was measured at 3540 rpm after installation in the MIST facility. At this speed, the measured head-flow characteristic was approximately 3% above design, with 10% higher than expected output flows at design point head rise. Operation on the design head-flow characteristic was possible by reducing the control setpoint for 100% speed. However, at the reduced speeds, pump operating points were still down from the design point along the head-flow characteristic, due to lower than plant-typical flow path hydraulic resistances.

Output flows for the pumps operating at 3540 rpm varied by 3% from the mean. This variation resulted from differences in hydraulic resistance for the four cold leg paths. To compensate for these differences, control system setpoints for 100% pump speed were determined which achieved approximately equal cold leg flow rates. Pump speeds were adjusted so that all four cold leg flow rates matched the lowest previous value. The resulting head-flow curves and pump speeds are shown in Figure 6.3.

The cold leg flow rate balance was repeated at 18% speed to verify the predictability of MIST pump performance. Head-flow curves were calculated for each pump operating at reduced speed based on the 100% speed curves determined above and centrifugal pump affinity laws. Measured pump head rise and output flow were predicted to within measurement uncertainty by the calculations, as shown in Figure 6.4.

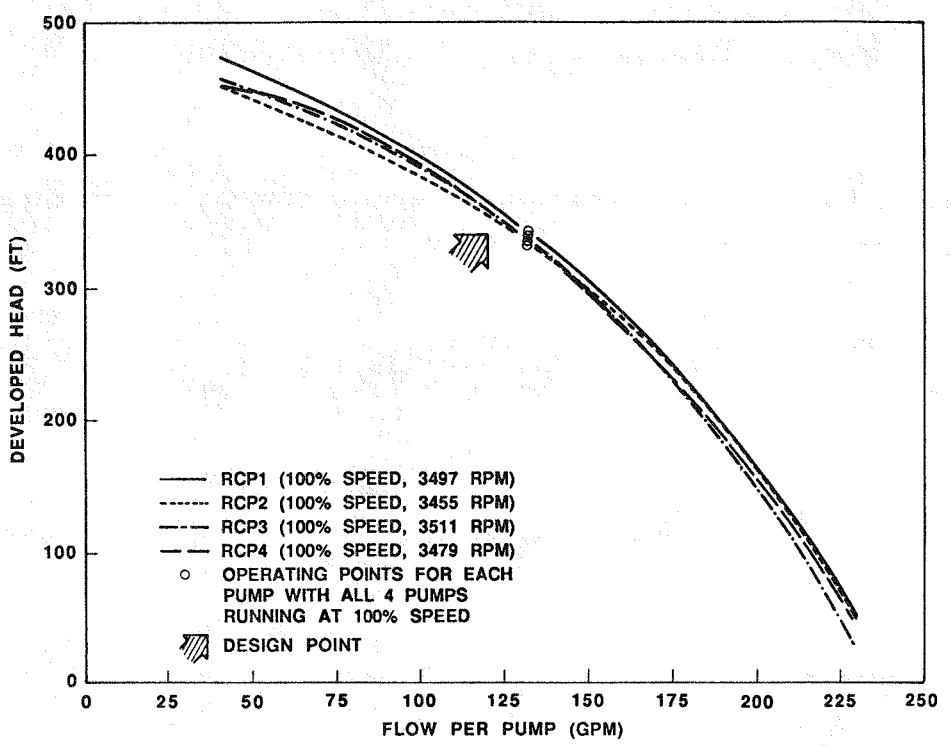

Figure 6.3 Reactor Coolant Pump Head-Flow Characteristics

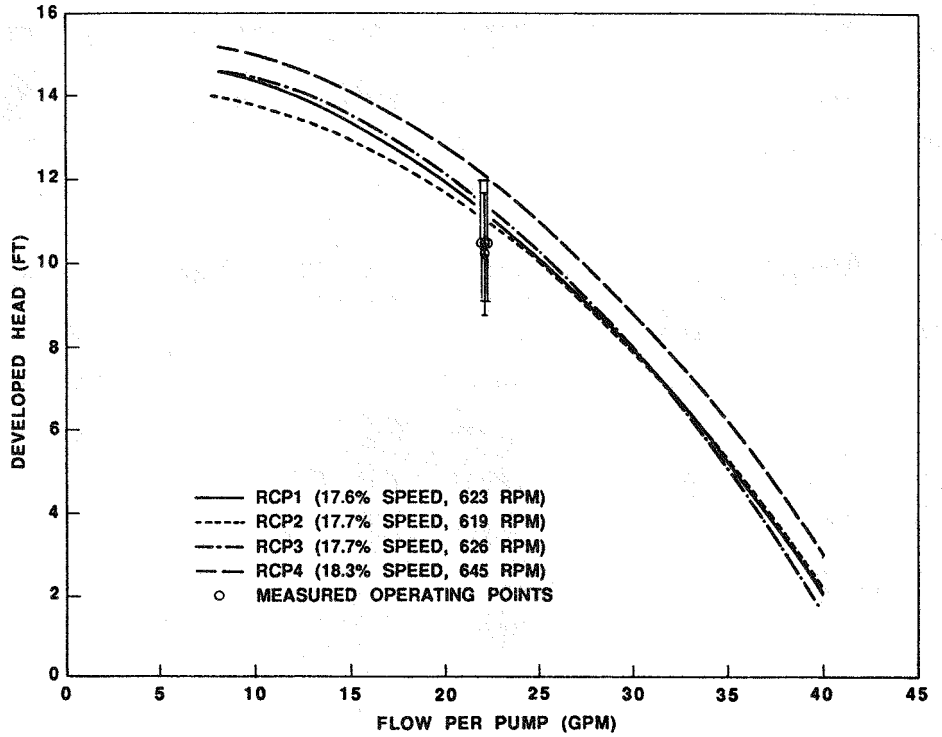

Figure 6.4 Reactor Coolant Pump Head-Flow Characteristics at 18% Speed

Pump locked-rotor hydraulic resistances were characterized as a function of scaled cold leg flow and are presented in Table 6.10. The resistance values are expressed as K/A^2 $[ft^{-4}]$ and include the additional resistance provided by the pump discharge orifices. Resistances given in Table 6.10 are measured values, except the values listed for 18.4% and 110.6% scaled flow. The values at 18.4% (22.1 gpm) and 110.6% (132.7 gpm) were obtained from a curve fit of the measured values.

Table 6.10

REACTOR COOLANT PUMP LOCKED-ROTOR RESISTANCE

Forward Flow Resistance -- K/A^2 $[ft^{-4}]$

Scaled Flow gpm	(%)	RCP1 (A1)	RCP2 (B1)	RCP3 (A2)	RCP4 (B2)	Average
4.7	(3.9)	2173800	2086500	2205600	2085400	2194700
22.1	**(18.4)**	**353400**	**394700**	**341700**	**286400**	**340700**
29.	(24.2)	247200	262600	247200	224000	243300
39.	(32.5)	179400	175100	175100	175100	176200
59.	(49.2)	134400	134400	143700	140000	138100
81.	(67.5)	121800	108900	130700	122800	121000
100.	(83.3)	115600	111700	120200	109100	114200
119.	(99.2)	110100	109200	112400	105100	109200
132.7	**(110.6)**	**109300**	**105400**	**108000**	**99600**	**105900**

Reverse Flow Resistance -- K/A^2 $[ft^{-4}]$

Scaled Flow gpm	(%)	RCP1 (A1)	RCP2 (B1)	RCP3 (A2)	RCP4 (B2)	Average
22.1	**(18.4)**	**301500**	**299700**	**299600**	**274700**	**299600**
29.	(24.2)	216300	216300	216300	196000	210500
39.	(32.5)	136700	162300	158000	141000	149500
59.	(49.2)	136200	143700	143700	132500	139000
81.	(67.5)	131700	138600	136600	126700	133400
100.	(83.3)	128000	134500	132500	121500	129100
119.	(99.2)	124300	129400	124800	118400	124200
132.7	**(110.6)**	**121800**	**127500**	**121500**	**114000**	**120300**

Plant-typical reactor coolant pump spinup and coastdown characteristics were simulated for MIST using a variable speed drive and the automatic control

described in Section 4.2. A linear ramp from 0 to 100% speed in 15 seconds was specified for the pump spinup characteristic. All pumps were observed to complete the spinup to 100% speed in 15 seconds, as specified. Pumps A1, A2, and B2 exhibited a delay (of less than 1 second) before beginning to rotate, but achieved the required ramp rate of 6.67% per second within 2.5 seconds. Recorded spinup ramps for each MIST reactor coolant pump are shown in Figure 6.5.

During a modeled reactor coolant pump coastdown, pump speed was to decrease from 100% to 20% speed in 33 ±3 seconds and complete the coastdown from 20% to 5% speed (or less) in a maximum of 75 seconds. The MIST reactor coolant pumps met these requirements as shown in Figure 6.6.

6.5 GUARD HEATER PERFORMANCE

The MIST facility guard heating concept and hardware are described in Section 3.3 of this document. Guard heater performance characterization tests and results are discussed in this section. These tests determined the guard heater power control functions which result in zero net heat loss (within tolerance) from the pipe wall at steady-state conditions over each of the 42 MIST loop guard heater zones. Control functions were derived from set-points determined at loop operating temperatures of approximately 400° and 550°F. The test points were performed with the loop inventory superheated to maximize the sensitivity of the characterization.

To perform the characterization tests, the guard heater power for each control zone was adjusted until the superheated vapor contained in the zone reached a steady-state temperature. When steady-state conditions were achieved, the total heat input to each zone offset the loss across the insulated pipe boundary plus local heat losses within each zone.

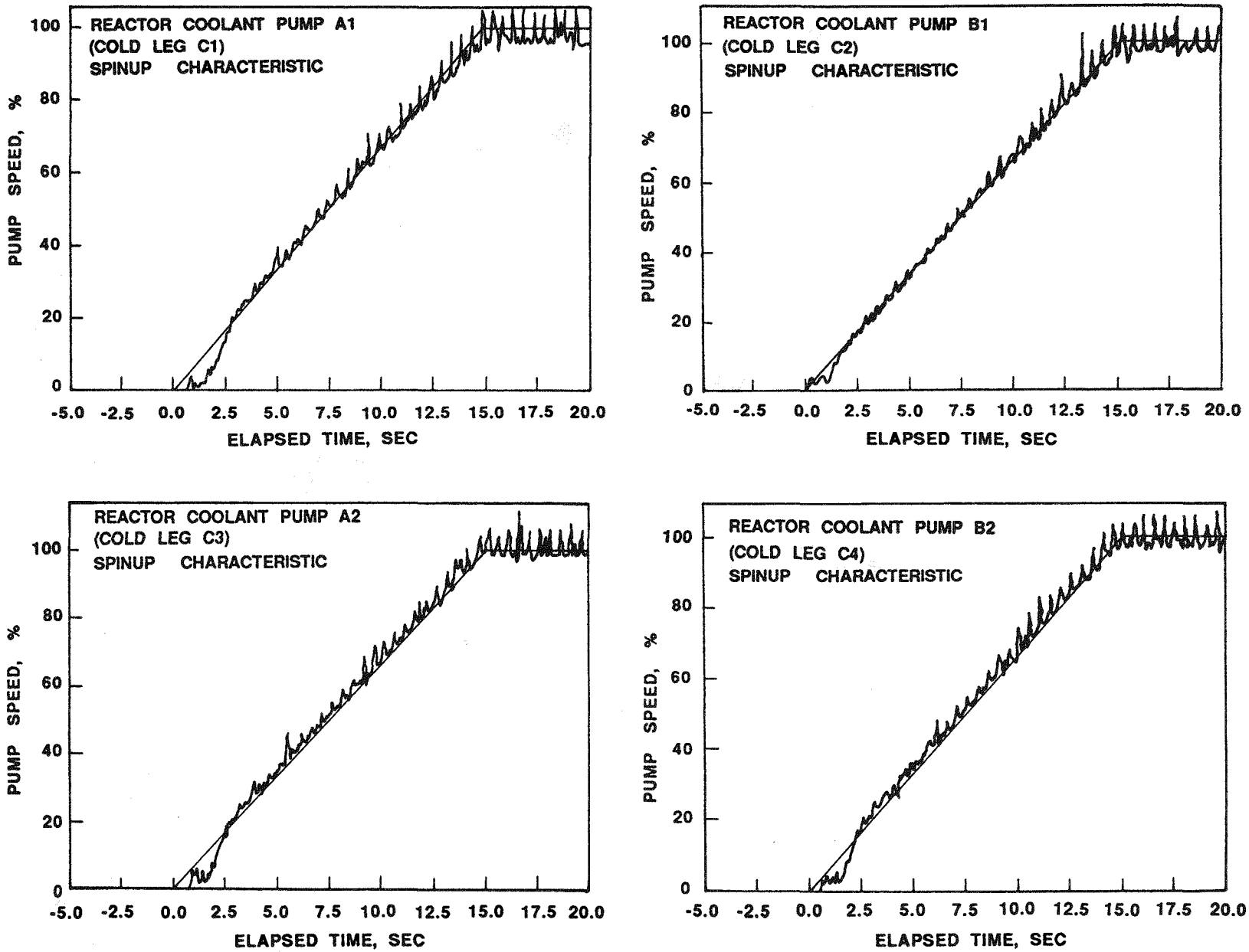

Figure 6.5 Reactor Coolant Pump Spinup Characteristics

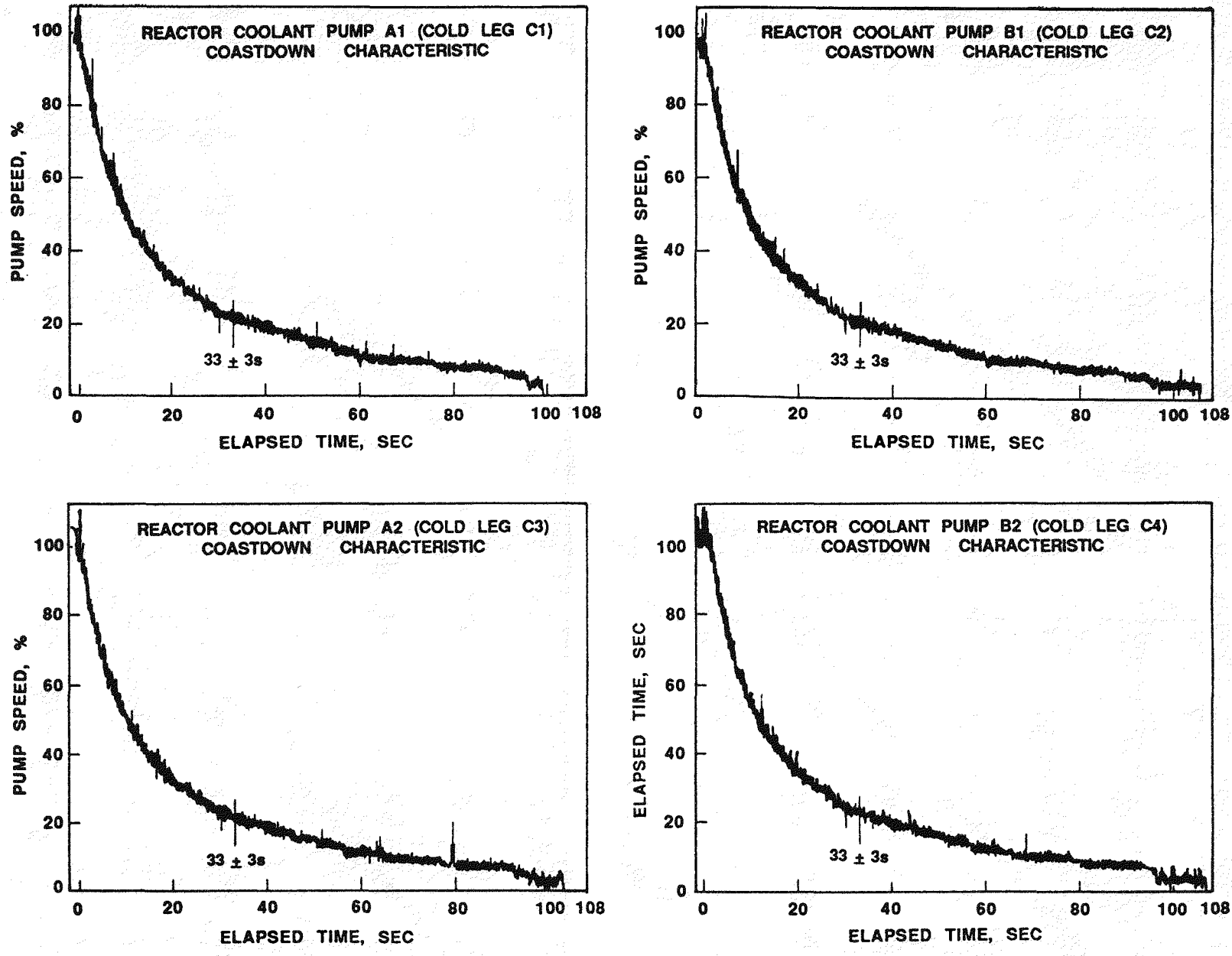

Figure 6.6 Reactor Coolant Pump Coastdown Characteristics

Steady-state criteria for each guard heater zone were based on achieving thermal equilibrium within 1 watt per foot of zone length, with corresponding time rates of temperature change computed for each zone depending on the diameter of the contained pipe. Steady-state acceptance required satisfaction of temperature change specifications for each guard heater zone with the vapor in each zone being superheated by at least 10°F. These acceptance criteria were satisfied for all guard heater zones during characterization tests at both 400° and 550°F loop operating temperatures.

The thermal independence of adjacent guard heater zones was confirmed by monitoring fluid temperature profiles. These measurements did indicate the presence of some local convection cells within components, but did not indicate net fluid flow around the loop. With loop conditions essentially stagnant, the energy transport across control zone boundaries was insignificant.

Pipe wall metal temperatures, differential temperatures across the control insulation layer, fluid temperatures, and guard heater power were recorded at two different loop operating points for each guard heater zone. Metal and differential temperatures and total guard heater power for each zone are reported in Table 6.11.

The insulation temperature gradient recorded for each zone provided an indication of the magnitude of local heat losses within the zone and their proximity to the differential temperature measurement location. In Table 6.11, relatively large negative differential temperatures indicate relatively large local heat losses within the zone which are remote to the measurement location. Positive differential temperatures indicate that the measurement site is influenced by a significant nearby local heat loss. Most zones show a combination of these influences on measured differential temperature.

Table 6.11

MIST GUARD HEATER CONTROL PARAMETERS

		Low Temperature (~400°F)			High Temperature (~550°F)		
Zone	Loop Location	Metal T[°F]	Delta T[°F]	GHPower [Watts]	Metal T[°F]	Delta T[°F]	GHPower [Watts]
01	Pressurizer Vessel	423.0	-12.21	418	587.2	-12.57	760
02	Pressurizer Surge Line	414.0	+ 2.53	269	557.7	+ 4.51	504
03	Pressurizer Spray Line		0.00			0.00	
04	RV Lower Plenum	390.0	-38.84	230	466	-34.36	266
05	RV Core Region	384.7	- 8.52	353	503	- 8.45	534
06	RV Upper Plenum	385.6	-43.68	127	453	-45.42	163
07	RV Top Plenum	398.2	-18.79	144	475.6	-23.28	225
08	RV Vent Valves	385.1	0.00	249	618.3	0.00	332
09	Continuous Vent Line	391.4	-19.40	354	594.0	-42.09	1035
10	Hot Leg A Lower Riser	399.5	- 7.78	280	556.3	- 5.87	576
11	Hot Leg A Middle Riser	403.8	- 4.25	383	551.7	+16.59	618
12	Hot Leg A Upper Riser	413.7	-12.03	344	473.4	-26.12	577
13	Hot Leg A OTSG Stub	404.8	+ 2.69	351	594.0	+ 9.09	623
14	Hot Leg B Lower Riser	401.8	-14.84	443	588.5	-14.19	740
15	Hot Leg B Middle Riser	387.2	-12.80	383	584.6	- 8.89	670
16	Hot Leg B Upper Riser	402.8	- 7.01	722	446.9	-10.65	880
17	Hot Leg B OTSG Stub	426.7	+12.73	359	592.0	+21.31	617
18	OTSG-A Lower Zone	421.7	- 8.56	384	589.7	- 5.56	835
19	OTSG-A Lower Middle Zone	413.7	-10.75	417	558.8	-13.75	788
20	OTSG-A Upper Middle Zone	392.5	-55.95	544	517.1	-66.62	814
21	OTSG-A Upper Zone	389.9	-26.61	494	599.5	-19.76	809
22	OTSG-A Downcomer	413.7	+ 0.94	668	616.8	+ 3.51	1449
23	OTSG-B Lower Zone	422.9	- 9.95	619	587.1	- 7.23	835
24	OTSG-B Lower Middle Zone	410.6	- 1.21	473	546.1	- 0.39	728
25	OTSG-B Upper Middle Zone	405.0	-33.13	541	529.0	-31.69	559
26	OTSG-B Upper Zone	410.4	-21.41	377	607.0	- 8.53	651
27	OTSG-B Downcomer	413.4	+ 3.67	720	588.2	+ 6.15	1388
28	Cold Leg A1 Lower Riser	443.0	- 7.69	425	615.5	- 9.21	749
29	Cold Leg A1 Upper Riser	457.7	+ 1.30	452	551.6	+ 9.01	611
30	Cold Leg A1 Discharge	408.9	-11.24	164	642.9	-13.80	328
31	Cold Leg B1 Lower Riser	450.8	+ 2.08	412	603.3	-12.47	786
32	Cold Leg B1 Upper Riser	435.7	- 6.15	505	569.7	+ 5.58	693
33	Cold Leg B1 Discharge	418.0	-15.59	174	633.5	-21.80	345
34	Cold Leg A2 Lower Riser	447.7	-18.77	469	591.8	- 5.01	651
35	Cold Leg A2 Upper Riser	452.6	+ 3.71	328	576.0	+ 4.06	551
36	Cold Leg A2 Discharge	403.5	-29.50	145	642.9	-14.35	296
37	Cold Leg B2 Lower Riser	431.1	-18.87	530	605.9	+ 0.97	713
38	Cold Leg B2 Upper Riser	455.7	+ 3.61	464	573.2	+ 2.88	690
39	Cold Leg B2 Discharge	381.3	-28.66	171	638.8	-16.71	322
40	RV Downcomer Upper Zone	421.2	-41.48	228	579.0	-37.56	358
41	RV Downcomer Middle Zone	418.0	- 7.95	201	581.1	- 6.93	339
42	RV Downcomer Lower Zone	397.7	+ 3.25	632	576.9	+17.05	1078

After characterization, control functions for 40 of the 42 guard heater zones were determined which required power control to achieve the specified relationship between the control insulation differential temperature and the pipe wall metal temperature. Control functions for the pressurizer spray line and the continuous vent line (installed for Davis-Besse tests only) required power control to achieve specified fluid temperature differences through the zones. The control functions for guard heater control system are presented in Table 6.12 with associated comments.

6.6 MIST LOOP HEAT LOSS WITHOUT GUARD HEATERS

MIST facility heat loss with guard heaters inactive was characterized as a function of loop temperature. Overall facility and individual component heat losses were characterized for steady-state loop operating temperatures between 350° and 510°F. Steady-state loop conditions were maintained for approximately 48 hours before recording data for the heat loss analysis.

Overall heat losses were indicated by the core power output required to maintain steady-state conditions at each recorded loop temperature. Component heat losses were determined from fluid mass flow rate and enthalpy change. Core power input was also required to determine the heat loss for the reactor vessel. Overall and component heat losses are presented graphically in Figures 6.7 through 6.14.

The total facility heat loss at natural circulation test initial conditions was estimated by extrapolating heat loss characterization data. Total heat loss (given by steady-state core power) was correlated against the approximate facility-to-ambient temperature difference $[(T_{hot}+T_{cold})/2-T_{amb}]$. The indicated total heat loss at test initial conditions was 36.8 kW.

Table 6.12

GUARD HEATER CONTROL FUNCTIONS

$$\Delta T = C_0 + C_1 \times MT$$

Zone	Loop Location	C_0	C_1	Comments
01	Pressurizer Vessel	-11.27	-0.0022	1
02	Pressurizer Surge Line	-3.15	0.0137	1,2
03	Pressurizer Spray Line	0.00	0.0000	3,4
04	Reactor Vessel Lower Plenum	-61.75	0.0587	5
05	Reactor Vessel Core Region	- 8.72	0.0005	1
06	Reactor Vessel Upper Plenum	-33.62	-0.0261	1
07	Reactor Vessel Top Plenum	4.30	-0.0580	1
08	Reactor Vessel Vent Valves	0.00	0.0000	6
09	Continuous Vent Line	24.43	-0.1120	7
10	Hot Leg A Lower Riser	-12.64	0.0122	8
11	Hot Leg A Middle Riser	-61.16	0.1409	1
12	Hot Leg A Upper Riser	85.59	-0.2360	1
13	Hot Leg A OTSG Stub	-10.99	0.0338	1
14	Hot Leg B Lower Riser	-16.23	0.0035	1
15	Hot Leg B Middle Riser	-20.48	0.0198	1
16	Hot Leg B Upper Riser	26.24	-0.0826	1
17	Hot Leg B OTSG Stub	-9.42	0.0519	1
18	OTSG-A Lower Region	-16.09	0.0179	1
19	OTSG-A Lower Middle Region	-2.20	-0.0207	1
20	OTSG-A Upper Middle Region	-22.33	-0.0857	1
21	OTSG-A Upper Region	-39.36	0.0327	1
22	OTSG-A Downcomer	-4.29	0.0127	1
23	OTSG-B Lower Region	-16.96	0.0166	1
24	OTSG-B Lower Middle Region	-3.68	0.0060	1
25	OTSG-B Upper Middle Region	-37.83	0.0116	1
26	OTSG-B Upper Region	-48.30	0.0655	1
27	OTSG-B Downcomer	-2.22	0.0142	1
28	Cold Leg A1 Lower Riser	-3.77	-0.0088	9
29	Cold Leg A1 Upper Riser	-36.28	0.0821	10
30	Cold Leg A1 Discharge	-6.77	-0.0109	1
31	Cold Leg B1 Lower Riser	45.07	-0.0954	1
32	Cold Leg B1 Upper Riser	-44.29	0.0875	1
33	Cold Leg B1 Discharge	-3.54	-0.0288	1
34	Cold Leg A2 Lower Riser	-61.53	0.0955	1
35	Cold Leg A2 Upper Riser	2.44	0.0028	1
36	Cold Leg A2 Discharge	-55.04	0.0633	11
37	Cold Leg B2 Lower Riser	-67.82	0.1135	12
38	Cold Leg B2 Upper Riser	6.42	-0.0062	1
39	Cold Leg B2 Discharge	-46.35	0.0464	13
40	RV Downcomer Upper Region	-51.94	0.0248	1
41	RV Downcomer Middle Region	-10.56	0.0062	1
42	RV Downcomer Lower Region	-27.39	0.0770	1

Table 6.12 (Continued)

GUARD HEATER CONTROL FUNCTIONS

Guide to Comments

Comment	Explanation
1	The noted ΔT versus MT CASCADE function was installed for all MIST Phase 3 and 4 transient tests.
2	Guard heater Zone 2 was in MANUAL control to establish required test initial conditions. CASCADE control based on ΔT versus MT was triggered at test initiation. In MANUAL control, guard heater power was adjusted to achieve a fluid temperature difference of 0°F between PZTC01 and H1TC10. Required power at steady-state initial conditions was approximately 620 Watts.
3	The pressurizer spray line was available for all tests using the reactor coolant pumps, beginning with 360514 on 13-Mar-1988.
4	Guard heater Zone 3 was controlled in AUTOMATIC to achieve a fluid temperature difference of 0°F between PZTC10 and C3TC07.
5	The ΔT measurement for Zone 4 (RVDT01) failed during loop heat up on 11-Aug-1987. After this date, Zone 4 guard heater power is a function of metal temperature (RVMT01) alone. The revised control function table is:

RVMT01	['F]	100.	200.	390.	466.	700.	750.
RVWM01	[Watts]	0.	230.	230.	266.	266.	0.

Comment	Explanation
6	The ΔT setpoint for Zone 8 is 0°F for all values of RVMT23. No attempt is made to offset the large heat losses at the reactor vessel vent valves using guard heater power.
7	The continuous vent line was installed for Davis-Besse plant-specific (Group 37) transient tests only. The noted function was determined to allow the specified heat loss, resulting in the specified fluid flow rate and direction.
8	The ΔT measurement for Zone 10 (H1DT01) failed prior to Phase 4 Test 4100B2. Zone 10 guard heater power is a function of metal temperature (H1MT01) for Tests 4100B2 and 4CR3T2. The revised control function table is:

H1MT01	['F]	90.	400.	474.	700.	700+
H1WM01	[Watts]	0.	280.	425.	425.	0.

A point at 556°F, 576 W was erroneously omitted from the function table. As a result, Zone 10 was under-powered when H1MT01 exceeded 474°F during Tests 4100B2 and 4CR3T2. No adverse impact is expected for these tests.

Table 6.12 (Continued)

GUARD HEATER CONTROL FUNCTIONS

Guide to Comments

Comment — **Explanation**

9 The ΔT measurement for Zone 28 (C1DT01) failed during loop heat up on 04-Feb-1987. After this date, Zone 28 guard heater power is a function of metal temperature (C1MT01) alone. The revised control function table is:

C1MT01	[°F]	100.	217.	443.	615.	750.	750+
C1WM01	[Watts]	0.	0.	425.	749.	749.	0.

10 The ΔT measurement for Zone 29 (C1DT02) failed prior to Phase 4 Test 4CR3T2. Zone 29 guard heater power is a function of metal temperature (C1MT02) for Test 4CR3T2. The revised control function table is:

C1MT02	[°F]	90.	458.	535.	650.
C1WM02	[Watts]	0.	452.	579.	0.

Points at 535°F, 579 W and 650°F, 0 W were incorrectly installed and should have been installed as 552°F, 611 W; 650°F, 661 W; and 750°F, 0 W in the function table. As a result, Zone 29 was underpowered when C1MT02 exceeded 535°F during Test 4CR3T2. No adverse impact is expected for this test.

11 The ΔT measurement for Zone 36 (C3DT03) failed during loop heat-up on 11-Aug-1987. After this date, Zone 36 guard heater power is a function of metal temperature (C3MT03) alone. The revised control function table is:

C3MT03	[°F]	100.	200.	404.	642.	700.	750.
C3WM03	[Watts]	0.	145.	145.	296.	296.	0.

12 The ΔT measurement for Zone 37 (C4DT01) failed during loop heat-up on 04-Feb-1987. After this date, Zone 37 guard heater power is a function of metal temperature (C4MT01) alone. The revised control function table is:

C4MT01	[°F]	100.	212.	431.	606.	750.	750+
C4WM01	[Watts]	0.	0.	530.	713.	713.	0.

13 The ΔT measurement for Zone 39 (C4DT03) failed during loop heat-up on 08-Oct-1987. After this date, Zone 39 guard heater power is a function of metal temperature (C4MT03) alone. The revised control function table is:

C4MT03	[°F]	32.	76.	381.	639.	750.	750+
C4WM03	[Watts]	0.	0.	171.	322.	322.	0.

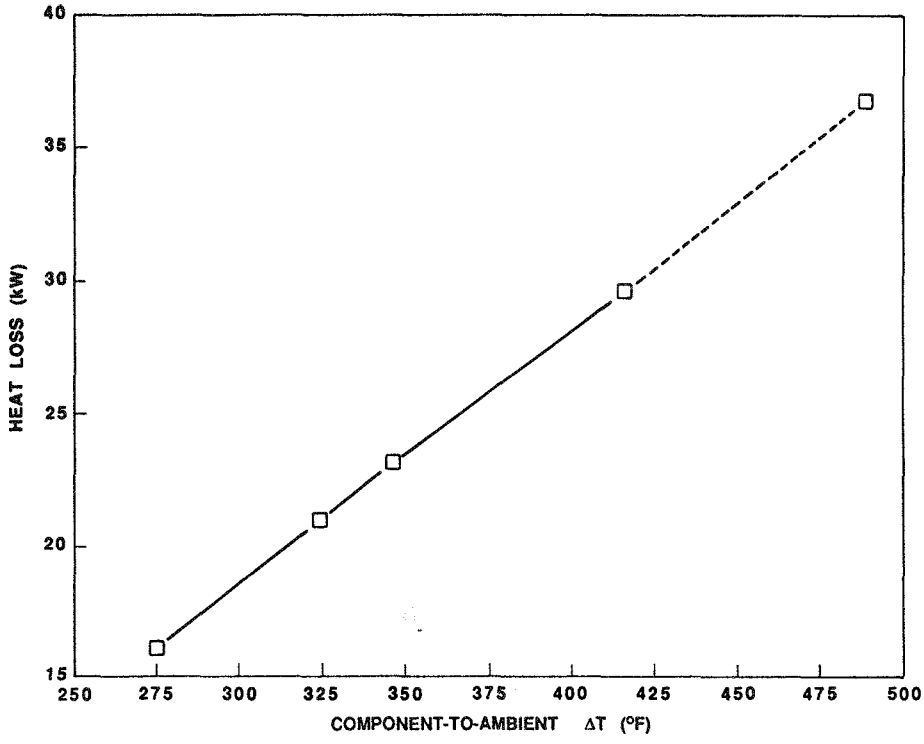

Figure 6.7 Facility Overall Heat Loss

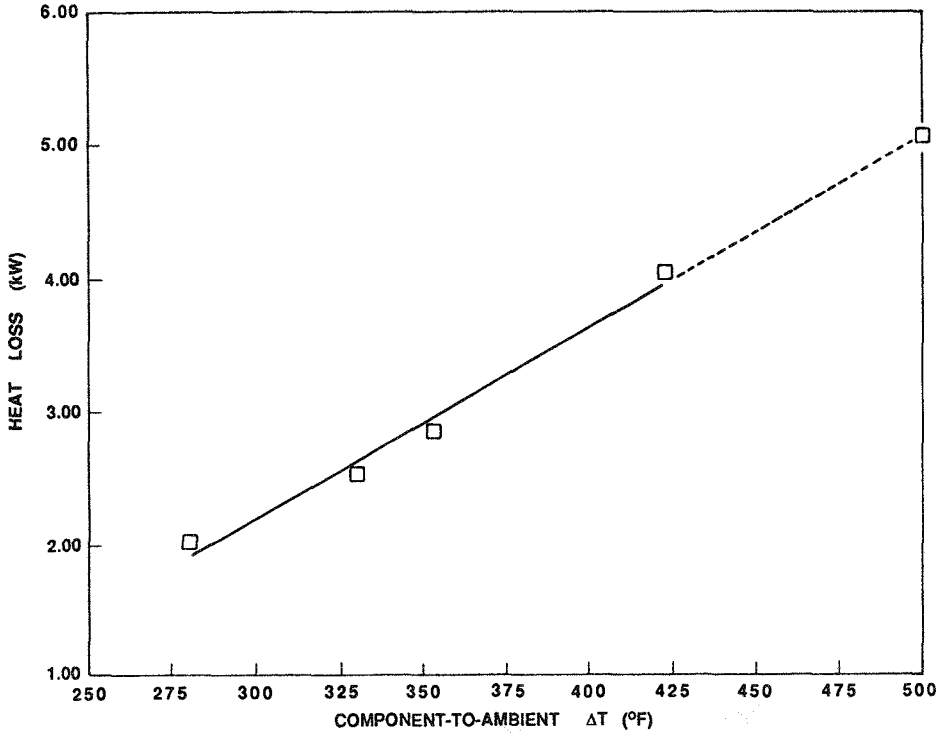

Figure 6.8 Reactor Vessel Heat Loss

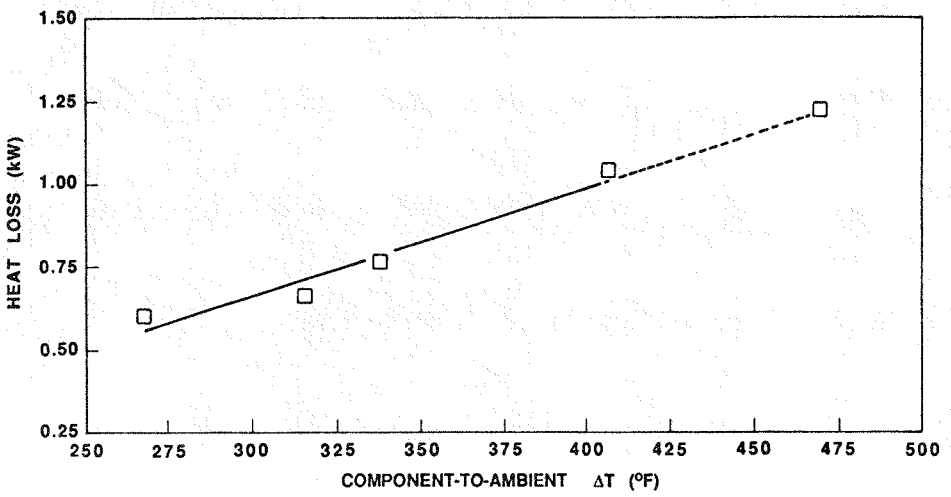

Figure 6.9 Reactor Vessel Downcomer Heat Loss

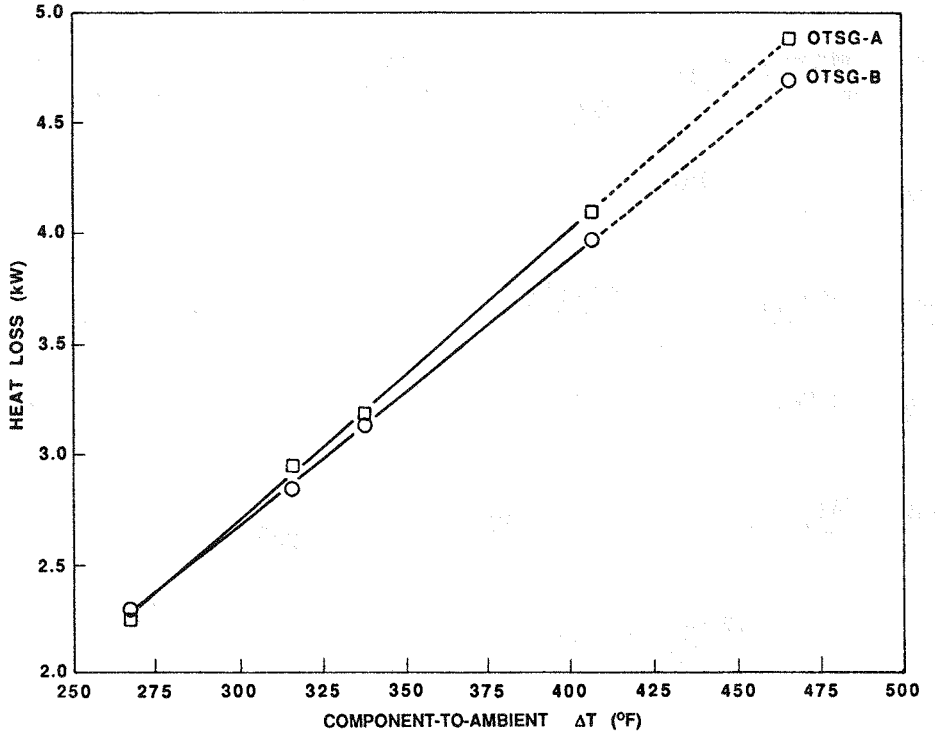

Figure 6.10 Steam Generator Heat Loss

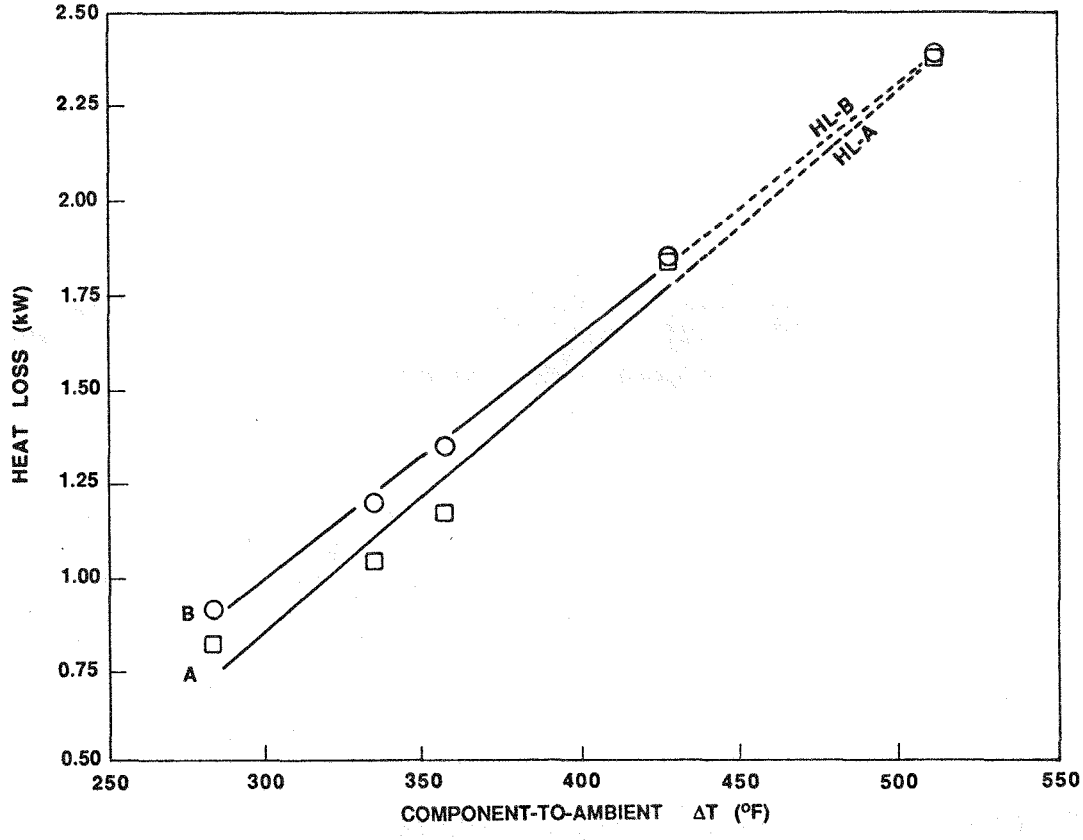

Figure 6.11 Hot Leg Heat Loss

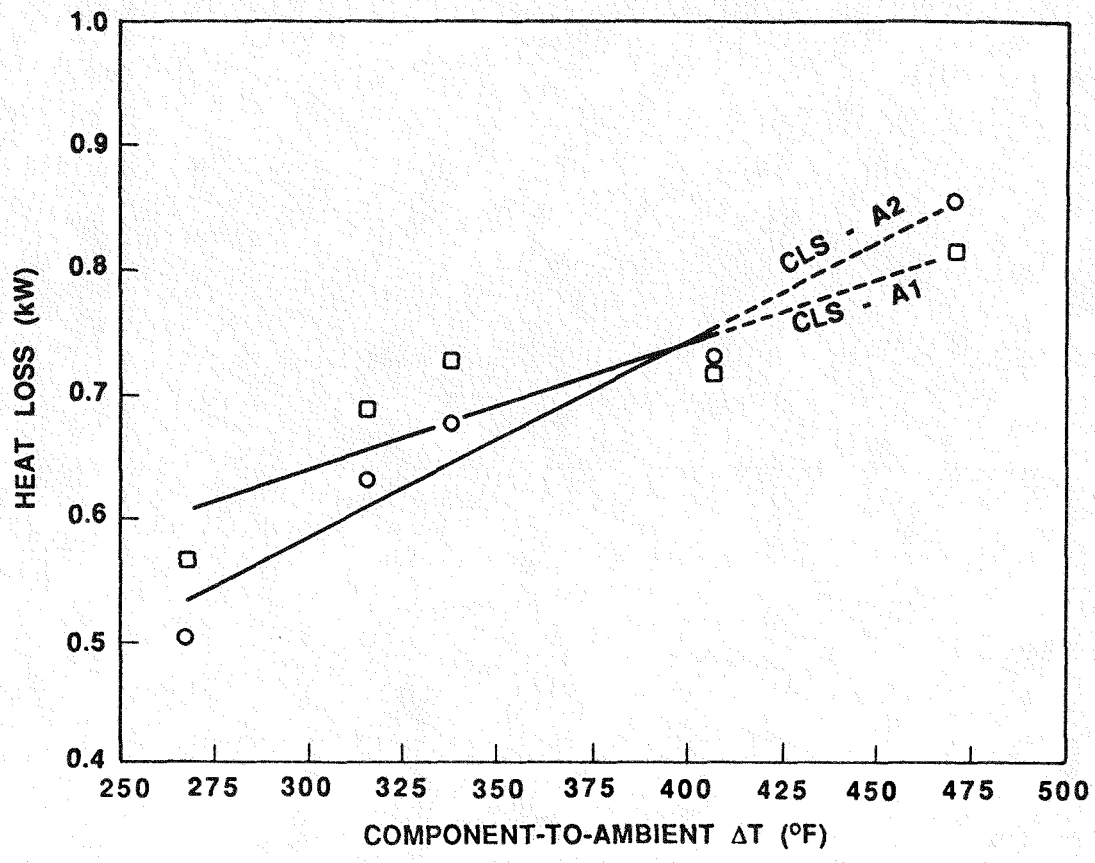

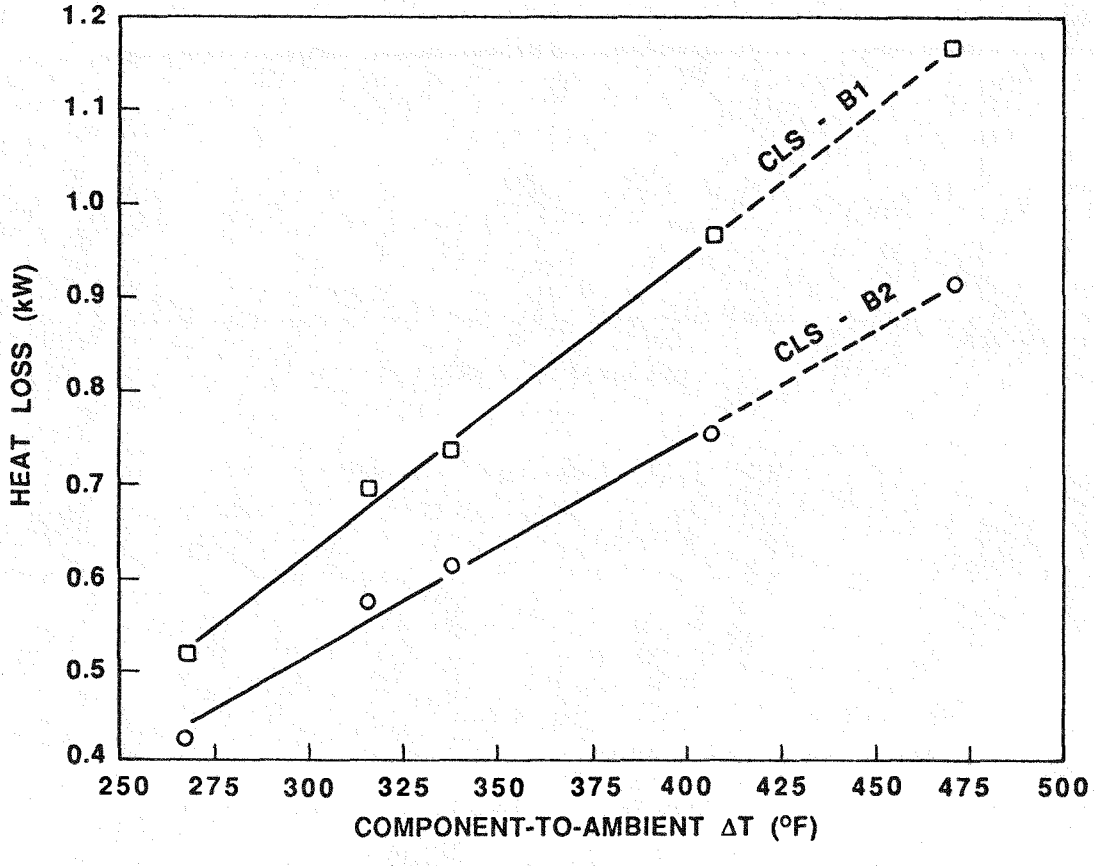

Figure 6.12 Cold Leg Suction Heat Loss

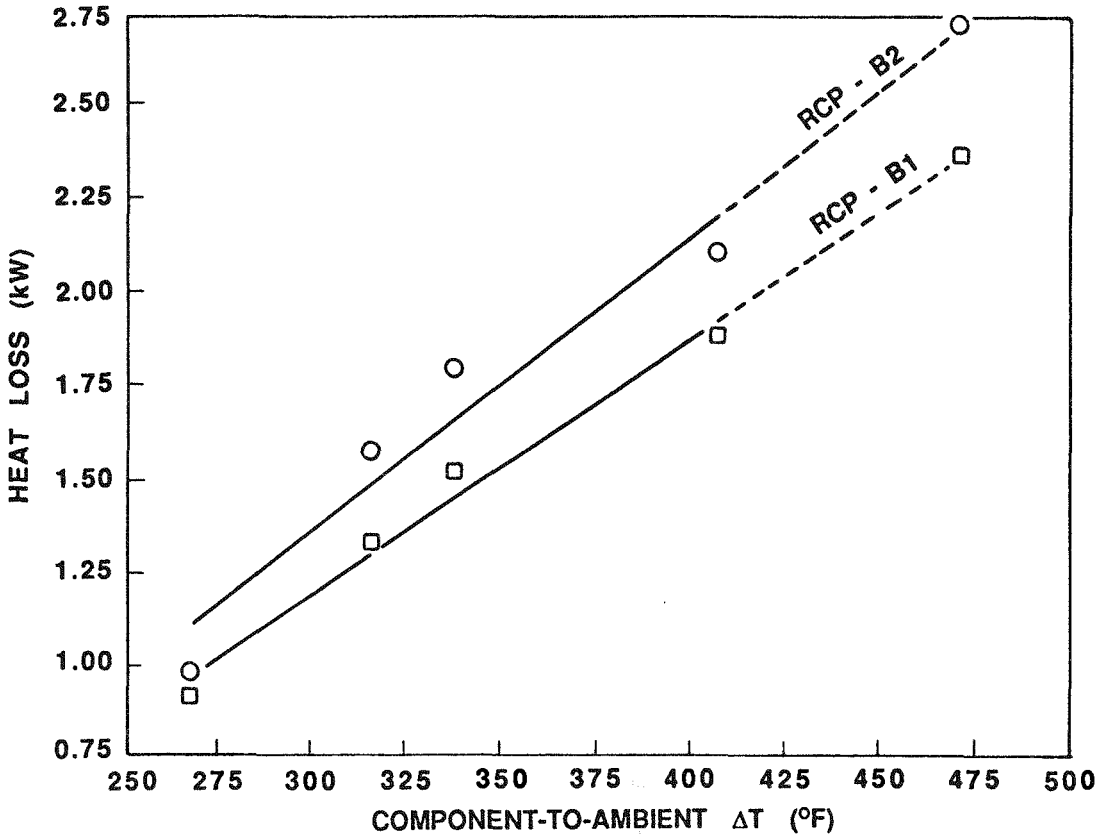

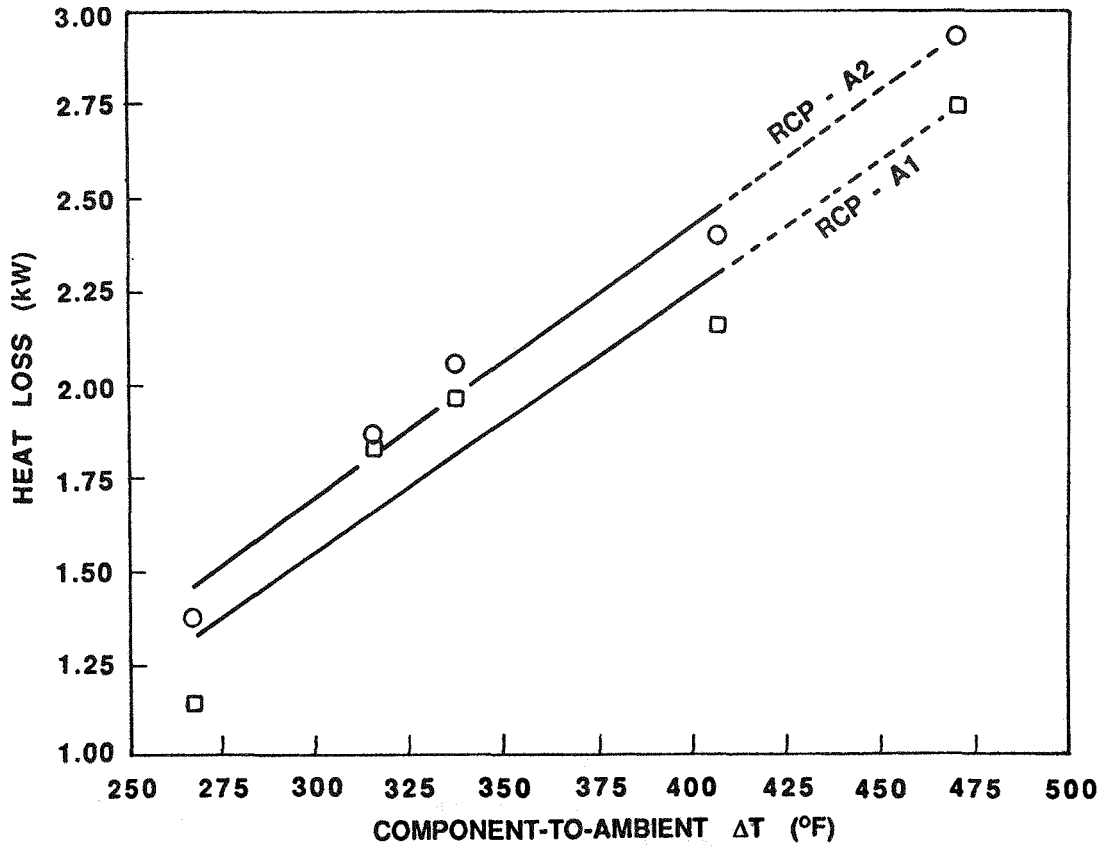

Figure 6.13 Reactor Coolant Pump Heat Loss

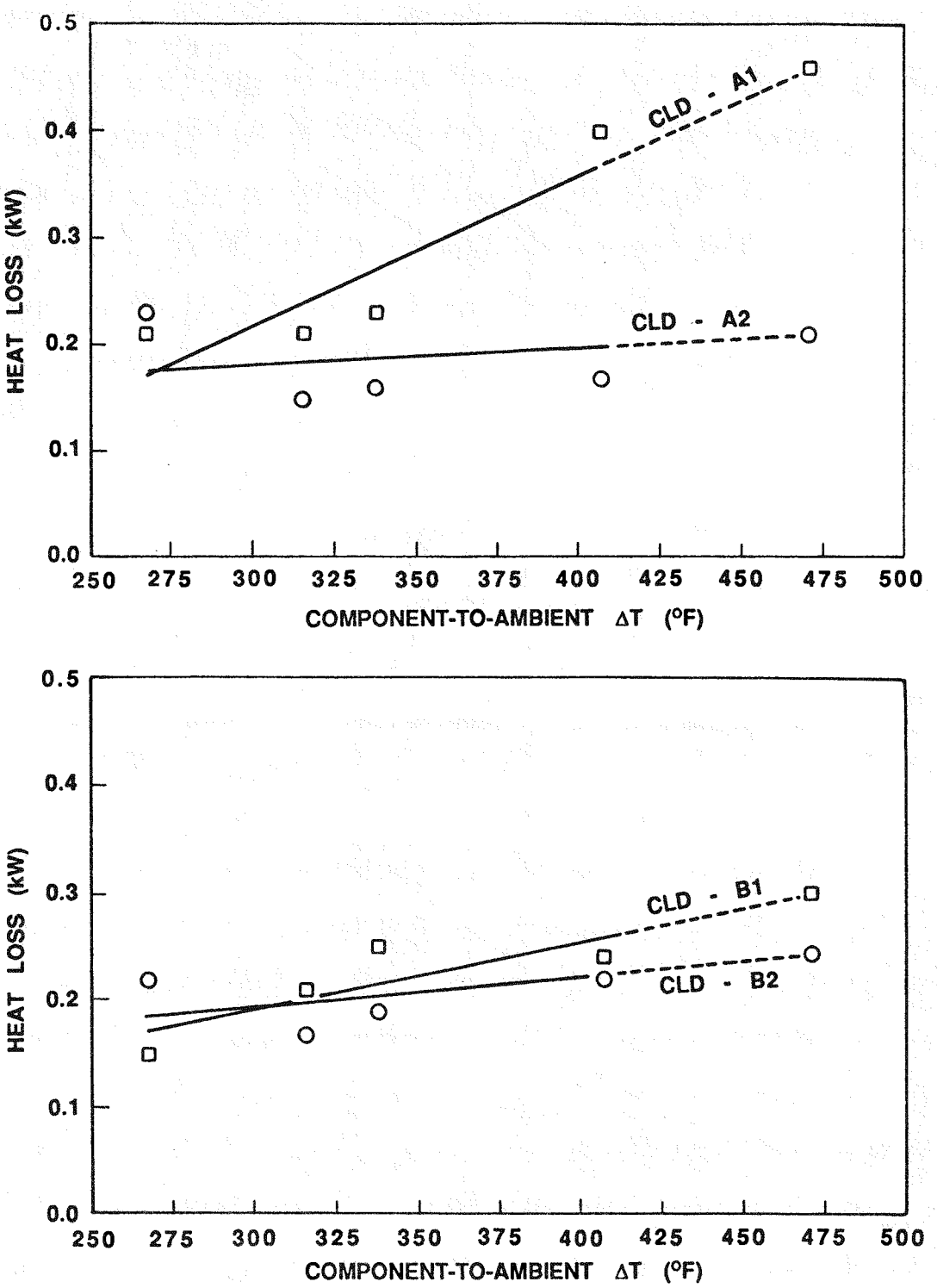

Figure 6.14 Cold Leg Discharge Heat Loss

Facility heat losses due to water cooling of the reactor coolant pumps, gamma densitometers, and the cooled thermocouple account for about one-half (18.8 kW) of total heat loss at natural circulation initial conditions and are offset by augmenting core power. The remaining 18.0 kW is lost through the passive insulation and at insulation discontinuities and penetrations. This portion of the total heat loss is offset by the guard heaters during normal operation. The locations of the major facility heat losses are listed in Table 6.13.

6.7 LEAK QUALITY SYSTEM PERFORMANCE

The MIST leak enthalpy system measures the energy content of cold leg discharge leak or the simulated reactor coolant pump seal leak effluent. The system operates by subcooling the initially two-phase leak effluent and computing leak enthalpy as the enthalpy of the subcooled fluid at the system outlet plus the specific energy transfer from the leak effluent to tower cooling water. Quality is then calculated from the enthalpy measurement and steam tables. Measurement uncertainty for the system is a strong function of the tower cooling water flow rate. Characterization testing was performed to optimize the cooling water flow rates for planned Phase 4 transient tests and minimize total measurement uncertainty.

For Phase 3 testing, tower cooling water flow rates were sufficient to assure subcooling at atmospheric pressure at the leak enthalpy system outlet for theoretical worst-case heat loads. Recorded heat loads were significantly less than than the assumed worst case, and reported uncertainties for leak enthalpy were impacted by the excess cooling water flow. During characterization, cooling water flow rates to the leak enthalpy heat exchangers were matched to actual heat loads for planned transient tests. Cooling water flow rates were further reduced by utilizing the backpressure provided by the single-phase leak system hardware downstream of the leak enthalpy system.

Table 6.13

LOCATIONS OF MAJOR FACILITY HEAT LOSSES

Component	Elevation [ft rel. SGUFLTS]	Description
Pressurizer	18.4 to 19.6	Main Heater Penetrations
	24.5	Vessel Support with Transite Block
	28.6	Relief Valve Connective Piping
	29.0	Vessel Cap; PORV and Spray
Pressurizer Surge Line	22.3	Pipe Support with Transite Block
Reactor Vessel	-1.3	Lower Flange (centerline)
	17.0	Upper Flange (centerline)
	21.3	Hot Leg Connections to Vessel
	22.3	Vessel Support with Transite Block
	24.2	RVVV Connections to Vessel
	29.4	Vessel Cap with Vent, etc.
Hot Legs (each)	21.2	Viewport Block and Densitometer Spool
	29.0	Viewport Block
	40.2	Pipe Support with Maranite Block
	43.9	Pipe Support Guide Clip
	50.1	Deck 3 Grating Interference
	60.0	Pipe Support with Maranite Block
	66.5	Viewport Block, Vent, etc.
Steam Generators (each)	-0.5	Guide Plate
	0.5	Main Feedwater Connection
	5.9	Low Auxiliary Feedwater Header
	32.0	Steam Bleed Connection to Vessel
	35.5	Pipe Support with Maranite Block
	50.0	Guide Plate
	50.8	High Auxiliary Feedwater Header
	51.6	Steam Line Connections to Vessel
OTSG Downcomer (each)	30.2	Pipe Support with Transite Block
	32.0	Steam Bleed Connection to Downcomer
Cold Leg Suction (each)	-7.4	Drain Valve
	-2.0	Guide Clip
	-0.5	Low Venturi Piezo Ring Pressure Tap
	0.6	Mid Venturi Piezo Ring Pressure Tap
	1.7	High Venturi Piezo Ring Pressure Tap
	21.4	Gamma Densitometer Spool
	25.8	Reactor Coolant Pump
Cold Leg Discharge (each)	21.3	Gamma Densitometer Spool
	25.8	Reactor Coolant Pump
Reactor Vessel Downcomer	4.0	Low Venturi Piezo Ring Pressure Tap
	5.4	Mid Venturi Piezo Ring Pressure Tap
	6.8	High Venturi Piezo Ring Pressure Tap
	24.2	Reactor Vessel Vent Valve Connections
	24.6	Downcomer Head Plate, Vent, Supports

Characterization test runs duplicated the transient test's leak mass and energy transport by reproducing the initial conditions and control actions for Phase 4 transient tests with saturated conditions expected at the cold leg leak sites. Three leak-ECCS scenarios, representing four Phase 4 transient tests, were investigated. The first represented tests 410AT3 and 410BD1 – scaled 10 cm^2 SBLOCA transients with HPI unavailable. The second represented test 4100B2 – a scaled 100 cm^2 SBLOCA with all emergency core cooling systems available. The third represented test 4SBO11, which simulated station blackout conditions with reactor coolant pump seal leakage equivalent to two scaled 0.25 cm^2 leaks and all ECCS except the core flood tank disabled. For each of the three scenarios, the peak cooling demand was noted immediately following leak saturation.

Results of leak quality system characterization tests are presented in Table 6.14 and Figures 6.15 and 6.16. Tower cooling water flow rates and leak enthalpy measurement uncertainty were reduced from Phase 3 values based on the results of this characterization testing. As shown in the figures, indicated uncertainties for leak enthalpy ranged from 10 to 90 Btu/lbm for the 10 cm^2 leak tests and from 10 to 130 Btu/lbm for the 100 cm^2 leak tests. These uncertainties are much less than the Phase 3 values of 50 to 350 Btu/lbm.

Optimum tower cooling water flow rates were too small to be maintained for the station blackout test. The specified cooling water flow for this test was the minimum which could be controlled and sustained.

Table 6.14

LEAK QUALITY SYSTEM CHARACTERIZATION DATA

Leak Size	Phase 4 Tests	Cooling Water Flow Rate	Peak Heat Load	Leak Rate at Peak Load	Peak LMTD	Minimum System Outlet Subcooling
10cm^2	410AT1 410BD1	3,350 lb/hr	315,000 Btu/hr	660 lb/hr	187°F	14.8°F
100cm^2	4100B2	15,800 lb/hr	1,430,000 Btu/hr	3360 lb/hr	302°F	12.0°F

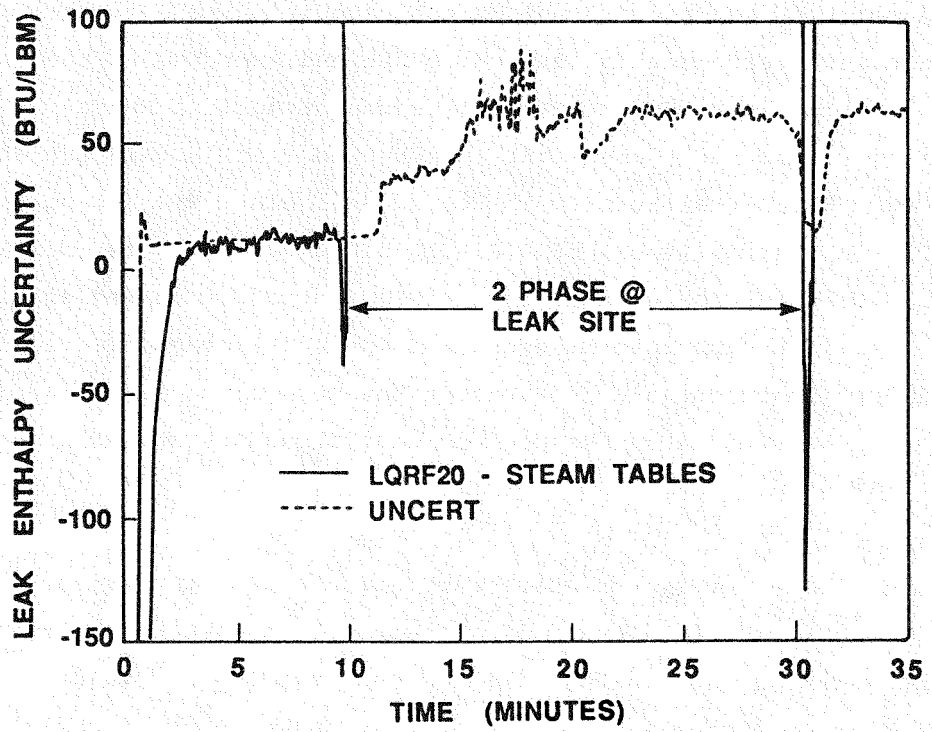

Figure 6.15 Leak Enthalpy Uncertainty for 10 cm^2 Leak Phase 4 Tests

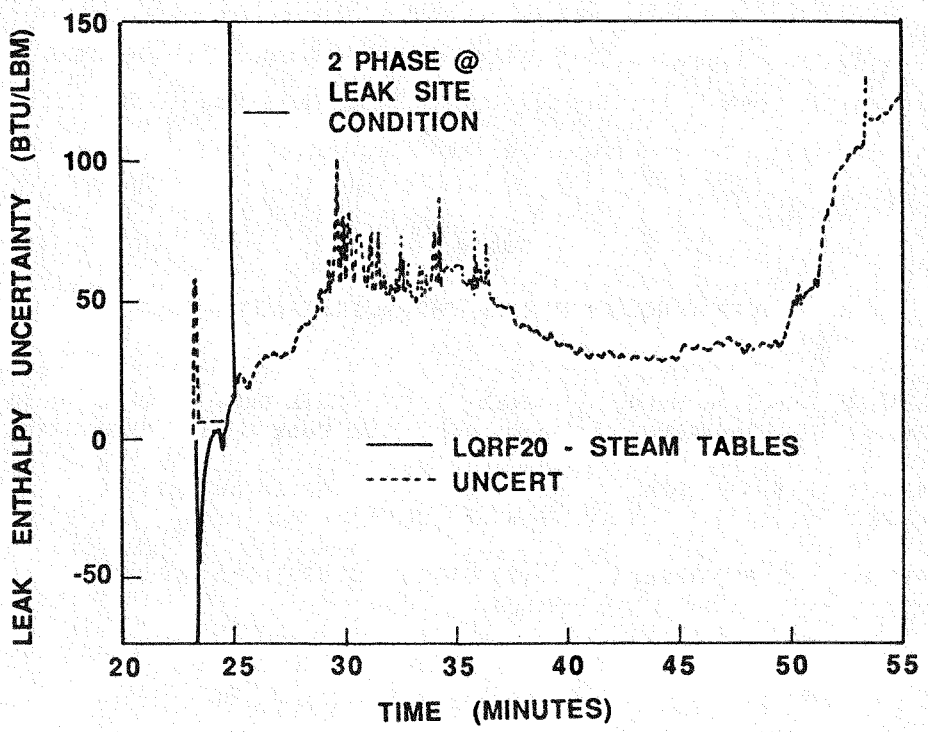

Figure 6.16 Leak Enthalpy Uncertainty for 100 cm^2 Leak Phase 4 Test

Section 7

TEST SPECIFICATIONS

The MIST test matrix was designed to address the issues formulated by the Technical Advisory Group (TAG). As listed in Table 7.1, the MIST testing was divided into eight different groups.

Table 7.1

MIST TEST GROUPS

Test Group 30	-- Mapping Tests
Test Group 31	-- Boundary System Variations
Test Group 32	-- Altered Leak and HPI Configurations
Test Group 33	-- HPI-PORV Cooling
Test Group 34	-- Steam Generator Tube Rupture
Test Group 35	-- Non-Condensibles and Venting
Test Group 36	-- Pump Operation and Core Uncovery
Phase 4	-- Additional MIST Testing

In the Test Group 30 mapping tests, integral systems data were obtained during a measured, controlled traverse through the initial events governing a small-break loss-of-coolant (SBLOCA). Whereas these early SBLOCA events ordinarily occur rapidly, in the mapping tests these events were greatly prolonged in time by controlling the rate of primary inventory depletion. Test Groups 31 through 36 were referred to as Transient Tests. In the boundary systems variations (Group 31), a single boundary system parameter was varied from their nominal condition to assess its effect. The boundary conditions so evaluated included reactor vessel vent valve control, heat loss control and augmentation, feed control and wetting, symmetry of steam generator secondary system depressurization for cooldown, an abnormal transient operating guideline (ATOG) operator-controlled test, and test repeatability. In altered leak and high-pressure injection (HPI) configurations (Group 32), leak size, leak location, isolation status, and HPI capacity were varied singly from the

nominal test condition. Feed and bleed, or HPI-PORV cooling (Group 33), was examined by interrupting feed to both steam generators and making inert the steam generator secondaries. Testing examined the timing of HPI actuation, HPI capacity, and the effects of surge line uncovery. In the steam generator tube rupture tests (Group 34), both single-ended rupture of one tube and double-ended rupture of 10 tubes were simulated. Methods of primary system depressurization, rupture elevation (top or bottom of generator), isolation status of the affected generator, and depressurization rate of the affected generator were varied from a nominal test condition. In the non-condensibles and venting tests (Group 35), the effects of non-condensible gases and venting on an SBLOCA were examined. Test variations included the effects of gas species, break location, and venting status. For the pump operation and core uncovery tests (Group 36), MIST was configured for forced flow. Test variations included a repeat of the nominal test with the new forced flow loop configuration, an ATOG operator test in which the pumps were available, pumps operation throughout an SBLOCA, pumps tripped at minimum inventory, and the effect of test initialization in forced flow. A core uncovery test involving pump operation was also tested.

Additional MIST testing beyond the above described program was performed in late 1987 and 1988. This MIST follow-on program – referred to as Phase 4 – both extended the earlier (Phase 3) data base, and explored transients and natural circulation phenomena that were previously not addressed. A 100 cm^2 SBLOCA transient was performed, extending the range of break sizes in the MIST data base. A low-pressure injection (LPI) system added for Phase 4 testing provided a more realistic simulation of the emergency core cooling system (ECCS) during low reactor coolant system pressure than was previously available. A repeat of the MIST nominal test was performed, but with modified post-trip core power and steam generator cooldown rates. This test was to provide insight into the known scaling compromise of having excess primary fluid volume. A series of steady-state steam generator performance tests were performed to supplement the current understanding of high-elevation auxiliary feedwater, as well as provide data on main feedwater operation. The areas previously not addressed included two SBLOCA transients without high-pressure injection. The variation on these tests was different strategies on utilizing the steam generator for loop cooldown. A station blackout transient was also

simulated in this phase of testing. One possible procedure for mitigating this postulated event was tested on the MIST facility. Two plant transients were simulated on the scaled MIST facility. The Crystal River 3 loss-of-offsite power event of June 1981, and the Rancho Seco loss-of-ICS event of December 1985 were simulated. The intent of these scaling tests was to provide insight into the scaling compromises known to exist in the MIST facility, and to provide code benchmarking data. These tests were completed in December 1987.

Finally, four natural circulation tests were performed in late 1988 to investigate phenomena observed at the TMI-1 plant during the conduct of natural circulation testing on October 7, 1985. A makeup and letdown flow systems simulation were added to MIST emergency core coolant system. The first natural circulation test was a simulation of the TMI-1 plant event. The other three natural circulation tests were repeats of the first test, but with 1) reactor vessel vent valves closed, 2) heat losses imposed on selected cold legs, and 3) active makeup and letdown flows.

The control of MIST during testing was specified to be both plant similar and reproducible. These somewhat conflicting aims were addressed by automating several MIST boundary systems, namely steam generator pressure and HPI flow rate, to simulate plant operator control. Certain test groups examine specific system control modes such as HPI-PORV cooling, venting, and pump operation. Also, the test loop operator performed a limited number of control actions simulating those of the plant. These include manual PORV actuation, core flood tank isolation, and venting. Finally, two MIST tests examined the effects of ATOG – a plant-trained operator is to control the loop using the Abnormal Transient Operator Guidelines.

MIST testing as well as its design thus strove for plant similarity. But the facility is not a plant. Certain interactions, notably mixing, liquid-liquid counterflow, and fluid-to-wall coupling, are necessarily distorted in a small-scale system. MIST was designed to provide accurate and relevant integral-system data with which to verify the prediction codes. These benchmarked computer codes are then the link between MIST and a plant.

In the following paragraphs, the mapping and transient test specifications are summarized. Detailed specifications of test initialization, test conduct, test specific boundary system control characteristics, and test specific measurement requirements are provided in References 9, 10, and 11.

7.1 MAPPING TESTS -- GROUP 30

The system conditions at the transitions among the early post-SBLOCA events were determined in the mapping tests. These events include saturated and two-phase natural circulation, intermittent circulation, flow interruption, and the boiler-condenser mode (BCM) heat transfer.

The early events are difficult to examine both during testing and in code predictions. They occur in quick succession and while both the boundary and system conditions are varying rapidly. These initial events are important to the subsequent transient. For example, sustained primary circulation supports heat transfer and primary depressurization, while prolonged flow interruption may cause primary repressurization.

The mapping tests were performed to traverse the early events slowly and with each of the boundary system controls held constant. Only the primary fluid mass was varied during a test. It was slowly decreased by imbalancing the HPI and leak flow rates. The transient system interactions were observed with these imposed nearly constant conditions. This technique will permit the relatively precise determination of the conditions governing each of the early events and the transitions among them. These determinations can be used directly to verify the ability of the system codes to predict the early interactions.

The observations from the mapping tests may also be used to correlate event occurrence to system conditions, i.e., to "map" performance versus conditions. The boundary system settings are selected to highlight the differences among the early transient sequences. Each of the mapping tests separately provided the primary conditions at which the early interactions occur.

Table 7.2 lists the mapping tests and contains six variables: pressurizer (PZR) status, core power, leak configuration, RVVV status, SG (secondary) level, and RCP status. The "Leak Configuration" column of the table lists the leak size and location. The leak size sets the HPI-leak energy removal capacity, rather than the rates of inventory loss and initial depressurization. This is because the HPI head-flow characteristics were not applied in the mapping tests. Rather, the HPI flow rate was set to the leak flow rate to obtain steady state, and subsequently reduced to effect a draining rate equal to the difference between the leak and HPI flow rates.

Table 7.2

MAPPING TESTS -- GROUP 30

Test Number		Status: PZR Status[1]	Core Power[2] %	Leak Configuration[3] Size (cm^2)/Location	Status: RVVV Status[4]	Status: SG Level[2] ft	Status: RCP Status
0	300001	Unisolated	3.5	10/DC	Auto	31.6	Off
1	3001BB	Isolated	3.5	5/DC	Auto	31.6	Off
3	3003AA	Unisolated	3.5	5/DC	Auto	31.6	Off
4	3004CC	Unisolated	1.0	1/DC	Auto	31.6	Off
5	300504	Unisolated	3.5	5/DC	Closed	31.6	Off
6	300605	Unisolated	3.5	5/DC	Auto	A=min,B=31.6	Off
7	3007CC	Unisolated	3.5	5/DC	Auto	Minimum	Off
8	300806	Unisolated	3.5	5/DC	Auto	31.6	On
9	3009AA	Unisolated	3.5	5/B1-CLD	Auto	31.6	Off

Notes:

(1) PZR status "Isolated": Pressurizer isolated after the steady state, at the beginning of the first drain.

(2) Augmented core power by 0.4% to offset losses to ambient.

(3) Leak configuration "DC" denotes the lower RV-DC leak site. As discussed in the text, the imposed leak size determines the HPI-leak heat removal capacity rather than the rate of inventory loss.

(4) The automatic ("Auto") RVVV settings are 0.125 and 0.04 psi to open and close, with control in automatic/independent.

(5) The 31.6-ft SG level corresponds to 95% on the Operate Range. "Minimum" denotes the lowest SG secondary level while retaining stable SG control. All use high-elevation AFW injection with AFW at 110 ± 20°F. Setting "A=Min, B=31.6" uses constant SG level control with the A-SG at the minimum level and the B-SG at 31.6 ft.

7.2 BOUNDARY SYSTEM TESTS -- GROUP 31

The boundary system tests examined the adequacy and impact of the major boundary system simulations of MIST, namely the RVVV, guard heating, and SG level controls. These tests were first to be conducted in the MIST transient test series to ensure that these boundary system simulations were well understood and that their optimum simulation mode has been selected, before the bulk of the MIST transient tests were performed. The eleven tests of Test Group 31 are listed in Table 7.3.

Table 7.3

BOUNDARY SYSTEM TESTS -- GROUP 31

All Tests: 10-cm^2 (scaled) B1-CLD leak, full HPI available, no non-condensible gas, no RCP operation

All Tests except ATOG effects (Test 6): Full HPI characteristics with throttling, no HPI/PORV cooling.

Test	Number	Description	Variable	Setting	Nominal Setting
0	310000	Nominal	(Nominal)	---	---
1	310101	Closed RVVVs	RVVV Control	Manually Closed	Auto
2	310201	Open RVVVs	RVVV Control	Manually Open	Auto
3	310302	No Guard Heating	Guard Heater Control	Off	Auto
4	310403	Band SG Level	SG Level Control	Band	Constant
5	3105AA	Throttled AFW	SG Level Control, δ	0.6 ft/m (Rate of Level Increase)	Constant
		Asymmetric SG Cooldown	SG Depressurization	Asymmetric	Symmetric ("ATOG")
6	310699	ATOG Effects	Loop Control	(See Text)	---
7	310702	No Core Power Augmentation	Core Power	No Augmentation	Augmented
9	3109AA	Nominal	(Nominal)	---	---
10	311000	Nominal Repeat	(Nominal)	---	---
11	3111AA	Maximum Feed Wetting	AFW Wetting	Maximum	Minimum

Test 0 (310000) is the MIST nominal test. These nominal test conditions include a scaled 10-cm^2 B1-CLD leak, full HPI and AFW available, no non-condensible gas injection, no reactor coolant pumps (RCPs) available, automatic RVVV actuation on differential pressure, automatic guard heater control, constant SG level control (after SG refill), and symmetric SG cooldown. (Test 0 was later supplanted by Nominal Test 9 and Nominal Repeat Test 10.)

Tests 1 and 2 (310101) and 310201) vary the RVVV operation. The MIST RVVV simulations are on/off control valves rather than the swing check valves of the plant. Control valves are required to provide positive position control and indication, but these control valves cannot replicate the smoothly varying performance of the plant check valves. This is especially apparent with vapor flow through the valves. The plant valves are expected to open only partially such that the relatively small differential pressure (generated by the steam flow rates associated with post-trip core power levels) is offset by the increased hydraulic resistance of the partially-open valves. The open/closed operation of the MIST RVVV simulation, on the other hand, tends to perform unstably. As continuing steam production increases the differential pressure across the closed valves, the valves open fully. The open valves deplete the differential pressure (ΔP) back toward the closing setpoint. To counteract this cyclic tendency, the RVVV simulation has been modified from the usual scaled configuration (which obtains the irrecoverable ΔP of the plant at power-scaled flow rates through the valves) in the following manner: The hydraulic resistance of the MIST RVVV simulation was increased to augment the ΔP across the open valves in steam flow; and the ΔP at which to close the MIST control valves was selected to approximately match the system conditions to those of the plant at closure.

Four RVVVs are used to simulate the eight valves of the lowered-loop plants. These four control valves may be actuated either independently or ganged. In the independent control mode, each valve is actuated separately, based on the differential pressure from the RV outlet plenum to the downcomer quadrant to which that valve discharges. (The individual RVVV ΔPs use a common RV outlet plenum pressure tap.) In contrast to this independent operation, in the ganged control mode all four valves open and close simultaneously in response to any single ΔP.

The independent rather than the ganged control mode permits asymmetric RVVV response to nonuniform downcomer conditions, and is the intended control mode for MIST testing. Tests 1 and 2 of Test Group 31 examine RVVV performance and impact to the SBLOCA transient.

Test 3 (310302) repeated the nominal transient but without guard heating. This test was performed with major component heat losses specifically minimized to give insight into the role of guard heating and heat losses during the SBLOCA transient.

The SG secondary controls were modified in Tests 4 (310403) and 5 (3105AA). Test 4 used band rather than constant level control after refill of the SG secondaries such that feed cycles are more pronounced than usual to impose time-varying asymmetries on the system. Test 5 imposes a reduced rate of SG refill and unequal rates of SG cooldown to increase the likelihood of AFW BCM. The unequal SG depressurizations after refill (to obtain 100°F/h cooldown in the A-SG versus 50°F/h in the B-SG) imposes long-term asymmetries on the system.

Test 6 (310699) examined the impact of operator guidelines (ATOG), quite unlike the other Group 31 tests. Rather than varying a single boundary system control feature as in the preceding tests, the operator employed ATOG to control the relevant systems.

Test 7 (310702) used no core power augmentation to offset uncompensated heat losses. Tests 9 and 10 (3109AA and 311000) were the nominal and nominal repeat tests. Finally, Test 11 (3111AA) used maximum feed wetting.

7.3 LEAK-HPI CONFIGURATION TESTS -- GROUP 32

The leak and high pressure injection (HPI) characteristics are varied in Test Group 32. These six tests are summarized in Table 7.4.

Table 7.4

LEAK-HPI CONFIGURATION TESTS -- GROUP 32

Test	Number	Description	Variable	Value	Nominal Value
1	320101	Reduced Leak Size	Leak Size, cm^2	5	10
2	320201	Increased Leak Size	Leak Size, cm^2	50	10
3	320302	CLS Leak	Leak Location	B1-CLS	B1-CLD
4	3204AA	PORV Break	Leak Location	PORV	B1-CLD
5	320503	Isolated Leak	Break Isolation	Isolated during flow interruption phase (see text)	Unisolated
6	320604	Reduced HPI Capacity	HPI Capacity	Evaluation Model	Full

Tests 1 and 2 (320101 and 320201) vary the break size. The reduced leak size in Test 1 halves the nominal leak flow rate. The increased leak size in Test 2 is five times the nominal leak rate and was selected in order to obtain core flood tank actuation. Both tests were performed with full HPI system (scaled) capacity.

The leak location was changed in Test 3 to vary the leak fluid temperature response to system conditions, as well as the impact of leak flow on inter-CL asymmetries. The PORV break (Test 4) was selected to discharge vapor initially, thus obtaining effects of increased HPI-leak cooling as well as an altered distribution of system inventory between the loop and the pressurizer. The break was isolated in Test 5, deleting HPI-leak cooling and thus elevating primary system pressures. Finally, the effects of reduced HPI capacity were examined in Test 6.

Control changes were introduced late in the transients of two tests. In Test 4 (PORV Break), the SG secondary control pressure was abruptly reduced over the final 50 psi of the controlled pressure reduction to induce SG activity. HPI-PORV cooling rather than HL venting was specified during the later stages of loop refill in Test 3 (CLS Leak).

7.4 FEED AND BLEED TESTS -- GROUP 33

Test Group 33 examined HPI-PORV ("feed and bleed") cooling. Four tests were specified, as outlined in Table 7.5. Another feed and bleed test with reactor coolant pump operation is included in Group 36, which is described later in Section 7.7. The four tests of Group 33 simulate that the RCPs are not available. In each test, a complete loss of feedwater is simulated. No leaks are used in these tests.

Table 7.5

FEED AND BLEED TESTS -- GROUP 33

(One feed and bleed test with RCP operation is included in Group 36)

All Tests: AFW is unavailable. No leak, non-condensible gas, or RCP operation. PORV keep open after actuation. Nominal RVVV control (automatic and independent actuation at 0.125 and 0.04 psi).

Automatic throttling of HPI to obtain 75°F core exit subcooling.

Test	Number	Description	Variable	Setting	Nominal Setting
1	3301BB	Nominal Feed and Bleed	(Nominal)	---	---
2	330201	Reduced HPI	HPI Capacity	Evaluation Model	Full
3	330302	Delayed HPI	Time of HPI Actuation	20 minutes	@ PORV Lift
4	330499	Surge Line Uncovery	(---------- See Text ----------)		

Test 1 (3301BB) is the nominal feed and bleed test. Full HPI characteristics were used with HPI being activated when the PORV opened. Test 2 used the evaluation model (EM) rather than the full HPI head-flow characteristics. The third test imposed delayed HPI activation. Thus, the PORV discharge was the only available energy removal mechanism for the first 20 minutes, other than fluid and metal heat capacity. Subsequent activation of HPI investigated the potential for precipitous condensation event. HL venting was employed later in this test transient. Test 4 addressed surge line uncovery, and institutes several of the operator actions and system characteristics relevant to Davis-Besse. The test was initiated in forced circulation.

7.5 STEAM GENERATOR TUBE RUPTURE TESTS -- GROUP 34

Test Group 34 imposed a series of simulated tube ruptures. The seven tests of this series are listed in Table 7.6. These tests were more rapid than the usual MIST transients and required a higher degree of test loop operator control and interaction. The operator procedures of these tests are based on, and are simplifications of, plant procedures for steam generator tube rupture events.

The nominal SGTR test (Test 1) simulated the (doubled-ended) rupture of 10 tubes at the top of the B-SG. Both steam generators were kept operational throughout this test; i.e., the "affected" (ruptured) SG was not to be isolated. A single-ended single tube (1.5 cm^2) rupture was simulated in Test 2. The operator was to perform a controlled single-loop cooldown and depressurization. Test 3 simulated a low-elevation SGTR to investigate the effect of extensive primary voiding before the rupture site is uncovered. The affected SG was isolated in Test 4 in order to observe the SG fill and idle-loop performance. A steam line break and a large SGTR were superimposed in Test 5. Test 6 was a repeat of Test 3 – the low-elevation, double-ended rupture of 10 tubes. Test 7 was a single-tube rupture, as is Test 2. The pressurizer vent was used for depressurization in Test 7; also, other methods of primary system depressurization were tested late in the transient.

Table 7.6

STEAM GENERATOR TUBE RUPTURE TESTS -- GROUP 34

An RCP-running SGTR test is included in Test Group 36. All tests: RCPs not available, Full HPI capacity available, Nominal RVVV control, no non-condensible gas. The nominal leak size (30.8 cm^2) simulates double-ended flow path from ten tubes; the reduced leak size (1.54 cm^2) represents a single flow path from one tube.

Test	Number	Description	Variable	Setting	Nominal Setting
1	340100	Nominal SGTR (Cooldown Using 2 SGs)	(Nominal)	---	---
2	340213	One Tube Rupture (1-loop Cooldown)	Leak Size (cm^2) Status of Affected SG	1.54 Isolated	Unisolated
3	340302	Low-Elevation SGTR	Leak Location	Bottom	Top
4	3404AA	SG Isolated	Status of Affected SG	Isolated	Unisolated
5	340504	Steam Line Break With SGTR	Steam Line Condition	Broken	Intact
6	3406AA	Repeat Low-Elevation SGTR	Leak Location	Bottom	Top
7	340799	One-Tube Rupture PZR Venting, De-Pressurization Method	(---------- See Text ----------)		

7.6 NON-CONDENSIBLE GAS AND VENTING TESTS -- GROUP 35

The six tests of Group 35 explored the effects of venting and non-condensible gases. Test 1 was a repeat of the nominal test (3109AA) but with vent actuation. The HLHPVs were operated continuously and symmetrically throughout

most of the test. Late in the loop refill phase, the venting was performed asymmetrically.

The non-condensible gas threshold was to be determined in Test 2. This is the maximum amount of non-condensibles which can be withstood before encountering a facility limit. The facility limits include: high primary system pressure, high core-region fluid and heater-sheath temperatures, low RV collapsed liquid level, high primary-to-secondary pressure difference, and maximum non-condensible gas collection capacity.

The threshold amount was determined based on effects rather than on the simulation of particular plant sources of gas. This threshold amount of non-condensible gas was then applied in transient Tests 3 through 5. No venting was used in Test 5; Test 3 used continuous HLHPV actuation (as in Test 1 which had no non-condensible gas) and Test 4 used continuous RVUHV actuation. The ability of the HL vents to remove non-condensible gas from the RV head was also examined in Test 3. A cold leg suction break was used in Tests 6 and 8. Nitrogen was used in Test 8 rather than helium. The features of the Group 35 tests are summarized in Table 7.7.

7.7 REACTOR COOLANT PUMP OPERATION TESTS -- GROUP 36

Test Group 36 and the core uncovery test (Test 3801AA) were performed after the loop had been reconfigured for forced flow. The major change was to replace the CL venturis with turbine meters. Because the venturis provide two-thirds of the required hydraulic resistance needed to simulate locked-rotor pumps, this change decreased the loop resistance below the scaled value with the model pumps off. Test 0 (3600AA) repeated the MIST nominal test (Test 3100AA) with the reconfigured loop to investigate the impact of the resistance change on integral system events, as well as an indication of test reproducibility. The remaining five tests of Group 36 use the model RCPs. These tests are summarized in Table 7.8.

The reactor coolant pumps were employed in Test 1 (3601AA). A plant-trained operator controlled the loop throughout testing and employed pump bumps as appropriate.

Table 7.7

NON-CONDENSIBLE GAS AND VENTING TESTS -- GROUP 35

Test Number		Title	Inter-Test Variations			
Short	Complete		Leak Site	NCG Species	Venting	Break Status
1	350101	Venting without NCG	CLD	None	HL	Open
2	3502CC	NCG Threshold	None	He	None	NA
3	350312	Hot Leg Venting with NCG	CLD	He	HL	Isolated
5	350502	NCG without Venting	CLD	He	None	Open
7	350700	Hot Leg Venting with NCG and Cold Leg Suction Leak	CLS	He	HL	Isolated
8	350800	Hot Leg Venting with Nitrogen and Cold Leg Suction	CLS	N_2	HL	Isolated

Notes

- Leak sites: "CLD" = Cold leg B1 discharge, "CLS" = Cold leg B1 suction (both scaled 10-cm^2).
- Venting: "HL" = Both hot leg high-point vents open throughout the test.
- Break status: "Isolated" = Break closed during test. Isolation times were test-dependent, and varied from 124 to 146 minutes.

Table 7.8

REACTOR COOLANT PUMP OPERATION TESTS -- GROUP 36

Test	Number	Description	Variable	Setting	Nominal Setting
0	3600AA	Nominal Repeat	(Nominal)	---	---
1	3601AA	Pump Bump: ATOG With RCPs Available	Loop Control RCP Status	(See Text) Available	(See Text) Unavailable
2	3602DD	Pumps On SBLOCA	RCP Operation	On	Off
3	360301	Worst Stop SBLOCA	RCP Operation	On Initially	Off
4	360499	Feed and Bleed With Pumps	RCP Operation	On, Trip On Loss of SCM	(Nominal Feed and Bleed) Off
5	360514	SGTR With Pumps	RCP Operation	On, Trip On Loss of SCM	(Nominal SGTR) Off

Tests 2 and 3 are related. Test 2 is to repeat the conditions of the nominal test but with the model RCPs kept in operation. The observed time of minimum primary fluid inventory in Test 2 was subsequently to be used to set the time at which to stop the pumps in Test 3 (Worst Stop SBLOCA).

Tests 4 and 5 were related to previous test groups. Both maintained the pumps in operation through test initiation, until the loss of subcooled margin. Test 4 repeats the conditions of the nominal feed and bleed test (Group 33) and Test 5 repeats those of the nominal SGTR test (Group 34).

The core uncovery test (Test 3801AA) examined phase separation when the pumps were stopped in a highly voided system, steam cooling of the core, and core reflood.

7.8 PHASE 4 TESTS

The MIST Phase 4 test matrix included two series of tests: 1) a set of eight tests which explored transients that were not addressed in the earlier MIST Phase 3 program and 2) a set of four tests which simulated phenomena observed during the conduct of actual plant natural circulation.

Test 4NOML3 was a repeat of MIST nominal test with modified post-trip power and ATOG cooldown rates.

Tests 410AT3 and 410BD1 examined the impact of the absence of the HPI system on the MIST nominal test. The ultimate refill and stabilization of the loop was accomplished by the core flood tank and the low-pressure injection (LPI) system. In Test 410AT3, the standard abnormal transient operation guideline (ATOG) was employed, i.e., constant steam generator pressure. Whereas, in Test 410BD1, a 50-psi/minute blowdown of the secondary system was implemented 30 minutes after test initiation.

Test 4100B2 was a 100-cm^2 SBLOCA transient which complements the spectrum of leak sizes performed in MIST Phase 3 tests.

Test 4SGPF2 included a series of steady-state steam generator performance tests. These tests were performed in two parts: the first utilized the main feedwater system while the second part used the high-elevation minimum-wetting auxiliary feedwater. In each part, a series of steady-state measurements were taken at various secondary levels while the primary side was in subcooled natural circulation.

A station blackout transient was examined in Test 4SB011. In addition, two plant transients were simulated: 1) the Crystal River 3 loss-of-offsite power event of 1981 which was simulated in Test 4CR3T2 and 2) the Rancho Seco loss-of-ICS event of December 1985 was simulated in Test 4SEC02.

The four natural circulation (NC) tests were performed similarly, but with different loop configurations. Test 4NCSM1 was a simulation of one phase of the TMI-1 natural circulation test where a "cold leg anomaly" was observed. The other three natural circulation tests repeated the nominal test (Test 4NCSM1) but with the reactor vessel vent valves closed in Test 4NCVV1, additional heat losses were imposed on cold legs A1 and B2 in Test 4NCHL1, and letdown and makeup flow simulations were employed in Test 4NCLM1.

The features of the Phase 4 tests are summarized in Table 7.9.

Table 7.9

PHASE 4 TESTS

Test	Description
4NOML3	Nominal test, modified core power decay and ATOG cooldown rate
410AT3	Nominal test, no HPI, ATOG control schemes for SG level and pressure
410BD1	Nominal test, no HPI, 50-psi/minute SG blowdown
4100B2	100-cm^2 leak
4SB011	Simulation of a station blackout transient
4CR3T2	Simulation the Crystal River 3 loss-of-offsite power event of 1981
4SECO2	Simulation of Rancho Seco loss-of-ICS event of December 1985
4SGPF2	Steady-state steam generator performance characterization
4NCSM1	Natural circulation simulation
4NCVV1	Repeat of 4NCSM1, with RVVV closed
4NCHL1	Repeat of 4NCSM1, with heat losses imposed on A1 and B2 cold legs
4NCLM1	Repeat of 4NCSM1, with letdown and makeup flows active

Section 8

REFERENCES

1. "Multi-Loop Integral System Test (MIST) Facility Specification," Alliance Research Center Report RDD:84:4091-01-01:01 (distributed November 1984).

2. Technical Advisory Group Final Report – "Integral System Testing Program for the B&W-Designed NSS," B&W Nuclear Power Division Report Number BAW-1787, June 1983.

3. Burchill, W.E., "Physical Phenomena of a Small-Break Loss-of-Coolant Accident in a PWR," Nuclear Safety 23, 5 (September - October, 1982).

4. "SAVER – Fluid Flow Network Pressure Drop Analysis Program," NPGD-TM-143, Revision 2, February 1978.

5. "Multi-Loop Integral System Test (MIST) Instrumentation," Alliance Research Center Report RDD:84:4127-30-01:03, Revision 3, (distributed March 1987).

6. "Once-Through Integral System (OTIS) – Final Report," NUREG/CR-4567, Babcock & Wilcox Report BAW-1905, Revision 2, September 1986.

7. "MIST Draft Characterization Report," IST Program PMG Transmittal 540, September 9, 1986.

8. "Emergency Operating Procedures Technical Bases Document," B&W Nuclear Power Division Technical Document Number 74-1152414-00, July 1985.

9. "MIST Test Specifications," Babcock & Wilcox Report BAW-1894, Revision 1, March 1986.

10. "Transmittal of MIST Phase 4 Test Specifications," IST Program PMG Transmittal 4-53, August 12, 1988.

11. "Transmittal of MIST Phase 4 Natural Circulation Test Specifications," IST Program PMG Transmittal 4-75, December 22, 1989.

12. "Thermal Analysis of MIST Guard Heating System," Alliance Research Center Report RDD:84:4127-15-01:01 (distributed November 1984).

13. "Auxiliary Feedwater Bench-Scale Tests," B&W Report LR:81:5168-05:01, March 15, 1981.